Molecular mechanisms of extracellular matrix dynamics at barrier tissues and control of molting in *Drosophila*

Dissertation

zur

Erlangung des Doktorgrades (Dr. rer. nat.)

der

Mathematisch-Naturwissenschaftlichen Fakultät

der

Rheinischen Friedrich-Wilhelms-Universität Bonn

vorgelegt von

Yanina-Yasmin Pesch

aus

Siegburg

Bonn, 2016

Angefertigt mit Genehmigung der Mathematisch-Naturwissenschaftlichen Fakultät der Rheinischen Friedrich-Wilhelms-Universität Bonn

1. Gutachter: Prof. Dr. Michael Hoch

2. Gutachter: PD Dr. Matthias Behr

Tag der Promotion: 20.03.2017

Erscheinungsjahr: 2017

Teile dieser Arbeit wurden bereits veröffentlicht in:

Pesch YY, Riedel D, Behr M (2015) Obstructor A organizes matrix assembly at the apical cell surface to promote enzymatic cuticle maturation in *Drosophila*. J Biol Chem 290(16):10071-10082.

Pesch YY, Riedel D, Patil KR, Loch G, Behr M (2016) Chitinases and Imaginal disc growth factors organize the extracellular matrix formation at barrier tissues in insects. Sci Rep 6:18340.

Pesch YY, Riedel D, Behr M (2016) *Drosophila* Chitinase 2 is expressed in chitin producing organs for cuticle formation. Arthropod Struct Dev. pii: S1467-8039(16)30172-30174. [Epub ahead of print]

Table of contents

1 - Introduction

1.1 - All arthropod species share chitinous structures as epithelial barriers and exoskeletons

Arthropods constitute more than 80% of all animal species on earth comprising 1 million described and 5 to 10 million estimated species (Odegaard, 2000; Xie et al., 2015). The arthropod phylum includes insects, crustaceans, arachnids and myriapods. Despite their enormous biodiversity, all arthropods share a chitin-containing exoskeleton that is provided by the epidermal cuticle and mediates stability of the body (Moussian, 2013a).

As the rigid exoskeleton restricts body growth, during their development all arthropods as well as nematodes have to undergo several periods of molting, which is the shedding of the cuticle (Locke & Huie, 1979; Chang, 1993; Merzendorfer & Zimoch, 2003; Ewer, 2005). It is believed that the complicated molting process, also called ecdysis, has arisen once during evolution. For this reason, arthropods and nematodes are grouped in the clade of ecdysozoa (Aguinaldo et al., 1997).

Chitin is the second most abundant biopolymer on earth after cellulose and is present in high amounts in the body walls of arthropods and fungi (Merzendorfer, 2006; Rathore & Gupta, 2015). Chitin was already identified as main component of the arthropod cuticle in the 19th century (Odier, 1823). However, almost 200 years later it is still not completely understood how the organization of chitin and other cuticle components to generate a stable matrix is mediated (Moussian, 2010; Moussian, 2013a).

In addition to the exoskeleton covering the epidermis, chitinous cuticular structures can also be found in parts of the arthropods gut in the peritrophic matrix (Richards & Richards, 1977; Lehane, 1997). In insects and myriapods, but not other arthropods, the tracheal system also possesses a chitinous cuticle (Moussian, 2013a).

The arthropod cuticle has different functions that are necessary for survival (Moussian, 2013a) (Fig. 1.1).

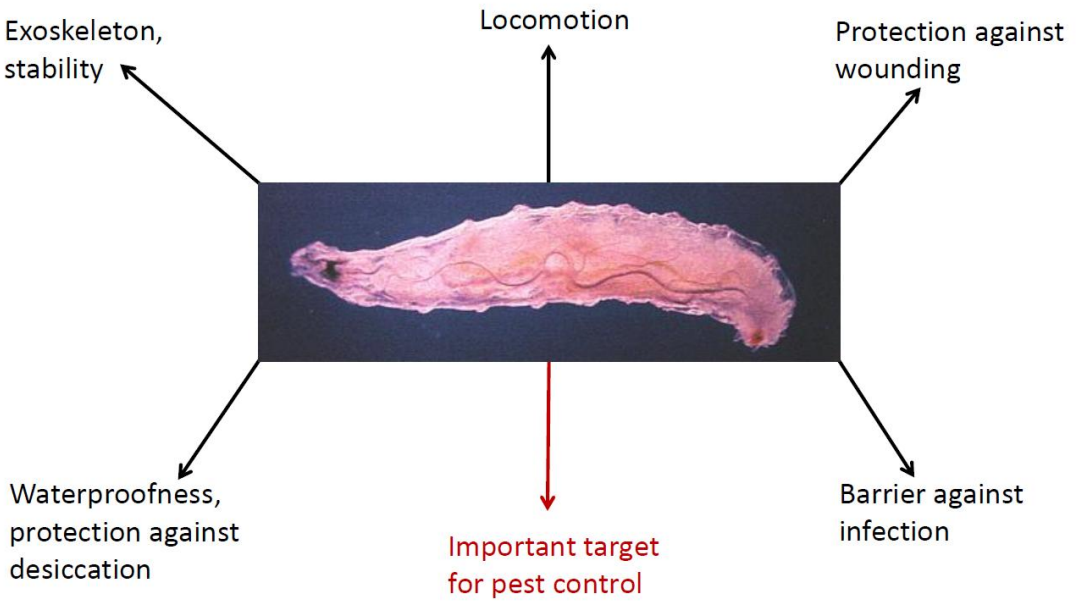

Fig. 1.1 - The cuticle protects insects throughout their life time. The cuticle acts as an exoskeleton, mediating stability, allowing locomotion and accomodating increasing body size. In addition the cuticle constitutes a barrier, mediating water homeostasis and protecting insects against wounding, predators and invading pathogens. All of these functions make the cuticle a target for pest control against harmful insects. Taken by an bright field microscope, the central picture shows a third instar *Drosophila melanogaster* larvae. The epidermal cuticle constitutes the outer larval body wall.

Most importantly, as the exoskeleton the cuticle defines body shape, mediates body stability and enables locomotion (Moussian et al., 2006a). The cuticle not only preserves the shape of the body but also forms body appendages and has influence on the shape of internal organs, such as the gut and the trachea (Moussian, 2013a). Thereby it protects against mechanical stresses, such as wounding and environmental hazards like predators. Additionally, it constitutes a crucial "first line of defense" against infection by invading pathogens (Barbakadze et al., 2006; Moussian et al., 2006a; Moussian, 2010; Petkau et al., 2012). Another important function of the cuticle is the prevention of water loss as desiccation is fatal for the animal (Beament, 1968; Parvy et al., 2012; Jaspers et al., 2014; Moussian, 2013a). This all makes the cuticle a protective shield against environmental circumstances, but also an important target for pest control (Kramer & Muthukrishnan, 1997; Arakane & Muthukrishnan, 2010; Zhang et al., 2011a; Rathore & Gupta, 2015).

This study makes use of *Drosophila melanogaster* as genetic model system to analyze epidermal cuticle dynamics and the hormonal control of molting. Because of the large variety of genetic and molecular tools and its simple genetics as well as its short generation time and easy handling, *Drosophila melanogaster* is an excellent model organism of choice for the analysis of gene functions and molecular mechanisms (Rubin & Lewis, 2000).

1.2 - Cuticle molting during the *Drosophila* life cycle

Drosophila melanogaster undergoes several different stages during its development. The generation time from egg laying to the mating of adult flies takes about 10 days at 25°C. During early embryonic development the body axes are established. The first mitotic divisions occur without division of the cytoplasm. In the process of cellularization, an epithelial cell monolayer is established on the surface of the developing embryo. By invagination of cells at the ventral part of the embryo, gastrulation is initiated and subsequently the three germ layers (ectoderm, endoderm and mesoderm) are formed (Sweeton et al., 1991; Campos-Ortega & Hartenstein, 1997). In the course of embryogenesis, segmentation and organ development is accomplished. Embryonic development takes about 24 hours and is completed by larval hatching from the eggshell.

Drosophila development comprises three larval stages, first (L1), second (L2) and third (L3) instar stage. The first and second instar larval stage take 24 hours each and are terminated by larval molting events, whereas the third instar stage lasts 48 hours and is followed by puparium formation. About 32 hours after molting to third instar stage larvae stop feeding and exhibit increased locomotor activity. At the end of the L3 stage larvae cease moving and initiate pupariation (Andres & Thummel, 1992; Sawin-McCormack et al., 1995; Mirth & Riddiford, 2007). During the pupal stage *Drosophila* undergoes metamorphosis, in which larval tissues are degraded while adult tissues are established from imaginal precursors (Chadfield & Sparrow, 1985; Thummel, 1996). After 4-5 days the adult fly ecloses from the puparium and is able to reproduce only few hours after hatching (Campos-Ortega & Hartenstein, 1997).

Each of the developmental transitions in the *Drosophila* life cycle - embryonic hatching, the larval molts, pupariation and metamorphosis - is concomitant with a pulse of the hormone

ecdysone (Andres & Thummel, 1992). Ecdysone biosynthesis and signaling is a major topic in this study and will be described in detail below (chapter 1.6.1).

Drosophila larvae constantly feed, thereby increasing their body mass 200-fold within 4 days, mostly due to *de novo* lipid biogenesis (Church & Robertson, 1966). The rigid nature of the chitinous exoskeleton restricts larval growth. Therefore, the massive increase in body size requires periodic shedding of the cuticle upon molting, marking the transitions between the larval stages (Chang, 1993; Chaudhari et al., 2011; Xie et al., 2015). Each molt requires the complete synthesis of a new cuticle and the full degradation of the old cuticle. As both processes occur at the same time, molting requires stringent organization of cuticle remodeling in order to prevent improper degradation of the old as well as damage to the new, nascent cuticle by lytic enzymes (Chaudhari et al., 2011). Furthermore, the composition of the pupal cuticle is essential for successful metamorphosis (Fristrom, 1965; Chadfield & Sparrow, 1985).

All in all, this indicates that proper organization of the cuticle matrix is crucial for development and survival, both during molting and pupariation when massive cuticle remodeling needs to occur as well as in intermolt stages upon wounding and during growth. How the chitin-matrix of the epidermal exoskeleton is organized during its synthesis and remodeling is one of the key questions of this study and is discussed in chapter 1.5.

1.3 - Molting to adapt to increasing body growth

The term "molting" is generally used for the shedding of an outer cover, such as feathers in birds or skin in snakes, but the molting process of arthropods, which includes replacement of the exoskeleton, is by far more complex. All insects have to undergo molting, also called ecdysis, several times during their development. Even though the elasticity of the cuticle allows growth to some extent, at some point further expansion is restricted by the rigidity of the exoskeleton, which therefore needs to be shed and replaced by a new, larger exoskeleton (Locke & Huie, 1979; Chang, 1993; Ewer, 2005).

The molting process is very complex and therefore needs strict control as the exoskeletal barrier is crucial for insect survival (chapter 1.1). Molting is initiated by pulses of the steroid hormone 20-hydroxyecdysone that initiates a coordinated gene expression program (Urness & Thummel, 1990; Urness & Thummel, 1995; Thummel, 1996). The behavior of molting

insects is also tightly regulated and comprises a stereotypic "molting sequence" (Park et al., 2002). The different steps of the molting process are depicted in Fig. 1.2, focusing on the epidermal cuticle:

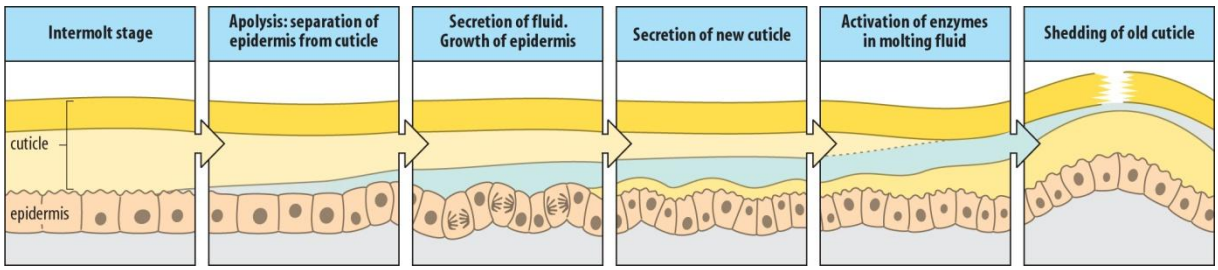

Fig. 1.2 - The molting process. During intermolt stages, the cuticle directly adheres to the epidermis. Upon initiation of molting, apolysis occurs, which is the separation of the cuticle from the epidermal cells. By secretion of fluids, also named "molting fluid", the space between the epidermis and the cuticle becomes larger during the process of molting. After the epidermis undergoes mitotic cell division, new cuticular material is secreted. The synthesis of the new cuticle occurs whilst the old cuticle is partly degraded by enzymes in the molting fluid. When synthesis of the new cuticle is completed, the old cuticle is shed. Adapted from Brian E. Staveley, Memorial University of Newfoundland (http://www.mun.ca/biology).

Before initiation of the molt the epidermal cells are strongly attached to the cuticle (Ewer, 2005). When the molting process is initiated, detachment between the two occurs. The separation of epidermis from cuticle is called apolysis. The so called exuvial space in between the epidermal cells and the cuticle grows through secretion of the "molting fluid" or "molting gel" by the cells. While the secretion of molting fluid continues, the epidermal cell layer grows by mitotic cell division. After mitosis is completed, the cells start to secrete cuticular material, starting with the outermost envelope layer (chapter 1.4.1), and lytic enzymes in the molting fluid such as chitinases and proteases are activated to degrade the old cuticle. This implies that the synthesis of the new and the degradation of the old cuticle occurs in parallel (Wigglesworth, 1960; Lensky et al., 1970; Locke and Huie, 1979; Reynolds & Samuels, 1996; Locke, 2001; Merzendorfer and Zimoch, 2003; Chaudhari et al., 2011). Interestingly, the lytic enzymes are not excluded from the newly synthesized cuticle, but its non-chitinous envelope layer most likely renders it insensitive against damage by molting fluid enzymes (Locke, 2001; Chaudhari et al., 2011). After synthesis of the new cuticle is finished, the old cuticle is shed and ecdysis is completed. Afterwards, the soft and fragile new cuticle hardens by enzymatic sclerotization (Dennel, 1944; Hopkins & Kramer, 1992;

Loveall & Deitcher, 2010). For this reason, molting always bears a risk for the insect as the full barrier function of the cuticle is compromised within a short time period after ecdysis and the animal is prone to dehydration and damage by predators (Ewer, 2005).

1.4 - Chitinous structures in *Drosophila*

The term "chitin" originates from the Greek word "chiton", which means "cover" or "shell". This already hints at chitin being the most important component of the arthropod exoskeleton. Chitin can not only be found in the arthropod cuticle, but also in the body walls of fungi and yeast and the inner shells of squids and cuttlefish (Merzendorfer, 2006; Rathore & Gupta, 2015; Younes & Rinaudo, 2015). There is evidence that chitin is also produced in certain vertebrates, including fish and amphibians, but the biological role of chitin in vertebrates remains elusive (Tang et al., 2015).

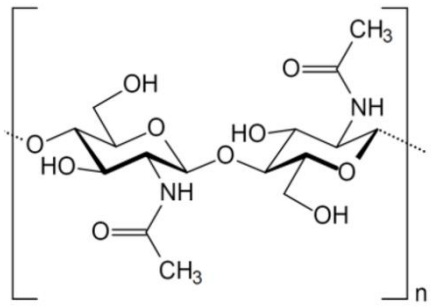

Chitin is a sugar polymer made up by N-acetyl-β-D-glucosamine (GlcNAc) residues that are linked via β-(1,4) glycosidic bonds (reviewed in Kramer and Muthukrishnan, 1997; Merzendorfer and Zimoch, 2003) (Fig. 1.3).

Fig. 1.3 - Chemical structure of chitin. Chitin consists of linear polymers of β-(1,4)-linked N-acetyl-β-D-glucosamine (GlcNAc) residues. Adapted from Younes & Rinaudo, 2015.

In *Drosophila* chitin-containing structures can be found in distinct organs, which are the digestive, the tracheal system, the head skeleton, spiracles and the epidermis (Richards & Richards, 1977; Lehane, 1997; Tonning et al., 2005; Moussian et al., 2006a; Petkau et al., 2012; Moussian, 2013a). There chitin is deposited by epithelial cells to form the apical extracellular matrix (aECM), which acts as a protective layer that is required for tissue integrity and stability (Tonning et al., 2006; Moussian et al., 2006a).

As my work concentrates on two specific chitin-matrix forming organs, namely the epidermis and the tracheal system, these will be discussed in more detail below (chapter 1.4.1 for the epidermis and 1.4.2 for the tracheal system).

1.4.1 - Structure and development of the epidermal cuticle

The *Drosophila* epidermis is a ectodermally derived single layered epithelium. It starts to form during early embryogenesis and finally encovers the whole animal at stage 15, followed by deposition of first cuticle material (Moussian et al., 2006a; Jacinto et al., 2012; Petkau et al., 2012).

The *Drosophila* epidermal cuticle consists of stratified aECM material produced by the epidermal cells (Wigglesworth, 1948; Moussian, 2010). Because of the high conservation of cuticle structure among all insects, results obtained from analyzing the *Drosophila* cuticle can most likely be transferred to other species (Moussian, 2010). Although several different terminologies exist, only the very common and widely accepted terminology by Locke, 2001, will be used in this thesis, dividing the cuticle into three main areas: The envelope, the epicuticle and the procuticle (Fig. 1.4).

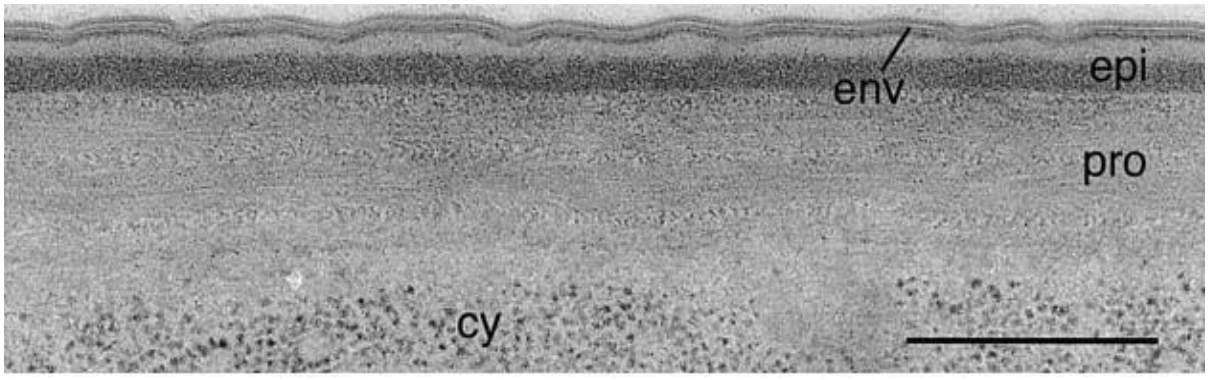

Fig. 1.4 - Epidermal cuticle structure in wild type *Drosophila* larvae. Three distinct layers are seen in this TEM picture: The outer envelope (env), the electron dense epicuticle (epi) and the procuticle (pro), which contains the chitin lamellae and lies on top of the monolayer of epidermal cells (cy - cytoplasm). The scale bar represents 500 nm. Adapted from Moussian et al., 2005a.

The uppermost layer of the cuticle, facing the external environment, is the envelope. The hydrophobic envelope consists mainly of neutral lipids and wax esters, but also contains proteins (Locke, 2001; Moussian, 2013a; Jaspers et al., 2014). The main function of the envelope is the protection of the animal against dehydration and soaking (Beament, 1968; Gibbs, 1998; Gibbs, 2011; Moussian, 2013a). This waterproof barrier is established by complex formation of sclerotin, which is a protein-quinone complex, polyphenols and the above-mentioned lipids (Wigglesworth, 1985; Moussian, 2013a). The envelope has a uniform

thickness and constitutes the first cuticle layer that is synthesized upon molting because of its important protective function (Locke, 2001; Moussian, 2013a).

The electron dense layer beneath the envelope is called the epicuticle (Locke, 2001). The epicuticle is devoid of chitin (Sass et al., 1994) and rather contains a multitude of proteins and lipids, but the exact composition of the epicuticle remains unknown (Moussian, 2013a). Both the correct composition of the chitinous procuticle and proper ecdysone signaling are necessary for epicuticle formation (Moussian et al., 2005b; Gangishetti et al., 2012).

The procuticle forms the thickest layer of the epidermal cuticle and mainly comprises chitin organized into stacked lamellae (Wigglesworth, 1948; Locke, 2001). Additionally, proteins can be found within the procuticle (Condoulis & Locke, 1966). Within the tightly packed procuticle about 17-20 anti-parallel chitin fibers form microfibrils by hydrogen bonding between the sugar chains. The microfibrils are about 3 nm in diameter and 300 nm in length. They align to form horizontal laminae that are stacked slightly shifted towards each other, resulting in helicoidal lamellar arrangement (Locke, 2001; Merzendorfer & Zimoch, 2003; Vincent & Wegst, 2004; Moussian et al., 2005a; Moussian et al., 2006a; Moussian et al., 2006b).

Cuticle synthesis is subdivided into three phases: First, the generation of layers is performed, second, cuticle thickening occurs, and third, laminae obtain their final orientation and the cuticle hardens via sclerotization (Hopkins & Kramer, 1992; Moussian et al., 2006a). The first layer that is synthesized during development and also during each molting event is the envelope layer (Wigglesworth, 1948; Locke, 2001; Moussian et al., 2006a). As soon as the envelope forms a nearly continuous layer covering the epidermal cells, procuticle synthesis begins (Moussian, 2010). During embryonic development envelope synthesis starts at stage 15 and first chitin is detected in stage 16. Epicuticle synthesis begins in late stage 16. During stage 17 the epicuticle becomes more organized and dense due to sclerotization, flattening of the epidermal cells occurs and the chitinous procuticle thickens significantly. However, no lamellar structure can be detected until the very end of embryogenesis at late stage 17, shortly before larval hatching (Moussian et al., 2006a).

Upon procuticle synthesis the apical membrane of the epidermal cells forms specialized microvilli-like structures, the apical undulae, which subdivide the membrane into functional clusters. The crests of the undulae harbor the chitin-synthesizing machinery, whereas at the grooves vesicle exocytosis containing newly synthesized cuticle material takes place

(Moussian et al., 2010). Cuticle synthesis occurs continuously in the larval stages with especially strong synthesis taking place during the last instar larval stage, which is the phase when the larval growth rate is highest (Kaznowski et al., 1985; Wolfgang & Riddiford, 1986).
Importantly, as noted above, the epidermal body wall cuticle needs to be very stable. The lamellar chitin structure of the procuticle confers both stability and elasticity to the cuticle (Vincent & Wegst, 2004; Tonning et al., 2006). The outer part of the procuticle, also called exocuticle, becomes hardened upon sclerotization, which is the crosslinking of proteins and chitin with catecholamines and phenols. This leads to a more rigid and stabilized cuticle (Dennel, 1944; Ostrowski et al., 2002; Moussian et al., 2005a; Moussian, 2010; Loveall & Deitcher, 2010).
The stratified lamellar architecture of the epidermal cuticle is in contrast to the non-lamellar chitin-structures in the tracheal system (Devine et al., 2005; Tonning et al., 2005; Moussian et al., 2006b; Moussian, 2013a; Moussian et al., 2013b) and the peritrophic matrix of the digestive system, which is not discussed in this thesis. An overview of chitin structure in the peritrophic matrix is given in Lehane, 1997.
Beneath the procuticle a monolayer of epidermal cells synthesizes the vast majority of cuticular material (Wigglesworth, 1960). As those few cells produce the thick and elaborate cuticle aECM, epidermal cells have an extensive secretory organelle machinery and an apical membrane with specialized structures (Wigglesworth, 1960; Uv & Moussian, 2010).
In between the above mentioned stratified chitin-matrix and the epidermal cell monolayer a morphological distinct, non lamellar structure can be detected, the so called "assembly zone" or "deposition zone". This region becomes very obvious in the epidermis but may exist also in other cuticles (Delbecque et al., 1978; Wolfgang et al., 1986; Wolfgang et al., 1987). The assembly zone is a stable and permeable matrix and is thought to be the area through which components, such as chitin fibrils or proteins, that have just been secreted by the epidermal cells pass before they are integrated into the stratified cuticle. It is supposed that the assembly zone is the area where this integration into the pre-existing, mature cuticle matrix takes place. Even though some unidentified proteins have found to be localized to the assembly zone (Wolfgang et al., 1987; Locke et al., 1994), these have not been further analyzed yet, leaving the molecular mechanism of cuticle formation and organization at the assembly zone largely elusive. What is already known about the molecular mechanisms of chitin-matrix production, maturation and degradation is discussed below in chapter 1.5.

1.4.2 - Development and structure of the tracheal chitin-matrix

The *Drosophila* tracheal system constitutes a combination of a pulmonary and vascular system and consists of a stereotypic network of about 10,000 branches. Its function is the transport of oxygen to tissues (Ghabrial et al., 2003; Wu & Beitel, 2004). In the *Drosophila* tracheal system a monolayer of epithelial cells forms a lumen through which oxygen can flow. Oxygenated air is taken up at the posterior spiracles and is transported through the ramified luminal network to the target tissue. The tracheal network is formed already at second half of embryogenesis by multiple morphological events, such as cell migration, tube fusion and expansion. Importantly, the tracheal network forms without cell proliferation and is regulated by membrane biogenesis at the apical cell surface and by secretion of liquid into the lumina to keep them open (Beitel & Krasnow, 2000; Ghabrial et al., 2003; Lubarsky & Krasnow, 2003; Hemphälä et al., 2003). As the size of tubular organs is very important for their function, with aberrant tube length or diameter leading to severe impairments, tracheal tube size is tightly genetically controlled (Behr et al., 2003; Lubarsky & Krasnow, 2003; Hemphälä et al., 2003). At the end of embryonic development, liquid clearance of the lumina is necessary to enable gas filling of the tracheal tubes and for establishing proper tube length (Behr et al., 2007).

The tracheal cuticle consists of the outward non-chitinous envelope and epicuticle as well as the chitinous procuticle, which covers the tracheal epithelial cells (Moussian et al., 2006b; Moussian, 2013a). The envelope consists mainly of lipids and faces the tracheal lumen (Moussian, 2013a). The synthesis of the epicuticle, which is a protein-lipid matrix devoid of chitin, starts from stage 15 onwards (Devine et al., 2005; Moussian, 2013a). The innermost cuticle layer, the procuticle, contains proteins and, most importantly, chitin (Moussian, 2013a). In the tracheal procuticle in contrast to the epidermal, chitin is not arranged into lamellae, but is present in long filamentous structures that are organized parallel with tube length (Devine et al., 2005; Tonning et al., 2005; Moussian et al., 2006b). Unlike the evenly shaped, smooth epidermal cuticle the tracheal cuticle has a less regular structure and is characterized by protrusions (Araújo et al., 2005; Uv & Moussian, 2010; Moussian, 2013a). Chitin synthesis starts at late stage 13 when it can be detected discontinuously in the lumen of the dorsal trunk, which is the main branch of the tracheal system. During stage 15 chitin lines all branches of the tracheal system (Devine et al., 2005).

The biological function of the tracheal chitin-matrix is to provide a viscoelastic extracellular matrix limiting tube diameter and length, and thus preventing dilated and/or oversized tubes (Dong & Hayashi, 2015). Loss or improper secretion of chitin affects cytoskeleton and aECM organization as well as stability of the developing epithelium, thereby affecting tube length and diameter (Tonning et al., 2005; Devine et al., 2005; Petkau et al., 2012).
Mutations affecting the chitin synthases *kkv (krotzkopf verkehrt)* and *cystic* lead to failure of tube size expansion, also resulting in local cyst-like structures (Araújo et al., 2005; Devine et al., 2005). Loss of the chitin deacetylases Serp (Serpentine) and Verm (Vermiform), which modify chitin and are necessary for its fibrillar structure, cause over-elongated tubes (Luschnig et al., 2006). Thus, the correct texture of chitin in the tubes also plays an important role in size regulation. The Knickkopf (Knk) protein organizes chitin fibril assembly, protects chitin-matrix structures in the trachea and was shown to be necessary for tube expansion (Devine et al., 2005; Moussian et al., 2006b; Petkau et al., 2012).
The chitin-binding protein Obstructor-A (Obst-A) forms a complex with the deacetylase Serp and Knk to mediate protection of chitin fibrils against the attack by chitinolytic enzymes. Loss of *obst-A* leads to premature chitin degradation and tube over-elongation (Petkau et al., 2012). Furthermore, Obst-A controls tube diameter in partial redundancy with the related Obst-C/Gasp protein (Tiklová et al., 2013). The function of Obst-A in the tracheal cuticle is discussed in detail in Chapter 1.5.4.

1.5 - Molecular factors required for cuticle formation and organization

The cuticle has to be replaced several times during insect development when molting occurs (chapter 1.3), but cuticle synthesis also takes place during intermolt stages in order to adapt to growth and wounding (Kaznowski et al., 1985; Chang, 1993; Galko & Krasnow, 2004; Chaudhari et al., 2011). Thus, cuticle formation requires strict genetic control (Moussian et al., 2005b; Moussian, 2010). Yet, not much is known how exactly cuticle components are organized into a highly ordered matrix (Moussian, 2010). The following chapter sums up the present knowledge about factors implicated in the regulation of cuticle organization, preservation and maturation.

1.5.1 - Factors implicated in chitin synthesis

Chitin synthesis starts during embryonic development and is continued throughout larval and pupal development (Kaznowski et al., 1985; Moussian et al, 2006a). This is enzymatically mediated by chitin synthases, which are inserted into the apical plasma membrane of the chitin-producing cells. Their function is to catalyze the β-1,4-linkage between UDP-GlcNAc (Uridine-diphosphate–N-acetyl-D-glucosamine) monomers that are used as substrate (Merzendorfer, 2006). Chitin monomers are connected within the cytoplasm and the growing sugar chains are shuttled outside, exiting via the pore-forming unit of the enzyme (Merzendorfer, 2006). *Drosophila* has two chitin synthases. Chitin Synthase-1, also called krotzkopf verkehrt (kkv), is responsible for chitin synthesis in the epidermis, the fore- and hindgut and the trachea, whereas Chitin Synthase-2 is implicated in chitin synthesis in the midgut (Ostrowski et al., 2002; Moussian et al., 2005b; Tonning et al., 2005; Öztürk-Çolak et al., 2016). Loss of *kkv/chitin synthase-1* leads to severe structural defects of the head cuticle and to compromised procuticle integrity, detachment of the procuticle from the epidermis, destabilized epicuticle, dysregulated sclerotization and altered epidermal cell morphology (Ostrowski et al., 2002; Moussian et al., 2005b).

Importantly, mutants lacking genes involved in the biosynthesis of the molting hormone ecdysone (chapter 1.6.1) fail to establish a proper embryonic cuticle, indicating the role of ecdysone in regulating chitin synthases and other genes that are crucial for cuticle formation (Nüsslein-Volhard et al., 1984; Jürgens et al., 1984; Wieschaus et al., 1984; Chávez et al., 2000).

1.5.2 - Factors involved in chitin-matrix maturation and protection

Chitin fibrils undergo spontaneous self assembly into microfibrils, which then form lamellar structures (Merzendorfer & Zimoch, 2003; Vincent & Wegst, 2004; Moussian et al., 2006a). However, this self assembly is not sufficient to establish an ordered, strong cuticle matrix (Moussian, 2010; Moussian, 2013a). Furthermore, cuticle remodeling upon molting requires degradation of old cuticle structures by chitinolytic enzymes (Chaudhari et al., 2011). The following chapter sums up the knowledge about factors and molecular processes that are required for dynamic cuticle assembly, maturation, protection and disassembly.

Chitin deacetylases Serpentine and Vermiform for maturation and preservation

One important process of chitin-matrix maturation is the deacetylation of chitin polymers. In insects this is controlled by chitin deacetylases, which are conserved in sequence and and function (Dixit et al., 2008). In *Drosophila* Serpentine (Serp) and Vermiform (Verm) most probably catalyze the enzymatic deacetylation of chitin at the acetamide groups, converting chitin into chitosan (Luschnig et al., 2006) (Fig. 1.3 for the chemical structure of chitin). This conversion alters the physicochemical properties (Tsigos et al., 2000; Yang et al., 2011; Hsiao et al., 2013), thereby changing composition and stability of the chitin-matrix and probably influencing the capability of chitin to interact with proteins (Luschnig et al., 2006; Moussian, 2010).

Drosophila Serp and Verm are expressed in the trachea and in the epidermis. Loss of the chitin deacetylases in *Drosophila* causes changes in the structural properties of chitin resulting in tracheal tube overelongation and to reduced epidermal procuticle deposition, thereby also influencing body shape. Altogether these defects lead to embryonic lethality (Luschnig et al., 2006; Wang et al., 2006). Surprisingly, new data indicate that Serp is produced and secreted by the fat body and is then taken up by tracheal cells, which shuttle the Serp protein into the tracheal lumen via transcytosis (Dong et al., 2014).

Knickkopf and related proteins for differentiation and protection

Knickkopf (Knk) is a GPI-anchored protein implicated in chitin organization and protection (Moussian et al., 2006b). It influences chitin deposition in *Drosophila* and associates with chitin (Ostrowski et al., 2002; Moussian et al., 2006b). Knk harbors a dopamine monooxygenase-like (Domon) domain, which may catalyze some redox reaction such as crosslinking of chitin with proteins or may be involved in the interaction of Knk with other proteins (Moussian, 2006b; Shaik et al., 2014). In the tracheal cuticle the Knickkopf protein mediates chitin fibril assembly and protection of chitin-matrix structures, making it necessary for tracheal tube expansion (Devine et al., 2005; Moussian et al., 2006b; Petkau et al., 2012).

Knk function has been studied well in *Tribolium castaneum* where Knk colocalizes with chitin in the procuticle and is implicated in the organization of chitin into laminae. Upon molting

Knk protects the newly synthesized cuticle against degradation by chitinolytic enzymes (Chaudhari et al., 2011).

Knk-like proteins can be found in all chitin-producing animal groups except for fungi (Chaudhari et al., 2011). In *Tribolium* three members of *knk*-like genes have been identified, which are all necessary for proper cuticle function, but play a role in different types of cuticle at different developmental stages (Chaudhari et al., 2014). In addition to its function in chitin organization and protection in the procuticle, Knk also plays a role in organization of the serosal cuticle and therefore is necessary for egg hatching (Chaudhari et al., 2015).

It was shown in *Tribolium* that the Retroactive (Rtv) protein is required to mediate the trafficking of Knk into the procuticle as loss of Rtv leads to retention of Knk within the epidermal cells, leading to molting defects and lethality (Chaudhari et al., 2013). *Drosophila* Rtv is not well known, but initial studies show that it binds chitin and probably supports orientation of newly formed chitin fibrils at the apical cell surface (Moussian et al., 2005a; Moussian et al., 2006b).

1.5.3 - Glyco18 family members as chitinolytic enzymes

Repetitive molting and wounding requires the concerted degradation of cuticle structures. Hydrolytic cleavage of the β-1,4-glycosidic bonds of chitin fibrils is mediated by Chitinases to form chitooligosaccharides and by β-N-acetyl-D-glucosaminidase for further processing into sugar monomers (Kramer & Muthukrishnan, 1997; Merzendorfer & Zimoch, 2003; Arakane & Muthukrishnan, 2010; Zhu et al., 2016). The resulting GlcNAc oligomers and monomers undergo recycling for chitin biosynthesis (Merzendorfer & Zimoch, 2003; Chaudhari et al., 2013).

As this thesis investigated *Drosophila* Chitinases, their function will be discussed in more detail. Chitinases are members of the Glycosylhydrolase Family 18 (Glyco18), which comprises both Chitinases (Chts) as well as the related Imaginal Disc Growth Factors (Idgfs) (Zhu et al., 2004). The Glyco18 family is highly conserved in arthropods, nematodes and fungi (Zhu et al., 2004; Arakane & Muthukrishnan, 2010). The common domain architecture that members of the Glyco18 family share is depicted in Fig. 1.5:

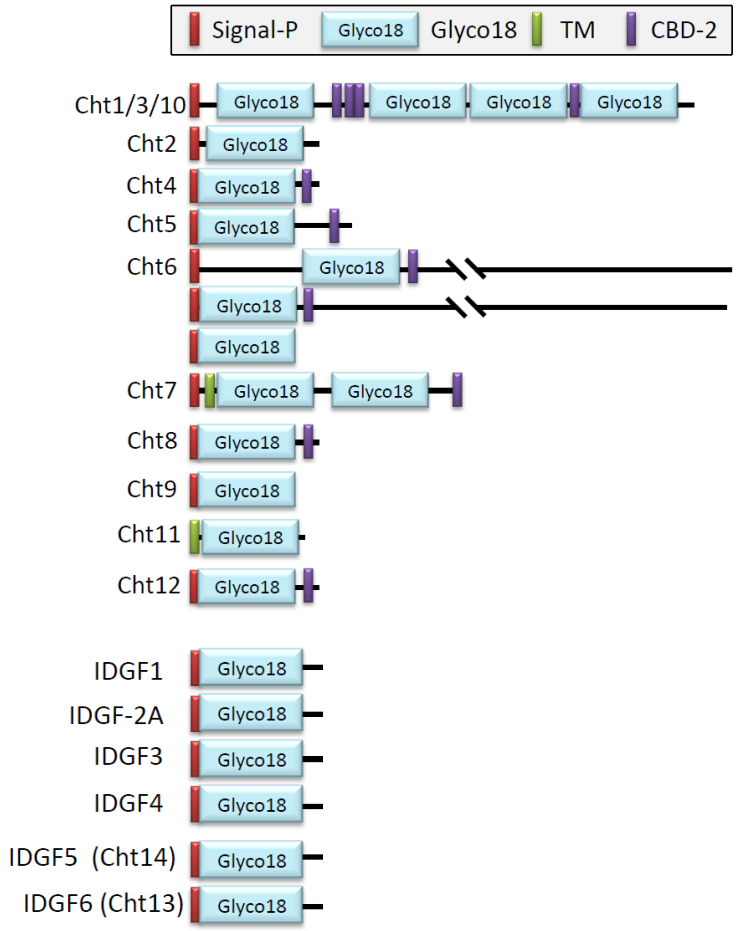

Fig. 1.5 - The Glyco18 protein family in *Drosophila*. In *Drosophila* there are 14 Chitinases and 4 Idgfs that share a similar domain organization and have strong sequence homology. Cht13 is also known as Idgf6 or DS47 and that Cht14 is also called Idgf5. Even though domain architecture varies to some extent, Glyco18 proteins typically contain a signal peptide that is cleaved upon maturation, a catalytic domain, a PEST-rich linker region (enriched in serine and threonine) and a chitin binding domain. The latter is not present in all Chts and in none of the Idgfs. Idgfs are catalytically inactive due to a point mutation in their active site.

Most Glyco18 members show the following domain architecture: An N-terminal catalytic region (Glyco18 domain) is followed by a PEST-linker region (enriched in proline, glutamate and especially serine and threonine) and a C-terminal Chitin Binding Domain (CBD) (Zhu et al., 2004). All Glyco18 members except for Cht11 have a signal peptide for secretion (Merzendorfer & Zimoch, 2003). Not all Chts and none of the Idgfs have CBDs, but interestingly, Idgf2 and Idgf4 are nonetheless capable of binding chitin (Arakane & Muthukrishnan, 2010). There is evidence that also the Chts lacking CBDs play a role in chitin remodeling and that the CBDs only increase the affinity of the Chts to chitinous structures (Zhu et al., 2004; Arakane & Muthukrishnan, 2010).

The catalytic activity of Chitinases is predicted for Cht1 to Cht11, but has only been demonstrated for Cht4, 5 and 9 (Zhu et al., 2008a). Cht12 as well as all Idgfs are not catalytically active due to a point mutation in the active enzymatic site (Zhu et al., 2004) and may act as lectins or be implicated in cell communication, immunity and the regulation of growth (Kawamura et al., 1999; Zhu et al., 2004). Indeed, Idgfs act in the imaginal discs stimulating growth, polarization and motility of disc cells (Kawamura et al., 1999).
It is thought that even though there are so many different Chitinases in insects there is no complete redundancy as different Chts show distinct specificities for the chain length of the chitin substrate (Merzendorfer & Zimoch, 2003). Knockdown screens in *Tribolium* show that some Chts are crucial for molting and survival (Zhu et al., 2008a; Zhu et al., 2008b).
Strikingly, homologs of Chitinases can also be found in organisms that do not synthesize chitinous structures, such as humans. Their function might be linked to immunity (Kirkpatrick et al., 1995; Merzendorfer & Zimoch, 2003; Arakane & Muthukrishnan, 2010).

1.5.4 - The Obstructor family of chitin-binding proteins

Two major classes of chitin-binding proteins have been identified in *Drosophila,* which promote stabilization of the chitin-matrix and might assist chitin-matrix assembly (Behr & Hoch, 2005). First, the R&R (Rebers & Riddiford) domain genes are found in multiple clusters in the genome and show peak expression upon molting (Rebers & Riddiford, 1988; Rebers & Willis, 2001; Togawa et al., 2008). One example of R&R proteins is resilin, which confers elasticity to the cuticle (Qin et al., 2009).
The second group of chitin-binding proteins was identified in *Drosophila* (Behr & Hoch, 2005) and named the "Obstructor family" due to a barrier phenotype in mutant embryos. This group belongs to the so called CPAP family (Cuticle Proteins Analogous to Peritrophins) that was also identified later on by sequence and domain arrangement analysis in many insects (Jasrapuria et al., 2010; Willis, 2010; Jasrapuria et al., 2012).
In general the CPAP family shares the peritrophin-A motif consisting of a Chitin Binding Domain Type 2 (CBD2) with six characteristically spaced cysteine residues. This makes the CPAPs unique as no other cuticle proteins containing cysteine residues have been identified (Jasrapuria et al., 2010; Willis, 2010). The study of Jasrapuria et al., 2010, found 42 CBD2-containing proteins in *Tribolium castaneum*, containing 13 chitin metabolizing enzymes and

29 proteins with signal peptides enabling secretion. Due to the three prominent CBD2 domains, members of the *obstructor* gene family are homologous to the CPAP3 subfamily (Jasrapuria et al., 2010).

The *obstructor* multigene family is highly conserved among arthropods

A database screen for genes exclusively expressed in cuticle-forming tissues led to the discovery of the CG17052 locus (Behr & Hoch, 2005). Since the mutant embryos showed a "barrier break down" phenotype, the locus was called "*obstructor*" (*obst*). By BLAST analysis four related genes with more than 50% DNA sequence identity were discovered. The first discovered gene was thereupon called *obst-A* and the other genes were named *obst-B* to *obst-E*. *Obst-C* is synonymous to the *gasp* gene that had previously been discovered (Barry et al., 1999; Tiklová et al., 2013). Five *obstructor* genes have a common domain architecture, consisting of an N-terminal signal peptide enabling protein secretion and three regularly spaced Chitin-Binding Domains type 2 (CBD2) also known as Peritrophin-A domain (Barry et al., 1999). Thus, these five proteins are classified as subgroup 1 of the Obstructor family (Fig. 1.6).

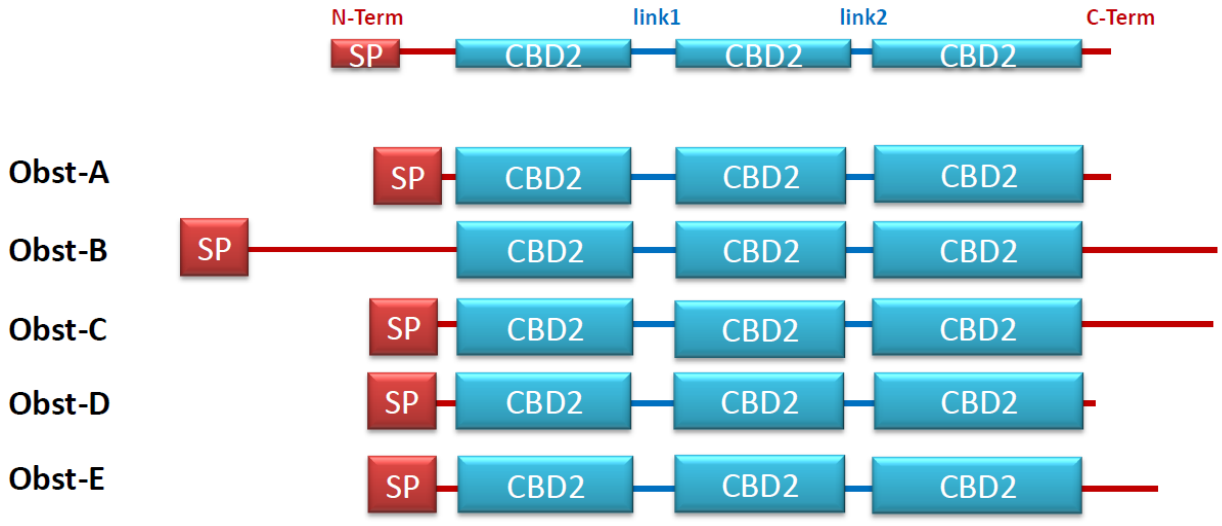

Fig. 1.6

Fig. 1.6 - Domain architecture of the Obstructor protein family (subgroup 1). The Obstructor (Obst) protein family includes the members Obst-A to E (subgroup 1), which have very high sequence similarity, and the members Obst-F to J (subgroup 2). All Obst proteins share the common domain architecture of an N-terminal signal peptide (SP; red) that indicates protein secretion and three Chitin-Binding Domains type two (CBD2; blue). The C-terminal portions of the Obst proteins are variable. The linking regions between the CBD2s of subgroup 1 Obst proteins have approximately the same size, which is not the case for subgroup 2 proteins. Adapted from Behr & Hoch, 2005.

The Obstructor subgroup 2 genes *obst-F* to *obst-J* also share the general domain architecture of the *obstructor* family, but the spacing between the CBDs is not even (Behr & Hoch, 2005).
RNA in situ hybridization data revealed the expression of *obstructor* subgroup 1 genes in chitin-secreting tissues such as the tracheal system, the epidermis and the gut during late embryonic stages starting shortly before first secretion of chitin occurs. This hints at a function of the Obstructor family in the packaging of chitin-fibrils where new cuticle material is established.
Phylogenetic analysis showed the presence of *obstructor* orthologs in invertebrate species including insects and the nematode *C. elegans*, but not in vertebrates. The results indicate a strong evolutionary conservation of the Obstructor group of chitin-binding proteins in invertebrates (Behr & Hoch, 2005).

Obstructor-A is necessary for apical extracellular matrix integrity in the trachea

Out of the *obstructor* gene family, the *obstructor-A* (*obst-A*) gene has been further investigated in the past years. *Obst-A* encodes two transcripts resulting in the same protein with a size of 27 kDa (Petkau et al., 2012). For the functional analysis of *obst-A*, two deletion lines ($obst\text{-}A^{d02}$, $obst\text{-}A^{d03}$) were generated by P-element jump out mutagenesis. Both were proven to be null mutant lines completely lacking *obst-A* transcription (Petkau et al., 2012).
It was shown that in the trachea Obst-A is co-localized with chitin and that the proper distribution of Obst-A is chitin-dependent. During the embryonic stages 14 to 16, chitin is strongly present within the tracheal tube lumina and afterwards degraded in stage 17 to enable gas filling of the trachea (Tonning et al., 2005; Moussian et al., 2006a). Obst-A associates with chitin fibrils and its loss leads to premature degradation of the chitin-matrix (Petkau et al., 2012). In *obst-A* mutants, accumulation of chitin in the tubes occurs normally until stage 15 suggesting that Obst-A does not have any impact on synthesis and secretion of

chitin. The main phenotype of *obst-A* mutants becomes visible from stage 16 onwards. As during stage 16 the chitin-matrix hinders further size expansion of the tracheal tubes, *obst-A* mutants show elongated tracheal tubes. Importantly, loss of *obst-A* also leads to irregular, premature degradation of the luminal chitin.

It was demonstrated in pulldown studies that the chitin deacetylase Serp, which is essential for the maintenance of chitin texture in the trachea, directly interacts with Obst-A (Petkau et al., 2012). Loss of Obst-A leads to a strong reduction of luminal Serp, but does not interfere with initial Serp secretion proving that Obst-A is needed for the correct localization of Serp. Furthermore, Obst-A interacts with the chitin-protecting protein Knk and is also necessary for its proper localization and persistence, but not for its initial secretion. Thus, Obst-A forms a core complex with Serp and Knk, which associates with the chitin lamellae for extracellular matrix protection (Fig. 1.7).

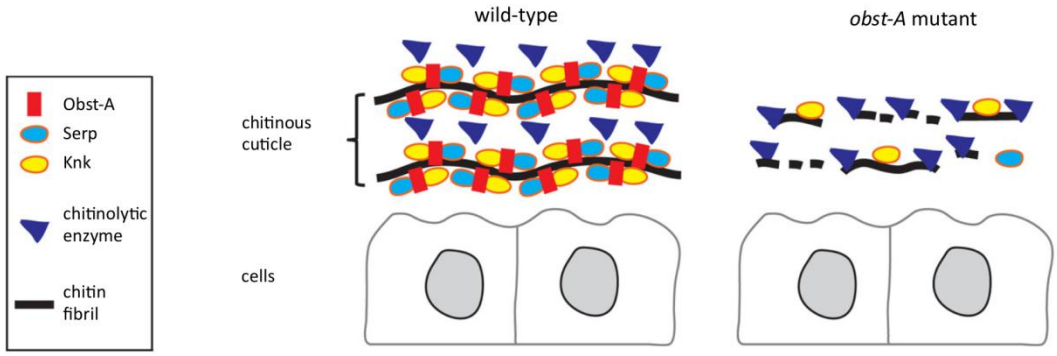

Fig. 1.7 - Obst-A builds a complex with Serp and Knk in the trachea for protection of chitin. The model illustrates the function of Obst-A in the tracheal system during late embryogenesis. There it builds a complex together with the chitin deacetylase Serp and the chitin protecting protein Knk along the chitin fibrils, which hinders the premature degradation of chitin by chitinolytic enzymes. In the *obst-A* mutant this complex cannot assemble, allowing premature chitin degradation. Adapted from Petkau et al., 2012.

The Obst-A mediated "core complex" is needed for the protection of the tracheal chitin fibrils against premature attack by chitinolytic enzymes (Petkau et al., 2012). Thereby, Obst-A preserves tracheal aECM structure and has an impact on tube size during late embryogenesis.

Obstructor-A is required for larval growth and molting

Obst-A null mutants suffer from a severe growth defect (Petkau et al., 2012) as they fail to increase their body size even though the passage of food through the gut is not affected, indicating a strong developmental delay. *Obst-A* mutants are lethargic in comparison to control larvae and loss of *obst-A* finally results in complete larval lethality (Fig. 1.8). *Obst-A* mutants already show partial embryonic lethality, but about 80-90% die during larval development. The main lethal phase is observed shortly after molting from first to second instar larval stage occurs in control larvae, but not in *obst-A* mutants, which are arrested at the molt (Petkau et al., 2012; chapter 3.3).

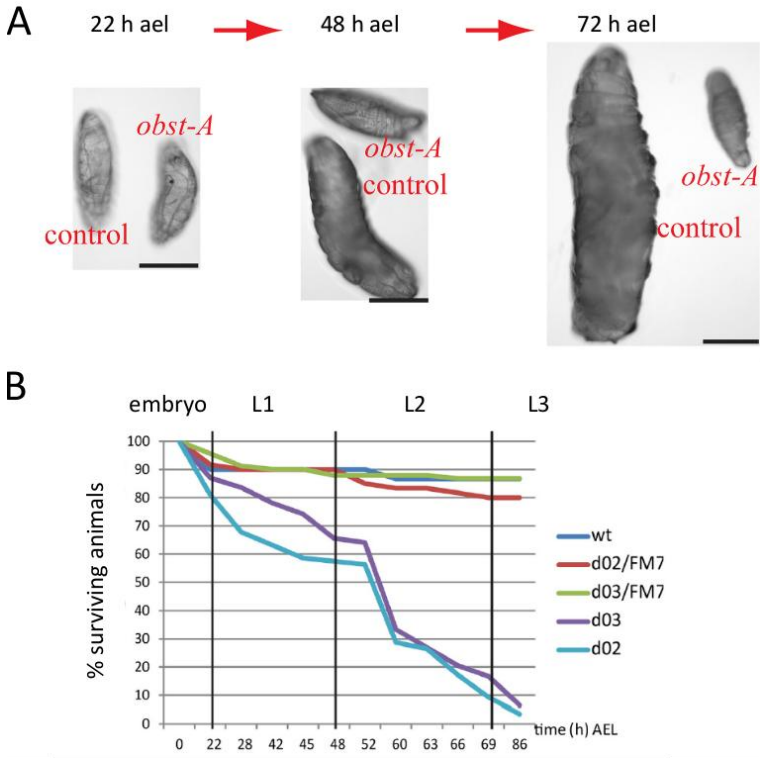

Fig. 1.8 - Growth defect and lethality profile of *obst-A* mutant larvae. A: Pictures show the size comparison of control and *obst-A* null mutant larvae 22 h, 48 h and 72 h after egg laying (ael), corresponding to first, second and third instar stage of the control larvae. It can be seen that *obst-A* mutants barely grow at all. B: Lethality profile of larvae with several genotypes. y-axis: surviving animals in %; upper x-axis: developmental stage; lower x-axis: time points corresponding to hours after egg laying. It can be seen that wild type (blue) as well as heterozygous *obst-A* mutants (d02/FM7, red; d03/FM7, green) survive well. In contrast both lines of hemizygous *obst-A* null mutants (*obst-A*^{d03} (d03), purple; *obst-A*^{d02} (d02), light blue) exhibit complete larval lethality. Note that *obst-A* null mutants are developmentally arrested in the first instar stage and that the most striking drop in mutant survival occurs shortly after control and heterozygous larvae undergo the transition to second instar stage. Adapted from Petkau et al., 2012.

Furthermore, *obst-A* mutant larvae revealed a severe epidermal cuticle integrity defect. When pricking wild type larvae laterally with a thin glass needle, they survive well with little or no bleeding. *Obst-A* mutants in contrast suffer from major injury after pricking as vital organs directly spill out resulting in immediate larval death. The molecular function of Obst-A in the epidermis, however, was not investigated in the study of Petkau et al., 2012, and is subject of my thesis. Cuticle preparations of *obst-A* mutant larvae showed molting defects in epidermis, trachea, head skeleton and spiracles (Petkau et al., 2012). Many larvae displayed double mouth hooks as the old first instar mouth hooks are not properly shed but the new second instar mouth hooks have already been fully developed.
Double mouth hooks and death at the transition between larval stages are characteristic for mutants affecting molting hormone signaling (Perrimon et al., 1985; Oro et al., 1990; Bender et al., 1997; Schubiger et al., 1998; Li & Bender, 2000; Bialecki et al., 2002; Oron et al., 2002; Gates et al., 2004; Gaziova et al., 2004; Ou et al., 2016). Altogether, this indicates that Obst-A may have a dual function, one in controlling cuticle formation in other tissues than the trachea and a second function in the hormonal regulation of molting. Both functions were investigated in this thesis.

1.6 - Hormonal control of molting

As molting is a complicated process that poses great risks for the animal, it has to be tightly regulated (Ewer, 2005). Molting in *Drosophila* is controlled by several hormonal pathways (Di Cara & King-Jones, 2013), which are discussed below.

1.6.1 - The molting hormone ecdysone regulates developmental transitions in *Drosophila*

Steroid hormones are small, lipophilic compounds that can pass through cell membranes and constitute important regulators of growth in many organisms, including humans. It is of great interest that both puberty in humans and metamorphosis in insects are regulated by peak production of steroid hormones and their binding to nuclear receptors. Even though the two processes are so diverse, both represent the conversion from a juvenile, immature to an adult, sexually mature organism (King-Jones & Thummel, 2005; Rewitz et al., 2010; Roa

et al., 2010; Yamanaka et al., 2013; Niwa & Niwa, 2016). Steroid hormones are involved in the hormonal control of molting in all insects as well as crustaceans indicating evolutionary conserved mechanisms (Horn et al., 1966). In insects the steroid hormone regulating growth and inducing developmental transitions is 20-hydroxyecdysone (20E) (Thummel, 1996; Kozlova & Thummel, 2000; King-Jones & Thummel, 2005). 20E is produced in peripheral tissues from ecdysone (E), which is synthesized within the endocrine prothoracic gland. Frequently, in the literature both ecdysteroid hormones E and 20E are summarized under the general term "ecdysone" (Yamanaka et al., 2013). The ecdysteroid titer fluctuates during *Drosophila* development, rising before and falling after each developmental transition (Kozlova & Thummel, 2000; Fig. 1.9).

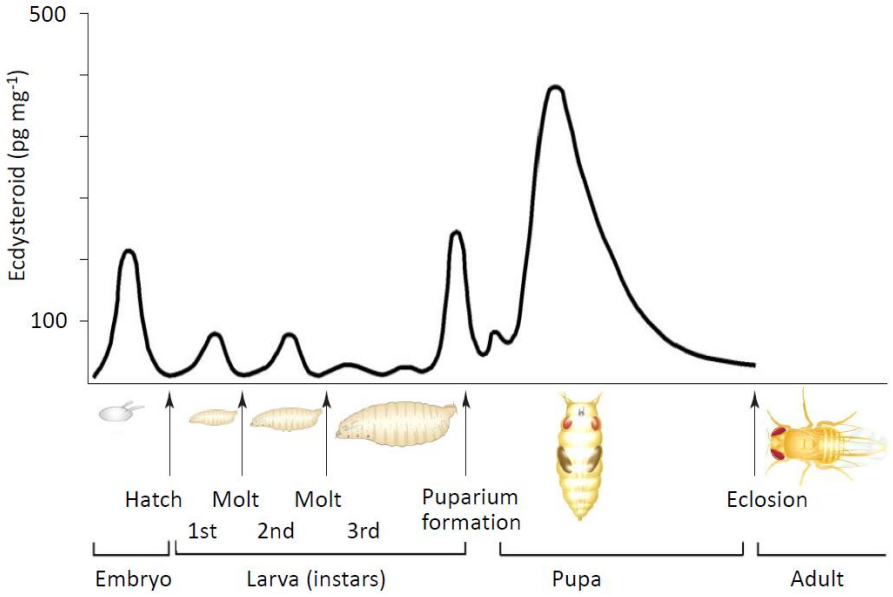

Fig. 1.9 - Ecdysteroid peak production precedes developmental transitions. Measurement of ecdysteroid levels (mostly ecdysone and 20-hydroxyecdysone) during *Drosophila* development. Note that distinct peaks in ecdysteroid production can be detected prior to each developmental transition: embryonic hatching, molt from first to second and from second to third instar larval stage, puparium formation and metamorphosis. The minor ecdysteroid peaks during the third instar larval stage correspond to the attainment of critical weight for pupariation and the onset of wandering behavior (Mirth & Riddiford, 2007). Modified from Kozlova & Thummel, 2000.

The first peak in ecdysteroid production can be seen during embryonic development preceding hatching into a first instar larva. Since rise of ecdysone levels are needed to induce the molecular processes leading to the larval molts, further ecdysteroid peaks are detectable prior to the molts from L1 to L2 and L2 to L3, respectively (Kozlova & Thummel, 2000).

During the L3 stage two minor ecdysteroid peaks can be detected, marking the achievement of the critical weight that is mandatory for metamorphosis and the beginning of wandering behavior (Mirth & Riddiford, 2007). The next peak is seen at the onset of puparium formation. The strongest rise in ecdysteroid level occurs upon metamorphosis when ecdysteroids are required for the differentiation of nascent adult structures (Kozlova & Thummel, 2000). Ecdysteroid levels drop again when the prothoracic gland is no longer necessary for pupal development and is degraded via apoptosis (Locke & Huie, 1979; Dai & Gilbert, 1991). It is still not completely understood how the timing, duration and amplitude of the different ecdysone pulses is regulated (Ou et al., 2016).

In addition to their role governing developmental transitions during embryonic, larval and pupal development, in adult flies ecdysteroids are involved in germline development, the regulation of the circadian clock, stress resistance, neuron activity and longevity (Uryu et al., 2015). The main source of ecdysone in adult flies is the ovary and ecdysone was shown to control oocyte lipid accumulation and whole-animal lipid metabolism to support oogenesis (Sieber & Spradling, 2015).

Ring gland structure and function

The *Drosophila* ring gland (RG) is an endocrine gland that is located between the two brain hemispheres. As it surrounds the aortic blood vessel, it was accordingly named "ring" gland. The RG consists of three distinct parts: The corpora cardiaca (CC), the prothoracic gland (PG) and the corpus allatum (CA) (King et al., 1966; Siegmund & Korge, 2001; Hartenstein, 2006; Sánchez-Higueras et al., 2014) (Fig. 1.10).

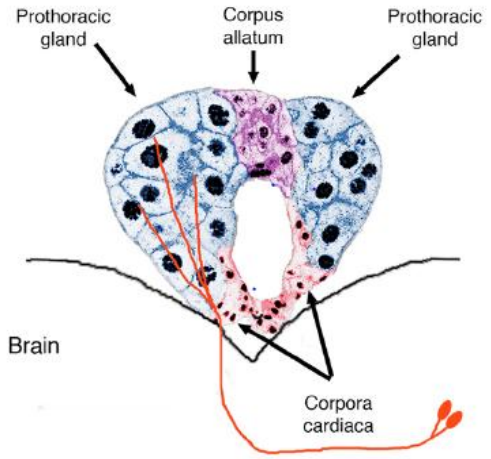

Fig. 1.10 - Structure of the *Drosophila* ring gland. The ring gland is a tripartite endocrine organ consisting of the corpora cardiaca (CC), the corpus allatum (CA) and the prothoracic gland (PG). The aorta passes through the central cavity of the ring gland. The CA lies in between the two lobes of the PG and produces the Juvenile Hormone, whereas the PG is the site of ecdysone production. The PTTH-producing neurons that innervate the PG and thereby regulate ecdysteroidogenesis are shown in red. Adapted from Talamillo et al., 2008.

Only in higher Diptera such as *Drosophila*, the three parts of the ring gland are fused together, whereas in other insects the PG, CC and CA form distinct structures at different locations throughout the insect body (Ou et al., 2016).

The CC have a function not related to molting, but rather linked to metabolic control and therefore are only briefly mentioned here. The CC are a binary structure that are directly attached to the brain via nerves and secrete the Adipokinetic Hormone (AKH) as well as glycemic factors and heart-accelerating factors (Siegmund & Korge, 2001; Hartenstein, 2006). The function of the CA is the production of the Juvenile Hormone (JH) (Wigglesworth, 1947). The PG is the site of ecdysteroid production (Chino et al., 1974; King et al., 1974) and consists of two lobes and can be easily distinguished from the CA and the CC because of the larger cell size. In both the CA and the PG the hormones are produced in the smooth ER (King et al., 1966). The function of the hormones JH from the CA and ecdysone from the PG is discussed in detail later in this chapter.

Ecdysone synthesis by the Halloween genes

Ecdysone and its derivatives are the main molting hormones of all arthropods (Gilbert et al., 2002). The substrate for ecdysteroid synthesis is dietary cholesterol that is taken up by the prothoracic gland. The first step is the conversion of cholesterol to 7-dehydrocholesterol by the Neverland dehydrogenase (nvd) in the ER of the PG cells (Gilbert et al., 2002; Yoshiyama et al., 2006). The next steps are catalyzed by the so called "Halloween" enzymes, a group of cytochrome P450 monooxygenases (Warren et al., 2002; Gilbert, 2004; Rewitz et al., 2006). The "*Halloween*" genes were identified in a screen for factors controlling embryonic morphogenesis by Nüsslein-Volhard, Wieschaus and coworkers and got their name because of the bloated pumpkin-like or ghost-like appearance of the mutant embryos, which is caused by impaired cuticle and head skeleton differentiation (Nüsslein-Volhard et al., 1984; Jürgens et al., 1984; Wieschaus et al., 1984). The first reactions catalyzed by members of the "Halloween" group, which result in the biosynthesis of β-ketodiol from 7-dehydro-cholesterol, are not yet completely understood (Saito et al., 2016). Therefore, these reactions are called the "Black Box", most probably including the rate limiting step of ecdysteroidogenesis (Gilbert et al., 2002; Saito et al., 2016). The known "Black Box" enzymes are Spookier (spok) (Namiki et al., 2005; Ono et al., 2006), Shroud (sro) (Niwa et al., 2010)

and the less well described Cyp6t3 (Ou et al., 2011). Ecdysteroidogenesis continues by the conversion of β-5 ketodiol to β-ketotriol by Phantom (phm) (Niwa et al., 2004; Warren et al., 2004). Next, 2-desoxyecdysone is generated by the disembodied (dib) enzyme. The final step of ecdysone biosynthesis is catalyzed by Shadow (sad) (Chávez et al., 2000; Warren et al., 2002). Ecdysone is released from the PG via the hemolymph into peripheral tissues where it is quickly converted into the active 20-hydroxyecdysone (20E) (King-Jones & Thummel, 2005; Rewitz et al., 2013). This reaction is mediated by the Shade hydroxylase (shd) (King et al., 1974; Petryk et al., 2003). 20E, which is 100 times more potent than unhydroxylated ecdysone (Riddiford, 1980), is able to bind to the ecdysone receptor complex, which consists of the ecdysone receptor (EcR) and Ultraspiracle (Usp). Upon binding of 20E the receptor complex initiates the transcription of ecdysone target genes (Fig. 1.11).

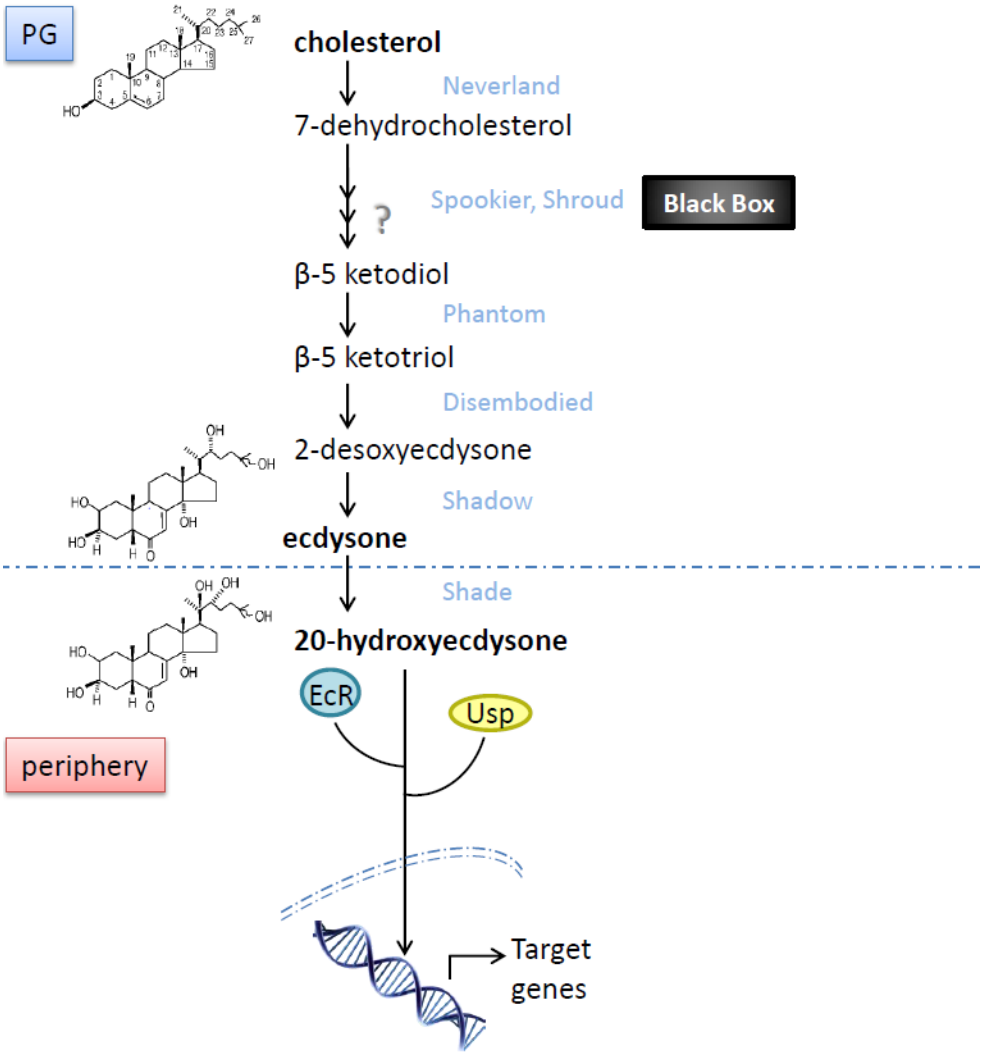

Fig. 1.11

Fig. 1.11 - Simplified scheme of the ecdysone pathway in larvae. In the prothoracic gland dietary cholesterol is converted to ecdysone in a multistep cascade by the Neverland dehydrogenase and the so called "Halloween" enzymes. Ecdysone is released into the periphery where it is hydroxylated into the active molting hormone 20-hydroxyecdysone (20E), which binds to the Ecdysone receptor complex consisting of the Ecdysone receptor (EcR) and Ultraspiracle (Usp). Once 20E is bound the receptor complex can activate the transcription of target genes. The biosynthetic enzymes are depicted in light blue, biosynthesis intermediates are listed in black. The structural formulas of the sterols printed in bold are shown on the left (modified from Warren et al., 2002). Some reactions of ecdysone biosynthesis are not yet understood and called "Black Box" as indicated by the question mark.

Ecdysone receptor binding and initiation of signaling

Nuclear receptors are transcription factors acting as key regulators of development and metabolic pathways in a wide range of organisms (King-Jones & Thummel, 2005; Nakagawa & Henrich, 2009). The insect ecdysone receptor (EcR) is an ortholog of the vertebrate farnesoid X receptor or liver X receptor, which play a role in lipid and bile acid sensing (Koelle et al., 1991; King-Jones & Thummel, 2005). Ultraspiracle (Usp), the partner of the EcR, is an ortholog of the vertebrate retinoid X receptor, which forms heterodimers e.g. with the thyroid hormone receptor and retinoic acid receptor (Oro et al., 1990; Dawson & Xia, 2012). Nuclear receptors dimerize and bind to specific genomic response elements to induce target gene transcription (Hall & Thummel, 1998; King-Jones & Thummel, 2005).

EcR heterodimerizes with Usp and, in case 20E is bound, associates with ecdysone specific DNA elements to regulate target gene expression. This was first discovered in the polytene chromosomes of the salivary gland where EcR/Usp binding causes loosening of the DNA structure, thereby forming certain "puffs" (Ashburner, 1971; Yao et al., 1992; Yao et al., 1993). The unliganded EcR-Usp dimer can suppress the transcriptional initiation of genes. This repression is released when 20E is bound during the subsequent ecdysone pulse (Schubiger & Truman, 2000).

There are different isoforms of the EcR, which show tissue-specific expression (Talbot et al., 1993; Schubiger et al., 1998). Different mutants lacking one or more *EcR* isoforms and *usp* mutants are either embryonic lethal or show arrest at molting or metamorphosis depending on the strength of the maternal component. Those that die upon molting frequently show double mouth hooks, which is often called the "ultraspiracle phenotype" (Perrimon et al., 1985; Oro et al., 1990; Hall & Thummel, 1998; Schubiger et al., 1998, Li & Bender, 2000;

Oron et al., 2002; Gaziova et al., 2004; Jones et al., 2010). Interestingly, *usp* mutants are still capable of forming the cuticle of the next stage, but fail to shed the old one. A possible explanation would be that EcR alone is sufficient to initiate the early molting events, while Usp is necessary to complete the last phase of the molt (Riddiford, 2007).

Upon 20E binding the EcR/Usp dimer initiates the transcription of a large number of target genes. Interestingly, many of the genes that are induced early are nuclear receptors such as E75, DHR3, DHR4 and ftz-f1 (Andres & Thummel, 1992; King-Jones & Thummel, 2005). E75 acts in a positive feedback loop elevating ecdysteroid titers (Bialecki et al., 2002), whereas DHR3 and DHR4 are transcriptional repressors of many genes upon metamorphosis (King-Jones & Thummel, 2005; Ou et al., 2011; Parvy et al., 2014). Acting together DHR3 and DHR4 control the transcription of β-Ftz-f1, which itself is a key regulator of the temporal control of ecdysone signaling. β-Ftz-f1 is the ortholog of the steroidogenic factor 1 (SF1) that is responsible for the maturation of steroid-producing organs in vertebrates (Parvy et al., 2005). The transient, temporaly highly controlled expression of β-Ftz-f1 is required for the proper execution of molting and metamorphosis (Broadus et al., 1999; Yamada et al., 2000; King-Jones & Thummel, 2005). Additionally, β-Ftz-f1 specifically induces the transcription of the Halloween genes *phm* and *dib* (Parvy et al., 2005).

Other very important genes that are directly induced by the liganded EcR/Usp receptor complex are *E74* and *broad*, which are necessary for the activation of other genes that play essential roles in initiating and executing developmental progressions (Thummel et al., 1990; Urness & Thummel, 1990; Karim et al., 1993; Fletcher & Thummel, 1995; Urness & Thummel, 1995; Crossgrove et al., 1996; Zhou & Riddiford, 2002).

Ecdysone target genes can be subdivided into two different classes. In the first step, a small subset of target genes is induced, the so called "early response genes" (such as the above-mentioned nuclear receptors, *E74* and *broad*), and in the second step a multitude of "secondary response genes" is induced. This second induction step is partly achieved by the early response genes out of which many act as transcription factors. In the end the secondary response genes mediate the stage- and tissue-specific biological reactions that lead to either molting or metamorphosis (Kozlova & Thummel, 2000; Thummel, 2002; Andres & Thummel, 2002).

The complexity of ecdysone signaling

In the past years many regulatory factors influencing ecdysone target gene induction and feedback loops between the different target genes have been identified (Yamanaka et al., 2013; Moeller et al., 2013; Parvy et al., 2014). The most important mechanisms will be briefly described.

Ecdysone pulses have to be controlled in intensity and duration. As long as ecdysteroid titers are low, ecdysone stimulates further ecdysteroid production and the EcR induces its own expression (Koelle et al., 1991; Rewitz et al., 2013; Moeller et al., 2013). When peak levels are reached, a second feedback mechanism comes into action reducing further ecdysteroid production (Rewitz et al., 2013). The two feedback mechanisms, which have antagonizing functions, are regulated by switching of isoform expression of the early response gene *broad* (Moeller et al., 2013). Concerning the duration of the pulse, steroid degradation is important to lower the concentration once peak levels are reached. The steroid degradation enzyme Cyp18a1 is induced in peripheral tissues by ecdysteroid pulses converting 20E into inactive ecdysonoic acid (Rewitz et al., 2013).

An additional level of complexity is added by the many cofactors of the EcR/Usp receptor complex (Nakagawa & Henrich, 2009). Many proteins associate with the receptor complex to either block or stimulate ecdysone signaling. Cofactors include the stimulatory factor Taiman (Bai et al., 2000) and Bonus, which represses β-*Ftz-f1* transcription (Beckstead et al., 2001). The cofactor rigor mortis shuttles between the nucleus and the cytoplasm and molecularly interacts with EcR, Usp, DHR3 and β-Ftz-f1. Loss of *rigor mortis* leads to a typical molting defect as mutant larvae die with double mouth hooks, a result of incomplete cuticle shedding (Gates et al., 2004). Co-inhibitors of the ecdysone receptor complex include SMRTR (Tsai et al., 1999) and the highly conserved Alien protein (Dressel et al., 1999; Papaioannou et al., 2007), each blocking the transcription of different regulatory factors. As loss of each of the described cofactors leads to a unique phenotype, it is very likely that they specifically control the induction or repression of a small subset of genes important for ecdysone production and signaling and that many of similarly acting regulators have not been identified yet (Yamanaka et al., 2013).

The transcription factors Ventral veins lacking (Vvl) and Knirps (Kni) are necessary for the proper expression of all ecdysone biosynthesis genes, whereas Molting defective (Mld)

specifically induces expression of the most upstream biosynthesis genes (Neubueser et al., 2005; Danielsen et al., 2014). The transcription factor Ouija board (Ouib) acts even more specifically by only inducing the expression of *spookier* (Komura-Kawa et al., 2015). The transcription factor Without children (Woc) is necessary for ecdysone production in late third instar larvae, but its exact mode of action is still debated (Wismar et al., 2000; Warren et al., 2001; Jin et al., 2005).

A very potent and the most well known regulator of ecdysone production is the prothoracicotropic hormone (PTTH), which will be discussed below.

PTTH as major regulator of ecdysone biosynthesis

The prothoracicotropic hormone (PTTH) is a small neuropeptide produced in a lateral pair of brain neurons in each hemisphere. The PTTH neurons directly innervate the PG in *Drosophila* (Kawamaki et al., 1990; Siegmund & Korge, 2001; McBrayer et al., 2007) (Fig. 1.10). PTTH binds to the Receptor Tyrosine Kinase Torso located in the membrane of the PG cells, thereby activating the Ras GTPase. This in turn leads to phosphorylation of Raf initiating a MAPK cascade, leading to stimulation of ecdysteroid production (Caldwell et al., 2005) inter alia by upregulation of certain Halloween genes including *phm* and *dib* (Rewitz et al., 2009).

PTTH is the key stimulatory factor in the PG increasing ecdysone biosynthesis (Kawamaki et al., 1990; Gilbert et al., 2002; Yamanaka et al., 2013) However, the exact molecular targets of PTTH action have not been identified yet (Ou et al., 2016). One described direct target of PTTH action is the DHR4 nuclear receptor. DHR4 downregulates ecdysteroidogenesis and was shown to be negatively regulated by PTTH signaling (Ou et al., 2011). In addition to its function as main stimulator of ecdysteroidogenesis, PTTH is also implicated in other signaling pathways such as endosomal trafficking and regulation of the composition of the cytoskeleton (Rewitz et al., 2009; Young et al., 2012).

Not only the targets of PTTH action, but also the factors influencing PTTH production and release are incompletely understood (Young et al., 2012). There is evidence that PTTH is under control of the circadian clock (Mirth et al., 2005; McBrayer et al., 2007; Ou et al., 2011; Schiesari et al., 2011; Yamanaka et al., 2013). PTTH expression is downregulated upon damage of imaginal discs (Halme et al., 2010; Jaszczak et al., 2016). Additionally, the metabolic status of the larvae as well as their body weight influences PTTH levels (Mirth et

al., 2005; Young et al., 2012). Starvation was shown to reduce PTTH levels (Young et al., 2012). PTTH secretion is increased once third instar larvae reached the critical weight that is required for undergoing pupariation, thereby resulting in augmented ecdysteroid synthesis that initiates wandering behavior, leads to a stop of growth and finally enables metamorphosis (Mirth et al., 2005).

The two other hormones responsible for the regulation of developmental transitions - 20-hydroxyecdysone and the Juvenile Hormone - also influence PTTH signaling. 20E was shown to increase PTTH levels via an indirect feedback mechanism, whereas JH might render the PG insensitive to PTTH action (Gu et al., 1997; Young et al., 2012; Yamanaka et al., 2013).

Loss of PTTH surprisingly does not lead to larval lethality, but delays the onset of metamorphosis resulting in larger pupae and eclosing adults due to the prolonged feeding period (McBrayer et al., 2007). This makes PTTH a regulator of developmental timing and final body size.

Other factors and pathways regulating ecdysone biosynthesis

For a long time it was presumed that PTTH is the only regulating factor that stimulates ecdysteroid biosynthesis in the PG. However, in the recent years this picture has gotten more complex since several other factors have been found that directly act on the PG to either elevate or reduce ecdysteroidogenesis (Yamanaka et al., 2013). Those include yet uncharacterized factors signaling the nutritional and metabolic state of the organism (Layalle et al., 2008; Yamanaka et al., 2013; Sarraf-Zadeh et al., 2013). However, the exact nature of these factors and the mechanisms how they act positively or negatively on ecdysone production are poorly understood. This makes the PG the "decision making center" that integrates various signals and environmental cues and then assesses whether to progress to the next developmental stage or not (Andersen et al., 2013; Yamanaka et al., 2013).

Other pathways that influence ecdysone production are the TOR pathway (Layalle et al., 2008; Montagne et al., 2010), Insulin signaling (Mirth et al., 2005; Colombani et al., 2005; Caldwell et al., 2005; Walkiewicz & Stern, 2009; Walsh & Smith, 2011; Koyama et al., 2014; Colombani et al., 2015), the TGFβ/Activin pathway (Gibbens et al., 2011); β3-octopamine receptor signaling (Ohhara et al., 2014), serotonergic signaling (Shimada-Niwa & Niwa, 2014) as well as Nitric Oxide signaling (Cacéres et al., 2011; Johnston et al., 2011).

It is of note that the PTTH-MAPK pathway and the TOR pathway share common targets (Shahbazian et al., 2006), which is indicative of crosstalk between the two pathways. Furthermore, the PTTH-MAPK pathway and Insulin signaling interact with one another (Kim et al., 2004). This makes the analysis of the influence of those three pathways on ecdysteroidogenesis very challenging.
All of this shows that the hormonal control of molting is extremely difficult and becomes even more complex as research progresses. On the whole, the regulation of the molting hormone pathways still remains incompletely understood (Ou et al., 2016).

1.6.2 - The Juvenile Hormone signals the maintenance of larval development

The Juvenile Hormone (JH) is produced by the corpus allatum of the PG (Wigglesworth, 1947). JH is responsible for initiating a larval molt instead of inducing pupal development (Schneiderman & Gilbert, 1964; Gilbert et al., 2000). It prevents the ecdysone-peak induced changes in cuticle composition upon puparium formation, thereby maintaining the "juvenile" status quo (Riddiford, 1980; Wolfgang & Riddiford, 1986). In the presence of JH a larval cuticle is formed again after molting, whereas in the absence of JH formation of a pupal cuticle occurs.
Even though JH was discovered in 1934 in Wigglesworth, the molecular mechanism of JH signaling still remains unclear and a JH receptor has long been searched for (King-Jones & Thummel, 2005). It was demonstrated that JH can bind to Usp *in vivo* (Jones et al., 2001), which enables crosstalk to ecdysone signaling. It is still not clear if the binding of JH to Usp has a biological function (Jindra et al., 2015). The partially redundant receptors Met (Methoprene tolerant) and Gce (Germ cell-expressed) most probably play the biggest role in transmitting JH-mediated signals and inducing JH-mediated transcription and have just recently been discovered (Jindra et al., 2015). Loss of both Met and Gce leads to pupal lethality in *Drosophila*, whereas loss of one of the components only has no obvious phenotype (Abdou et al., 2011). Interestingly, both Met and Gce heterodimerize with the EcR-cofactor Taiman (Zhang et al., 2011b; Jindra et al., 2015; Jindra, personal communication), indicating interplay between the ecdysone and the JH signaling pathway.

A different evidence of interaction between ecdysone and JH comes from a microarray study, which showed that some genes are upregulated only if 20E and JH are present at the same time, whereas some JH-induced genes can be blocked by 20E (Beckstead et al., 2007).

1.6.3 - Eclosion hormone and ecdysis triggering hormone initiate the molting sequence

The peptide hormones EH (eclosion hormone) and ETH (ecdysis triggering hormone) are crucial for the correct molting performance (Hesterlee & Morton, 1996; Park et al., 2002).
When molting is initiated, ETH stimulates the behavioral sequence that triggers shedding of the cuticle (Park et al., 2002; Roller et al., 2010). It was recently reported that EH is essential for the stimulation of pre-ecdysis behavior (Krüger et al., 2015).
ETH is produced by the Inka cells, which are small peritracheal cells that release peptide hormones when ecdysis occcurs. Inka cells are present in all insect classes (Zitnan et al., 1999; Zitnan et al., 2003). ETH is induced during ecdysteroid peaks and secreted from the Inka cells as soon as ecdysteroid peaks, which at this time have already initiated the first steps of molting, drop down again (Zitnan et al., 1999). ETH release signals the CNS to produce the Eclosion Hormone (EH), the Crustacean Cardioactive Peptide (CCAP) and Bursicon (Krüger et al., 2015), which all play a role in molting. EH is produced by two pair of brain neurons and was shown to increase further ETH synthesis and to regulate the ecdysis response of the CNS (Hesterlee & Morton, 1996; Krüger et al., 2015). Furthermore, EH and ETH coordinate the air-filling of the tracheal system after the molt (Clark et al., 2004).

1.7 - Aim of the study

Even though the synthesis of chitin by the epidermal cells is well described (Merzendorfer & Zimoch, 2003; Merzendorfer, 2006), not very much is known about the mechanisms by which newly secreted chitin fibrils are organized into a stable, differentiated lamellar matrix within the epidermal cuticle (Moussian, 2010).
The main goal of my study was to identify and analyze factors that are implicated in the processes of epidermal cuticle assembly and organization in *Drosophila melanogaster*.

During my master thesis I performed a RNAi-mediated knockdown screen to analyze the function of Chitinases and the related Imaginal Disc Growth Factors in the epidermal cuticle. The strongest phenotype was observed upon knockdown of *Chitinase 2* (*Cht2*) in cuticle-forming tissues resulting in complete larval and pupal lethality, severe impairment of epidermal cuticle integrity as well as a thinned epidermal cuticle. For this reason, the function of Cht2 in epidermal cuticle formation was further investigated in this PhD thesis. The aim of my analysis was to characterize how Cht2 influences epidermal cuticle integrity. In addition, the generation of a peptide antibody recognizing Cht2 was intended to decipher its expression pattern throughout embryonic and larval development.

The major part of this PhD thesis constituted the analysis of the chitin-binding protein Obstructor-A (Obst-A) in epidermal cuticle assembly. As it was previously known that Obst-A is a cuticular protein essential for tracheal cuticle function and that its loss causes epidermal integrity defects (Behr & Hoch, 2005; Petkau et al., 2012), I wanted to study its function in epidermal cuticle assembly in detail. Therefore, the defects in epidermal cuticle structure in *obst-A* mutants were analyzed in order to address the function of *obst-A* in the epidermal cuticle. The objective was to identify potential genetic interaction partners and to reveal the molecular mechanism by which Obst-A regulates the assembly and organization of the cuticular chitin-matrix.

Moreover, I wanted to find out the reasons for severe growth defect of the *obst-A* mutants and their inability to molt to second instar stage, which cannot be entirely explained only by the function of Obst-A in chitin-matrix organization. Strikingly, the mutants' growth and molting defects strongly resemble the phenotype caused by deficiency of the molting hormone ecdysone or defective ecdysone signaling (Perrimon et al., 1985; Oro et al., 1992; Bender et al., 1997; Schubiger et al., 1998; Hall & Thummel, 1998; Freeman et al., 1999; Li & Bender, 2000; Yamada et al., 2000; Bialecki et al., 2002; Oron et al., 2002; Gates et al., 2004; Gaziova et al., 2004; Ou et al., 2016). Thus, the question asked was if and how the small chitin-binding protein Obst-A can influence ecdysone signaling, which is one of the major hormone pathways in *Drosophila* and regulates larval molts, pupariation and metamorphosis. To find out more about the potential involvement of Obst-A in the hormonal control of molting, the expression of ecdysone biosynthesis enzymes and the induction of ecdysone signaling was investigated in *obst-A* mutants.

2 - Materials and Methods

2.1 - Materials

Devices, disposables and glassware

Equipment	Manufacturer
1.5 ml/ 2 ml/ 15 ml/ 50 ml tubes	Sarstedt, Nümbrecht, D
Agarose gel chambers	Peqlab, Erlangen, D
Agarose gel documentation Alpha Digi Doc	Biozym, Hessisch Oldendorf, D
Autoclave H+P Dampfsterilisator EP-2	H+P Labortechnik, Oberschleißheim, D
Bacterial shaker Innova 44	New Brunswick Scientific (Eppendorf), Hamburg, D
Balance KERN ew 4200-2NM	Kern & Sohn, Balingen, D
Balance BL 150 S	Sartorius, Göttingen, D
BEEM Embedding Mold	Ted Pella, Redding, USA
Binocular Zeiss Stemi 2000	Carl Zeiss, Jena, D
Centrifuge Allegra X-15R	Beckman Coulter, Krefeld, D
Centrifuges Eppendorf 5415 R; 5424 R	Eppendorf, Hamburg, D
Cover slips 24x40 mm; 24x60 mm	Menzel, Braunschweig, D
Developer machine Curix 60	AGFA, Bonn, D
Glass beads	Roth, Karlsruhe, D
Glassware (Erlenmeyer flasks, beakers)	VWR, Darmstadt, D
Heating plate	Leica, Solms, D
HPTLC silica gel plate	Merck Millipore, Darmstadt, D
Homogenizer Precellys	Peqlab, Erlangen, D
Incubators (18 °C, 25 °C)	Rubarth Apparate GmbH, Laatzen, D
Incubators (29 °C, 37 °C)	Memmert, Schwabach, D
LSM 710 Confocal microscope	Carl Zeiss, Jena, D
LSM 780 Confocal microscope	Carl Zeiss, Jena, D

Microscope slides	VWR, Darmstadt, D
Olympus AX70 light microscope	Olympus, Hamburg, D
Olympus SZX 12 fluorescent binocular	Olympus, Hamburg, D
Parafilm	Pechiney Plastic Packaging, Chicago, USA
PCR machine C1000 Thermal Cycler	Bio-Rad, Munich, D
PCR machine PTC-200 Peltier Thermal Cycler	MJ Research, St. Bruno, CA
PCR stripes	Sarstedt, Nümbrecht, D
Petri dishes	VWR, Darmstadt, D
pH-Meter FiveEasy FE20	Mettler-Toledo, Columbus, USA
Photometer Nano Drop 2000	Peqlab, Erlangen, D
Photometer	Bio-Rad, Munich, D
Pipettes	Eppendorf, Hamburg, D Starlab, Hamburg, D
PVDF membrane	Merck Millipore, Darmstadt, D
qRT-PCR Machine CFX96	Bio-Rad, Munich, D
qRT-PCR plastic plates 96 well	Bio-Rad, Munich, D
qRT-PCR plate plastic cover film	Bio-Rad, Munich, D
Screw cap glass tubes	Pyrex, Darmstadt, D
Shaking platform TL 10	Edmund Bühler, Tübingen, D
Speed-Vac SPD111 Savant	Thermo Fisher Scientific, Waltham, USA
Superfrost glass slides	Thermo Fisher Scientific, Waltham, USA
Thermomixer	Eppendorf, Hamburg, D
Turning wheel Rotator SB3	Stuart, Staffordshire, UK
Ultramicrotome Ultracut E	Reichert-Jung (Leica), Solms, D
Voltage Source Power Pac	Bio-Rad, Munich, D
Vortex Genie 2	Scientific Industries, New York, USA
Water bath SW22	Julabo, Seelbach, D
Western Blot Equipment	Bio-Rad, Munich, D
X-Ray Film Fuji Medical Super RX	Fujifilm, Tokio, Japan

Chemicals

Standard chemicals were purchased from one of the following companies:

Roche, Mannheim, D

Calbiochem, Darmstadt, D

Merck, Darmstadt, D

Applichem, Darmstadt, D

Sigma-Aldrich, Taufkirchen, D

Macherey-Nagel, Düren, D

VWR, Darmstadt, D

Gibco-Invitrogen, Karlsruhe, D

Roth, Karlsruhe, D

Non-standard chemicals are listed in the table below.

Chemical	**Manufacturer**
2-log DNA ladder	New England Biolabs, Ipswich, USA
20-hydroxyecdysone	Sigma-Aldrich, Taufkirchen, D; Cayman Chemical, Hamburg, D
7-dehydrocholesterol	Sigma-Aldrich, Taufkirchen, D
cholesterol	Sigma-Aldrich, Taufkirchen, D
Alkaline Phosphatase	Roche, Basel, CH
ECL Western Blotting Substrate Pierce SuperSignal West	Thermo Fisher Scientific, Waltham, USA
ECL Western Blotting Substrate Pierce SuperSignal West Femto	Thermo Fisher Scientific, Waltham, USA
Donkey serum	Sigma-Aldrich, Taufkirchen, D
Fluoromount-G DAPI	SouthernBiotech, Birmingham, USA
Go-Taq Polymerase	Promega, Madison, USA
iQ SYBR Green Supermix	Bio-Rad, Munich, D
Oligonucleotides/Primers	Invitrogen, Karlsruhe, D IDT Technologies, Leuven, BE

Phusion Hot Start II Polymerase	Thermo Fisher Scientific, Waltham, USA
PCR Nucleotide Mix	Roche, Basel, CH
Precision Plus Protein All Blue Standard	Bio-Rad, Munich, D
Protease Inhibitor Cocktail Complete	Roche, Basel, CH
Restriction endonucleases	New England Biolabs, Ipswich, USA
SYBR Safe DNA stain	Invitrogen, Karlsruhe, D
T4 Ligase	Roche, Basel, CH
Trypsin	Sigma Aldrich, Taufkirchen, D
Vectashield H-1500	Vector laboratories, Burlingame, USA

Kits

Kit	**Manufacturer**
BCA Protein Assay Pierce	Thermo Fisher Scientific, Waltham, USA
JB-4 Plus Embedding Kit	Polysciences, Warrington, USA
NucleoBond AX100 Midiprep Plasmid Purification Kit	Macherey-Nagel, Düren, D
NucleoSpin Gel and PCR Clean-up	Macherey-Nagel, Düren, D
NucleoSpin RNA II Purification Kit	Macherey-Nagel, Düren, D
QuantiTect Reverse Transcription Kit	Qiagen, Hilden, D

Fly food and media

Apple juice agar plates

Apple juice	500 ml
Sugar	50 g
Agar	43.5 g
Nipagin	30 ml

For apple juice agar plates the agar was dissolved in 1.5 l distilled water and the mixture was autoclaved. Nipagin was added after the mixture had cooled down to 60°C. The agar was poured into small petri dishes and stored at 4°C.

Fly food

Yarn agar	130 g
Yeast	248 g
Cornmeal	1223 g
Sugar beet syrup	1.5 l
10 % nipagin	300 ml

Fly food was prepared by boiling yarn agar in 15 l water. Yeast and cornmeal were heated separately in 5 l water each. First, sugar beet syrup was added to the agar, afterwards cornmeal and yeast. Nipagin was added after cooling of the mixture.

LB-Agar

Agar	1.5 % (w/v)
NaCl	1 % (w/v)
Trypton	1 % (w/v)
Yeast-Extract	0.5 % (w/v)

- add 1 l ddH_2O; pH 7.4

The mixture was autoclaved. If necessary antibiotics were added after cooling of the mixture to 60°C and Agar plates were poured in petri dishes.

LB-Medium

NaCl	1 % (w/v)
Trypton	1 % (w/v)
Yeast-Extract	0.5 % (w/v)

- add 1 l ddH_2O; pH 7.4

The medium was autoclaved. As for LB-Agar, if needed antibiotics were added to the cooled medium.

Used antibiotics for LB-Agar and LB-Medium:

Ampicillin - Stock: 50 mg/ml (frozen at -20°C)

Final concentration in selection media: 50 µg/ml

Chloramphenicol - Stock 50 mg/ml (frozen at -20 °C)

Final concentration in selection media: 25 µg/ml

Bacteria

Bacterial strain used for plasmid amplification: *E. coli* DH5α

Bacterial Strain	**Genotype**	**Source**
E. coli DH5α	F-endA1 deoR (φ80lacZΔM15) recA1 gyrA (Nal_r) thi-1 hsdR17 (r_K-, m_K +) supE44 relA1 Δ(lacZYA-argF) U169	Stratagene, La Jolla, USA

Buffers and Solutions

If not noted otherwise, all buffers and solutions were made with double distilled water (ddH_2O) and were stored at room temperature.

For immunostainings:

1x PBS:

NaCl	137 mM
KCl	2.7 mM
$Na_2HPO_4 \bullet 2\ H_2O$	10 mM
KH_2PO_4	2 mM

- pH 7.4

1x PBT:

1x PBS + 0,2% Triton X-100

Sodium citrate buffer:

Sodium citrate	10 mM

- pH 6.0

Trypsin buffer:

Tris	50 mM
Trypsin	0.001 % (w/v)

- pH 7.8

Blocking Solution:

10 % Donkey Serum (v/v) in PBS (for sections) or PBT (for other stainings)

Wheat Germ Agglutinin (WGA):

5 mg dissolved in 1 ml PBS, used 1:250 for stainings

For Western Blot:

RIPA Lysis Buffer:

Na_2HPO_4	10 mM
NaH_2PO_4	10 mM
SDS	0.1 %
Sodium fluoride	40 mM
EDTA	2 mM
Triton X-100	1 %
Sodium desoxycholate	0.1 %
Protease Inhibitor	1x

- pH 7.2; stored at 4 °C

5x Laemmli Buffer:

Tris-HCl	100 mM
SDS	3 % (w/v)
Glycerol	10 % (v/v)
Bromophenol Blue	0.01 % (w/v)
β-Mercapto ethanol	5 % (v/v)

- pH 6.8

10x SDS Running Buffer:

Tris	250 mM
Glycine	192 mM
SDS	1 % (w/v)

10x Transfer Buffer:

Tris	250 mM
Glycine	1.5 M

1x Transfer Buffer:

Transfer Buffer 10x	100 ml
Methanol	10 ml

- add 1 l ddH_2O

10x TBS: - pH 7.5

Tris	100 mM
NaCl	500 mM

1x TBST:

1x TBS + 0.2 % (v/v) Tween 20

Blocking solution:

1x TBST + 5 % (w/v) milk powder

For cloning:

TELT Buffer:

Tris	50 mM
EDTA	62.5 mM
LiCl	2.5 M
Triton X-100	4 % (v/v)

- pH 8.0; stored at -20 °C

6x DNA Loading dye:

Bromophenol Blue	0.25 % (v/v)
Xylencyanol	0.25 % (v/v)
Glycerol	30% (v/v)

1x TAE Buffer:

Tris	200 mM
EDTA	10 mM

- pH 8.0 was adjusted with acetic acid

Antibodies and dyes for immunofluorescent stainings

Antibody	Host Species	Dilution	Source/Reference
α-Spectrin (α-Spec)	mouse	1:10	3A9; DSHB, Iowa City, USA
Chitinase 2 (Cht2)	guinea pig	1:50 (sections) 1:100 (whole mount)	Pineda, Berlin, D; evaluated in this thesis
Chitinase 2 (Cht2)	rabbit	1:50 (sections) 1:100 (whole mount)	Pineda, Berlin, D; evaluated in this thesis
Chitin Binding Probe (CBP)-A488 conjugate		1:50	New England Biolabs, Ipswich, USA
Ecdysone Receptor (EcR)	mouse	1:10	10F1; DSHB, Iowa City, USA
Fasciclin II (FasII)	mouse	1:10	1D4; DSHB, Iowa City, USA
GFP	chicken	1:600	ab13970; Abcam, Cambridge, UK
Knickkopf (Knk)	rabbit	1:333	Moussian et al., 2006b
Obstructor-A (Obst-A)	rabbit	1:300	Petkau et al., 2012
Serpentine (Serp)	rabbit	1:175*	Luschnig et al., 2006
Vermiform (Verm)	rabbit	1:175*	Luschnig et al., 2006
Wheat Germ Agglutinin (WGA)-A633 conjugate		1:250	Molecular Probes, Carlsbad, USA

The antibodies marked with an asterisk require special antigen retrieval for JB-4 sections (see Methods chapter 2.2.3). Donkey secondary antibodies against the primary antibodies from different species (conjugated with either A488, Cy3, A647) were purchased from

Dianova, Hamburg, D, or JacksonImmuno, Baltimore, USA, and were all used in a 1:250 dilution.

qRT-PCR Primers and their efficiency

Gene	Forward primer sequence (5'→3')	Reverse primer sequence (5'→3')	Effi-ciency	Reference
rp49 (*ribosomal protein L32*) House-keeping gene	GCTAAGCTGTCGCACAAATG	GTTCGATCCGTAACCGATGT	100.0 %	Lechner et al., 2007
obstructor-A (*obst-A*)	GCAGTGCGACAAGTTCTACG	GAACTTGCGGTTGAGTGGAT	103.0 %	this thesis
serpentine (*serp*)	CAAGGCCACCTACTTCGTGT	ACTGCGATCTCGTGTCCTTT	99.6 %	this thesis
vermiform (*verm*)	GTGGCTGAAGTCGAAGAAGG	TTGGTCACGAAGAACACGTC	98.4 %	this thesis
knickkopf (*knk*)	GGGGCGGATACGTTTTTCTG	TCCAGAATGTTGGTTTTGCCAT	94.8 %	this thesis
E74A	TGTCCGCGTTTCATCAAGT	GTTCATGTCCGGCTTGTTCT	98.4 %	Gündner et al., 2014
neverland (nvd)	GGAAGCGTTGCTGACGAC-TGTG	TAAAGCCGTCCACTTCCTGCGA	97.0 %	McBrayer et al., 2007
spookier (spok)	TATCTCTTGGGCACACTCGCTG	GCCGAGCTAAATTTCTCCGCTT	109.7 %	McBrayer et al., 2007
shroud (sro)	AGCAGCTGAAGGTCGATAGC	GCGATTCGTGGCAGTAAAC	109.4 %	Moeller et al., 2013
phantom (phm)	GGATTTCTTTCGGCGCGATGTG	TGCCTCAGTATCGAAAAGCCGT	102.9 %	McBrayer et al., 2007
disembodied (dib)	TGCCCTCAATCCCTATCTGGTC	ACAGGGTCTTCACACCCATCTC	105.7 %	McBrayer et al., 2007
shadow (sad)	CCGCATTCAGCAGTCAGTGG	ACCTGCCGTGTACAAGGAGAG	112.3 %	McBrayer et al., 2007

shade (shd)	TCGCTTAATGCAGGGACTG	ACGCTCTGGGGTAAACTGC	96.9 %	this thesis
EcR common	CAGGTGAGGGCGTTGTAGTG	TGCGAAGAGCAAGAAGG	96.7 %	this thesis
ultraspiracle (usp)	CCTGTGCCAAGTGGTCAAC	GCAGAATCACCTGGTCGTC	100.0 %	this thesis
br-Z1	CCAGACCAACACCCACACAC	ACATTCGCTTCCTTCGTCCT	95.2 %	Moeller et al., 2013
br-Z4	CAAAGGCACACACACACACA	TCGGTCGGTTCTTCTCCTTC	96.8 %	Moeller et al., 2013
Ftz-f1	GAATGGCAGACGCAACTGT	TTCTGGTCGAGCACTTTGC	95.7 %	this thesis
ptth	GTTTGGACGAGATGGTGGGT	TTCGATGTACTGCGATCGGG	115.0 %	Fresán et al., 2015
ventral veins lacking (vvl)	CACTCCTGCATCCCTCAATAG	GGTGTATTCGGTGTGTGCTG	101.5 %	Danielsen et al., 2014
Knirps (kni)	GGAAGTGGAAAGAGATAGGGACA	TGTGAGTGTGTGTGTTGGTGGT	107.2 %	Danielsen et al., 2014
molting defective (mld)	CTGGAGGTGGAGATGAACGA	ATCGGCTGGAGTGAGGAAC	96.9 %	Danielsen et al., 2014
without children (woc)	GCAGTTATCCTTCTCGCACA	CTGCGGTGGATAGAATCGTA	96.9 %	this thesis
npc1a	TTGCAACCAAGCAGTTAGCA	CAATTTTGAAGGGCTCTGGA	98.6 %	Danielsen et al., 2014
Cyp18a	GAGATCGAGAAGGCCAAGG	GCGGAGAACAGATCGATGA	100.2 %	this thesis
eth	ATGGGATTTGGAAACGAG	AAGGAGCGTATTCGAGTTG	98.5 %	Gauthier & Hewes, 2006
eh	TAGTCAGCTCCCCAAACA	ATTGCAACTGCCACAAAG	117.3 %	Gauthier & Hewes, 2006
Rigor mortis (rig)	ACCAACTCCGTGCTGATGA	CGGCAGTAGGTGTTGGATG	99.5 %	this thesis

Primers for molecular cloning of pUAST-*obst-A GFP* vector

Primer name	**Sequence**
Obst-A repo forward 1step	GATACTGCAGTAGCGGCCGCCAATGAAGTTATTT
Obst-A repo reverse new	GATTGGTACCCGGTCCTTCTTGTCGTCC

Vectors

pMJ Green - Maxeiner et al., 2005

pUAST - Brand & Perrimon, 1993

pOT2 - Karunakaran et al., 2005

Software and Databases

Adobe Illustrator CS4	Adobe, San José, USA
Adobe Photoshop CS4	Adobe, San José, USA
BLAST	NCBI, USA
Cell'F	Olympus, Hamburg, D
CFX Manager	Bio-Rad, Munich, D
ConSite	Sandelin et al., 2004
Flybase	FlyBase *Drosophila* research community
GraphPad Prism	GraphPad, La Jolla, USA
ImageJ	Wayne Rasband, USA
Inkscape	Inkscape Community
JASPAR	Mathelier et al., 2014
OligoCalc	Northwestern University, USA
Microsoft Office	Microsoft, USA
Primer3	University of Massachusetts, USA
Serial Cloner	Serial Basics
ZEN 2010	Carl Zeiss, Jena, D
ZEN 2012	Carl Zeiss, Jena, D

Fly lines

	Fly line	**Genotype**	**Identifi-cation number**	**Source/Reference**
control	w- (w^{1118})	$\frac{+}{+/y}; \frac{+}{+}; \frac{+}{+}$	Bl-6236	Bloomington *Drosophila* Stock
	w- (Dahomey)	$\frac{+}{+/y}; \frac{+}{+}; \frac{+}{+}$		Linda Partridge lab; Broughton et al., 2005
GAL4 driver *Expression pattern noted in italic*	69B Gal4 *Whole ectoderm*	$\frac{+}{+/y}; \frac{+}{+}; \frac{69BG4}{69BG4}$	Bl-1774	Bloomington *Drosophila* Stock; Brand & Perrimon, 1993
	Aug21 Gal4 CyO actGFP *Corpus allatum*	$\frac{+}{+/y}; \frac{Aug21G4}{CyOactGFP}; \frac{+}{+}$		Christen Mirth lab; Siegmund & Korge, 2001
	phm Gal4-22 *Prothoracic gland*	$\frac{+}{+/y}; \frac{+}{+}; \frac{phmG4}{TM6b}$		Christen Mirth lab; Mirth et al., 2005
	P0206 Gal4 *Corpus allatum + Prothoracic gland (weak)*	$\frac{+}{+/y}; \frac{P0206G4}{P0206G4}; \frac{+}{+}$		Christen Mirth lab; Mirth et al., 2005
	Mai60 Gal4 *Prothoracic gland (strong) + salivary glands + imaginal discs*	$\frac{+}{+/y}; \frac{Mai60G4}{Mai60G4}; \frac{+}{+}$	Bl-30811	Walker et al., 2013
	Eth Gal4 *Inka cells*	$\frac{+}{+/y}; \frac{ethG4}{ethG4}; \frac{+}{+}$	Bl-51982	Diao et al., 2015

UAS responsive lines	UAS *Cht2* RNAi	$\frac{+}{+/y}; \frac{UAS\ Cht2}{UAS\ Cht2}; \frac{+}{+}$	CG2054 V-102249	Vienna *Drosophila* stock center (VDRC)
	UAS *Cht2*		CG2054	Anne Uv lab; Tonning et al., 2005
	UAS *obst-A* RNAi	$\frac{+}{+/y}; \frac{UAS\ obst-A\ RNAi}{UAS\ obst-A\ RNAi}; \frac{+}{+}$	CG17052 V-102591	Vienna *Drosophila* stock center (VDRC)
	UAS *obst-A*	$\frac{+}{+/y}; \frac{UAS\ obst-A}{UAS\ obst-A}; \frac{+}{+}$		Petkau et al., 2012
	UAS *verm* RNAi	$\frac{+}{+/y}; \frac{UAS\ verm\ RNAi}{UAS\ verm\ RNAi}; \frac{+}{+}$	CG8756 V-109518	Vienna *Drosophila* stock center (VDRC)
	UAS *serp* RNAi	$\frac{UAS\ serp\ RNAi}{UASserp\ RNAi/y}; \frac{+}{+}; \frac{+}{+}$	CG32209 V-15466	Vienna *Drosophila* stock center (VDRC)
	UAS *knk* RNAi	$\frac{+}{+/y}; \frac{UAS\ knk\ RNAi}{UAS\ knk\ RNAi}; \frac{+}{+}$	CG6217 V-106302	Vienna *Drosophila* stock center (VDRC)
	UAS *EcR-A*^{F645A} *Homozygous*			Brown et al., 2006
mutants	*obst-A*^{d03}	$\frac{obst-A^{d03601}}{FM7actGFP/y}; \frac{CyO}{Sp}; \frac{+}{+}$	CG17052	Petkau et al., 2012
	serp^{RB}	$\frac{+}{+/y}; \frac{+}{+}; \frac{serp^{RB}}{TM3ftz}$		Luschnig et al., 2006
	verm^{ex7}	$\frac{+}{+/y}; \frac{+}{+}; \frac{verm^{ex7}}{TM2twiGFP}$		Luschnig et al., 2006
	serp^{RB}*verm*^{KG}	$\frac{+}{+/y}; \frac{+}{+}; \frac{serp,verm}{TM3twiGFP}$		Luschnig et al., 2006
	knk^{f01902}	$\frac{+}{+/y}; \frac{+}{+}; \frac{knk^{f01902}}{TM6b}$	Bl-18487	
Balancer stocks	4x multi-balancer	$\frac{+}{+}; \frac{if}{CyO}; \frac{MKRS\ Sb}{TM6\ Tb\ Hu}$		
	GFP balancer 3rd chromosome	$\frac{+}{+/y}; \frac{+}{+}; \frac{Sb}{TM3SerGFP}$		

Self made	UAS *obst-A GFP* (II)	$\frac{+}{+/y}; \frac{UAS\ obst-A\ GFP}{UAS\ obst-A\ GFP}; \frac{+}{+}$
	UAS *obst-A GFP* (III)	$\frac{+}{+/y}; \frac{if}{CyO}; \frac{UAS\ obst-A\ GFP}{TM6Tb\ Hu}$
	obst-A rescue (to be crossed with different Gal4 lines)	$\frac{obst-A^{d03601}}{FM7actGFP/y}; \frac{UAS\ obst-A}{UAS\ obst-A}; \frac{+}{+}$
	knk mutant (GFP balancer)	$\frac{+}{+/y}; \frac{+}{+}; \frac{knk^{f01902}}{TM3SerGFP}$
	Transheterozygous *obst-A serp verm* triple mutant	$\frac{obst-A^{d03601}}{+}; \frac{+}{+}; \frac{serp,verm}{+}$
	Transheterozygous *obst-A knk* double mutant	$\frac{obst-A^{d03601}}{+}; \frac{+}{+}; \frac{knk}{+}$

For generation of UAS Obst-A GFP flies, flies that were positive for insertion of the *obst-A GFP* construct were repeatedly crossed with the 4x multibalancer line as described in chapter 2.2.12.2.

The generation of the *obst-A* rescue line is described in Supplementary Fig. S9.

Knk mutant flies balanced with TM6b were crossed with a GFP balancer for 3rd chromosome to establish a *knk* mutant line balanced with TM3SerGFP.

Transheterozygous *obst-A*/+;*serp,verm*/+ and *obst-A*/+;*knk*/+ mutants were established by crossing heterozygous *obst-A* mutants with *serp*, *verm* double mutants or *knk* mutants, respectively.

2.2 - Methods

2.2.1 - Working with *Drosophila melanogaster*

2.2.1.1 - Handling of flies

Drosophila melanogaster flies were handled under standard procedures. Flies were reared in food vials at different temperatures (18 °C, room temperature, 25 °C, 29 °C) depending on the experiment. Usually, for stock keeping flies were kept at 18 °C or room temperature and for experimental purposes they were kept at 25 °C or 29 °C.

Flies were made unconscious with carbon dioxide in order to sort and collect them. For collection of offspring embryos and larvae, flies were placed in cages in which the mated females laid eggs on apple juice agar plates that had a drop of yeast paste in the middle.

Egg collections were performed for different time intervals according to experimental needs, ranging from 2 h to 24 h. Shorter time points were chosen when developmental synchrony of the animals was required, longer time points were chosen when large numbers of offspring animals were needed and developmental staging was less important.

Until the developmental stage of interest was reached, collection plates were kept at the desired experimental temperature (usually at 25 °C or 29 °C in the incubator providing constant humidity and a 12 h/12 h light/dark cycle).

2.2.1.2 - Crossing of flies

Flies were made unconscious with carbon dioxide for their collection. For crossing of flies, freshly eclosed virgin females of a desired genotype were collected and mated with male flies of a different genotype.

For multistep crosses that only required a small amount of progeny, one virgin female was crossed to one male and held in fly food vials. Crosses that were intended to collect larger numbers of offspring animals were placed in egg laying cages. For these crosses larger numbers of virgins (15-60) were mated with approximately half the number of males.

The Gal4-UAS system (Brand & Perrimon, 1993) is a binary genetic tool for manipulating gene expression and was frequently used in this thesis. In this system the transcriptional

activator and the target gene are separated on two fly lines. The transcriptional activator Gal4 is expressed under control of a tissue specific enhancer in the first fly line, which is called the "driver line". The Gal4-responsive UAS (Upstream activating sequence) precedes the target gene in the second fly line. Only when those two fly lines are crossed, the Gal4 protein is able to bind to the UAS sequences, thereby activating target gene expression. As the Gal4 transcriptional activator is controlled by a tissue and/or developmental time point specific enhancer, the target gene expression is only achieved in the tissues in which Gal4 is expressed. This allows the functional analysis of genes in certain tissues and developmental stages. The Gal4-UAS system can be used for induced gene overexpression as well as induced gene knockdown (Dietzl et al., 2007). In the latter case, the UAS sequence is followed by an inverted repeat, which is transcribed into a hairpin double-stranded mRNA complementary to the mRNA of the gene that is intended to be knocked down. The hairpin is recognized and processed by the RNAi-machinery and can bind to the mRNA of interest, thereby preventing its translation (Zamore, 2001; Ghildiyal and Zamore, 2009).
In experiments using the Gal4-UAS system, females of the Gal4-carrying driver line were crossed with males of the UAS-responsive line (UAS *geneX* or UAS *RNAi-geneX*) to allow target gene overexpression or knockdown in the progeny. If not otherwise noted when using the Gal4-UAS system the crosses were kept at 29°C to allow full activation of target gene expression.

2.2.1.3 - Selection of larvae

In order to distinguish homo- or hemizygous from heterozygous mutant larvae, they were selected for presence of GFP signal at the fluorescence binocular. In all genetic setups, heterozygous larvae carried one copy of a balancer chromosome with a GFP marker, while homo/hemizygous mutants lacked this balancer chromosome.
E.g. heterozygous *obst-A*^{d03}/FM7actGFP mutant larvae have a GFP signal, whereas hemizygous *obst-A*^{d03}/y larvae do not have the FM7i,P{ActinGFP} balancer chromosome and therefore do not fluoresce when under the binocular.
Each separate groups of desired larvae was transferred to a new apple juice agar plate with yeast paste.

2.2.2 - JB-4 embedding of larvae and generation of sections

As it is very difficult to obtain high quality sections from soft larval material that is very likely to rupture upon sectioning, JB-4 glycol methacrylate resin was used for embedding of larvae. It has the advantage of preserving tissue integrity while still being suitable for most types of histological and immunofluorescent stainings. A protocol for the generation of JB-4 sections for *Drosophila* larvae was developed in the course of my master thesis with the help of Melanie Thielisch.

First, second and third instar larvae, respectively were collected and fixed in 1 ml 4 % paraformaldehyde in PBS overnight at 4 °C. For third instar larvae, about 10-15 larvae were used for fixation. For first and second instar stage, a higher number of larvae was fixated accordingly (up to 100 freshly hatched L1 larvae). Afterwards, dehydration was performed in an ascending ethanol series:

60 % ethanol (2x, 15 min)

70 % ethanol (15 min)

80 % ethanol (15 min)

90 % ethanol (15 min)

96 % ethanol (15 min)

100 % ethanol (2x, 30 min)

In each dehydration step 1 ml ethanol solution was added and tubes were incubated at room temperature on a turning wheel for the indicated time. For changing solutions, larvae were allowed to sink down to the bottom of the tube and the supernatant was discarded.

After dehydration, the larvae were infiltrated for embedding with JB-4 Plus Resin (Polysciences, Warrington, USA). As components of the JB-4 kit are toxic, all of the following steps were carried out under a fume hood.

The infiltration solution was prepared by adding 0.625 g benzoyl peroxide to 50 ml JB-4 Plus "Solution A" and mixing until the benzoyl peroxide was completely dissolved. The ethanol from the tubes with the larvae was discarded and 0.5 ml infiltration solution was added to each tube. After 1 h incubation at room temperature under gentle rocking on a shaking platform infiltration solution was changed and tubes were placed on an equivalent shaker at 4 °C. Final incubation took place overnight or up to 48 h, until larvae became a little

translucent and sank down to the bottom of the tube. Excess infiltration solution was stored at 4 °C for up to two weeks.

Infiltrated larvae were positioned in plastic embedding molds using forceps. Three first instar larvae, six second instar larvae or up to 15 first instar larvae, respectively, were placed parallel to each other in one mold. For preparation of embedding solution, 1.25 ml JB-4 Plus "Solution B" was added to 25 ml freshly made infiltration solution. The embedding mixture was stored on ice to prevent early polymerization and was pipetted gently, but rapidly into the embedding molds containing the larvae. In case larvae were swept away upon adding the solution, they were repositioned. The molds were filled to overflowing and small strips of parafilm were placed gently on top of the molds. Air bubbles were avoided to separate the embedding solution from oxygen, which prevents polymerization. The embedding molds were placed at 4 °C as the polymerization of JB-4 resin is a strongly exothermic reaction. After 24 h to 48 h the reaction was terminated and JB-4 blocks were taken out of the embedding molds, labeled and used for generation of sections.

The resin blocks were clamped into the block holder of the Ultracut E ultramicrotome (Reichert-Jung, D). A triangular sharp glass knife was used for first trimming the block until larval material was reached. Then 7 µm sections were cut and were gently taken with a forceps. They were placed on a preheated drop of water on a Superfrost glass slide that was placed on a heating plate set at 42 °C. This enabled unfolding and stretching of the sections and thereby better adhesion of the sections to the slide. On each slide about 20-30 consecutive sections were placed, with more anterior sections on the left side of the slide and more posterior sections on the right. Glass slides were dried overnight before they were used for staining procedures.

2.2.3 - Immunostaining

In the course of this thesis, immunostainings were performed on different materials: JB-4 sections, on embryos and on dissected larval tissues. For each of these three variants the general protocols had to be adapted. Thus, they are described in separate chapters below. In all cases stainings were performed at least three times (n=3) with material from more than 10 larvae (sections, dissected larvae) or 30 embryos, respectively. Appropriate negative

controls were used, such as secondary antibody controls in which the primary antibodies were omitted and only the secondary antibodies were used.

2.2.3.1 - Immunostaining of JB-4 sections

In order to prevent evaporation of the working solutions and dehydration of the sections, which impairs quality of the staining and enhances the background signal, all of the described steps were performed in a humid chamber.

As JB-4 is a very hydrophobic material, sections first had to be rehydrated before they could be used for immunostainings. The rehydration was performed using a descending ethanol series including the following steps:

96% ethanol

80% ethanol

70% ethanol

For each of these steps 500 µl of the respective ethanol dilution was added to the objective slide with the sections for 5 min. As the small sections often do not adhere strongly to the glass slides, changing solutions was always performed very carefully by gently tilting the slide so that the liquid runs down into tissue paper. Then, the next solution was added by pipetting slowly. The last step of rehydration was the adding of 600 µl PBS to the slides for 3 min.

The paraformaldehyde fixation, which can cross-link epitopes as well as the harsh treatment of tissues during JB-4 embedding and the dense JB-4 resin, which cannot be penetrated well by some antibodies, frequently requires antigen retrieval. Otherwise epitopes are masked and staining intensity is very poor.

In general, unmasking was performed by treating sections three times for 5 min each with a 10 mM sodium citrate buffer, pH 6.0, which was heated up in the microwave until boiling and then directly added to the slides (500 µl/slide).

For the antibodies against the Serp and Verm proteins a harsher demasking was required in order to achieve an intense staining. For this reason, they were incubated for 2 h at 65 °C in a glass cuvette filled with sodium citrate buffer and afterwards incubated with 500 µl 0.001% trypsin in 0.05 M Tris, pH 7.8, at 37 °C for 1 h.

In the next step, 500 µl blocking solution (10 % donkey serum (DS) in PBS) was added to the slides for 30 min at room temperature. Sections were washed three times for 5 minutes with 500 µl PBS and then 250 µl of primary antibody solution was added to each slide. For secondary antibody controls (without primary antibody), PBS with 1 % DS was added to the slides. Primary antibodies used in this study and their respective dilutions are listed in chapter 2.1.

On the next day sections were washed three times for 5 min with PBS and then secondary antibody solution was added for 2 h at room temperature. Fluorescently conjugated (either A488, Cy3, A647) donkey secondary antibodies directed against the primary antibodies from different species were diluted 1:250 in PBS supplemented with 1% DS were added and incubated. In general for all immunostainings (sections, embryos, larvae) the incubation with secondary antibody solution as well as all following steps were performed in the dark in order to prevent photobleaching of the coupled fluorophores.

Fluorescently coupled dyes such as CBP-A488 (Chitin Binding Probe; 1:50) as well as WGA-A633 (Wheat Germ Agglutin, 1:250) were added to the secondary antibody mix. CBP, which was synthesized according to a protocol provided from New England Biolabs, is a recombinant A488-conjugated protein harboring a Chitin Binding Domain. Therefore, it can be used for selective labeling of chitinous structures. WGA is a A633-conjugated lectin that selectively recognizes N-acetyl-D-glucosamine, which is the main constituent of chitin, and N-acetylneuraminic acid residues (Peters & Latka, 1986). For this reason WGA was used as marker for cell surfaces, which are rich in glycoproteins, as well as for recognizing chitinous material.

After incubation with the secondary antibodies, sections were washed three times for 5 min with PBS and mounted in Vectashield H-1500 with DAPI. They were stored for at least 24 h at 4 °C before confocal imaging.

2.2.3.2 - Immunostaining of whole-mount embryos

Embryos were rinsed from egg laying plates and dechorionated in 2.5 % sodium hypochlorite for 5 min and washed with deionized water. Afterwards, they were transferred into a glass vial containing a 1:1 mixture of 4 % formaldehyde and heptane. Fixation was carried out for

20 min, followed by devitellinization in a 1:1 mixture of heptane and methanol for 10 min. Embryos were shortly washed with methanol and were stored in fresh methanol at -20 °C.
Each step of the immunostaining was performed on a turning wheel. Embryos were washed three times for 20 min with 1 ml PBT (PBS + 0,2% Triton X-100) and blocked for 30 min with 1 ml PBT supplemented with 4 % BSA. As the BSA solution is not stable for long time at room temperature or 4 °C, for each staining an aliquot frozen at -20 °C was thawed. After blocking, the primary antibodies diluted in PBT were added and incubated at 4 °C for 72 h. For each sample 75 µl of primary antibody solution was used. Primary antibodies used in this study and their respective dilutions are listed in chapter 2.1.
Afterwards embryos were washed three times for 20 min with PBT and secondary antibodies (1:250) linked with fluorescent dyes and, if used for the staining, WGA were added for 2 h at room temperature. 150 µl secondary antibody solution was added to each slide. After three washing steps (20 min each, with PBT) embryos were placed on a glass slide, mounted in Vectashield H-1500 with DAPI and stored for at least 24 h at 4 °C before confocal imaging.

2.2.3.3 - Immunostaining of dissected larval material and dissection procedure

For immunostaining of larval material, larvae had to be dissected first in staining dishes filled with PBS. The exact dissection procedure depended on the developmental stage and on the genotype of the larvae.
Due to their cuticle integrity defect, *obst-A*^{d03} null mutant larvae were only pricked dorsally at the anterior-to-middle part of the larvae. This was sufficient to cause organ spill out. Because of the small larval size and in order to avoid loss of the tiny organs, *obst-A*^{d03} null mutant larvae were not further dissected before immunostaining.
First and second instar larvae of other genotypes were held with one forceps while they were opened dorsally at the posterior part with the second forceps. The dorsal cuticle was pulled away in a posterior-to-anterior movement.
Third instar larvae were prepared in an "inside-out" fashion. For this, the posterior third of the larva was cut off. The anterior two third were held with one forceps. At the same time the tip of another forceps was used to push the mouth hooks backwards so that the larva was turned inside-out with the organs exposed to the outside and the epidermal cuticle on the inside.

Opened larvae were transferred into staining dishes with 1 ml 4 % paraformaldehyde in PBS and fixated for 1 h at room temperature. Samples were washed three times for 20 min with 1 ml PBT (PBS + 0,2% Triton X-100) and blocked with 500 µl 10% Donkey Serum (DS) in PBT for 30 min. The primary antibodies (for the dilutions see chapter 2.1) were diluted in PBT + 1 % DS and incubated overnight at 4 °C on a shaking platform under gentle rocking. For each staining dish filled with larvae 250 µl of primary antibody mix was used.

On the next day larvae were washed three times for 20 min with 1 ml PBT. Secondary antibodies (1:250) and if needed fluorescent dyes were diluted in PBT + 1 % DS and 250 µl of the mix was added to each staining dish. After 2 h incubation at room temperature larvae were washed three times for 20 min with 1 ml PBT and placed on a glass slide for dissection and mounting.

The final dissection procedure depended on the tissue that was investigated in the stainings. In general, the tissues of interest were gently taken away by forceps and arranged on the glass slide in a drop of PBT. For preparation of ring glands, the anterior part of the larva was taken and one forceps was used to gently pull at the mouth hooks. This resulted in pulling out the brain-ring-gland complex still attached to the proventriculus and the gut. The connections (mostly nerves) of the brain-ring-gland complex to the gut were cut and the brains were arranged on the slides in a way that the ring gland was fully exposed for imaging. Dissected tissues were mounted in Fluoromount G with DAPI and stored for at least 24 h at 4 °C prior to confocal imaging.

2.2.3.4 - Generation and evaluation of anti-Chitinase 2 antibodies

In order to investigate the expression pattern of the Chitinase 2 (Cht2) a peptide antibody was generated. Cht2 has a predicted size of 484 amino acids, corresponding to a predicted molecular weight of 54.13 kDa.

The stretch of fifteen amino acids " WDPQTSQVLAKSERN" at position 335 to 349 was chosen as an epitope because it is part of the Glyco18 domain but exposed to the outside of the protein and not conserved in other Chitinases. The peptide was synthesized by Pineda, Berlin, and injected for immunization into two rabbits and two guinea pigs. After each 30 days a serum sample was sent by Pineda for testing. For this, immunostainings were

performed comparing the signal from the serum samples from immunized animals, serum samples from the same animals before immunization and secondary antibody controls.
After 150 days of immunization a strong specific signal was detected for serum from all four animals. Thus, the antibodies were purified from the blood of the animals (by Pineda) and were objected to testing by Western Blot (protocol see below, chapter 2.2.11) and immunostaining. For both applications, different antibody dilutions, incubation times and blocking variants were tested. In the end a dilution of 1:50 for JB-4 sections, 1:100 for other staining applications and the standard staining protocol without any modifications proved to be optimal. The anti-Cht2 antibodies were used 1:5000 for Western Blots.
The specificity of the four different anti-Cht2 antibodies was tested first in Western Blotting for recognition of a single prominent band at 54 kDa. In immunostainings specificity was tested by pre-immune serum and secondary antibody controls, overexpression controls (69B Gal4> UAS *Cht2*), knockdown controls (69B Gal4> UAS *Cht2* RNAi) as well as peptide competition. For peptide competition the Cht2 antibody was treated for 1h with the anti-Cht2 peptide that was used for immunization (0.5 µg/µl antibody) before adding the solution to the embryos/ larvae/ sections. This method efficiently blocks the epitope binding sites of the antibodies so that specific staining is blocked (Wingen et al., 2009).
Aliquots were either stored at 4 °C, at -20 °C (with 50 % glycerol) or snap-frozen in liquid nitrogen and stored at -80 °C. Only aliquots stored at -80 °C proved to be suitable for long term use.

2.2.4 - Microscopic imaging

Immunofluorescent stainings were imaged with the Zeiss LSM 710 and LSM 780 confocal microscopes (Carl Zeiss, Jena, D). Images and Z-stacks (sequential scans) were taken using the ZEN 2010 and ZEN 2012 software (Carl Zeiss, Jena, D). Standard settings were used but always adjusted to get excellent image quality. “Airy unit 1” settings were used to receive signals from the focal plane only. In order to avoid cross-excitation of fluorophores, the sample was sequentially scanned using separate fluorescence tracks: A488 and A633/A647 were imaged in the same track; Cy3 was imaged together with transmission light; DAPI was imaged in a separate track. For high-resolution subcellular studies the Zeiss 63x LCI Plan Neofluar objective was used.

For bright-field microscopy (DIC) the Olympus AX70 microscope as well as the Olympus SZX 12 fluorescent binocular (without or combined with fluorescence). Samples were imaged with the Cell'F software. Figures were designed using ImageJ, Adobe Photoshop, Inkscape and Adobe Illustrator.

2.2.5 - RNA isolation and generation of cDNA

For the isolation of RNA, carefully staged larvae were collected into the buffer RA1 (NucleoSpin RNA II kit, Macherey-Nagel) and frozen at -80 °C. About 10 third instar larvae, about 30 second instar larvae or about 60 first instar larvae were collected per sample.
For homogenization samples were thawed on ice and glass beads were added. The Precellys homogenizator was used with the following program: 3x15 s with 5000 rpm. After homogenization samples were stored on ice and β-mercapto ethanol was added to a final concentration of 1 % (v/v).
RNA was prepared using the NucleoSpin RNA II kit according to the manufacturer's instruction. RNA was eluted with ddH_2O, the samples were immediately placed on ice and RNA concentration was measured with the Nano Drop Spectrophotometer. 500 ng RNA was subjected to a second genomic DNA digestion and cDNA synthesis using the QuantiTect Reverse Transcription Kit (Qiagen) as described by the manufacturer. RNA was stored at -80 °C and cDNA was stored at -20 °C.

2.2.6 - Quantitative Real-Time PCR

Quantitative Real-Time PCR was used to determine the relative mRNA expression of certain genes. The primers used in this study are listed in chapter 2.1.

2.2.6.1 - Generation of primers and primer efficiency test

Primers for quantitative Real-Time PCR (qRT-PCR) were designed with the Primer3 Software using standard adjustments for qRT-PCR primers (amplicon size 80-110 nucleotides, primer size 18-20 nucleotides, melting temperature 58-62 °C, CG content 40-60 %). The mRNA sequence for all genes for which primers were designed was taken from FlyBase. All

designed primers were tested for specificity with the BLAST database and physicochemical properties and putative self-complementarity was checked with the OligoCalc Database (Kibbe, 2007). Primers that were already published were nevertheless tested with the BLAST and the OligoCalc Database.

Primers were manufactured by Invitrogen or IDT Technologies and primer pairs were diluted to a concentration of 5 pmol/µl in ddH_2O. All qRT-PCR primers were tested for efficiency using a cDNA dilution series and melt curve analysis. Primer efficiency was determined with the CFX Manager software (Bio-Rad). Only primers with minimum 75 % efficiency and without any unspecific by-products as seen by melt curve analysis, were used for qRT-PCR analysis.

2.2.6.2 - Quantitative Real-Time PCR procedure and analysis

For qRT-PCR analysis the following reaction mixture was used (15 µl):

cDNA	0.75 µl
ddH_2O	6 µl
Primer pair (5 pmol/µl)	0.75 µl
SYBR green mix	7.5 µl

Reactions were performed in technical duplicates or triplicates in clear 96 well plates in the CFX96 cycler (Bio-Rad) in which the SYBR green fluorescence was measured after each cycle. The following PCR program was used:

Denaturing	95 °C	3 min	
Denaturing	95 °C	10 s	45 cycles
Annealing	55 °C	10 s	
Elongation	72 °C	30 s	
Melt curve	65 - 95 °C		

Negative controls (-RT, where no Reverse Transcriptase (RT) was added upon cDNA synthesis) and no-template controls were used and samples were subjected to melt curve analysis to check for unspecific by-products.
For each qRT-PCR experiment if not otherwise noted five biological replicates were tested. All expression values were normalized to the expression of the housekeeping gene *rp49* (*Ribosomal protein L32*). Data was analyzed according to the ΔΔCT Method (Livak & Schmittgen, 2001) using the CFX Manager software and Microsoft Excel. Significance was tested using one-way ANOVA or Student's t-test (Graph Pad Prism 6). In all figures p-values are indicated by asterisks (*p<0.05, ** p<0.01, *** p<0.001, **** p<0.0001) and error bars show the standard error of the mean (SEM).

2.2.7 - Survival assays

Survival assays were frequently used in course of this thesis to determine the developmental stage at which lethality occurs in certain mutants and knockdown larvae. For this, the survival of animals was monitored throughout their entire development from late embryonic stages or early first instar stage to the adult stage.
Survival assays are subdivided in "Standard survival assays" in which only the lethal stage was monitored and "Sterol feeding assays" in which sterols were added to the food in an approach to overcome lethality. For each experimental condition 100 embryos or larvae, respectively, were placed on apple juice agar plates with yeast (25 larvae per plate) and monitored in short time intervals throughout their development. For all survival assays yeast paste was freshly prepared by adding 10 ml deionized water to a fresh yeast block (42 g).
All experiments included appropriate control conditions and were performed at least three times (n≥3, corresponding to ≥300 larvae per analyzed condition) and statistically analyzed by Student's t-test (Microsoft Excel). In the figures p-values are indicated by asterisks (* p<0.05, ** p<0.01, *** p<0.001) and error bars show the standard error of the mean (SEM).

2.2.7.1 - Standard survival assays

For standard survival assays embryos were rinsed from egg laying plates and dechorionated using 2.5% sodium hypochlorite for 5 min. After washing with ddH_2O, 25 living stage 17 embryos were placed on an apple juice agar plate supplemented with yeast paste. The same amount of yeast paste was used for all plates (~0.25 g/plate for 25 animals). As most experiments made use of the Gal4-UAS system that is fully activated at 29 °C (Brand & Perrimon, 1993) the apple juice plates were kept in a 29 °C incubator providing constant humidity.

The survival and developmental progression of the animals was monitored twice daily. After the hatching of adult flies they were transferred into food vials and monitored for two more days. Survivors were classified as "viable adults".

2.2.7.2 - Sterol feeding assays

Sterols for the feeding assays were prepared in glass vials in absolute ethanol and heated up to 65 °C until dissolving. Due to massive crystallization of the sterols, stocks were prepared freshly each time a new survival assay was conducted.

The concentrations of the stock solutions and the final working concentrations in the yeast, which are similar to the concentrations used in Huang et al., 2005, can be seen below:

Sterol	**Concentration in stock**	**Final concentration in yeast (50 µl stock/g yeast)**
cholesterol	20 mg/ml	1 µg/g
7-dehydrocholesterol	20 mg/ml	1 µg/g
20-hydroxyecdysone	10 mg/ml 15 mg/ml	0.5 µg/g 0.75 µg/g

50 µl of the corresponding stock solutions were added to 1 g of yeast paste, mixed by stirring until homogenous and distributed on apple juice agar plates (0.25 g yeast paste/ plate). As control condition, absolute ethanol only was added to the yeast paste.

Plates supplemented with 7-dehydrocholesterol, which is instable under light exposure (Yoshiyama et al., 2006) were constantly wrapped in thick paper towels to still allow breathing of the larvae.

25 early first instar mutant, knockdown or control larvae were placed on each apple juice plate. All sterol feeding experiments were performed at 25 °C in an incubator providing constant humidity and a constant 12 h/ 12 h light/ dark cycle. The constant light/ dark rhythm is an important prerequisite for the analysis of the ecdysone pathway that is under control of the circadian clock (McBrayer et al., 2007; Ou et al., 2011). For this reason many publications in the ecdysone field use a 12 h/ 12 h light/ dark cycle for their survival experiments (amongst others Yoshiyama et al., 2006; McBrayer et al., 2007; Gibbens et al., 2011; Moeller et al., 2013; Danielsen et al., 2014).

Note that also assays featuring Gal4-UAS knockdown larvae were performed at 25 °C in order to achieve full comparability to the other experiments and because the knockdown phenotype for the analyzed lines was beforehand tested to be highly similar at 25 °C and 29 °C.

As the complex molting phenotype of *obst-A* null mutant and knockdown larvae appeared relatively shortly before their death and decomposition of the dead larvae occurred quickly, monitoring in short time intervals was necessary. Larvae were monitored every 4 h during the day and were additionally assessed once during the night.

According to their molting phenotype *obst-A* null mutant and knockdown larvae that died during the first instar stage were classified into one of the following categories:

	Double mouth hooks	**Partial cuticle shedding**
dead before molt	**-**	**-**
dead upon initiation of molt	**+**	**-**
dead after partial molt	**+**	**+**

In the end the number of larvae in each category as well as the number of escapers into second and third instar stage was counted and compared and the effect of the different sterols on survival was statistically analyzed.

2.2.8 - Cuticle integrity assay

For cuticle integrity assays 6 h to 10 h old first instar larvae were placed on a glass slide and gently laterally pricked with a glass needle and immediately monitored for hemolymph bleeding and organ spill out by Nomarski microscopy (DIC, Olympus AX70) and Cell'F software.

For each experiment, the test was repeated at least three times with a minimum of 30 larvae each time. The number of larvae showing organ spill out was counted and significance was determined using Student's t-test (Microsoft Excel). In all figures p-values are indicated by asterisks (* $p<0.05$, ** $p<0.01$, *** $p<0.001$) and error bars show the standard error of the mean (SEM).

2.2.9 - Transcription factor binding site analysis

In order to analyze if *obstructor-A* is a target of the ecdysone transcription factor machinery, the JASPAR (Mathelier et al., 2014; http://jaspar.binf.ku.dk) and ConSite (Sandelin et al., 2004; http://consite.genereg.net) databases were used.

The analyzed sequence was taken from FlyBase and consisted of the 2 kb upstream of the *obst-A* gene (putative promotor sequence) and the *obst-A* gene sequence.

For the JASPAR database "JASPAR CORE Insecta" was chosen, transcription factors to be analyzed were selected and the cut-off ("relative profile score threshold") was subsequently changed in 5 % steps from the default 80 % to a value of 95 % in order to reduce the number of false positive hits.

For the ConSite database the option "Analyze single sequence" was chosen and all transcription factors from the "taxonomic supergroup insects" were selected for analysis. As for the JASPAR database the default 80 % cut-off ("TF score cut-off") was raised in 5 % steps up to 95 % to exclude false positive results.

2.2.10 - Triacylglycerol measurement by thin layer chromatography

To analyze the triacylglycerol (TAG) content of larvae, lipids were extracted and analyzed by thin layer chromatography. First for each sample about 200 first instar larvae were snap

frozen in liquid nitrogen and stored at -80 °C until start of the experiment. Thawed larvae were smashed with a pestle in 150 µl water per sample and protein concentration of the extracts was determined using the BCA Protein Assay Kit (Thermo Fisher Scientific). All samples were normalized to the one with the lowest protein concentration. 100 µl of each sample was taken for lipid extraction. 375 µl of a 1:2 chloroform/methanol mixture was added. After vigorous vortexing 125 µl chloroform was added, the samples were vortexed again, 125 µl ddH_2O was added and the samples were centrifuged for 1 min at full speed. The lower phase was transferred to a new tube and dried in the SpeedVac at 45 °C for 20 min or until completely dried. Lipids were dissolved in 15 µl of a 1:1 chloroform/methanol mixture. For thin layer chromatography a HPTLC silica gel plate (Millipore) was used. The standards (butter and oil prepared in a 1:1 chloroform/methanol mixture) as well as the samples were added on the plate (about 1.5 cm apart from the lower rim). The plate was run in a glass apparatus filled with the running solvent (70:30:1 n-hexane/di-ethylether/acetic acid) until migration was completed. The plate was completely dried and placed for 20 s in a 10 % copper sulfate/8 % phosphoric acid solution. After drying the plate was developed in a preheated oven (180 °C, top and bottom heat) for about 3 min until bands were clearly visible.

2.2.11 - Western Blot

Generation of protein extracts

Embryos, larvae, pupae or adult flies were frozen in liquid nitrogen and stored at -80 °C until they were used for the generation of protein lysates. Alternatively, animals were freshly collected. After washing, animals were transferred into RIPA buffer (100 µl/sample) and homogenized using glass beads and the Precellys machine (Peqlab). A small aliquot (4 µl) of the lysate was used for determination of the protein concentration with the BCA Protein Assay Kit (Thermo Fisher Scientific). The samples were adjusted to the one with the lowest measured protein concentration and Laemmli Buffer supplemented with 10 % β-mercapto ethanol was added. Samples were boiled at 95 °C for 5 min and afterwards subjected to SDS-PAGE.

SDS-PAGE

SDS-PAGE (Sodium Dodecyl Sulfate Polyacrylamide Gel Electrophoresis) is a method that separates proteins under electric current according to their molecular weight (Laemmli, 1970). Gels were prepared according to the following scheme (volumes sufficient for two gels):

10% Dissolving Gel		**5% Stacking Gel**	
ddH_2O	4.8 ml	ddH_2O	2.9 ml
Acrylamide Mix (29:1)	2.5 ml	Acrylamide Mix (29:1)	0.5 ml
1.5 M Tris pH 8.8	2.5 ml	1 M Tris pH 6.8	0.5 ml
10 % SDS	100 µl	10 % SDS	40 µl
10 % APS	100 µl	10 % APS	40 µl
Freshly added:		Freshly added:	
TEMED	6 µl	TEMED	6 µl

At first the dissolving gel was poured and covered with isopropanol. After polymerization the stacking gel was poured on top and a comb with the appropriate number of wells was inserted. SDS-gels wrapped in paper towels soaked with running buffer could be stored for several days at 4 °C.

SDS-gels were inserted into the electrophoresis apparatus and covered with 1x Running Buffer. Samples and the marker (Precision Plus Protein All Blue Standard, Bio-Rad) were added and the electrophoresis was conducted at 80 V until the samples reached the Dissolving Gel. Then the voltage was elevated to 110 V for 1 h.

Blotting

A PVDF membrane (Millipore) was activated in methanol and the Blot sandwich was assembled according to the following scheme:

Cathode

sponge

2x Whatman paper

gel

membrane

2x Whatman paper

sponge

Anode

The Blot sandwich was placed into a Blotting apparatus together with a cooling block and a magnetic stir bar and filled with transfer buffer containing methanol. To avoid the generation of heat, blotting was performed in the cold room (4 °C) under magnetic stirring. Blotting was performed for 2 h (for 1 blot at 70 V; for 2 blots at 100 V) and the cooling block was exchanged after 1 h.

Antibody incubation and Blot development

After blotting successful protein transfer was tested by PonceauS staining. The membrane was rinsed with TBS-T and blocked for 2 h with 5 % milk powder in TBS-T. The primary antibody was diluted in 2.5 % milk powder in TBS-T and incubated over night at 4 °C on a shaking platform. Following three washing steps using TBS-T (10 min each) the secondary antibody solution was added (HRP conjugated goat antibody directed against the species from which the primary antibody was purified). Secondary antibodies were diluted 1:15000 in 2.5 % milk powder in TBS-T and incubated for 2 h at room temperature. The membrane was washed again three times for 10 min with TBS-T and then developed with ECL reagent (Thermo Scientific). The X-ray developer Curix60 was used to visualize chemiluminescence on X-ray films. For each membrane different exposure times were tested. If after 20 min no signal was seen on the films the membrane was washed and developing was repeated using the ECL Femto reagent (Thermo Scientific).

2.2.12 - Generation of an UAS Obst-A GFP fly line

A UAS Obst-A GFP fly line was generated for future use as reporter line showing *obst-A* expression *in vivo*. Furthermore, the putative phenotypes of *obst-A* overexpression in different tissues and the protein trafficking can be analyzed in UAS Obst-A GFP animals.
Molecular cloning was performed using standard methods. A 666 bp fragment containing the *obst-A* sequence was amplified from the cDNA clone LD43683 by PCR in a way that appropriate restriction sites were added. This allowed cloning of the purified and digested fragment into the pMJ Green vector in frame with the included GFP. The pMJ *obst-A GFP* vector is thought to be a tool for the analysis of Obst-A in cell culture. To generate a reporter fly line, the *obst-A GFP* cassette was cut out of the pMJ vector and subcloned into the pUAST vector resulting in a final pUAST *obst-A GFP* vector.

2.2.12.1 - Molecular cloning

Genomic DNA extraction and PCR

The LD43683 cDNA clone (pOT2 vector) was used as template for amplification of the *obst-A* sequence. PCR was performed using the Phusion Hot Start Polymerase (Thermo Scientific) as described by the manufacturer. DMSO was added to the PCR reactions to avoid secondary structures. The PCR mix was set up as following in a 50 µl reaction volume:

5x Buffer HF	10 µl
10 mM dNTP	1 µl
Primer forward	0.25 µl
Primer reverse	0.25 µl
cDNA template	1 µl
DMSO	3 µl
ddH_2O	34 µl
Phusion polymerase	0.5 µl

The following PCR program was used to amplify the *obst-A* sequence:

Denaturing	98 °C	30 s	
Denaturing	98 °C	20 s	5 cycles
Annealing	55 °C	15 s	
Elongation	72 °C	1 min	
Denaturing	98 °C	20 s	24 cycles
Annealing	65 °C	15 s	
Elongation	72 °C	30 s	
Final elongation	72 °C	10 min	

The primers were designed in a way that restriction sites were integrated in the sequences. The PCR product was let run on an 1 % agarose gel with SYBR safe. Bands were excised under UV light and the PCR product was extracted with the NucleoSpin Gel and PCR Clean-up Kit (Macherey-Nagel).

Restriction digest and ligation

The purified DNA as well as the vector backbone were digested with restriction endonucleases (NEB) in a 50 µl reaction volume for 2 h at 37 °C. Alkaline phosphatase (Roche) was used for phosphorylation of the vector backbone as described by the manufacturer. The reaction volume of 20 µl was incubated for 20 min at 37 °C the 2 min at 72 °C. For ligation of DNA fragments the T4 DNA Ligase (NEB) was used.
A vector:insert ratio of 1:3 was used for ligation in a 10 µl reaction volume with 1 µl T4 Buffer and 1 µl T4 Ligase. Ligation reactions were incubated over night at 16 °C.

Transformation

The ligation mixture was transformed into competent DH5α *E. coli* cells. Per ligation mixture 50 µl bacteria were thawed on ice and 50-100 ng DNA was added. After 20 min incubation on ice the bacteria were heat shocked at 42 °C for 30 s. The bacteria were incubated again on ice for 2 min. Then 1 ml LB medium (without antibiotics) was added and the bacteria

were placed into a heating block set to 37 °C and incubated for 1 h under gentle shaking (200 rpm). Bacteria were streaked out on LB agar plates (with the appropriate antibiotic), which were incubated over night at 37 °C. The next day the plates were assessed for the growth of colonies and clones were inoculated in 3 ml LB medium (with the appropriate antibiotic) over night at 37 °C and 180 rpm.

Plasmid preparation

For test-scale plasmid preparation (miniprep) 1.5 ml of the overnight bacterial culture was centrifuged (1 min 13000 g). The pellet was resuspended in 350 µl TELT buffer supplemented with 35 µl lysozyme solution (10 mg/ml stock) and 2 µl RNase (10 mg/ml stock). The mixture was incubated for 5 min at room temperature and then boiled at 99 °C for 3 min. The tubes were directly placed into a centrifuge cooled down to 4 °C and were centrifuged for 15 min at full speed. 300 µl of the supernatant, but not the debris, was transferred into a new tube and 300 µl of isopropanol was added. The tube was inverted several times and incubated for 5 min at room temperature. After a 20 min centrifugation step at full speed and room temperature, the supernatant was discarded and the pellet was washed with 800 µl 70 % ethanol. Following another centrifugation step for 5 min at full speed and room temperature, the supernatant was discarded. The pellet was dried and reconstituted in 50 µl ddH_2O. DNA content was measured using the NanoDrop spectrophotometer.

For larger scale plasmid preparation (midiprep) 50 ml LB medium with the appropriate antibiotic was inoculated and the bacterial culture was grown overnight at 220 rpm and 37 °C. The NucleoBond AX100 Midiprep Plasmid Purification Kit (Macherey-Nagel) was used according to the manufacturer's instruction, but with the major modification that the plasmid precipitation step in isopropanol was lengthened from 20 min to 1 h as this resulted in a higher DNA yield. The pellet containing the plasmid DNA was reconstituted in 50 µl ddH_2O and the DNA concentration and purity was measured spectrophotometrically with the NanoDrop.

For both mini- and midiprep analytical test digests with restriction endonucleases (20 µl reaction volume) were performed and analyzed by agarose gel electrophoresis.

Plasmid sequencing and injection

Plasmids were sequenced by Seqlab (Göttingen, D). Final plasmids with the correct sequence were sent for injection into fly embryos to BestGene (Chino Hills, USA).

2.2.12.2 - Mapping of fly lines and generation of stable stocks

10 fly lines were sent by BestGene, out of which all flies are progeny of a fly with successful integration of the pUAST *obst-A GFP* vector. However, for all lines the genomic integration site of the P-element still needed to be determined and stable stocks had to be generated.
For this a red eyed male of each of the lines was crossed to a female fly of the white-eyed 4x balancer stock with the following genotype:

$$\frac{+}{+}; \frac{if}{CyO}; \frac{MKRS\ Sb}{TM6\ Tb\ Hu}$$

Red eyed males from this crossing were crossed again with a virgin from the 4x balancer stock and the offspring was assessed for the presence of markers and the eye color.
If f.ex. in the progeny, red eyed flies occur that have both if (narrow eyes) and CyO (curly wings) markers, the insertion cannot be on the second chromosome; if red eyed flies occur with both Sb (short back hairs) and Tb (short thick body shape) Hu (additional hair on humeri) markers, the insertion cannot be on the third chromosome. If only red eyed females hatch but no red eyed males, the insertion is likely on the first (X) chromosome.
Red eyed offspring of the mapping crosses were crossed again with the 4x balancer stock to generate stable stocks that were maintained and tested for GFP signal after crossing with Gal4 driver lines.

3 - Results

In epithelial tissues the extracellular matrix often exerts a barrier function. In *Drosophila* not much is known about the molecular mechanisms how chitin-matrix forms at the epithelia.
During my PhD I characterized a key region through which all newly secreted cuticle components pass and become organized into dense, stratified structures. This region is called cuticle assembly zone (chapter 1.4.1) (Delbecque et al., 1978; Wolfgang et al., 1986; Wolfgang et al., 1987). I have characterized two essential factors to be involved in the chitin-matrix formation in this region, namely Obstructor-A (Obst-A) and Chitinase 2 (Cht2). In summary, my data suggest that Obst-A is a key mediator of chitin-matrix formation at the assembly zone, which additionally requires Cht2. These data have recently been published (Pesch et al., 2015, Pesch et al., 2016a; Pesch et al., 2016b) and are presented in the first two parts of the results section. Furthermore, during my PhD I discovered an additional and surprising function of Obst-A in the hormonal control of molting. These data are presented in the third part of the results section.

3.1 - Analysis of Chitinase 2 in cuticle formation

A surprising role of Chitinases and the related Imaginal Disc Growth Factors in epidermal cuticle stability was discovered by Dr. Matthias Behr and Kapil Patil.
In an approach to analyze this phenotype on a molecular level, during my master thesis (supervision Dr. Matthias Behr, LIMES Institute, University of Bonn) I performed a knockdown screen investigating the function of Chts and Idgfs in the epidermal cuticle.
I followed up on this project during my PhD and completed the knockdown screen with the remaining *Cht* and *idgf* lines with the help of the internship students Michael Beilharz and Dennis Holzkämper (data not shown). So far it was only known that some Chitinases probably play a role in the enzymatic breakdown of chitin fibrils into oligomers or monomers (Merzendorfer & Zimoch, 2003; Chaudhari et al., 2013). An amino acid substitution in the catalytic site renders Idgfs enzymatically inactive (Kawamura et al., 1999). They act as growth factors in the imaginal discs, but their function in the epidermis was previously completely elusive.

However, the roles of Chitinases and Idgfs have not been systematically investigated so far (see 1.5.3) leaving the basic question unanswered if all or even specific genes of the large Glyco18 multigene family contribute to cuticle formation in insects. The data I have generated together with co-workers were recently published in Scientific Reports (Pesch et al., 2016a) and Arthropod Structure & Development (Pesch et al., 2016b). To sum this up, we were able to show that Chts and Idgfs are essential for cuticle integrity and correct cuticle organization as knockdown of the individual *Chts* and *Idgfs* led to specific structural abnormalities of the chitin-matrix.

Importantly, the strongest phenotype was seen in *Chitinase 2* knockdown larvae. For this reason further analysis of Cht2 function in cuticle forming organs was performed.

In the RNAi-mediated knockdown screen of *Chitinases* and *Idgfs*, which I performed during my master thesis, and in the phenotypic analysis of *Cht* and *Idgf* knockdown larvae by Dr. Matthias Behr and Kapil Patil, especially *Cht2* knockdown animals showed severe cuticle defects, molting defects and complete lethality before reaching the adult stage. Only few adult flies hatched, but died immediately. Cuticle integrity, as assessed in a wounding assay, was heavily compromised and immunostainings revealed that the chitin-matrix was structurally defective. Strikingly, loss of each *Cht* and *Idgf* led to individual structural defects in the procuticle suggesting different non-redundant functions of Chitinases in the chitinous cuticle. Here I only show data obtained during my PhD study and exemplarily only the data for *Cht2* is presented.

3.1.1 - Chitinase 2 is required for epidermal lamellar cuticle thickening

My studies clearly show the importance of Cht2 in chitin-matrix formation during larval intermolt stages when cuticle material is massively produced but not degraded. This is presented in the next chapters.

3.1.1.1 - Knockdown of *Chitinase 2* results in diminished cuticle size and altered localization of important cuticle proteins

For knockdown of *Cht2* in cuticle forming tissues 69B Gal4 flies were crossed with UAS RNA interference (RNAi) flies. As the 69B driver is specific for the ectoderm, this results in RNAi-

mediated reduction of *Cht2* levels in the offspring in ectodermal tissues such as the epidermis and the trachea (Brand & Perrimon, 1993; Huang et al., 2005; Dietzl et al., 2007).

For labeling of the chitin-matrix by confocal analysis I generally used Chitin Binding Probe (CBP) that specifically labels chitin and Wheat Germ Agglutinin (WGA) which is a lectin binding to certain sugar residues in chitin and at cell surfaces. As Obst-A (chapter 1.5.4) is a protein detected in the chitin-matrix (chapters 3.2.2, 3.2.3) also this marker was used.

To analyze potential cuticle structure defects sections of third instar 69B Gal4> UAS *Cht2* RNAi larvae were generated and stained with CBP, WGA and an anti-Obst-A antibody (Fig. 3.1.1).

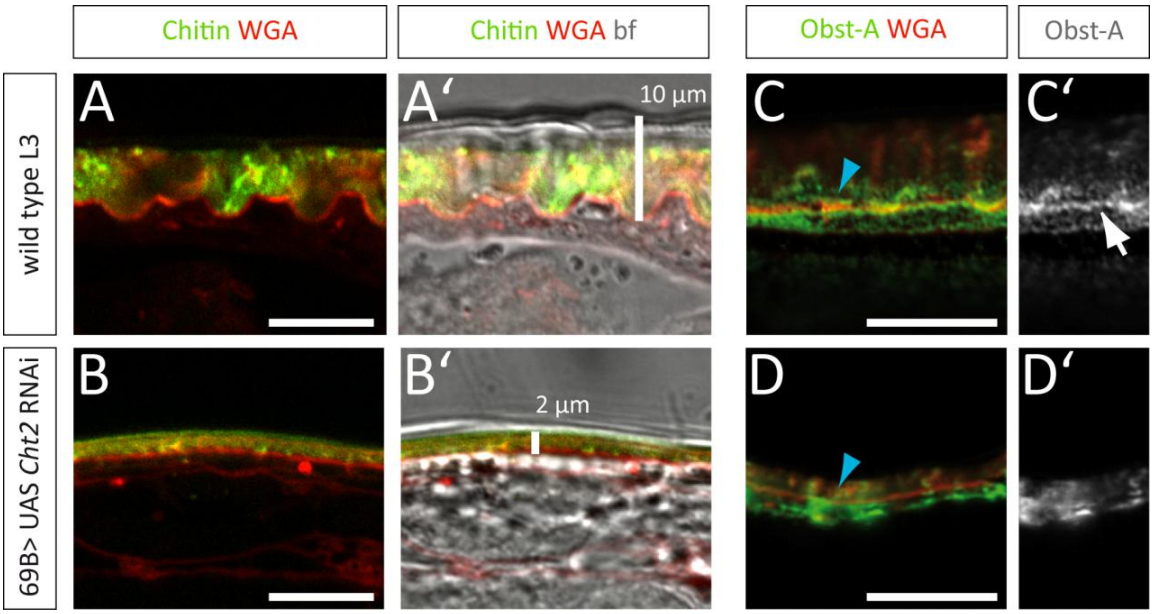

Fig. 3.1.1 - Cuticle thickness and Obst-A enrichment at the cuticle assembly zone is reduced in 69B Gal4> UAS *Cht2* RNAi knockdown larvae. Representative immunostaining on JB-4 sections of wild type (A, A', C, C') and 69B Gal4> UAS *Cht2* RNAi (B, B', D, D') late third instar larvae. The left panel (A and B) shows Chitin (CBP, green) and WGA (red) staining marking the chitinous procuticle and the cell surfaces. To give an overall orientation of the epidermal cuticle, Chitin (green) and WGA (red) staining is merged with the brightfield image in the second panel (A' and B'). The dimensions of the cuticle are indicated by bars demonstrating the reduced thickness of the epidermal cuticle in 69B Gal4> UAS *Cht2* RNAi larvae (2 µm compared to 10 µm in the wild type control). Images were taken with the same magnification. The third panel (C, D) shows WGA (red) and Obst-A staining (green). The blue arrowheads mark the apical epidermal cell surface. Note that in the wild type (C) colocalization (yellow) of WGA and Obst-A staining is seen at the apical cell surface. In C' and D' single channel Obst-A staining is depicted in grey. Enrichment of Obst-A at the apical cell surface in the wild type (C') is indicated by an arrow. In 69B Gal4> UAS *Cht2* RNAi larvae (D') this enrichment is weakened. Scale bars represent 10 µm. Adapted from Pesch et al., 2016a.

Chitin staining in sections (Fig. 3.1.1) revealed that the cuticle is thinned in *Chitinase 2* knockdown larvae. In wild type third instar larvae average cuticle thickness comprises 10 µm. The cuticle is narrowed to 2 µm in 69B Gal4> UAS *Cht2* RNAi knockdown larvae.

As described in chapter 1.5.4, Obst-A is a chitin-binding protein that has an important function in the tracheal chitin-matrix. Since epidermal cuticle integrity is compromised in *obst-A* deficient larvae, the presence of Obst-A was expected in the epidermis of wild type third instar larvae. There Obst-A was found to be present in the epidermal cells and also within the chitinous procuticle, but clear enrichment was seen in the cuticle assembly zone (Fig. 3.1.1 C, also see Fig. 3.2.4, 3.2.5).

The assembly zone is a non-lamellar area that is located on top of the apical epidermal cell surface but below the lamellar procuticle. Most likely it represents a stable, but permeable matrix through which chitin fibrils and proteins that have just been secreted by the epidermal cells pass through before their integration into the stratified cuticle occurs (Delbecque et al., 1978; Wolfgang et al., 1986; Wolfgang et al., 1987). Even though several proteins were found to localize to the assembly zone, these remain completely uncharacterized (Wolfgang et al., 1987; Locke et al., 1994). Thus, Obst-A constitutes the first identified molecular marker of the cuticle assembly zone. The function of Obst-A in the cuticle assembly zone is discussed in detail later in chapter 4.6. Obst-A localization in the assembly zone is dependend on Cht2 as the enrichment of Obst-A at the apical cell surface was strongly reduced in *Cht2* knockdown larvae (Fig. 3.1.1 D').

In addition to Obst-A, the localization of three other cuticle factors was determined in 69B Gal4> UAS *Cht2* RNAi knockdown larvae. Localization of the chitin protector Knk was not affected in *Cht2* knockdown larvae, but the chitin deacetylases Serp and Verm were mislocalized (Supplementary Fig. S1). The localization and function of Serp, Verm and Knk in the epidermal cuticle of wild type larvae is analyzed in detail in chapter 3.2.4. This altogether implicates that Cht2 may somehow contribute to mechanisms that are required for Obst-A mediated chitin-matrix formation.

3.1.1.2 - Knockdown of *Chitinase 2* causes reduction of the cuticle assembly zone

As described above, cuticle thickness is severely reduced in *Cht2* knockdown larvae. To analyze chitin-matrix structure, TEM analysis was performed by Dietmar Riedel, Max Planck Institute for Biophysical Chemistry, Göttingen. This analysis revealed strong structural defects in the knockdown larvae (Supplementary Fig. S2 A-B'). In third instar wild type larvae the procuticle comprised up to 50 distinct chitin lamellae, whereas in 69B Gal4> UAS *Cht2* RNAi knockdown larvae only up to 8 lamellae can be detected. In immunogold labeling studies (Supplementary Fig. S2 C-C') strong reduction of the cuticle assembly zone, which in electron microscopy is normally seen as a distinct zone above the epidermal cells, was observed in 69B Gal4> UAS *Cht2* RNAi knockdown larvae. In line with the reduction of the number of lamellae, this indicates a function of *Cht2* in the lamellar thickening of the epidermal cuticle.

3.1.2 - Chitinase 2 is expressed in chitin-secreting and non-chitinous tissues during embryonic and larval development

In order to establish a tool for the analysis of Cht2 function in cuticle thickening polyclonal anti-Cht2 antibodies were generated by immunizing two rabbits and two guinea pigs with a peptide fragment of the Cht2 C-terminus as described in chapter 2.2.3.4. After purification all four antibodies were tested in Western Blot analysis and immunofluorescent stainings including appropriate controls. All four antibodies work, but the antibody derived from "guinea pig 2" yields the most specific signals. Hence, only the results for the anti-Cht2 antibody "guinea pig 2" are shown. This antibody specifically recognized one single band at the expected size in Western Blot analysis and signals in immunofluorescent labeling were reduced in negative control stainings (Fig. 3.1.2).

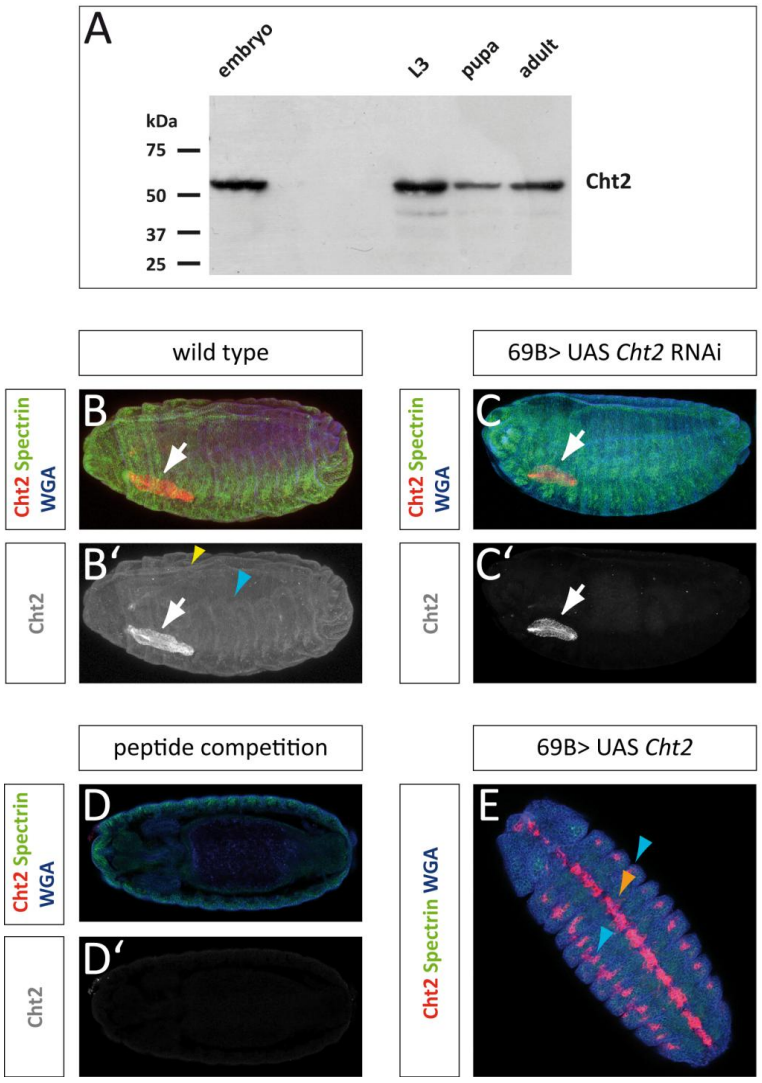

Fig. 3.1.2 - Evaluation of specificity of the anti-Cht2 antibody. A: Western Blot analysis using lysates from embryo, L3 larvae, pupae and freshly eclosed adult flies. Molecular weight is indicated on the left side. The anti-Cht2 antibody specifically labels one band above 50 kDa. This corresponds to the predicted molecular weight of Cht2 which is 56 kDa. Cht2 expression appears highest in third instar stage. Equal loading was tested by PonceauS stain. B-E: Representative immunofluorescent staining on embryos from different genotypes. 3D projections of whole embryos are shown. For comparison of staining intensity all images were taken with the same laser settings. B, B': wild type control (stage 16); C, C': 69B Gal4> UAS *Cht2* RNAi knockdown (stage 16); D, D': peptide competition on wild type embryo (stage 16); E: 69B Gal4> UAS *Cht2* overexpression (stage 11). Costaining of Cht2 (red) together with α-Spectrin (green) and WGA (blue), which both label cell surfaces, is shown in B, C, D, E and single channel Cht2 staining in grey is depicted in B', C', D'. In the wild type (B, B') the Cht2 antibody labels the salivary glands (arrows), the epidermis (yellow arrowhead) and the tracheal system (blue arrowhead). In the 69B Gal4> UAS *Cht2* RNAi knockdown embryo (C, C') the Cht2 signal in the salivary gland (arrows) is still visible, but the staining in the epidermis and tracheal system is absent. Peptide competition (D, D') completely abolishes Cht2 antibody staining. Overexpression of *Cht2* (69B Gal4> UAS *Cht2*) (E) causes strong Cht2 staining in the tracheal system (blue arrowheads) and the ventral midline (orange arrowhead), which is in line with the expression pattern of the 69B Gal4 line at embryonic stage 11.

In late stage wild type embryos Cht2 staining could be detected in the salivary glands, the epidermis and the tracheal system (Fig. 3.1.2 B-B'). In 69B Gal4> UAS *Cht2* RNAi knockdown embryos staining in the epidermis and the tracheal system was diminished (Fig. 3.1.2 C-C'). A signal in the salivary glands was still present, but a little weaker than in the wild type. In the "peptide competition" control the Cht2-peptide that was used for immunization of the animals was added to the antibody solution. As a result the antibody binds to the excess peptide in solution instead of the Cht2 epitope on the embryo. Peptide competition resulted in complete absence of Cht2 staining (Fig. 3.1.2 D-D') proving the specificity of the anti-Cht2 antibody. In an overexpression control using 69B Gal4> UAS *Cht2* embryos strong Cht2 signal was detected according to the expression pattern of the 69B driver line (Fig. 3.1.2 E). Altogether, the results imply that the newly generated anti-Cht2 antibody specifically recognizes its epitope and thus can be used for the analysis of Cht2 expression.

3.1.2.1 - Chitinase 2 expression in embryos

The newly tested anti-Cht2 antibody was used for analysis of Cht2 expression in embryos by immunostainings. Cht2 expression was detected in cuticle-forming organs such as the epidermis, the tracheal system, the spiracles, but also in the non-chitinous salivary glands (Fig. 3.1.3).

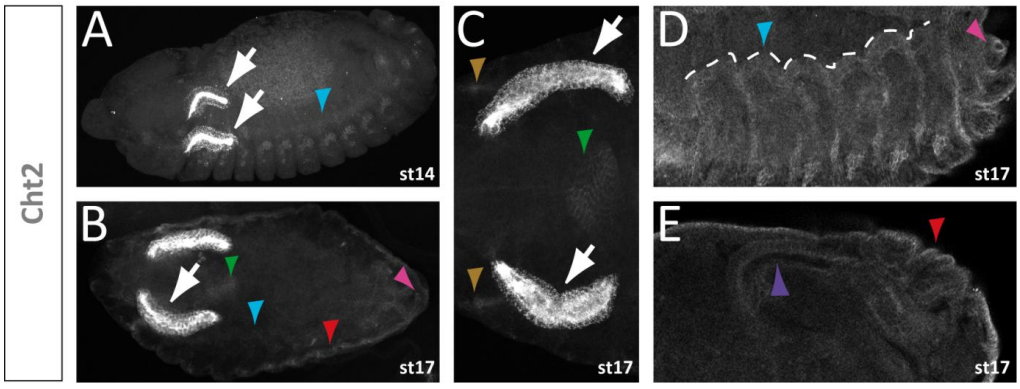

Fig. 3.1.3 - Cht2 staining is detected in different embryonic tissues including chitin-producing organs. Representative immunostaining. All images show single channel Cht2 staining in grey. A: stage 14 (st14) embryo, B-E: stage 17 (st17) embryo. Arrows (in A, B, C) point at the salivary glands, which are strongly positive for Cht2 staining. Blue arrowheads (in A, B, D) indicate Cht2 staining in the tracheal system. The shape of the tracheal dorsal trunk is depicted with white dashes in D. Green arrowheads (in B, C) show Cht2 staining in the proventriculus, red arrowheads (in B, E) point at the strong Cht2 staining in the epidermis. Anterior (beige; C) and posterior (pink; B, D) spiracles are also recognized by the anti-Cht2 antibody. Cht2 signal in the hindgut is indicated by a purple arrowhead in E. Adapted from Pesch et al., 2016b.

In embryonic stage 14 strong Cht2 signal was observed in the salivary glands and weaker signal was seen in the tracheal system (Fig. 3.1.3 A). In stage 17 embryos (Fig. 3.1.3 B-E), which constitutes the last stage of embryogenesis, in addition to signal in the salivary glands, Cht2 expression was detected in the tracheal system, the epidermis, anterior and posterior spiracles, the proventriculus and the hindgut. Altogether, immunofluorescent analysis indicates the expression of Chitinase 2 in both cuticle-forming and non-chitinous organs.

3.1.2.2 - Chitinase 2 expression in larvae

As a next step the expression pattern of Cht2 in larvae was determined in whole-mount preparations and sections. Cht2 staining in third instar larvae is depicted in Fig. 3.1.4.

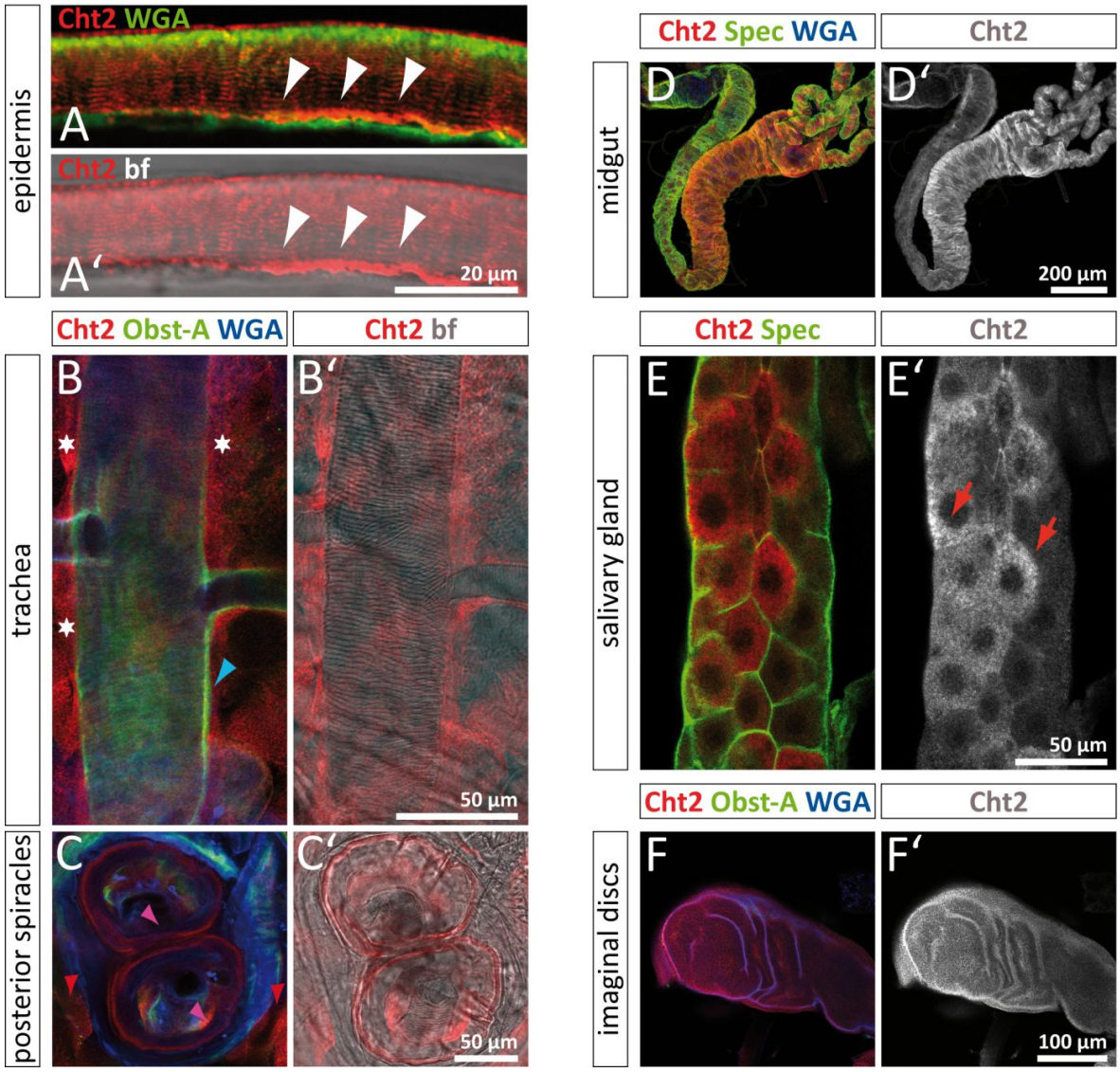

Fig. 3.1.4

Fig. 3.1.4 - Cht2 is expressed in diverse larval tissues including chitin-producing organs. Representative immunostaining of dissected tissues derived from wild type third instar larvae. Scale bars represent the size indicated in the respective picture. A and A' show Cht2 expression in the epidermis. A: Cht2 (red) and WGA (green) signal. WGA staining is distributed in the chitinous procuticle and the epidermal cells. Cht2 localizes to the apical cell surface of the epidermal cells where its signal weakly overlaps with WGA staining. Cht2 staining is also present at the distinct chitin lamellae, which is best seen in the merge of the Cht2 signal (red) with the brightfield image (A'). Arrowheads indicate the enrichment of Cht2 at the apical cell surface. In B and B' Cht2 staining in the tracheal system is illustrated. B: Merge of Cht2 (red), Obst-A (green) and WGA (blue) staining. The Obst-A protein, which is important in the tracheal system of embryos, localizes to the tracheal lumen and the apical cell surface where also Cht2 is detected (blue arrowhead). Cht2 is predominantly found in the tracheal cells as highlighted by asterisks. B': Cht2 staining (red) is shown together with the brightfield image to underline the mostly cellular localization. C and C' portrays Cht2 staining at the posterior spiracles. C: Merge of Cht2 (red), Obst-A (green) and WGA (blue) signal. Obst-A staining appears weak, but Cht2 is found in high levels at the posterior spiracles (pink arrowheads) as also seen in the merge of Cht2 signal (red) with the brightfield image in C'. Additionally, Cht2 signal is detected in the epidermis (see red arrowheads in C). D, D: Maximum intensity projection of Cht2 staining in the anterior midgut. D: Merge of Cht2 (red), α-Spectrin (Spec; marker of cell surfaces) and WGA (blue) staining demonstrating the strong Cht2 expression in the midgut. Single channel Cht2 (grey) staining is shown in D'. E, E': Cht2 staining in the salivary glands. In E cell surfaces are labeled by α-Spectrin (Spec; green) and Cht2 (red) is detected in the cytoplasm. The cytoplasmic localization of Cht2 is indicated by red arrows in the single channel image (E'; Cht2 in grey). Note that Cht2 staining is much stronger in some cells than in others. Staining shown in F and F' was performed by Bachelor student Michelle Dassen. F, F': Cht2 signal in imaginal discs. F: Cht2 expression (red) is shown together with the stainings for Obst-A (green), which is weakly detected in imaginal discs, and WGA (blue). Cht2 is expressed in the whole imaginal disc as also depicted in the single channel image (F', Cht2 in grey). Adapted from Pesch et al., 2016b.

In third instar wild type larvae, Cht2 expression was detected in the chitin-producing organs epidermis, the tracheal system, the posterior spiracles and the anterior midgut. In these organs Cht2 was localized both intracellular and extracellular in the chitinous aECM (Fig. 3.1.4 A-D'). This hints at a function of Cht2 in the cuticle of different chitin-producing organs. Moreover, Cht2 expression was detected in the salivary glands, in particular in the cytoplasm of certain cell clusters, and in the imaginal discs (Fig. 3.1.4 E-F').

In the epidermis Cht2 was found along the chitin lamellae but was strongly enriched in the cuticle assembly zone. Since the localization of Obst-A, which also normally localizes to the assembly zone, was altered and the assembly zone was diminished in *Cht2* knockdown larvae, the results altogether suggest an important role of Chitinase 2 in chitin-matrix formation at the cuticle assembly zone.

3.2 - Analysis of the Obstructor-A protein in epidermal cuticle formation

One major focus of this thesis was the functional analysis of the Obstructor-A (Obst-A) protein in the *Drosophila* epidermal cuticle.

As described in the introduction of this thesis (chapter 1.5.4), Obst-A is a chitin-binding protein, which is crucial for larval growth and development. The role of Obst-A in maintaining chitin structures in the tracheal system was characterized in detail in the study by Petkau et al., 2012. However, there are morphological differences among distinct chitin-matrices, showing the need for the analysis of Obst-A function in the epidermis. For example the tracheal chitin-matrix is thin, viscous and flexible but has to resist mechanical pressure, while the epidermal body wall cuticle has to withstand massive environmental forces and moreover needs to stabilize the whole organism (Moussian, 2010; Petkau et al., 2012). Accordingly, the tracheal chitin-matrix is rather thin while the epidermal chitin-matrix is compact and organized into lamellae. The underlying mechanisms of cuticle formation in the distinct organs is poorly known.

In addition to the tracheal defects, the study by Petkau et al., 2012, also describes other phenotypes of *obst-A* mutants including growth reduction and strong molting defects, which were further analyzed in this thesis in chapter 3.3. As *obst-A* deficient larvae also show strong defects in epidermal cuticle integrity (Petkau et al., 2012), this suggests a role of Obst-A in the epidermal chitin-matrix, which is presented in this chapter of the results section.

3.2.1 - Analysis of the *obstructor-A* null mutant phenotype during larval stages

As a first step in the further functional characterization of the Obst-A protein the null mutant phenotype was intensified with a focus on the epidermal integrity defect, including the analysis of epidermal cuticle structure. The results are depicted below.

3.2.1.1 - Loss of *obstructor-A* causes growth impairment and epidermal integrity defects

The general phenotype of *obst-A* null mutants was described in Petkau et al., 2012. In this study two different *obst-A* deletion mutants were generated by P-element excision and

analyzed. As both deletions result in transcript null mutants (*obst-A*^{d02} and *obst-A*^{d03}), for simplicity only *obst-A*^{d03} mutants were used in the present thesis.

Obst-A mutants are completely larval lethal and are not capable of increasing body size (Petkau et al., 2012). A quantification of the growth defect in *obst-A*^{d03} mutants is depicted in Fig. 3.2.1.

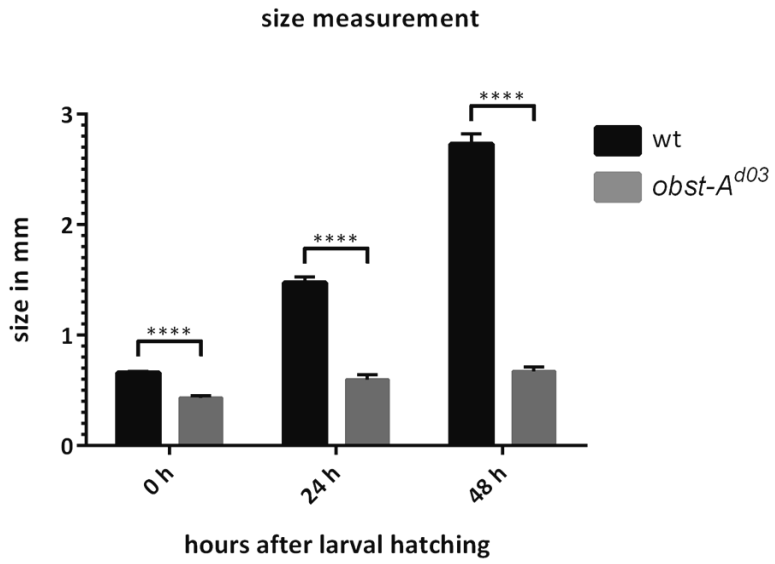

Fig. 3.2.1 - Quantification of the growth defect in *obst-A*^{d03} null mutant larvae. Grey bars: *obst-A*^{d03} mutant larvae; black bars: wild type (wt) control larvae. y-axis: larval size in mm. x-axis: hours after larval hatching. 0 h: freshly eclosed first instar larvae; 24 h: wild type control has reached early second instar stage (*obst-A* mutant arrested in L1); 48 h: wild type control has reached early third instar stage (*obst-A* mutant still arrested in L1, only very few *obst-A* mutant larvae survive for 48 h). n=10 larvae were measured for each condition. Error bars represent SEM. ****p<0.0001.

As seen in Fig. 3.2.1 *obst-A* mutants basically do not grow at all, whereas wild type control larvae increase in size from less than 1 mm in first instar stage to about 3 mm in early third instar stage. Already upon larval hatching *obst-A* mutants were found to be significantly smaller than the control and this size difference became even bigger as development progressed. At 48 h after larval hatching, the few surviving *obst-A* mutant larvae were about the same size as freshly eclosed control larvae.

In addition to the growth defect, *obst-A* null mutants have an epidermal phenotype as cuticle stability tests (Galko & Krasnow, 2004) in *obst-A* mutant larvae revealed a severe epidermal cuticle integrity defect. When pricking wild type larvae laterally with a thin glass needle, they survive well with little or no bleeding. *Obst-A* mutants in contrast suffer from major injury after pricking as vital organs directly spill out resulting in immediate larval death

(Petkau et al., 2012). The molecular function of Obst-A in the epidermal cuticle, however, was not investigated in the study of Petkau et al., 2012, and is subject of my thesis. The cuticle integrity test that was already performed in Petkau et al., 2012, was repeated and larval survival after wounding was quantified (Fig. 3.2.2).

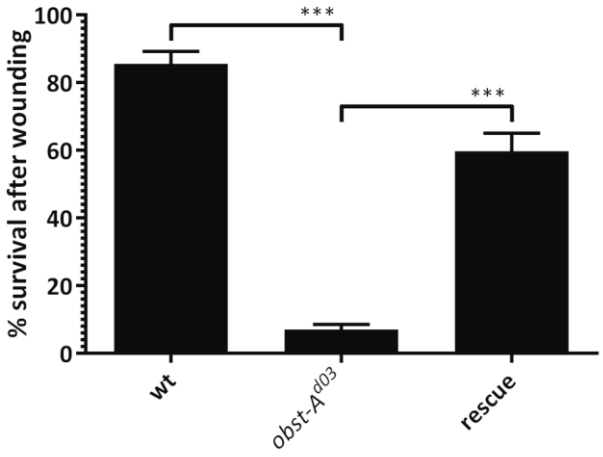

Fig. 3.2.2 - Quantification of survival after wounding. y-axis: % survival of animals after gentle lateral pricking with a thin glass needle. x-axis: analyzed genotype**.** The cuticle integrity test was performed in early first instar wild type control larvae (wt), *obst-A*^{d03} null mutant larvae and *obst-A* rescue larvae (*obst-A*^{d03}/y; UAS *obst-A*/CyO; 69B Gal4/+). n≥30 larvae for each condition. Error bars represent SEM. ***p<0.001.

In the wild type 85 % of larvae survived the pricking, whereas only 7 % of *obst-A* mutants survived. The other 93 % died immediately due to organ spill out. The epidermal integrity phenotype could be partly rescued by re-expression of *obstructor-A* in the mutant background resulting in about 60 % survival after wounding.

3.2.1.2 - Body shape and epidermal cuticle structure is severely affected in *obstructor-A* mutants

To further investigate the epidermal integrity defect in *obst-A* mutants, the overall architecture of the epidermal cuticle in both mutants and wild type larvae was analyzed. This was assessed by generating JB-4 sections and staining them with Chitin Binding Probe, which specifically labels chitin (Fig. 3.2.3).

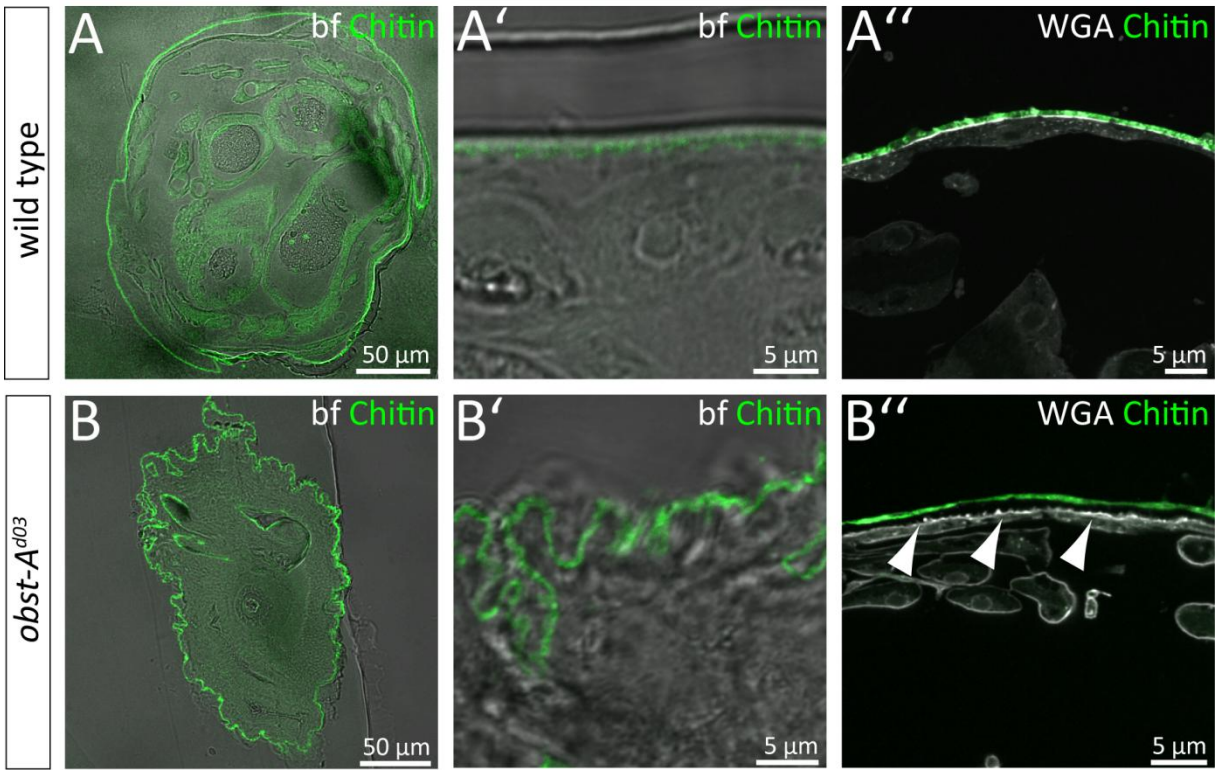

Fig. 3.2.3 - Cuticle structure and body shape is severely compromised in *obst-A* null mutants. Representative immunostaining of JB-4 sections generated from late first instar larvae. A-A'': wild type control. B-B'': *obst-A*^{d03} mutant. All images (A-B'') show chitin staining (CBP) in the procuticle in green. Brightfield (bf) images are shown in A-B'. WGA staining is depicted in A'' and B''. Size of scale bars is indicated in each picture. Note that in 97% of wild type control larvae (n=27) body shape is circular (A) and the epidermal chitin layer, which is seen as a green line surrounding the body, is smooth and even (A, magnification in A'). In contrast, the chitinous cuticle in 54% of *obst-A*^{d03} mutant larvae (n=24) is completely wrinkled (B, magnification in B') resulting in deformed body shape. In the wild type (A'') the chitinous cuticle (marked in green) directly lies on top of the epidermal cells (marked in grey by WGA staining), whereas 29 % of *obst-A*^{d03} mutant larvae show a detachment phenotype in which the cuticle segregates from the epidermal cells (B''). The gap in between the epidermal cell surface and the procuticle is marked by arrow heads in B''.

In wild type larvae the epidermal cuticle evenly lines a roundish body as seen by chitin staining in Fig. 3.2.3 and the chitin layer is connected to the epidermal cells. In *obst-A*^{d03} mutants, however, cuticle structure is compromised. Body shape was massively deformed in half of the investigated *obst-A* mutants, which displayed a completely wrinkled, ragged chitinous cuticle. This constitutes a novel phenotype that has never been observed upon loss of any known cuticle regulator. The intensity of chitin staining was comparable in wild type and mutant larvae, but cuticle organization was strongly affected in the mutant. In about one third of *obst-A*^{d03} mutants detachment of the cuticle from the epidermal cells was observed.

These results show that loss of *obst-A* causes significant defects in cuticle structure. On the other hand, overexpression of *obst-A* in cuticle producing organs using the ectoderm-specific 69B Gal4 driver line (Brand & Perrimon, 1993; Huang et al., 2005) did not lead to any visible phenotype (data not shown). A pUAST-*obst-A GFP* vector was cloned and UAS Obst-A GFP reporter fly lines were established. Larvae expressing *obst-A GFP* under control of the 69B Gal4 driver line showed strong *obst-A GFP* signals in all ectodermal tissues including the epidermis, but survived normally to adulthood (chapter 3.3.5). Apparently loss of *obst-A* is detrimental for epidermal cuticle structure and for survival of larvae, whereas overexpression of *obst-A* does not have any obvious biological consequences.

3.2.2 - Obstructor-A is expressed in ectodermal tissues throughout larval development

In embryos expression of Obst-A was shown in tracheal tube lumina and at the epidermal cell surface (Petkau et al., 2012). To enable further functional characterization of Obst-A in tissues other than the trachea, an expression study in larvae was conducted. For this wild type larvae were dissected or sectioned and stained with an antibody that specifically recognizes the C-terminus of the Obst-A protein. In *obst-A* null mutants no staining is detected when using this antibody (data not shown).

In third instar wild type larvae Obst-A expression was detected in the epidermis (Fig. 3.2.4 A-A'') and the lumina of the tracheal system (Fig. 3.2.4 B-B''), which is in line with the embryonic expression data in Petkau et al., 2012. In the epidermis Obst-A was detected in the epidermal cells and in lower levels within the chitinous procuticle. Obst-A signal was enriched in the cuticle assembly zone, which is located above the apical cell surface (chapter 1.4.1). Strong colocalization of Obst-A with chitin was observed at the lowest chitin lamella. The epidermal localization of Obst-A is further studied in chapter 3.2.3.

Additionally, Obst-A staining was found in the ectodermal parts of the gut such as the proventriculus (Fig. 3.2.4 C-C'') and in the imaginal discs (Fig. 3.2.4 D-D''). In the imaginal discs Obst-A signal was weak except for a few cells strongly positive for Obst-A that were found in clusters located mostly near the margins of the discs.

Obst-A staining in the hormone producing ring gland (Fig. 3.2.4 E-E'') is analyzed in detail in chapter 3.3.4.

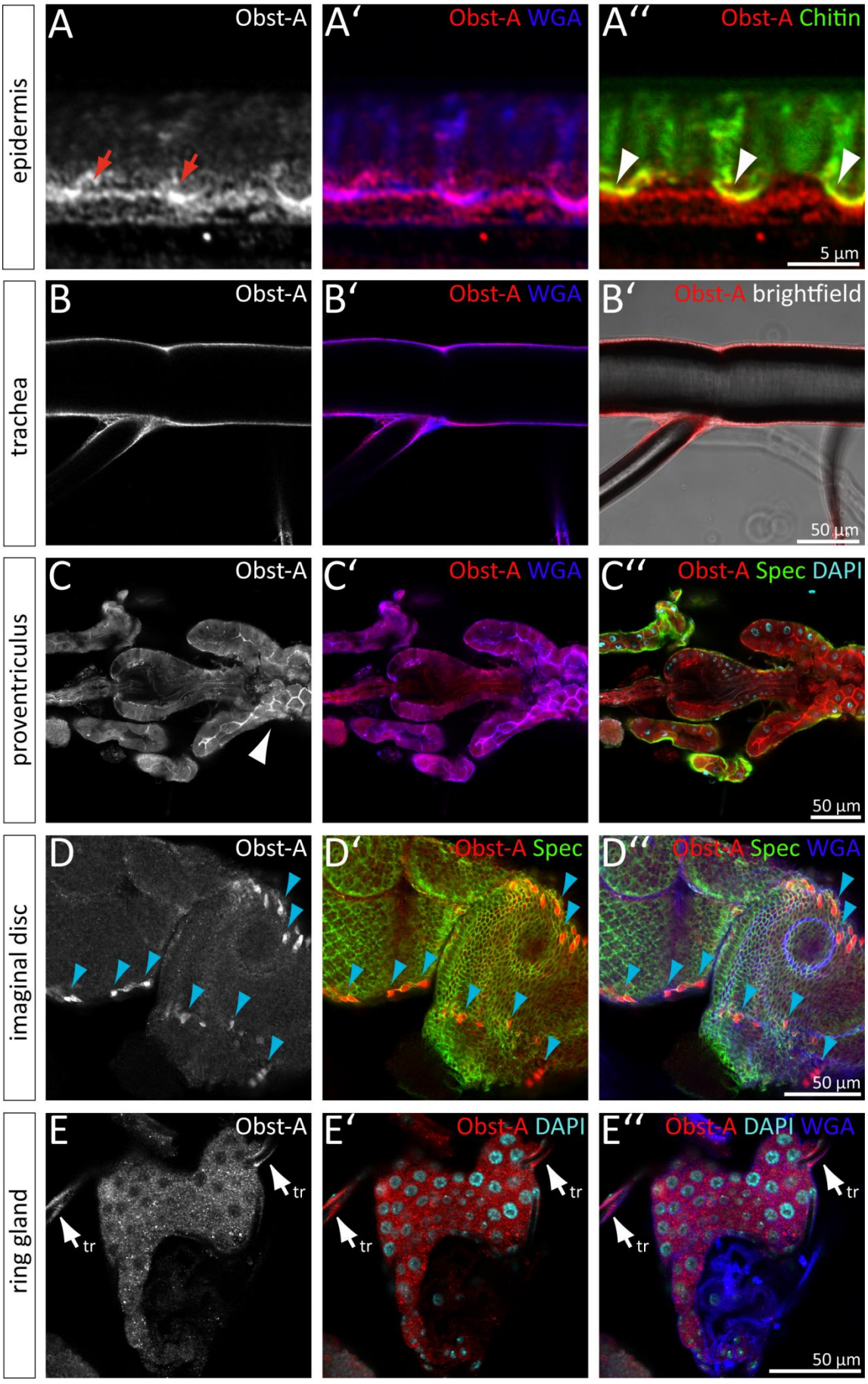
epidermis
A
Obst-A
A'
Obst-A WGA
A''
Obst-A Chitin
5 µm
trachea
B
Obst-A
B'
Obst-A WGA
B'
Obst-A brightfield
50 µm
proventriculus
C
Obst-A
C'
Obst-A WGA
C''
Obst-A Spec DAPI
50 µm
imaginal disc
D
Obst-A
D'
Obst-A Spec
D''
Obst-A Spec WGA
50 µm
ring gland
E
Obst-A
tr
tr
E'
Obst-A DAPI
tr
tr
E''
Obst-A DAPI WGA
tr
tr
50 µm

Fig. 3.2.4

Fig. 3.2.4 - Obst-A is expressed in various tissues of ectodermal origin. Representative immunofluorescent stainings of JB-4 sections (A-A'') and whole mount preparations (B-E'') of wild type third instar larvae. A to E show staining with anti-Obst-A (single channel) in grey. A' to E' and A'' to E'' show costainings of Obst-A (in red) with various other markers as indicated in the figure. A', B', C', D'', E'': WGA, a fluorescently linked lectin that marks sugar residues e.g. in chitin structures and at cell surfaces, in blue; A'': Chitin marked by CBP (Chitin Binding Probe), in green; C'', D', D'': staining with anti-Spec (α-Spectrin), which labels cell membranes, in green; C'', E', E'': DAPI, which stains nuclei, in cyan. Brightfield image is depicted in B''. Size of scale bars is indicated in the respective images. The analyzed tissues are specified on the left side. A-A'': Obst-A staining is found in the epidermis. Obst-A signal is detected in the epidermal cells (bottom) and the epidermal procuticle. The strongest Obst-A staining is detected between the apical epidermal cell surface and the chitinous procuticle. The enrichment of Obst-A signal is indicated by red arrows in A. Obst-A staining overlaps with the WGA signal in A', which is also enriched in the cuticle assembly zone. The dimensions of the procuticle can be seen by the chitin staining in A''. Colocalization of Obst-A staining and chitin staining at the lowest chitin lamella in A'' is marked by white arrowheads. B-B'': Obst-A staining is detected in the lumina of the tracheal system. The luminal localization of Obst-A can be seen in the costaining with WGA (B') and in the merge of Obst-A signal and the brightfield image (B''). C-C'': In the proventriculus Obst-A signal is found both in the cytoplasm and enriched at the cell surfaces (as indicated by the white arrowhead in C). The enrichment of Obst-A at cell surfaces is in complete colocalization with the WGA staining (C'). Colabeling of Obst-A with α-Spectrin and DAPI is depicted in C''. D-D'': Weak overall Obst-A staining can be seen in imaginal discs. The blue arrowheads indicate small groups of single cells that are located near the margins of the discs and stain strongly for Obst-A. The localization of strong Obst-A signal in single cells can be seen in the costaining with α-Spectrin (D'; D'') and WGA (D''). E-E'': Cytoplasmic Obst-A staining is detected in a dotty vesicle-like pattern in the endocrine ring gland. The absence of Obst-A in the nuclei is made clear by the DAPI costaining in E'. Colabeling of Obst-A with WGA and DAPI is shown in E''. The arrows labeled with "tr" point at small trachea near the ring gland that also show Obst-A staining.

Highly similar expression results were yielded for earlier larval stages (data not shown). Altogether, these data indicate that throughout larval development Obst-A is expressed in several different tissues of ectodermal origin, which include but are not limited to chitin-producing organs.

3.2.3 - Obstructor-A is a chitin-binding protein enriched at the epidermal cuticle assembly zone

As *obst-A* null mutants showed severe epidermal cuticle integrity defects and strongly altered body shape, a function in the epidermal cuticle was hypothesized. To investigate the role of Obst-A in the epidermal cuticle, next, its localization in the epidermal cuticle and the underlying cells was analyzed in different larval stages by immunofluorescent labeling showing that Obst-A is found in the epidermal cuticle throughout larval development (Fig. 3.2.5).

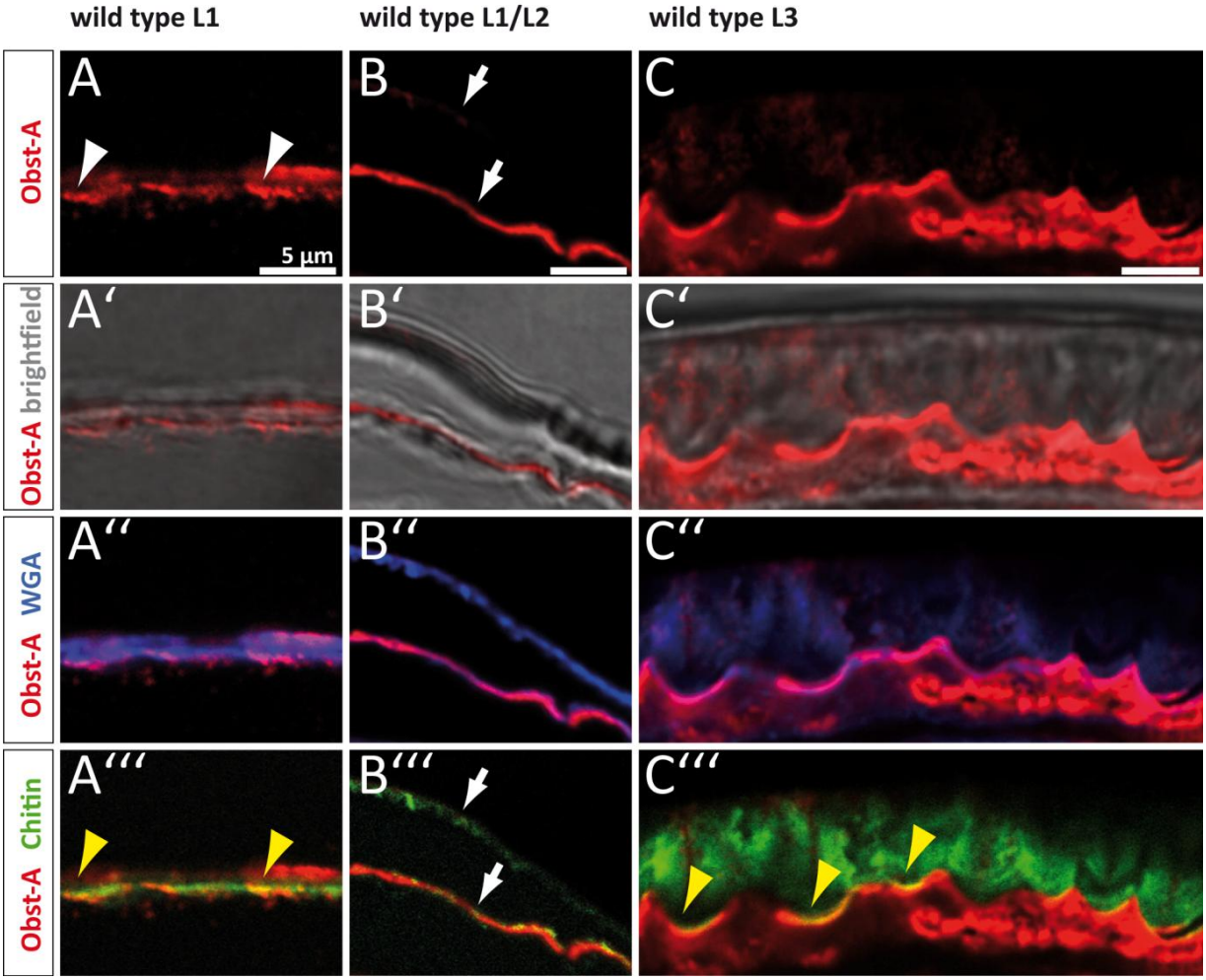

Fig. 3.2.5

Fig. 3.2.5 - Obst-A localizes to areas of cuticle assembly throughout larval development. Representative immunofluorescent stainings of JB-4 sections of wild type larvae. Left panel (A to A'''): first instar; middle panel (B to B'''): first to second instar transition; right panel (C to C'''): third instar. The upper panel (A-C) shows single channel Obst-A staining in red. The second beneath (A'-C') displays the overlay of the bright field image and Obst-A staining (red). In the third panel (A''-C'') Obst-A (red) costaining with WGA (blue) is depicted and in the lowest panel (A'''-C''') Obst-A (red) costaining with chitin (CBP, green) is illustrated. In the first instar stage (A to A''') Obst-A is found throughout the cuticle with strong enrichment at the lowest part of the chitinous procuticle (white arrowheads in A) where it partially colocalizes with chitin (yellow arrowheads in A'''). At the transition from first to second instar stage (B-B''') two distinct cuticles (arrows in B and B''', note the two chitin layers in B''') can be detected. These constitute the old cuticle that is degraded during the molt (upper cuticle) and the new cuticle that is established at the same time (lower cuticle). Obst-A staining is predominantly detected in the new, lower cuticle, whereas only very faint Obst-A signal is found in the old, upper cuticle that is prone to degradation (arrows in B). During the third instar stage (C-C''') very strong Obst-A expression is seen within the epidermal cells and weaker Obst-A signal is found within the chitinous procuticle along the chitin lamellae. Obst-A staining is strongly enriched above the apical epidermal cell surface in the cuticle asembly zone. Partial colocalization of Obst-A with the lowest chitin lamella is indicated by yellow arrowheads in C'''. Scale bars represent 5 µm. Adapted from Pesch et al., 2015.

This analysis of epidermal Obst-A expression throughout all larval stages suggests that Obst-A is localized wherever new cuticle material is deposited. In the first instar stage Obst-A could be detected throughout the entire chitinous cuticle, but staining was enriched in the lower part of the procuticle where new chitin material is deposited (Fig. 3.2.5 A'''). During molting, when at the same time the old cuticle is degraded and a new cuticle is formed (Chaudhari et al., 2011), Obst-A was observed to be present in high levels within the entire new cuticle, while only faint Obst-A staining was detected in the old cuticle that undergoes degradation (Fig. 3.2.5 B'''). In the third instar stage, which marks the developmental phase in which most cuticle synthesis occurs with about one new lamella being added each hour (Kaznowski et al., 1985), very strong Obst-A expression was found in the epidermal cells and with special enrichment in the cuticle assembly zone. The localization of Obst-A in the cuticle assembly zone is also seen in Fig. 3.1.1. and 3.2.4.

Importantly, electron microscopy data by our cooperation partner Dietmar Riedel, Max Planck Institute Göttingen, revealed that the cuticle assembly zone is absent and lamellar chitin arrangement is disturbed in *obst-A* mutants (Supplementary Fig. S3). This represents an important finding for the study of Obst-A function, linking its role in the epidermal cuticle to the assembly zone.

In third instar larvae (Fig. 3.2.5 C-C''') Obst-A signal could also be detected scattered along the chitin lamellae, in partial colocalization with chitin. Obst-A staining at the lamellae is seen more clearly in Fig. 3.2.6.

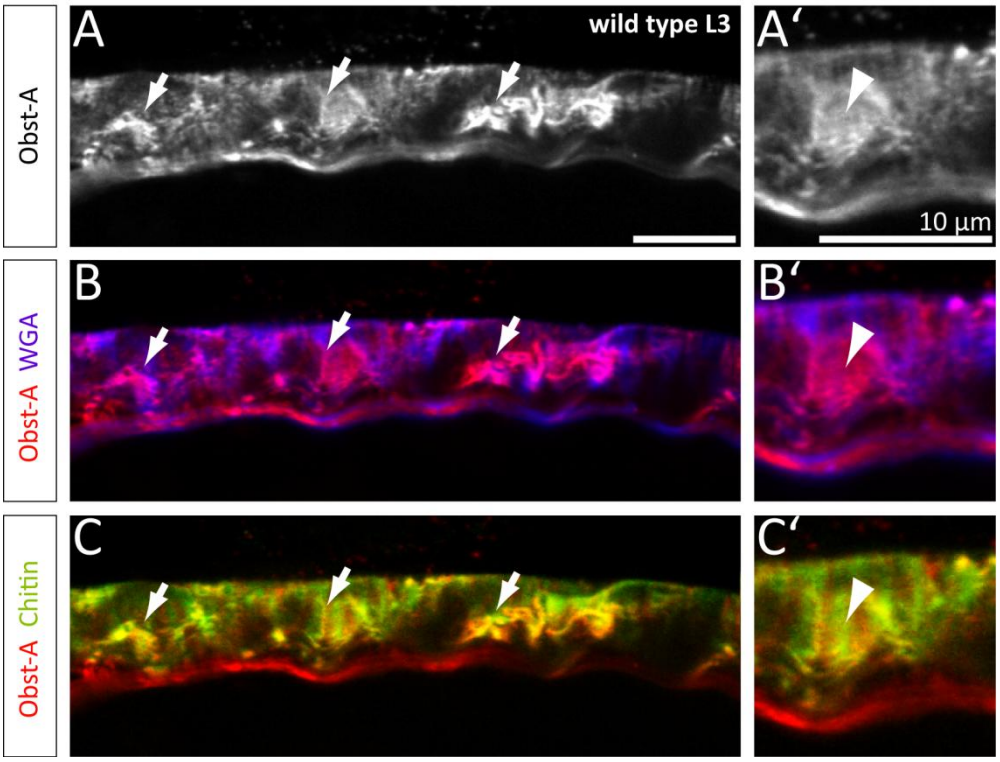

Fig. 3.2.6 - Obst-A is expressed in the larval epidermis and binds to lamellar chitin. Representative immunofluorescent stainings of JB-4 sections of wild type third instar larvae. A and the magnification in A' show staining with anti-Obst-A (single channel) in grey. Obst-A staining is detected in the epidermal cells but also found within the chitinous procuticle. Distinct chitin lamellae can be seen in the Obst-A single channel proving that Obst-A binds to lamellar chitin. In B and the magnification in B' colabeling of Obst-A (red) and chitin (CBP, green) is depicted. Yellow areas represent partial colocalization of Obst-A and chitin staining at lamellae. In C and the magnification C' costaining of Obst-A (red) and WGA (blue) is illustrated with colocalizing signals appearing in pink color. Staining of Obst-A at chitin lamellae is indicated by arrows in the left panel (A-C) and arrowheads in the magnifications in the right panel (A'-C'). Scale bars represent 10 µm.

In the epidermal cuticle WGA staining was detected in the chitin layer with enrichment at the apical cell surface of the epidermal cells. Chitin staining appeared in stacked horizontal lines, which represent the distinct chitin lamellae (Fig. 3.2.6).

Obst-A staining was not only detected within the epidermal cells, but also within the procuticle, in partial colocalization with the chitin lamellae (Fig. 3.2.6). It was previously shown in biochemical assays that the chitin-binding protein Obst-A is indeed capable of

binding to chitin (Petkau et al., 2012; data Matthias Behr). Thus, it can be concluded that Obst-A associates with the chitin lamellae of the epidermal cuticle.

3.2.4 - Obstructor-A builds a network with other factors for epidermal cuticle assembly and organization

The previously described results show that Obst-A localizes to the cuticle assembly zone and that loss of *obst-A* severely affects cuticle structure. To find out more about Obst-A function, its interaction with already described factors that are important in the epidermal cuticle was investigated. But as knowledge about these proteins is limited, at first their mRNA and protein expression had to be analyzed. Subsequently *obst-A* mutants were examined for possible changes in the expression and/or localization of these factors.

3.2.4.1 - The chitin deacetylases Serpentine and Vermiform are enriched in the cuticle assembly zone and the chitin protecting protein Knickkopf is localized within the chitinous procuticle

The chitin deacetylases Serpentine (Serp) and Vermiform (Verm) are implicated in the maturation of chitin-matrices, most probably by the conversion of chitin into chitosan (Luschnig et al., 2006; Wang et al., 2006), and the Knickkopf (Knk) protein protects chitin in the cuticle (Moussian et al., 2006b) (introduction chapter 1.5.2).
In the tracheal system Obst-A builds a complex with Serp and Knk to preserve chitin structures (Petkau et al., 2012) suggesting that Obst-A could interact with these two factors in the epidermal cuticle as well.
The localization of the deacetylase Serp, the highly similar Verm and the chitin protector Knk and their mRNA expression profile is depicted in Fig. 3.2.7.

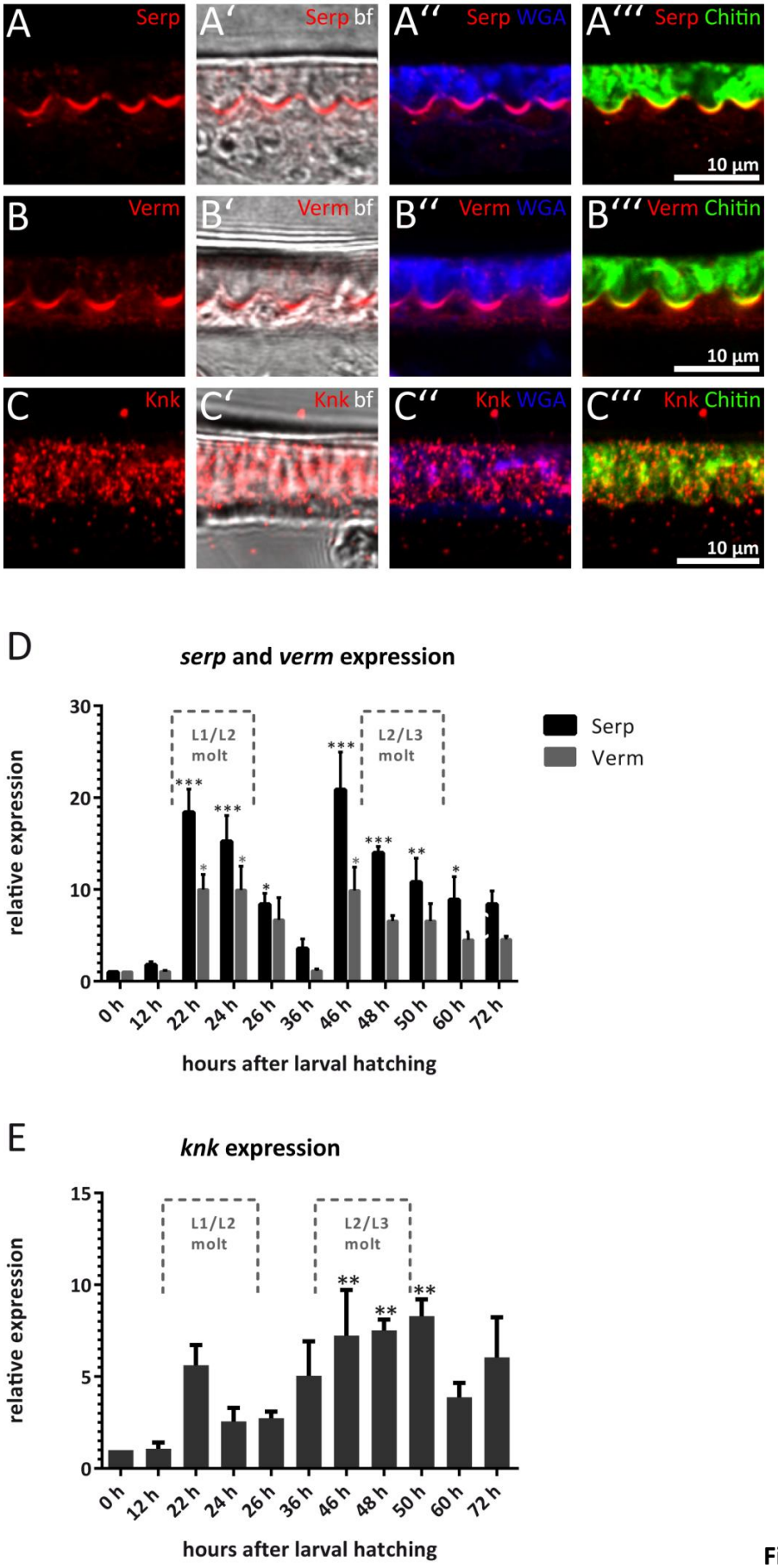
A
Serp
A′
Serp bf
A″
Serp WGA
A‴
Serp Chitin
10 µm
B
Verm
B′
Verm bf
B″
Verm WGA
B‴
Verm Chitin
10 µm
C
Knk
C′
Knk bf
C″
Knk WGA
C‴
Knk Chitin
10 µm
D
serp and verm expression
relative expression
30
20
10
0
L1/L2 molt
L2/L3 molt
Serp
Verm
0 h
12 h
22 h
24 h
26 h
36 h
46 h
48 h
50 h
60 h
72 h
hours after larval hatching
E
knk expression
relative expression
15
10
5
0
L1/L2 molt
L2/L3 molt
hours after larval hatching

Fig. 3.2.7

Fig. 3.2.7 - Protein localization and mRNA expression of the cuticle factors Serp, Verm and Knk. A-C''': Representative immunofluorescent staining of Serp (A-A'''), Verm (B-B''') and Knk (C-C''') on JB-4 sections of third instar wild type larvae. The left panel shows single channel Serp (A), Verm (B) and Knk (C) staining in red. In the second panel the merge of the Serp (A'), Verm (B') and Knk (C') staining (all in red), respectively, and the corresponding bright field image is depicted. In the third panel costainings of WGA (blue) with Serp (A''), Verm (B'') and Knk (C'') (all in red) and in the right panel costainings of Chitin (CBP, green) and Serp (A'''), Verm (B''') and Knk (C''') (all in red) are shown. Both Serp (A-A''') and Verm (B-B''') localize predominantly to the cuticle assembly zone and are found in partial colocalization with the lowest chitin lamella. Knk staining (C-C''') is distributed in a dotty pattern in the entire chitinous procuticle. Scale bars indicate 10 µm. D, E: Temporal profile of *serp, verm* (D) and *knk* (E) mRNA expression throughout larval development. n≥5. y-axis: relative expression normalized to the housekeeping gene *rp49*. x-axis: different time points of analysis. The expression at the 0 h time point, corresponding to larval hatching, is set to 1. Error bars represent SEM. Note that *serp* (black bar) and *verm* (grey bar) have a similar expression profile showing upregulation when molting occurs. *Knk* expression also peaks upon molting and is generally elevated during third instar stage. Adapted from Pesch et al., 2015.

In immunofluorescent stainings both Serp and Verm were mostly detected in the cuticle assembly zone at the apical cell surface, also localizing to the lowest chitin lamella. This represents the identification of two more molecular markers of the assembly zone (Fig. 3.2.7 A, B). In contrast, Knk was localized throughout the entire procuticle with a weak enrichment seen at the apical cell surface (Fig. 3.2.7 C).

Regarding *serp* and *verm* mRNA levels a similar expression pattern was detected showing strong upregulation during both the first to second and the second to third instar larval molt (Fig. 3.2.7 D). Also *knk* levels were found to be increased during molting. After the peak at second molt *knk* levels stayed elevated (Fig. 3.2.7 E). The localization of Serp and Verm in the assembly zone and the localization of Knk in the procuticle and the upregulation of all three factors upon molting suggests an important function in the epidermal cuticle.

3.2.4.2 - Serpentine and Vermiform are mislocalized and their gene expression is downregulated in *obstructor-A* mutants

Next the localization of Serp and Verm in *obst-A*^{d03} mutants was determined and indeed, differences to the wild type were detected (Fig. 3.2.8).

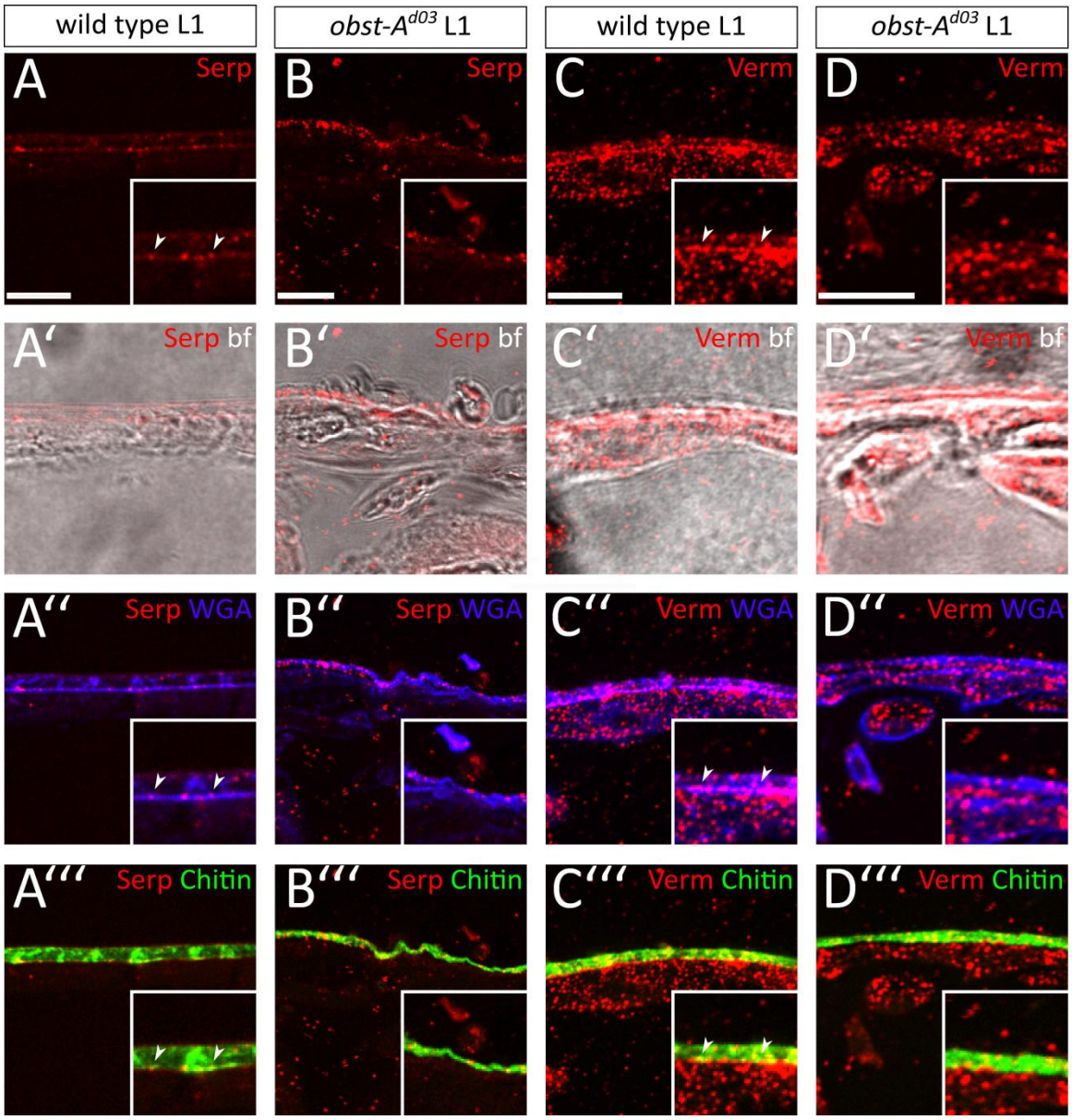

Fig. 3.2.8 - Serp and Verm are mislocalized in *obst-A*^{d03} mutants. Representative immunofluorescent staining of Serp (A-A'''; B-B''') and Verm (C-C'''; D-D''') using JB-4 sections of third instar wild type larvae. First panel (A-A''') and third panel (C-C'''): wild type control, first instar. Second panel (B-B''') and fourth panel (D-D'''): *obst-A*^{d03} mutant, first instar. A-D show single channel Serp (A, C) and Verm (B, D) staining in red. A'-D': Serp (A', C') and Verm (B', D') staining (red) is depicted together with the brightfield image. A''-D'' illustrates costaining of Serp (A'', C'') and Verm (B'', D'') with WGA (blue). A'''-D''': Costaining of Serp (A''', C''') and Verm (B''', D''') (red) is shown together with chitin staining (CBP, green). Insets show magnifications of the epidermal cuticle. In wild type larvae Serp (A'-A''') and Verm (C'-C''') can be found throughout the cuticle and clear enrichment at the cuticle assembly zone is seen (indicated by arrowheads in the insets). In *obst-A*^{d03} mutants, however, this enrichment is absent and Serp (B-B''') and Verm (D-D''') are mislocalized throughout the entire cuticle. Scale bars indicate 10 µm. Adapted from Pesch et al., 2015.

Already in first instar larvae an enrichment of Serp and Verm staining at the cuticle assembly zone was observed (Fig. 3.2.8) where the two deacetylases were found at the lowest chitin lamella. In contrast, in *obst-A* null mutants, which were shown to lack the assembly zone, Serp and Verm were diffusely localized throughout the whole cuticle and appeared in small aggregates (Fig. 3.2.8). qRT-PCR analysis revealed that *serp* and *verm* mRNA expression is altered in *obst-A* deficient larvae (Fig. 3.2.9).

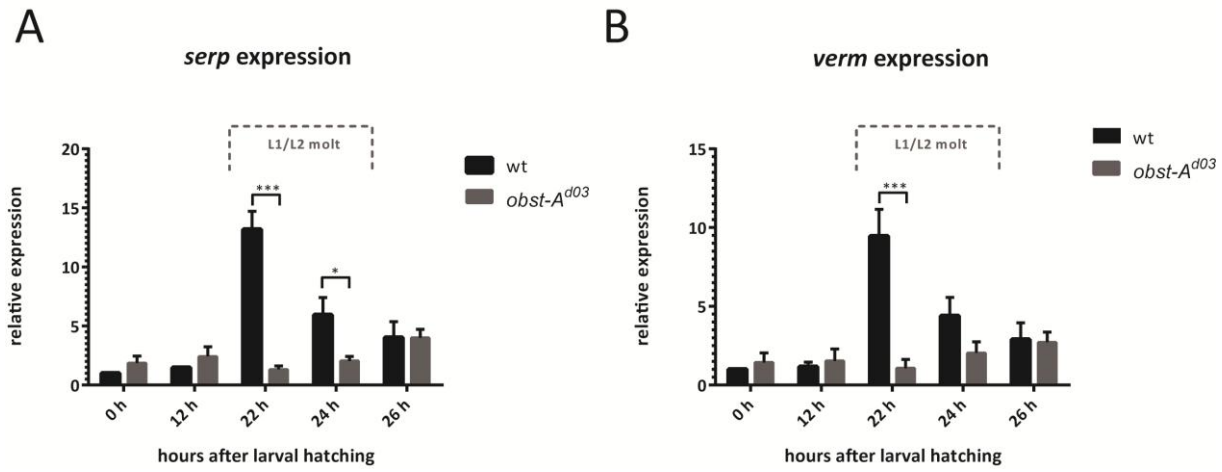

Fig. 3.2.9 - S*erp* and *verm* mRNA expression is misregulated in *obst-A*^{d03} mutant larvae. n≥5 for each condition. Grey bars: *obst-A*^{d03} mutant larvae; black bars: wild type (wt) control larvae. y-axis: relative expression normalized to the housekeeping gene *rp49*. x-axis: different time points of analysis. The expression at the 0 h time point, corresponding to larval hatching, is set to 1. Error bars represent SEM. Both *serp* (A) and *verm* (B) expression are elevated at the molt from first to second instar stage in the wild type. In *obst-A*^{d03} mutants that are not capable of reaching second instar stage this upregulation is absent, but a small elevation in *serp* and *verm* mRNA levels is detected at the latest investigated time point shortly before larval death.

In *obst-A*^{d03} mutants *serp* and *verm* expression was found to be significantly lower than in the wild type at 22 h after larval hatching, which corresponds to the time point when normally larval molting occurs. In *obst-A* mutant larvae, which are not capable of molting, only shortly before larval death a slight upregulation of *serp* and *verm* levels was detected, but expression levels as in the wild type were not reached.

As Serp and Verm play a role in maturation of chitin and thereby enhance chitin-matrix stability (Luschnig et al., 2006; Wang et al., 2006), the misexpression of the deacetylases in the *obst-A* mutant most probably contributes to its severe epidermal integrity defect.

3.2.4.3 - Knickkopf localization is unaffected, but its expression is upregulated in *obstructor-A* mutants shortly before their death

To test if the cuticle-matrix defects in the *obst-A* mutants might originate from compromised protection of chitin, localization and expression of Knk was investigated (Fig. 3.2.10).

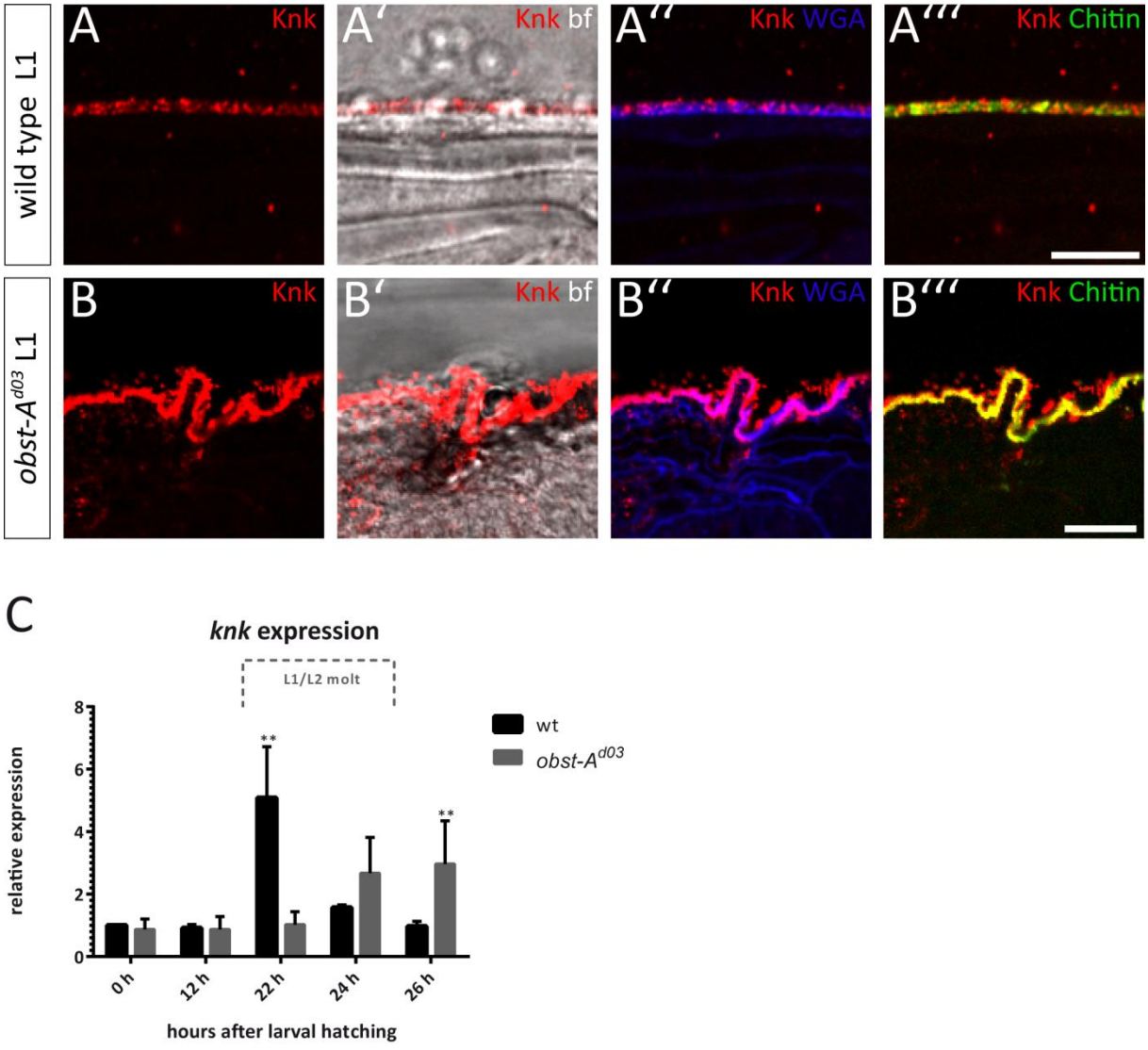

Fig. 3.2.10 - Knk is not mislocalized, but its mRNA expression is misregulated in *obst-A*^{d03} mutants. A-B''': Immunofluorescent stainings on JB-4 sections. A-A''': wild type late first instar; B-B''': late stage *obst-A*^{d03} mutant. Single channel Knk staining (A, B) is shown in red. The overlay of Knk staining (red) with the brightfield image (A', B'), WGA staining (blue; A'', B'') and chitin staining (CBP, green; A''', B''') is illustrated. In the wild type (A-A''') Knk staining appears in a dotty pattern (A) and is restricted to the chitinous procuticle that is visible in the brightfield image (A') and is marked by WGA (A'') and chitin staining (A'''). Knk is seen in partial colocalization with chitin. In the *obst-A* mutant (B-B''') the chitin layer is wrinkled, but Knk normally localizes to the procuticle (B, B'). Obst-A signal strongly overlaps with WGA (B'') and chitin staining (B'''). In comparison to the wild type Knk levels seem to be enriched in the

procuticle. C: B: qRT-PCR analysis of *knk* mRNA expression in both wild type (wt, black bars) and *obst-A*^{d03} mutant (grey bars) larvae. n≥5 for each condition. y-axis: relative mRNA expression normalized to the housekeeping gene *rp49*. x-axis: different time points of analysis. The expression at the 0 h time point, corresponding to larval hatching, is set to 1. Error bars represent SEM. Note that the expression of *knk* is upregulated in the wild type when molting occurs. In the *obst-A* mutant, which cannot molt, this peak expression is absent, but *knk* levels are elevated at later time points shortly before most *obst-A* deficient larvae die. Scale bars show 10 µm. Adapted from Pesch et al., 2015.

In *obst-A*^{d03} mutants Knk was found normally distributed throughout the defective, wrinkled chitin-matrix where it strongly colocalized with chitin (Fig. 3.2.10 B'''). In comparison to wild type late first instar larvae (Fig. 3.2.10 A''') Knk seemed to be present in higher levels in late *obst-A* mutant larvae. Indeed, mRNA expression of Knk was elevated shortly before larval death, whereas the *knk* peak that is normally present in the wild type when it undergoes molting was absent in *obst-A* deficient larvae (Fig. 3.2.10 C).

3.2.4.4 - Knockdown of *serpentine*, *vermiform* and *knickkopf* causes epidermal integrity defects, lethality, defective chitin-matrix organization and reduction of Obstructor-A in the assembly zone

As described above alterations in expression and localization of known cuticle factors were detected in *obst-A* null mutant larvae, which might contribute to the severe cuticular defects in the mutant. Vice versa, the effect of reduction of these factors on cuticle structure and Obst-A expression was analyzed.

Serp, *verm* and *knk* null mutants are embryonic lethal (data not shown). Thus, knockdown larvae were used for studies in larval stages in which levels of *serp*, *verm* and *knk*, respectively, were reduced using the 69B Gal4 driver line that leads to RNAi-mediated knockdown in cuticle forming organs. Knockdown efficiency ranged between 88 and 93% (data not shown). To check for cuticle integrity defects in the knockdown larvae the wounding assay, in which larvae are gently pricked with a glass needle, was conducted (Fig. 3.2.11).

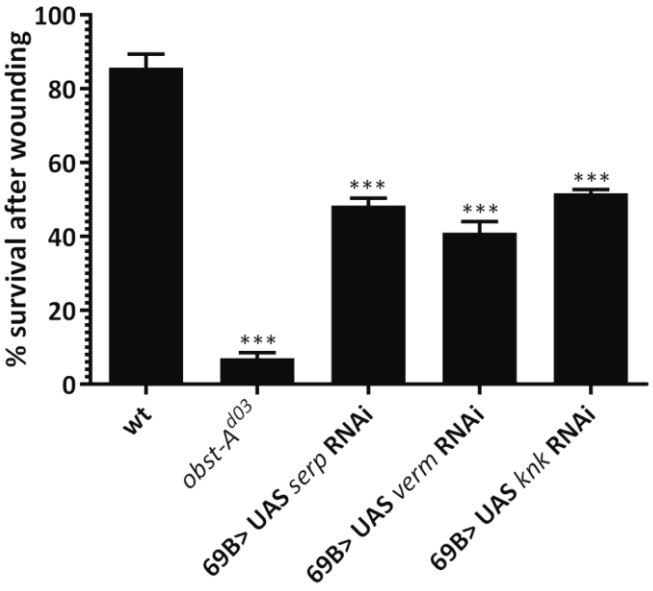

Fig. 3.2.11 - Quantification of survival after wounding in *serp*, *verm* and *knk* knockdown larvae. y-axis: % survival of animals after gentle lateral pricking with a thin glass needle. x-axis: analyzed genotype**.** The cuticle integrity test was performed in early first instar wild type control larvae (wt), *obst-A*^{d03} null mutant larvae, 69B Gal4> UAS *serp* RNAi larvae, 69B Gal4> UAS *verm* RNAi larvae and 69B Gal4> UAS *knk* RNAi larvae. n≥30 larvae for each condition. Error bars represent SEM. ***p<0.001.

As shown in Fig. 3.2.11, 85 % of wild type larvae, but only 7 % of *obst-A* deficient larvae survived gentle pricking with a thin glass needle. 69B Gal4> UAS *serp* RNAi, 69B Gal4> UAS *verm* RNAi and 69B Gal4> UAS *knk* RNAi knockdown larvae showed significant cuticle integrity defects as only about 40-55 % of larvae survived the injury. The defects are not as dramatic as in the *obst-A* mutant, but still severe.

To further analyze the phenotype, lethality as well as Obst-A localization was studied in *serp*, *verm* and *knk* knockdown larvae (Fig. 3.2.12).

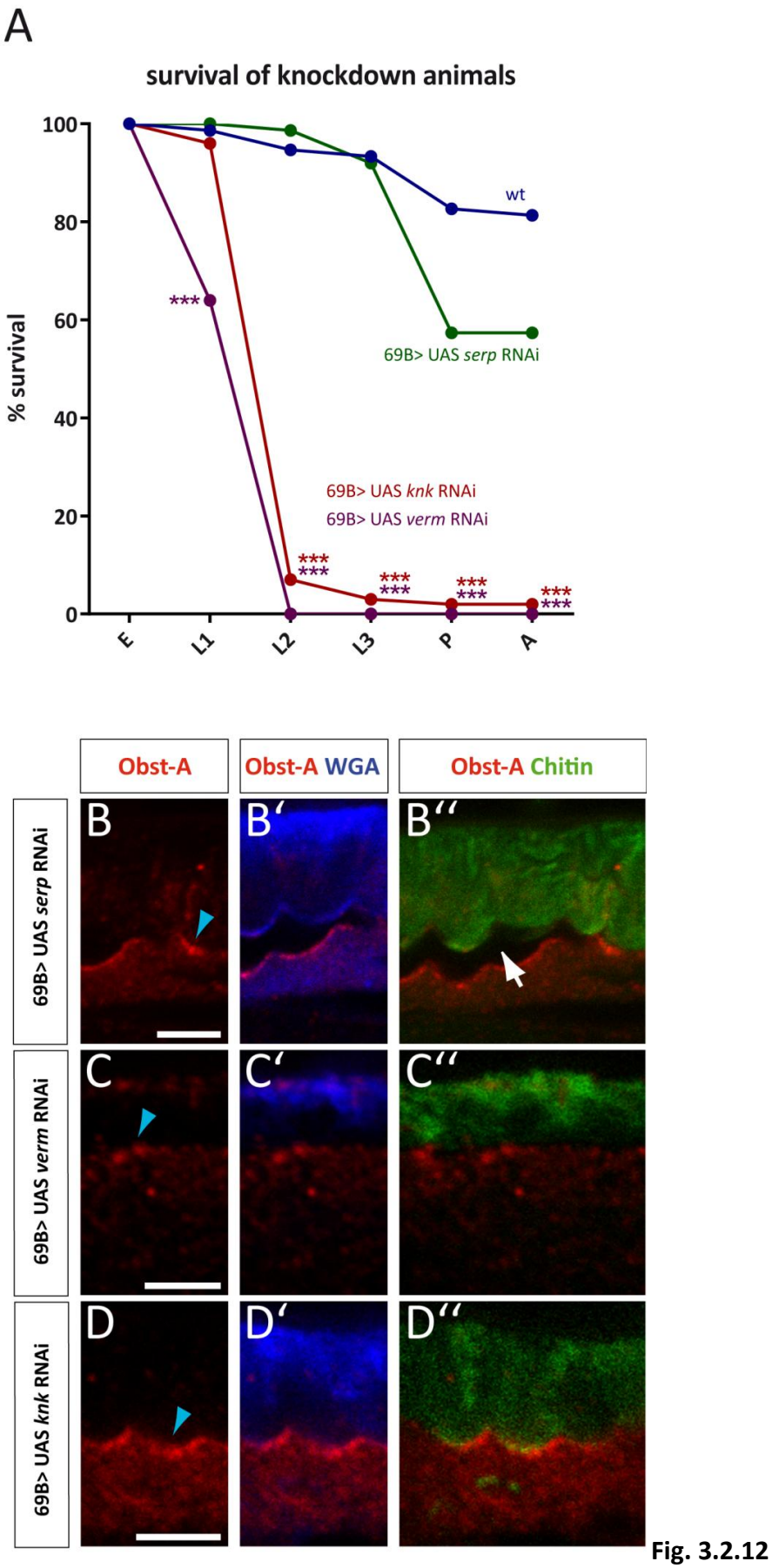
A
survival of knockdown animals
% survival
100
80
60
40
20
0
E
L1
L2
L3
P
A
wt
69B> UAS serp RNAi
69B> UAS knk RNAi
69B> UAS verm RNAi
***
Obst-A
Obst-A WGA
Obst-A Chitin
69B> UAS serp RNAi
69B> UAS verm RNAi
69B> UAS knk RNAi
B
B'
B''
C
C'
C''
D
D'
D''

Fig. 3.2.12

Fig. 3.2.12 - Knockdown of *serp*, *verm* and *knk* is partially lethal and causes cuticle defects. A: Survival of 69B Gal4> UAS *serp*, *verm* and *knk* RNAi knockdown larvae. y-axis: % of knockdown animals surviving to particular developmental stage. x-axis: developmental stage; E: late embryo; L1: first instar; L2: second instar; L3: third instar; P: pupa; A: adult. Dark blue line: wild type (wt); green line: 69B Gal4> UAS *serp* RNAi; purple line: 69B Gal4> UAS *verm* RNAi; dark red line: 69B Gal4> UAS *knk* RNAi. n=4 for each condition, each n includes 25 larvae. The mean of the four experiments is depicted. Statistical analysis was performed with Student's t-test (Microsoft Excel). *** represents $p<0.001$ compared to the wild type control. B-D'': Representative immunofluorescent staining using JB-4 sections of third instar 69B Gal4> UAS *serp*, *verm* and *knk* RNAi knockdown larvae. B-B'': 69B Gal4> UAS *serp* RNAi third instar larvae. C-C'': 69B Gal4> UAS *verm* RNAi third instar larvae. D-D'': 69B Gal4> UAS *knk* RNAi third instar larvae. The left panel (B, C, D) shows single channel Obst-A staining in red. In the middle panel (B', C', D') Obst-A staining (red) is depicted together with WGA staining (blue). The right panel (B'', C'', D'') shows Obst-A staining (red) merged with chitin staining (CBP, green). In 69B Gal4> UAS *serp* RNAi larvae (B-B'') the cuticle detaches from the epidermal cells (see arrow in B''). In all three different knockdown larvae Obst-A enrichment at the apical epidermal cell surface is weak in comparison to the wild type, which is illustrated by blue arrowheads in B, C, D. Scale bars represent 5 µm. Adapted from Pesch et al., 2015.

Null mutants lacking either *knk*, *serp* or *verm* expression are embryonic lethal (data not shown). Even though knockdown efficiency of the different lines was very high (in between 88 and 93 %, data not shown), the small residual expression of *knk*, *serp* and *verm* rescued most *knk* and *verm* knockdown larvae to first instar stage and more than half of *serp* knockdown larvae to adult stage. The strongest lethal phases were seen in *verm* knockdown larvae during late embryogenesis and first instar stage resulting in complete lethality before reaching second instar stage (Fig. 3.2.12). Most *knk* knockdown larvae died during first instar stage and only few animals reached adulthood. *Knk* knockdown animals (n=100) were also strongly developmentally delayed, with 80 % of larvae still in early first instar stage at 24 h after larval hatching when 90 % of wild type control larvae (n=75) had reached second instar stage. Lethality was less severe in *serp* knockdown larvae, which were partially lethal in third instar stage, with a little more than 55 % of larvae surviving to adult stage (Fig. 3.2.12). The survival profile of 69B Gal4> UAS *obst-A* RNAi larvae is depicted in detail later in chapter 3.3.5.

Concerning Obst-A localization in *knk*, *serp* and *verm* knockdown larvae, in third instar animals from all three different genotypes Obst-A staining was very weak. Reduction of Obst-A enrichment at the cuticle assembly zone, when compared to the wild type (Fig. 3.2.5 for comparison), was detected (Fig. 3.2.12). Especially in *verm* knockdown larvae Obst-A was

barely detectable in the assembly zone. Lamellar chitin organization was moderately disturbed in all three knockdowns (Fig. 3.2.12). Strikingly, in many *serp* knockdown larvae the cuticle was detached from the epidermal cells (Fig. 3.2.12B'').

3.2.4.5 - *Serpentine, vermiform* and k*nickkopf* genetically interact with *obstructor-A* to build a network that regulates epidermal cuticle formation and chitin-matrix organization

To further investigate the potential interplay of *obst-A* with *serp*, *verm* and *knk*, transheterozygous animals were generated by crossing of heterozygous *obst-A* mutant females (*obst-A*/FM7actGFP) with either *serp*,*verm*/TM3twiGFP or *knk*/TM3SerGFP heterozygous males. In the offspring some larvae carry one wildtypic and one mutant allele of *obst-A* and either *serp* and *verm* (*obst-A*/+;*serp*,*verm*/+) or *knk* (*obst-A*/+;*knk*/+). Severe epidermal integrity defects in these transheterozygous larvae were detected in wounding assays (Fig. 3.2.13).

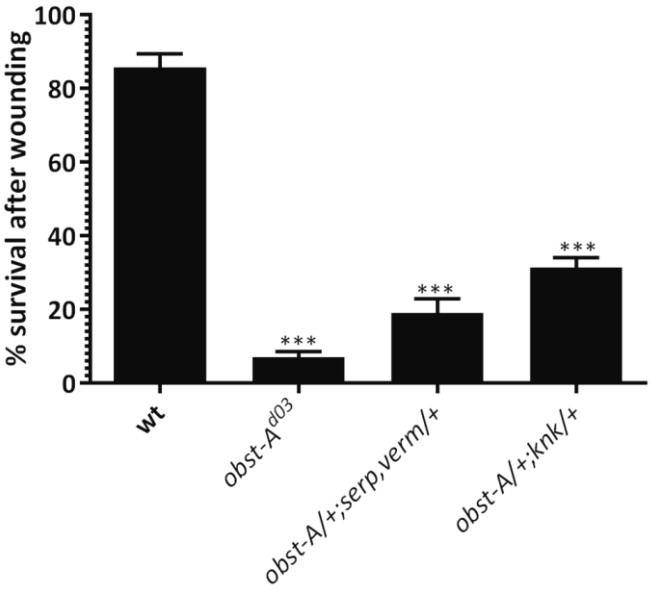

Fig. 3.2.13 - Quantification of survival after wounding in transheterozygous larvae carrying single mutant alleles of either *obst-A*, *serp* and *verm* or *obst-A* and *knk*. y-axis: % survival of animals after gentle lateral pricking with a thin glass needle. x-axis: analyzed genotype**.** The cuticle integrity test was performed in early first instar wild type control larvae (wt), *obst-A*^{d03} null mutant larvae, *obst-A*/+;*serp*,*verm*/+ and *obst-A*/+;*knk*/+ transheterozygous larvae. n≥30 larvae for each condition. Error bars represent SEM. ***p<0.001.

In comparison to the wild type control, in which 85 % of first instar larvae survived the injury, less than 20 % of *obst-A*/+;*serp*,*verm*/+ larvae and less than 40 % of *obst-A*/+;*knk*/+ transheterozygous larvae stayed alive after wounding, indicating highly compromised cuticle integrity. Tremendous structural chitin-matrix defects and mislocalization of the cuticle factors were detected in *obst-A*/+;*serp*,*verm*/+ and *obst-A*/+;*knk*/+ transheterozygous larvae in immunofluorescent stainings (Fig. 3.2.14).

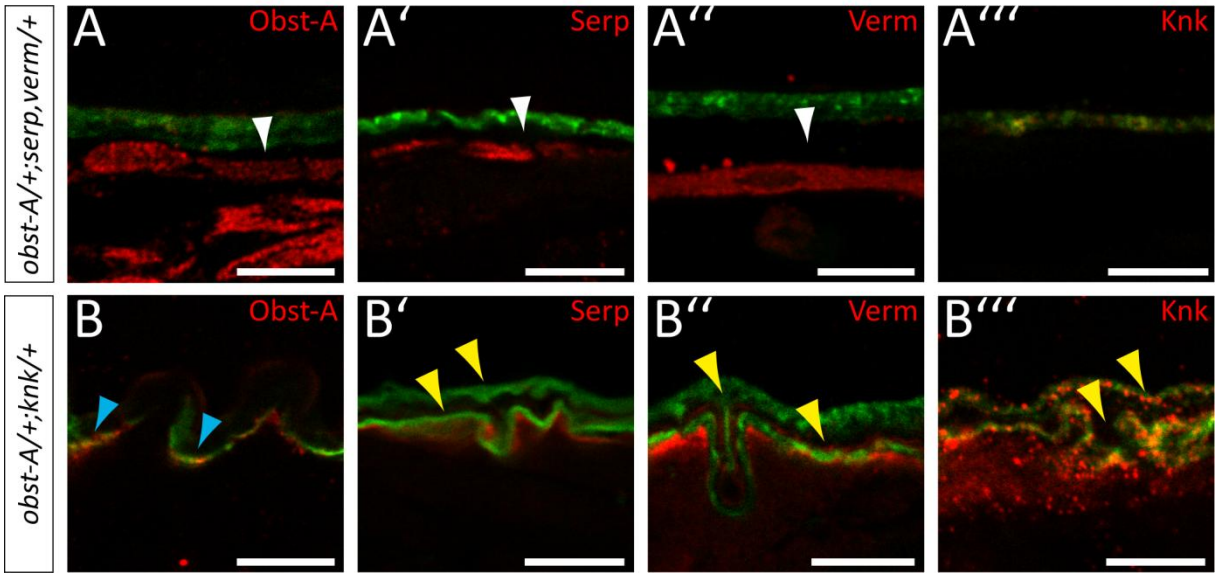

Fig. 3.2.14 - All cuticle factors are mislocalized and epidermal cuticle structure is immensely defective in transheterozygous *obst-A*/+;*serp*,*verm*/+ and *obst-A*/+;*knk*/+ larvae. A-A''': *obst-A*/+;*serp*,*verm*/+ third instar larvae. B-B''': *obst-A*/+;*knk*/+ third instar larvae. In all images costaining of chitin (CBP, green) and the indicated cuticle factor (red; A, B: Obst-A; A', B': Serp; A'', B'': Verm; A''', B''': Knk) is depicted. Note that in larvae from both genotypes Obst-A, Serp, Verm and Knk are not normally distributed in the cuticle. Reduction of Obst-A enrichment in the cuticle assembly zone in *obst-A*/+;*knk*/+ is indicated by blue arrowheads in B. Detachment of epidermal cells from the cuticle (see white arrowheads in A, A', A'') is observed in 43 % (n=14) of *obst-A*/+;*serp*,*verm*/+ larvae. Approximately half of *obst-A*/+;*knk*/+ third instar larvae (n=6) have a wrinkled cuticle phenotype just as *obst-A* null mutant larvae and have two chitin layers, which indicates molting defects at the second to third instar transition as the old cuticle is not shed and the newly synthesized cuticle is structurally abnormal (see yellow arrowheads pointing at the two cuticles in B'-B'''). Scale bars represent 10 µm. Adapted from Pesch et al., 2015.

For comparison, the normal cuticle structure and the localization of Obst-A, Serp, Verm and Knk in wild type third instar larvae is seen in Fig. 3.2.5 and 3.2.7.

In transheterozygous *obst-A*/+;*serp*,*verm*/+ third instar larvae frequently detachment of the chitin layer from the epidermal cells was observed similar to *obst-A* null mutant larvae (Fig.

3.2.14). The chitinous procuticle appeared thinned and neither Obst-A (Fig. 3.2.14 A), nor Serp (Fig. 3.2.14 A') and Verm (Fig. 3.2.14 A'') was detected within the chitin-matrix or at the apical epidermal cell surface. Instead Obst-A, Serp and Verm were restricted to the epidermal cells. Knk was normally distributed within the procuticle, but staining intensity was weak in comparison to the wild type.

About half of the transheterozygous *obst-A*/+;*knk*/+ third instar larvae had obvious molting defects as they possessed two distinct chitin layers, which most likely represent the second instar cuticle that was failed to shed and the newly synthesized third instar cuticle (Fig. 3.2.14 B'-B'''). Especially the new, inner cuticle appeared completely wrinkled, which is a phenotype that is frequently seen in *obst-A* null mutant larvae (Fig. 3.2.3). Extracellular enrichment of Obst-A, Serp and Verm was reduced when compared to the wild type (Fig. 3.2.14 B-B'') and Knk was detected in the procuticle to a lesser extent than in the wild type. Relatively strong Knk signal was also seen within the epidermal cells suggesting that Knk might not be properly secreted (Fig. 3.2.14 B''').

The severe defects in *obst-A*/+;*serp*,*verm*/+ and *obst-A*/+;*knk*/+ larvae indicate genetic interaction of *obst-A* with *serp*, *verm* and *knk* to mediate proper chitin organization and establish epidermal cuticle integrity.

3.3 - Analysis of Obstructor-A function in the hormonal control of molting

In the last part of the results section, the function of Obstructor-A in the control of molting was investigated. It was previously reported that *obst-A* null mutants are unable to molt to second instar stage (Petkau et al., 2012). However, the reason for this molting defect has not been investigated.

One very likely possibility is that the severe epidermal cuticle integrity defects of the mutants, which were described in the second part of the results section, lead to the inability to molt since Obst-A might be necessary for procuticle remodeling upon molting. To test this hypothesis, the expression level of *obst-A* upon molting was tested. As shown before Obst-A protein was detected in high levels in the newly synthesized, but not the old cuticle during the molt (Fig. 3.2.5).

However, the *obst-A* mutant molting phenotype cannot be entirely explained by the cuticle defects only. Upon molting a new cuticle is established and at the same time the old cuticle is partly degraded and eventually shed (Chaudhari et al., 2011). *Obst-A* mutant larvae are still capable of synthesizing a second instar cuticle as can be seen by the presence of double mouth hooks and double spiracles in late first instar *obst-A* deficient larvae (Petkau et al., 2012). This indicates that the mutants are not able to shed the first instar cuticle, a phenotype that is also characterized in more detail later in chapter 3.3.2.1.

Literature research for other mutants that are specifically arrested upon molting because of the inability to shed the old cuticle resulted in a large number of hits (Perrimon et al., 1985; Oro et al., 1992; Bender et al., 1997; Schubiger et al., 1998; Hall & Thummel, 1998; Freeman et al., 1999; Li & Bender, 2000; Yamada et al., 2000; Bialecki et al., 2002; Oron et al., 2002; Gates et al., 2004; Gaziova et al., 2004; Ou et al., 2016). Curiously, all of the described mutants are lacking a gene that plays a role in either the synthesis, the sensing or the regulation of signaling of the molting hormone ecdysone. The so called "ultraspiracle" (= double spiracles and mouth hooks) phenotype of these mutants, which strongly resembles the *obst-A* phenotype, was even described as characteristic for defects in the ecdysone machinery (Gates et al., 2004).

Additionally, two other publications describe mutants with similar phenotypes that are defective for two other hormones implicated in the control of molting, namely the Ecdysis Triggering Hormone (Park et al., 2002) and the Juvenile Hormone (Jones et al., 2011).

The high resemblance of the *obst-A* molting phenotype with the defects in those mutants opened up the question if Obst-A could itself be involved in the hormonal control of molting by a yet completely unknown mechanism. For this reason, the different molting hormone pathways were studied in *obst-A* deficient larvae. The surprising outcome is depicted in this part of the results section.

3.3.1 - *Obstructor-A* is a target gene of ecdysone signaling

A microarray study by the Thummel lab showed that *obst-A* is a target gene of ecdysone and that its expression is dependent on the EcR (Beckstead et al., 2005). However, the exact influence of ecdysone on *obst-A* expression has not been studied in detail. For this both the expression of *obst-A* at different time points during larval development (molt vs. intermolt) was analyzed and a bioinformatic transcription factor binding site was conducted in order to find out which transcription factors are putative direct regulators of *obst-A* transcription.

3.3.1.1 - *Obstructor-A* expression is upregulated upon molting

To analyze how *obst-A* expression changes during larval development qRT-PCR was conducted using carefully staged wild type larvae (Fig. 3.3.1).
The results revealed a relatively low *obst-A* expression during first instar stage. At about 22 h after larval hatching, when the molting from first to second instar larval stage begins, *obst-A* was strongly upregulated reaching a 25 fold higher expression than upon hatching. As molting progressed the *obst-A* expression gradually decreased. *Obst-A* expression was at a medium level during intermolt and rised drastically during molting from second to third instar stage reaching its highest expression value (32-fold upregulation). *Obst-A* expression declined after molting and stayed at a constant level during L3 stage (Fig. 3.3.1).

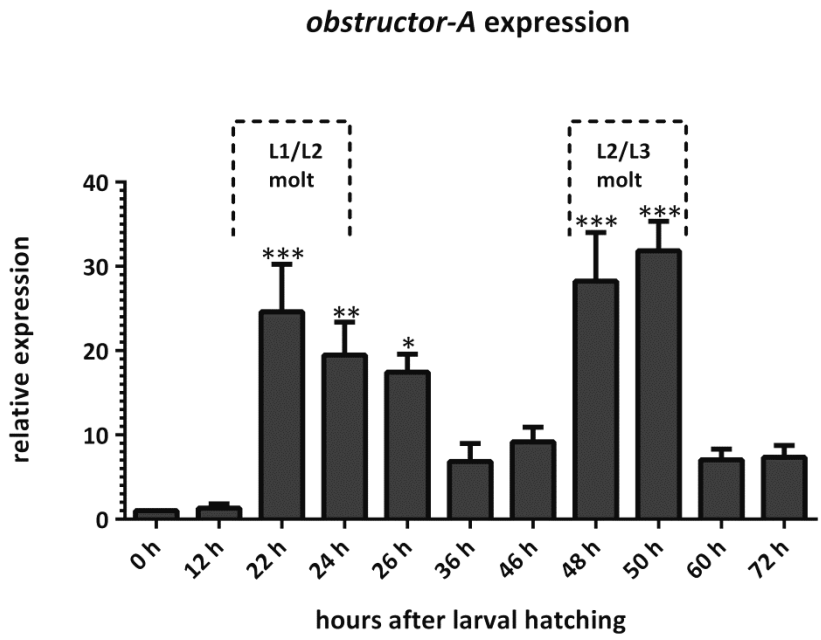

Fig. 3.3.1 - Temporal profile of *obst-A* mRNA expression throughout larval development. n≥5. y-axis: relative expression normalized to the housekeeping gene *rp49*. x-axis: different time points of analysis. The expression at the 0 h time point, corresponding to larval hatching, is set to 1. Error bars represent SEM. Note that peaks in *obst-A* expression correspond to the molt from first to second and from second to third instar stage.

The other *obstructor* genes (*obst-B, -C, -D*) also show a similar expression pattern being upregulated at times of molting (data not shown).

3.3.1.2 - Bioinformatic analysis predicts *obstructor-A* to be regulated by transcription factors of the ecdysone pathway

To further analyze if *obst-A* is a target gene of ecdysone signaling, a bioinformatic transcription factor binding site prediction analysis was conducted using *the obst-A* gene sequence as well as the 2 kb upstream, representing the putative promotor of *obst-A*. For this the two databases JASPAR and ConSite were used. The cut-off value (80 % probability of a binding site being functional *in vivo*) was raised in several steps to reduce the number of false positive hits.

EcR and Usp form a binary receptor complex that binds to ecdysone responsive DNA elements and upon 20E binding induce the transcription of "early response genes" (King-Jones & Thummel, 2005). The "early response proteins" E74A (Thummel et al., 1990; Karim & Thummel, 1991), the different isoforms of the broad complex (br-Z1,2,3,4) (Karim et al.,

1993; Crossgrove et al., 1996; Riddiford et al., 2003) and ftz (Broadus et al., 1999; Parvy et al., 2005; Yamada et al., 2000) were chosen for analysis as they all act as transcription factors inducing different other genes upon ecdysone pulses (Thummel, 2002). Vvl and Kni are transcription factors that are required for the induction of the ecdysone specific gene expression program (Moeller et al., 2013). Binding sites for all these ecdysone-related transcription factors were identified in the analyzed sequence and results are depicted in Table 3.1.

Number of binding sites	**JASPAR 80 %**	**ConSite 80 %**	**JASPAR 90 %**	**ConSite 90 %**	**JASPAR 95 %**	**ConSite 95 %**
br-Z1	21	22	0	0	0	0
br-Z2	79	79	10	10	3	3
br-Z3	50	50	5	5	1	1
br-Z4	49	49	3	3	0	0
Usp	6	6	0	0	0	0
EcR/Usp	21	n.a.	1	n.a.	1	n.a.
E74A	38	38	5	5	3	3
ftz	51	n.a.	3	n.a.	0	n.a.
Vvl	145	n.a.	28	n.a.	7	n.a.
Kni	7	n.a.	1	n.a.	0	n.a.

Table 3.1 - Transcription factor binding site analysis for the *obst-A* gene and its putative promotor. The JASPAR and the ConSite database were used, yielding similar results, and three different cut-off values were chosen (the default 80 % as well as 90 % and 95 %, meaning that the binding sites are functional in vivo with the respective probability). The *obst-A* sequence includes many transcription factor binding sites for ecdysone-related transcription factors, especially the different broad isoforms and Vvl. n.a. - not available.

3.3.2 - *Obstructor-A* mutants have a typical ecdysone deficiency phenotype

The molting hormone ecdysone is crucial for developmental transitions in *Drosophila*. Thus, its loss leads to the inability to reach the next developmental stage. This could either result in death after a prolonged larval stage, without any signs of developmental progression, or in death at the transition between stages (Perrimon et al., 1985; Oro et al., 1992; Bender et al., 1997; Schubiger et al., 1998; Hall & Thummel, 1998; Freeman et al., 1999; Li & Bender, 2000; Yamada et al., 2000; Bialecki et al., 2002; Oron et al., 2002; Gates et al., 2004; Gaziova et al., 2004; Ou et al., 2016). As described above, a phenotype that is indicative of ecdysone deficiency is also detected in *obst-A* mutants, opening up the question if Obst-A somehow controls ecdysone signaling.

3.3.2.1 - *Obstructor-A* mutants reveal severe molting defects

Loss of *obstructor-A* is completely larval lethal, since 100 % of the larvae die before reaching second instar stage (Petkau et al., 2012). About half of the larvae die exhibiting signs of initiated molting, but cannot complete the molt (see exact analysis in chapter 3.3.6).
The molting phenotype of *obst-A* null mutants was already published (Petkau et al., 2012), but has not been studied in detail. Obst-A mutants show the classical "ultraspiracle" phenotype as described above (Fig. 3.3.2). While wild type control larvae normally molt to second instar stage, *obst-A* mutants are still able to synthesize the second instar cuticle (Fig. 3.3.2 B, B''), but cannot progress much further. Whereas wild type larvae molt to second instar stage at 25 °C in the time interval from 22 h to 24 h after larval hatching, *obst-A* mutants show the double mouth hook phenotype from 26 h after larval hatching onwards. The mutant is not capable of discarding the full cuticle including the old mouth hooks, but instead only sheds the posterior part, which the larvae often drag around like a tail (Fig. 3.3.2 B''). Even though few larvae can get rid of this posterior part of the cuticle including the spiracles, they die soon after, in close proximity to the shed cuticle part.

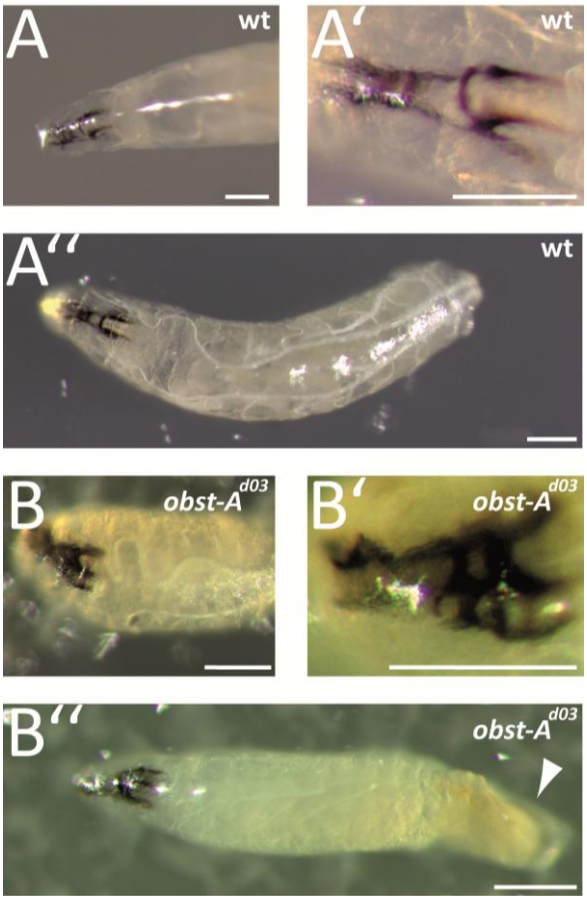

Fig. 3.3.2 - *Obst-A*^{d03} mutants are unable to molt to second instar stage. A-A'': wild type early second instar control (26 h after larval hatching). B-B'': *obst-A*^{d03} mutant 26 h after larval hatching (which would correspond to early second instar in control larvae). In the wild type the mouth hook appears normal for second instar stage (A, magnification in A') and the larva has completely shed its first instar cuticle (A''). *Obst-A*^{d03} mutants, however, fail to shed their first instar cuticle, but are capable of synthesizing the second instar cuticle as seen by the double (first and second) instar mouth hooks in B (magnification in B'). The arrow in B'' indicates the partial cuticle shedding in the mutant. Scale bars represent 200 µm.

This phenotype is typical for mutants suffering from ecdysone deficiency (see above) as well as mutants lacking the ecdysis triggering hormone (ETH) (Park et al., 2002). Both ecdysone and ETH pathway were tested in *obst-A* mutants.

3.3.2.2 - The eclosion hormone/ecdysis triggering hormone pathway is affected in *obstructor-A* mutants

The ecdysis triggering hormone and the eclosion hormone are responsible for inducing molting behavior in *Drosophila* larvae (Park et al., 2002). ETH is expressed in the peritracheal Inka cells (Zitnan et al., 1999) and induces EH release from neurosecretory cells (Krüger et

al., 2015). Obst-A expression was detected in the Inka cells of third instar wild type larvae and both *eth* and *eh* expression was reduced in *obst-A* mutants (Fig. 3.3.3).

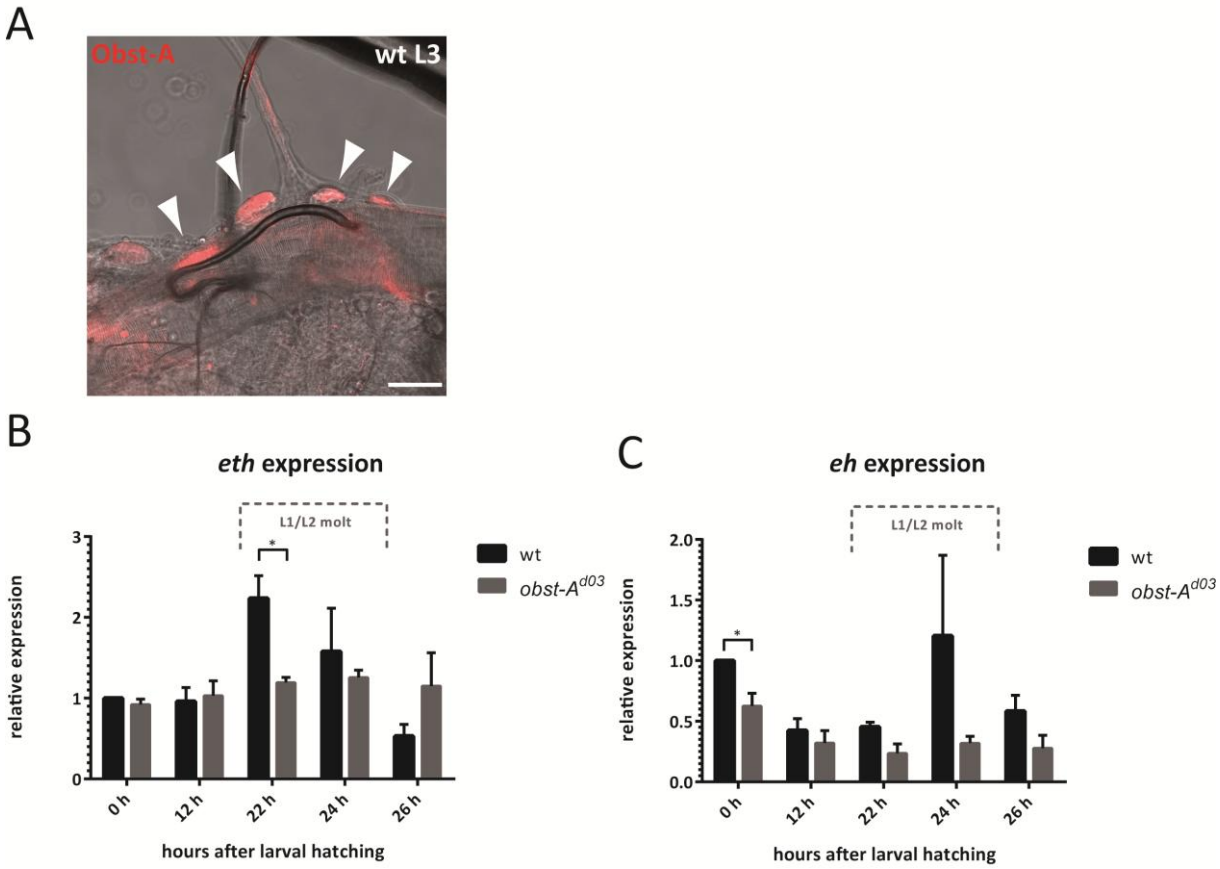

Fig. 3.3.3 - Obst-A is expressed in Inka cells and *eth* and *eh* expression is reduced upon loss of *obst-A*. A: Immunostaining of a wild type wandering third instar larva showing bright field image and Obst-A staining (red). Arrowheads label Obst-A signal in Inka cells that are located next to the tracheal dorsal trunk. Scale bar indicates 50 µm. B: qRT-PCR analysis of *eth* mRNA expression. C: qRT-PCR analysis of *eh* mRNA expression. B, C: analysis in both wild type (wt, black bars) and *obst-A*^{d03} mutant (grey bars) larvae. n≥4 for each condition. y-axis: relative mRNA expression normalized to the housekeeping gene *rp49*. x-axis: different time points of analysis. The expression at the 0 h time point, corresponding to larval hatching, is set to 1. Error bars represent SEM. Note that the expression of *eth* and *eh* is more or less unchanged in the *obst-A* mutant, whereas a peak expression can be seen in the wild type upon molting.

Both *eth* and *eh* expression show clear peaks in the wild type control when molting occurs. In contrast, the expression levels remain rather low in *obst-A* mutants (Fig. 3.3.3). This indicates problems in inducing ETH/EH signaling and might explain the disturbance of molting in the mutant. However this is no proof that Obst-A directly acts on the EH/ETH pathway as ETH is induced by ecdysone and EH is induced by ETH (Zitnan et al., 1999). Thus, next the ecdysone pathway was tested in *obst-A* mutants.

3.3.2.3 - *Prothoracicotropic hormone* expression is downregulated in *obstructor-A* mutants and TAG levels are reduced

The neuropeptide prothoracicotropic hormone (PTTH) is a major regulator of ecdysone synthesis stimulating ecdysteroid production (Gilbert et al., 2002; Yamanaka et al., 2013). *Ptth* expression levels were found to be reduced in *obst-A* mutants throughout their life time (Fig. 3.3.4 A).

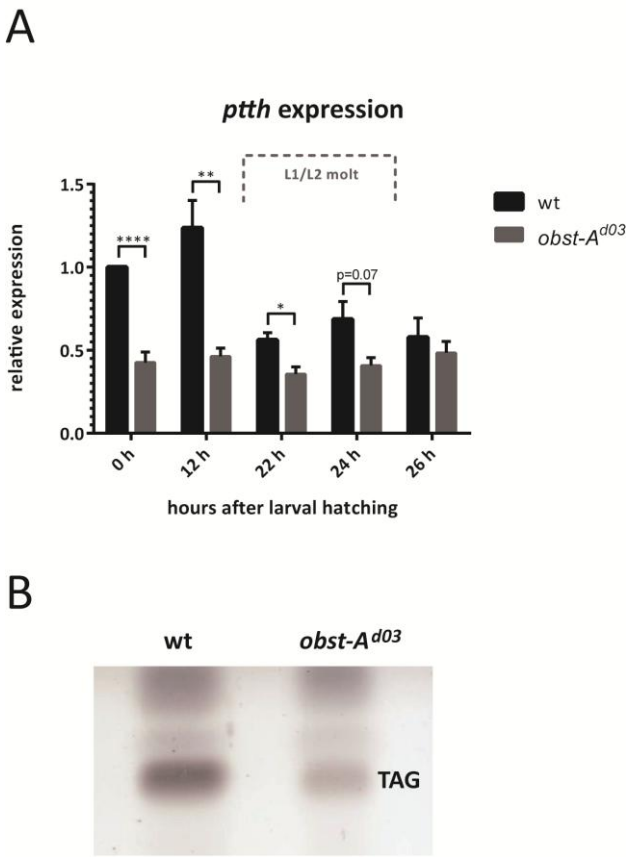

Fig. 3.3.4 - Expression levels of the *prothoracicotropic hormone* and TAG analysis by thin layer chromatography in *obst-A* null mutant and wild type control larvae. A) qRT-PCR analysis of *ptth* expression. n≥4 for each condition. Grey bars: *obst-A*^{d03} mutant larvae; black bars: wild type (wt) control larvae. y-axis: relative mRNA expression normalized to the housekeeping gene *rp49*. x-axis: different time points of analysis. The expression at the 0 h time point, corresponding to larval hatching, is set to 1. Error bars represent SEM. *ptth* expression in *obst-A* mutants remains unchanged, whereas peaks are visible in wild type control larvae. *ptth* expression is lower in *obst-A* mutants than in the control at all investigated time points. B) Representative thin layer chromatography of material from wild type control (26 h after larval hatching) and *obst-A* mutant larvae (26 h after larval hatching) reveals lower triacylglycerol (TAG) levels in the mutant.

Ptth expression was constant in *obst-A* mutants, while in the wild type oscillating expression levels were seen that has been reported previously (McBrayer et al., 2007). At all investigated time points the expression of *ptth* was lower in *obst-A* mutants compared to the wild type control. The regulation of *ptth* expression is incompletely understood (Young et al., 2012), but what is known is that *ptth* is under control of the circadian clock (Mirth et al., 2005; McBrayer et al., 2007) and that the metabolic status of the animal and its weight has an influence on *ptth* expression (Mirth et al., 2005; Young et al., 2012). Indeed, triacylglycerol (TAG) levels were reduced in *obst-A* mutants as can be seen in Fig. 3.3.4 B.
To avoid any influence of the circadian clock the 12 h/12 h light/dark cycle was kept the same for wild type and mutants and corresponding samples were collected at the same time (see discussion chapter 4.10).
Since *ptth* is in a positive feedback loop with 20E, meaning that its expression is also induced by 20E (Young et al., 2012; Yamanaka et al., 2013), the induction of ecdysone signaling had to be tested in *obst-A* mutants.

3.3.2.4 - Ecdysone signaling is not properly induced in *obstructor-A* mutants, preventing larval molt

A gene that is commonly used as a readout for ecdysone production is *E74A* as it is an early response gene that shows strong and specific peak expression following each ecdysone pulse during *Drosophila* development (Thummel et al., 1990; Karim & Thummel, 1991; Gündner et al., 2014) As *E74A* is only expressed after high ecdysteroid concentrations have been reached, it is a "sensitive indicator for ecdysone signaling" (Gates et al., 2004). Therefore, qRT-PCR analysis of *E74A* expression is a meaningful tool to detect delayed or lowered ecdysone pulses. Surprisingly, in *obst-A* mutants *E74A* levels remained at basal levels (Fig. 3.3.5 A) showing that ecdysone signaling is not induced in the mutant larvae.

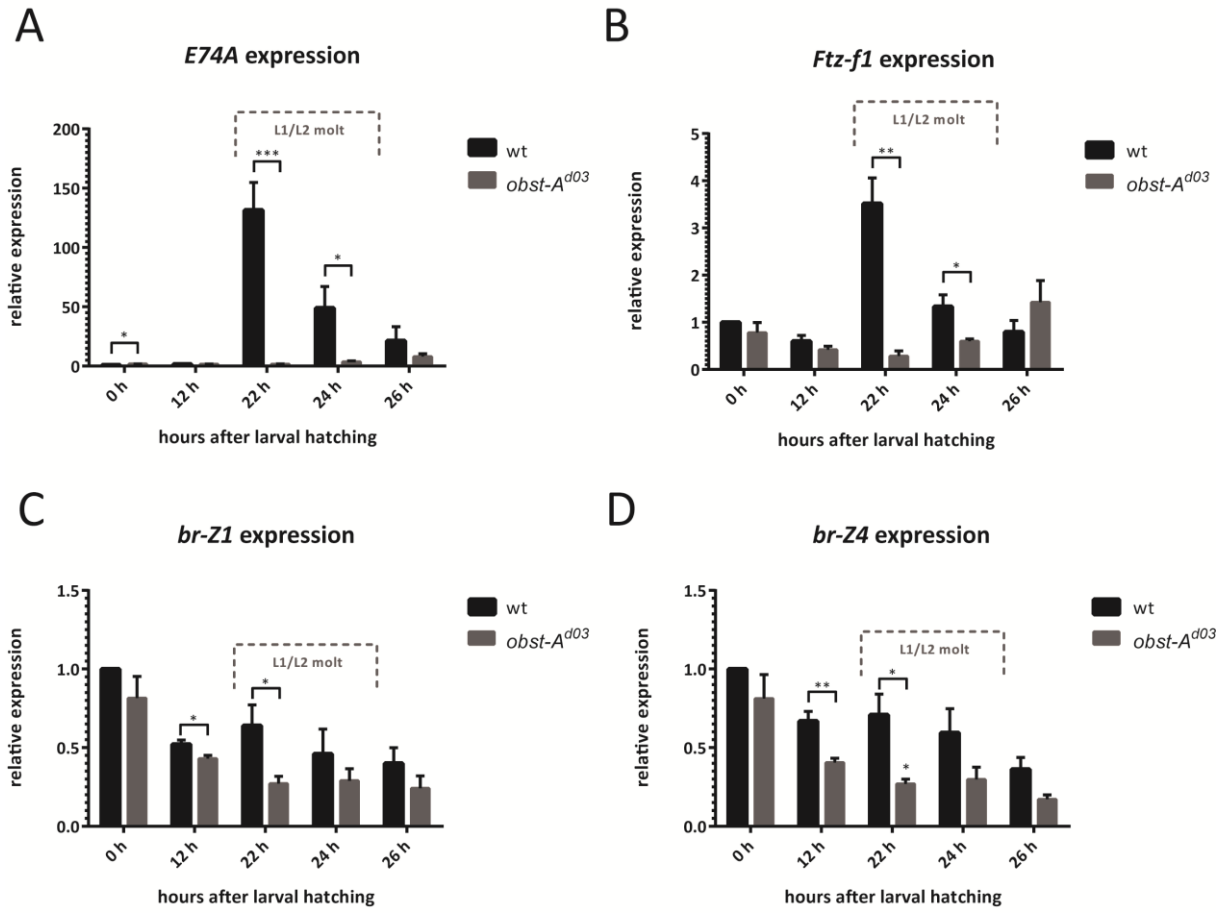

Fig. 3.3.5 - Expression levels of the ecdysone-target genes *E74A*, *Ftz-f1*, *br-Z1* and *br-Z4* in *obst-A* null mutant and wild type control larvae. qRT-PCR analysis. n=3 for *Ftz-f1*; n≥5 for all other conditions. Grey bars: *obst-A*^{d03} mutant larvae; black bars: wild type (wt) control larvae. y-axis: relative mRNA expression normalized to the housekeeping gene *rp49*. x-axis: different time points of analysis. The expression at the 0 h time point, corresponding to larval hatching, is set to 1. Error bars represent SEM. The most striking difference between wild type and *obst-A* mutant can be seen for *E74A* expression (A), which is 150-fold upregulated in the wild type when molting occurs. In the *obst-A* mutant, in contrast, *E74A* is not induced showing that the ecdysone response is abolished. *Ftz-f1* (B) peak expression is visible in the wild type upon molting but not detected in the *obst-A* mutant. Both broad isoforms br-Z1 (C) and br-Z4 (D) were found to be expressed in lower levels in the *obst-A* mutant at all investigated time points.

When molting takes place, *E74A* was strongly induced in the wild type, reaching a 150-fold expression level that gradually drops as molting progresses. Shortly before their death occurs, in the *obst-A* mutant only a very minor *E74A* peak was seen that reaches only a mere fraction of the amplitude of the peak in the wild type. E74A is an important regulator of stage-specific expression of ecdysone target genes (Fletcher & Thummel, 1995) implying that if *E74A* is not induced, other ecdysone target genes will be misexpressed as well.

Further target genes tested were *Ftz-F1* (Fig 3.3.5 B), which is a very important regulator of stage-specific ecdysone target gene induction (Broadus et al., 1999; Yamada et al., 2000), as well as *br-Z1* (Fig. 3.3.5 C) and *br-Z4* (Fig. 3.3.5 D), which are two isoforms of the early response gene complex *broad* (chapter 1.6.1) (Karim et al., 1993; Crossgrove et al., 1996; Riddiford et al., 2003).

Ftz-f1 (Fig. 3.3.5 B) was upregulated in the wild type when molting occurs, but this response was absent in *obst-A* mutants. In late stage *obst-A* mutants (26 h after hatching) a minor induction of *Ftz-f1* was seen.

The expression values of *br-Z1* (Fig. 3.3.5 C) and *br-Z4* (Fig. 3.3.5 D) were consistently lower in the *obst-A* mutant when compared to the wild type control.

3.3.3 - Ecdysone biosynthesis machinery and downstream signaling is disturbed in *obstructor-A* mutants

The previously described results clearly show that *obst-A* mutants are not capable of mounting a proper ecdysone response. This could either be caused by insufficient ecdysone production and/or disturbed ecdysone signaling. Both possibilities were tested by expression analysis.

3.3.3.1 - The ecdysone-producing *Halloween* genes are misregulated in *obstructor-A* mutants

The *neverland* gene and the *Halloween* genes *spookier*, *shroud*, *phantom*, *disembodied* and *shadow* encode for enzymes that mediate the modification of dietary cholesterol into ecdysone within the prothoracic gland (Gilbert, 2004; Rewitz et al., 2006). Reduced expression of *neverland* and the *Halloween* genes would indicate impaired ecdysteroidogenesis. To test for ecdysone biosynthesis in *obst-A* mutants, the expression levels of the above-mentioned genes were analyzed in wild type and mutant larvae by qRT-PCR (Fig. 3.3.6).

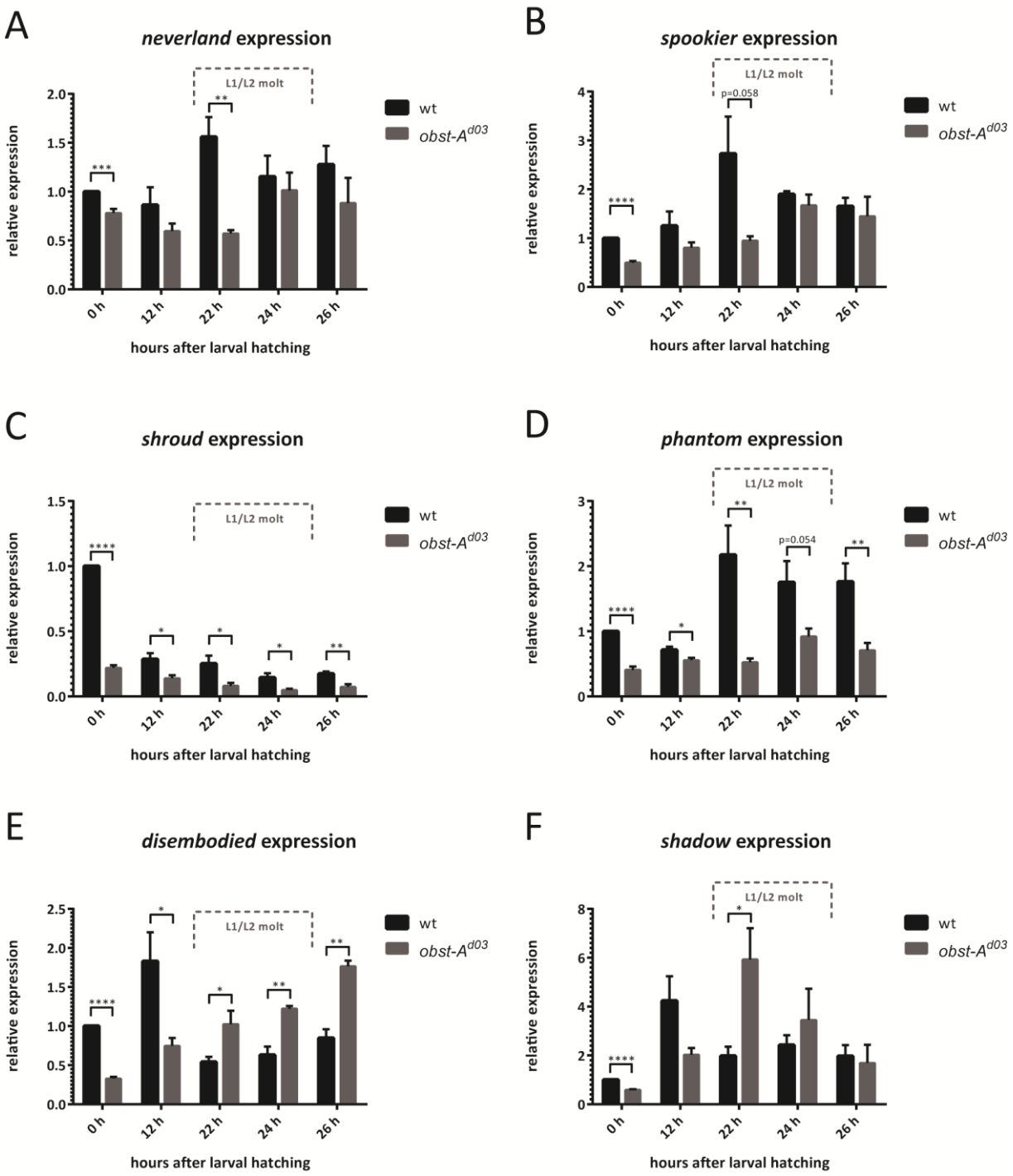

Fig. 3.3.6 - Expression levels of the ecdysone-producing *Halloween* genes in *obst-A* null mutant and wild type control larvae. qRT-PCR analysis. n≥5 for each condition. Grey bars: *obst-A*^{d03} mutant larvae; black bars: wild type (wt) control larvae. y-axis: relative mRNA expression normalized to the housekeeping gene *rp49*. x-axis: different time points of analysis. The expression at the 0 h time point, corresponding to larval hatching, is set to 1. Error bars represent SEM. Note that the expression of *neverland* (A), *spookier* (B), *shroud* (C) and *phantom* (D) is lower in *obst-A* null mutants than in the control at all time points of analysis. For the genes *disembodied* (E) and *shadow* (F) the expression is initially lower in *obst-A* mutants, but is higher than in the wild type control at later time points.

The mRNA expression of the biosynthetic enzymes *neverland* (Fig. 3.3.6 A), *spookier* (Fig. 3.3.6 B) and *phantom* (Fig. 3.3.6 D) was upregulated in the wild type when molting takes place. In *obst-A* mutants in contrast this upregulation was not detectable and at all investigated time points the expression of the biosynthetic enzymes was lower than in the wild type control. *Shroud* (Fig. 3.3.6 C) showed a different expression pattern, with a strong peak seen in the wild type upon embryonic hatching followed by lower expression at later stages. In the *obst-A* mutant *shroud* expression was constantly lower than in the wild type. The highest expression of *disembodied* (Fig. 3.3.6 E) and *shadow* (Fig. 3.3.6 F) was detected at 12 h after larval hatching in the wild type. In the *obst-A* mutant the expression of both *disembodied* and *shadow* was initially lower than in the wild type, but rised at later stages. At 22 h and 24 h (and 26 h in case of *disembodied*) after larval hatching the expression level in the mutant exceeded expression in the wild type. This could hint at a possible feedback mechanism trying to enhance ecdysone production in the *obst-A* mutant (chapter 4.10).

3.3.3.2 - Important regulatory factors of ecdysone signaling are misregulated in *obstructor-A* mutants

In addition to the biosynthesis genes that are expressed in the prothoracic gland, peripheral genes associated with ecdysone signaling were analyzed in *obst-A* mutants. The hydroxylase Shade modifies ecdysone, which is released from the PG into the periphery, into the active molting hormone 20-hydroxyecdysone (20E) (Petryk et al., 2003). 20E then binds to the receptor complex consisting of EcR and Usp and several cofactors such as rigor mortis (Ashburner, 1971; Li & Bender, 2000; Gates et al., 2004).

Shade, *EcR*, *usp* and *rigor mortis* expression in both wild type and *obst-A* mutant larvae is depicted in Fig. 3.3.7.

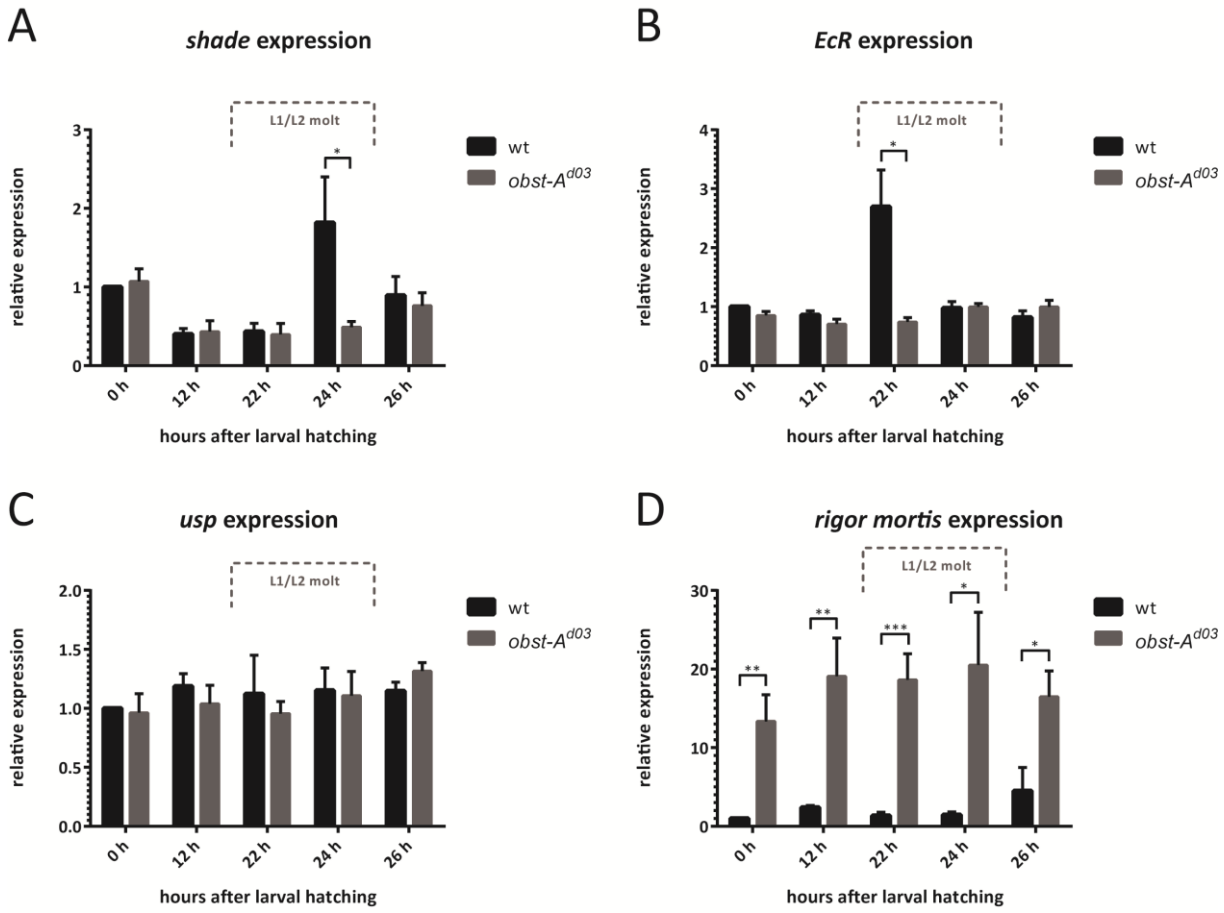

Fig. 3.3.7 - Expression levels of the ecdysone hydroxylase *shade*, the receptor components *EcR* and *usp* and the receptor cofactor *rigor mortis* in *obst-A* null mutant and wild type control larvae. qRT-PCR analysis. n≥5 for each condition. Grey bars: *obst-A*^{d03} mutant larvae; black bars: wild type (wt) control larvae. y-axis: relative mRNA expression normalized to the housekeeping gene *rp49*. x-axis: different time points of analysis. The expression at the 0 h time point, corresponding to larval hatching, is set to 1. Error bars represent SEM. Wild type larvae show peak expression of *shade* (A) and *EcR* (B) when molting occurs, whereas the peak is absent in the *obst-A* mutant. *Usp* levels are stable in both wild type and mutant larvae (C). The EcR cofactor *rigor mortis* is strongly upregulated in *obst-A* mutants at all time points of analysis (D) reaching 15- to 20-fold expression compared to the wild type control.

Both *shade* (Fig. 3.3.7 A) and *EcR* (Fig. 3.3.7 B) mRNA expression showed peak expression during molting, whereas the expression of both genes stayed at a basal level in *obst-A* mutants, indicating the absence of induction of the molt. *Usp* expression (Fig. 3.3.7 C) remained at a stable level, which is similar in wild type control and mutant larvae. Most surprisingly, the expression of the EcR cofactor *rigor mortis* (Fig. 3.3.7 D) was tremendously upregulated in *obst-A* mutants at all investigated time points with about 15- to 20-fold higher expression than in the wild type.

Next, the mRNA expression levels of factors that are known to influence ecdysteroidogenesis were tested in *obst-A* mutants and wild type larvae (Fig. 3.3.8). Kni, Vvl and Mld are transcription factors inducing the expression of the *Halloween* genes (Neubueser et al., 2005; Danielsen et al., 2014) and Woc is a transcription factor of yet incompletely understood function, which most likely regulates *neverland* expression (Wismar et al., 2000; Warren et al., 2001; Jin et al., 2005).

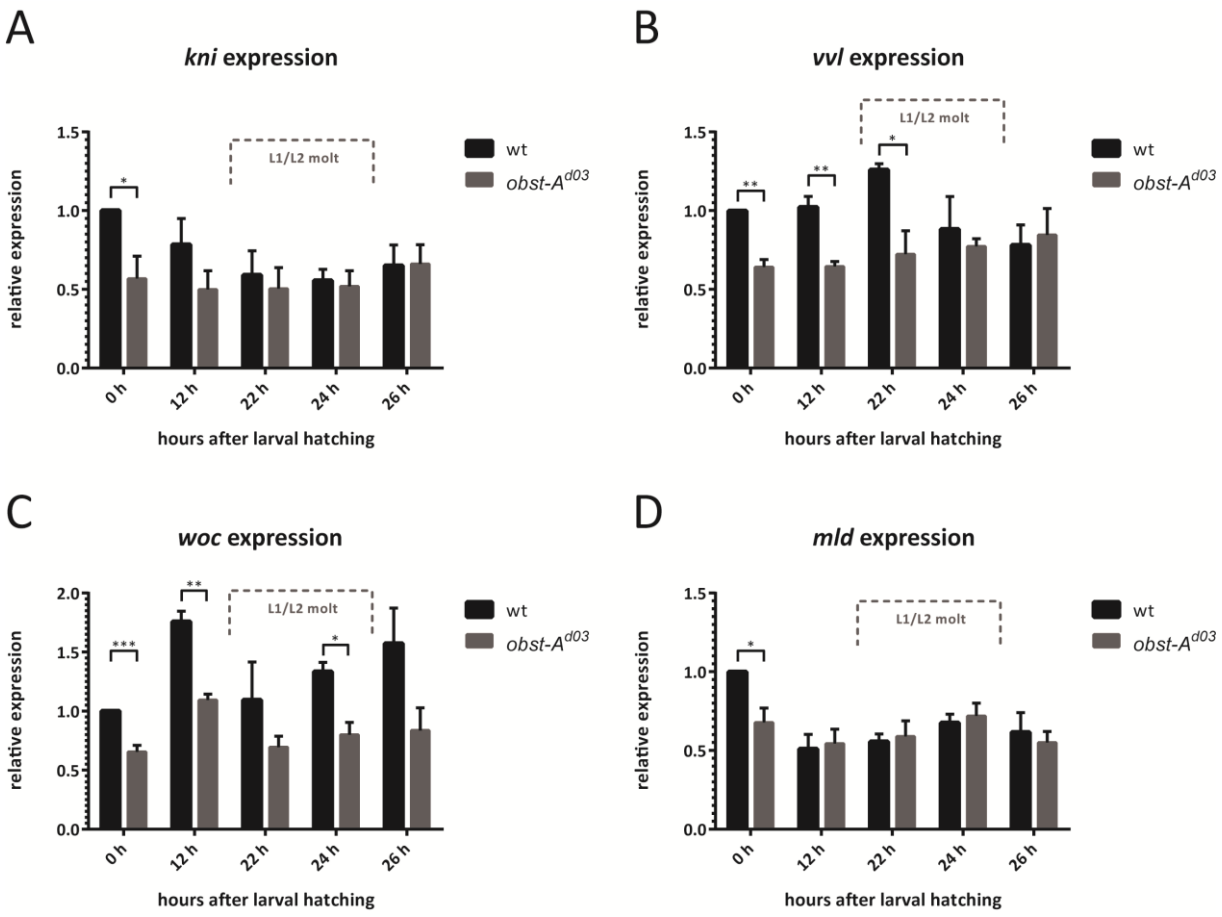

Fig. 3.3.8 - Expression levels of the ecdysone-related factors *kni*, *vvl*, *woc* and *mld* in *obst-A* null mutant and wild type control larvae. qRT-PCR analysis. n≥4 for each condition. Grey bars: *obst-A*^{d03} mutant larvae; black bars: wild type (wt) control larvae. y-axis: relative mRNA expression normalized to the housekeeping gene *rp49*. x-axis: different time points of analysis. The expression at the 0 h time point, corresponding to larval hatching, is set to 1. Error bars represent SEM. The expression of *kni* (A), *vvl* (B) and *woc* (C) is lower in *obst-A* null mutants than in the control at most time points of analysis, whilst *mld* expression (D) remains mostly unchanged in the mutant.

The transcription factors *kni* (Fig. 3.3.8 A), *vvl* (Fig. 3.3.8 B) and *woc* (Fig. 3.3.8 C) were expressed in lower levels in *obst-A* mutants compared to wild type larvae with the largest difference seen for *vvl* and *woc*. In contrast *mld* expression (Fig. 3.3.8 D) was largely unaffected in *obst-A* mutants.

3.3.3.3 - Feedback mechanisms regulating substrate import and ecdysone levels try to upregulate the ecdysone titer in *obstructor-A* mutants

Ecdysteroid titers are not only controlled by the rate of biosynthesis, but also by the import of cholesterol as substrate for ecdysone production via the npc1a transporter (Huang et al., 2005) and by the degradation of ecdysone via the cyp18a enzyme (Rewitz et al., 2010; Rewitz et al., 2013). In *obst-A* null mutants upregulation of *npc1a* and lack of *cyp18a* peak expression was observed (Fig. 3.3.9).

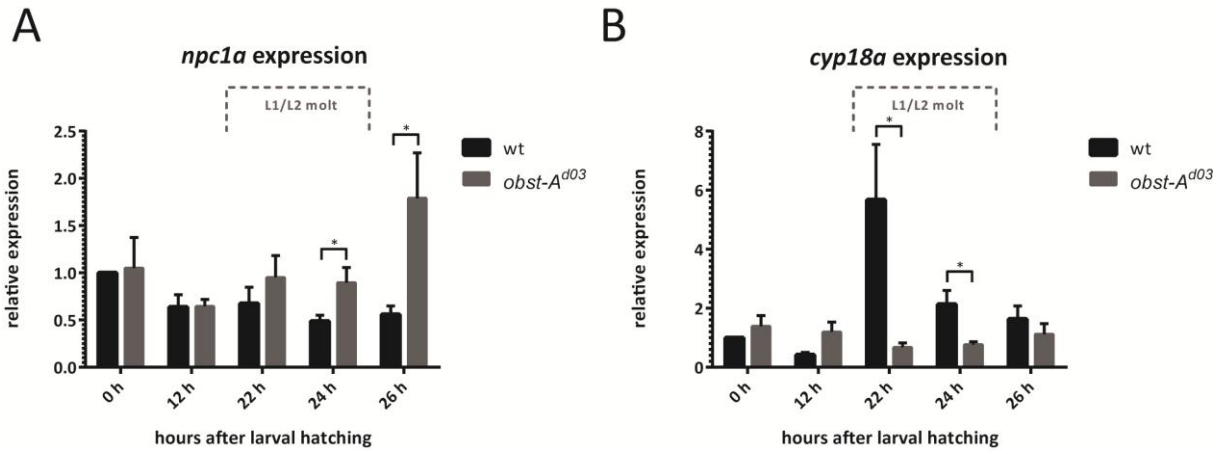

Fig. 3.3.9 - Expression levels of the cholesterol importer *npc1a* and the ecdysone degrading enzyme *cyp18a* in *obst-A* null mutant and wild type control larvae. qRT-PCR analysis. n≥5 for each condition. Grey bars: *obst-A^{d03}* mutant larvae; black bars: wild type (wt) control larvae. y-axis: relative mRNA expression normalized to the housekeeping gene *rp49*. x-axis: different time points of analysis. The expression at the 0 h time point, corresponding to larval hatching, is set to 1. Error bars represent SEM. The expression of *npc1a* (A) is elevated in *obst-A* mutants at the time when molting occurs in the wild type control, but not in the mutant. *Cyp18a* expression (B) is more or less unchanged in *obst-A* mutants, whereas a clear peak expression is seen in the wild type at 22 h after larval hatching.

Npc1a expression levels (Fig. 3.3.9 A) were comparable to the wild type control in early *obst-A* mutants, but exceeded the wild type levels in later stages meaning that more cholesterol is imported into the PG cells of the mutants in an attempt to increase ecdysone titers.

Additionally, upregulation of the ecdysone degrading enzyme *cyp18a* was detected in the wild type in the early stages of the molt to limit the ecdysone peak both in amplitude and length (Rewitz et al., 2010). In the *obst-A* mutant, however, *cyp18a* expression remained at a basal level (Fig. 3.3.9 B). As a consequence of elevated *npc1a* but reduced *cyp18a* expression, ecdysone levels should rise in *obst-A* mutants shortly before their death representing a potential feedback mechanism trying to overcome the inability to molt.

3.3.4 - Obstructor-A is expressed in the ring gland and necessary for its morphology

All results described above suggest that biosythesis of ecdysone is somehow affected in the *obst-A* mutant. The underlying process is regulated in the ring gland (chapter 1.6.1), an endocrine complex attached to the larval brain. As Obst-A is indeed expressed in non-chitinous structures including the ring gland (Fig. 3.2.4), ring gland morphology in *obst-A* mutant larvae was characterized to find out if the disturbed ecdysone production originates from defects in this endocrine organ.

3.3.4.1 - The ecdysone receptor is still nuclear, but the ring gland is strongly malformed in *obst-A* mutants

Brain ring gland complexes from *obst-A* mutant larvae and age-matched wild type control larvae were dissected and stained for the ecdysone receptor (EcR) (Fig. 3.3.10).

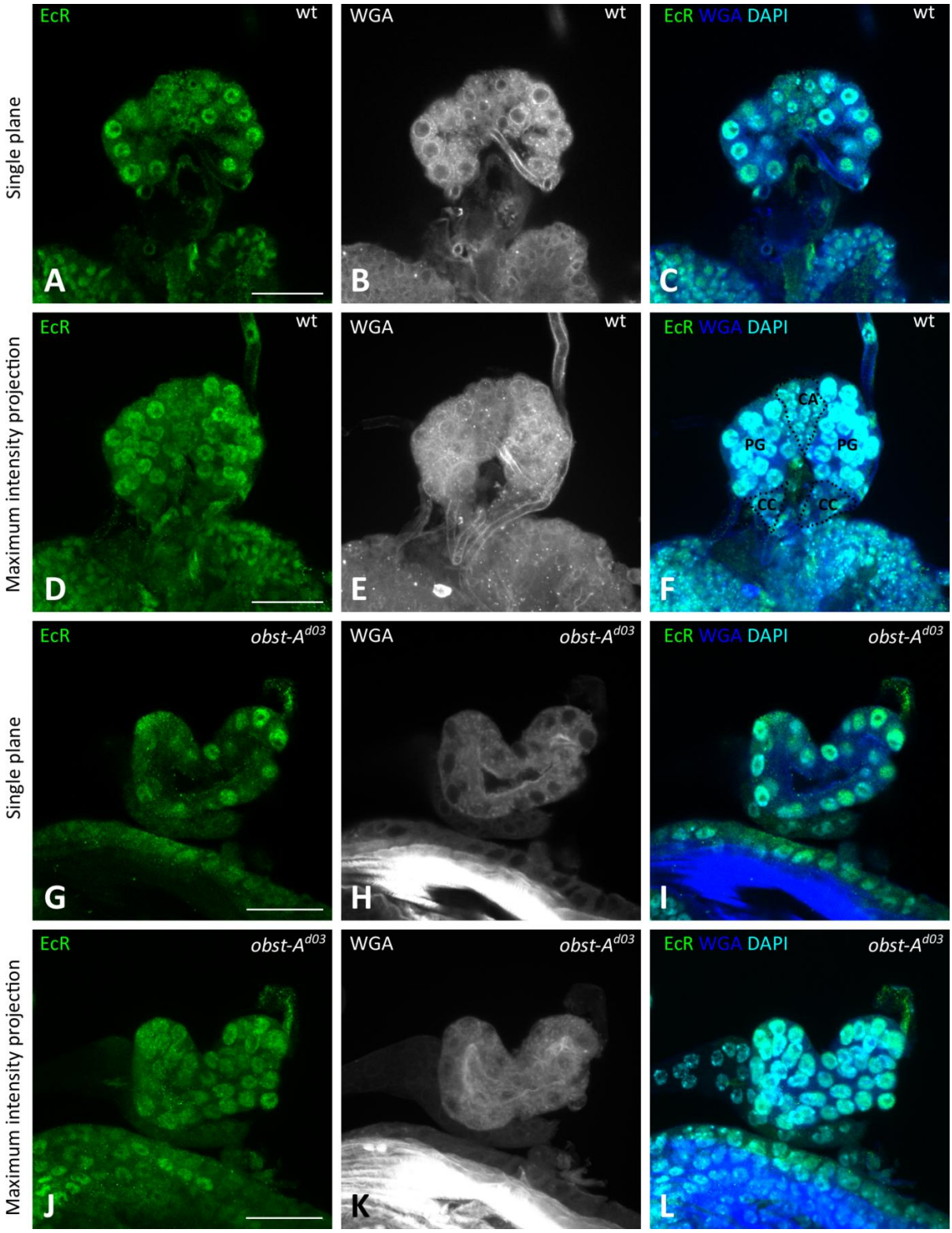
Single plane
Maximum intensity projection
Single plane
Maximum intensity projection
EcR
WGA
EcR WGA DAPI
wt
obst-A^d03
A
B
C
D
E
F
G
H
I
J
K
L
CA
PG
PG
CC
CC

Fig. 3.3.10

Fig. 3.3.10 - In *obst-A* mutants the EcR is normally localized within the nucleus, but structural abnormalities of the ring gland are visible. Representative immunofluorescent staining on whole mount ring glands using the EcR antibody (green), WGA (blue) and DAPI (cyan). Wild type and mutant were imaged with the same laser settings. Single channel images for WGA are depicted in grey. Scale bar represents 20 µm. A-F: ring gland of a first instar wild type larva, G-L: ring gland of an age-matched first instar *obst-A*^{d03} mutant larva. In the wild type control, the different cell sizes of the distinct ring gland cell types are visible in the single planes of a Z-stack (A, B, C) and the different lobes of the ring gland are seen in the maximum intensity projection of the same Z-stack (D, E, F). Note that the EcR staining is predominantly nuclear in both wild type (A, D) and *obst-A*^{d03} mutant (G, J) ring glands and appears in similar intensity as can also be seen in the merge with DAPI and WGA (C, F for wild type; I, L for mutant). The WGA channel (B, E for wild type; H, K for mutant) shows the general cellular architecture, leaving the nucleus unstained. The wild type shows a normal ring gland architecture. The different lobes are indicated by dashes in F: PG - prothoracic gland (large nuclei); CA - corpus allatum (small nuclei, in between the two lobes of the PG); CC - corpora cardiaca (small nuclei). This lobular architecture is not detected in the *obst-A*^{d03} mutant, in which the whole ring gland does not show its normal shape (compare B and H; C and I; E and K; F and L) and all nuclei have the same size (compare F and L). This makes the distinction of the cells into the PG cells, the CA cells and the CC cells impossible.

In *obst-A* mutants the EcR (Fig. 3.3.10 G, J) was detected in normal nuclear localization, just as in wild type larvae (Fig. 3.3.10 A, D). However, the unexpected observation was made that the ring gland structure was altered in *obst-A* mutants (Fig. 3.3.10 I, L for mutant compared to C, F for wild type). In the wild type the lobular architecture of the gland was visible as the cells of the prothoracic gland could be discriminated from the cells of the corpus allatum and the corpora cardiaca because of the difference in size of the nuclei. In the *obst-A* mutant, in contrast, all ring gland cells had the same size. In addition, the overall shape of the ring gland was different in the mutant showing an indentation at the place where in the wild type the small cells of the corpus allatum would be located.

3.3.4.2 - Obstructor-A is expressed in the ring gland throughout larval development and its loss leads to absence of the corpus allatum

As the ring gland was found to be malformed in *obst-A* mutant larvae, the next step was to test for Obst-A expression in the ring gland. The FasII antibody was used to label the corpora cardiaca and corpus allatum to facilitate the discrimination of the different ring gland lobes. Representative immunostainings are shown in Fig. 3.3.11 (A to F) for wandering third instar stage and early second instar stage at 26 h after hatching, which corresponds to the time point when *obst-A* mutant larvae show dramatic lethality and molting defects.

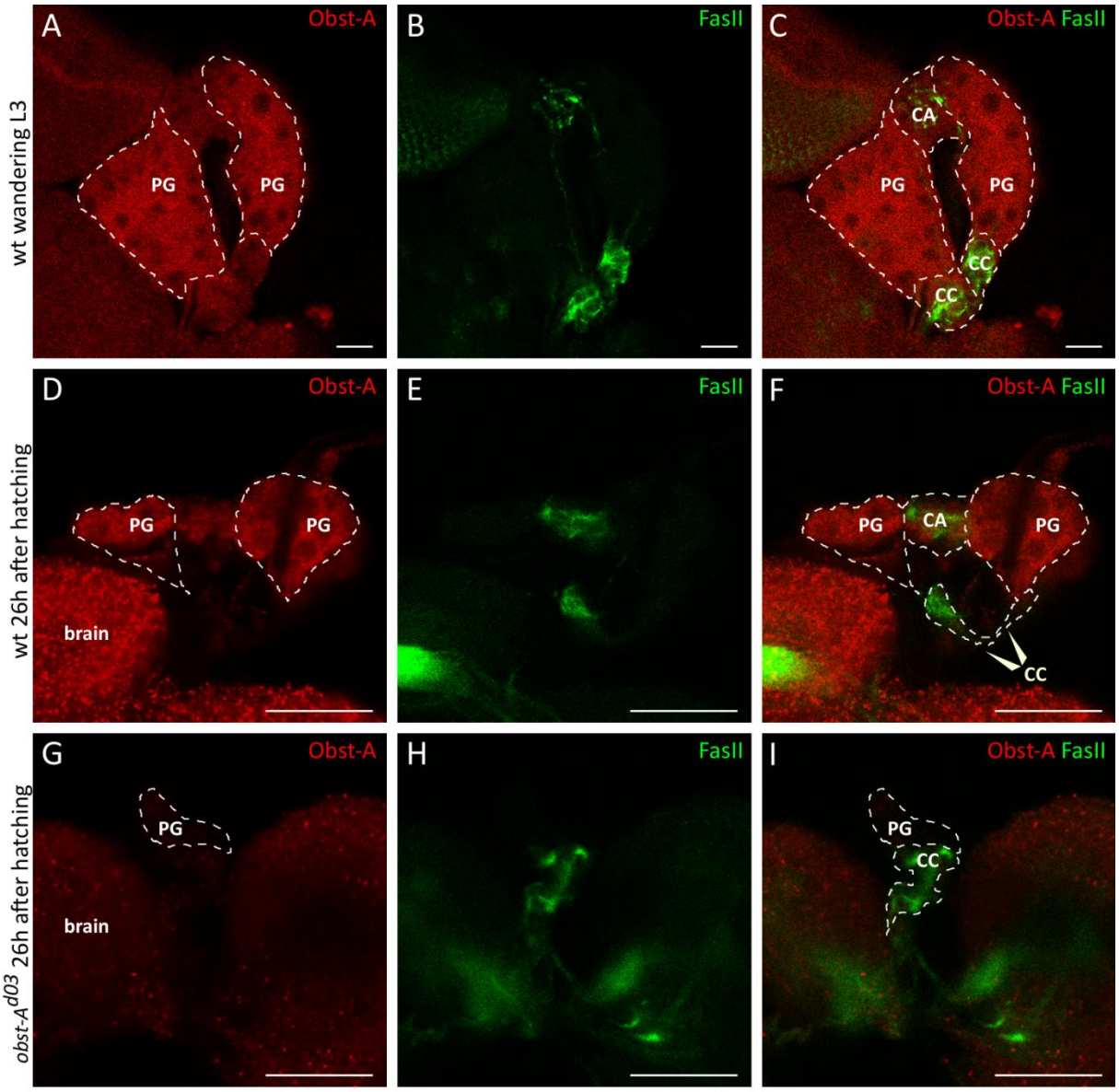

Fig. 3.3.11 - Obst-A is expressed in the prothoracic gland and its loss causes reduced ring gland size and absence of the corpus allatum. Representative immunostaining on whole mount ring glands using the anti-Obst-A (red) and FasII (green) antibodies. Scale bars represent 20 µm. All images were taken with the same laser settings. A-C: Wandering third instar wild type ring gland. D-F: Early second instar wild type (26 h after larval hatching) ring gland. G-I: late stage *obst-A*^{d03} mutant (26 h after larval hatching) ring gland. PG - prothoracic gland; CA - corpus allatum; CC - corpora cardiaca. In both third instar (A) and second instar (D) wild type larvae, a strong cytoplasmic Obst-A staining can be detected in the PG cells of the ring gland (indicated by white dashes). FasII (B, E) is used as a marker for the CA cells (top) and the CC cells (bottom) of the ring gland. The overall ring gland architecture can be seen in the Obst-A and FasII colabeling in C (third instar) and F (second instar). The ring gland is normal in the wild type as two lobes of the PG and CC, respectively, and one lobe of the CA in between the PG lobes can be seen. In the *obst-A* null mutant (G, H, I) the Obst-A signal is largely absent and only faint background staining can be detected (G, I). Note that there is only one lobe of the PG detectable, which is extremely reduced in size in comparison to the wild type. Additionally, FasII only labels one subset of cells, which corresponds to the CC (H, I). While the CC look normally developed, the CA is completely absent in the *obst-A* mutant.

Strong cytoplasmic Obst-A staining was detected in the wild type prothoracic gland at all developmental stages. Obst-A staining was also found in the corpus allatum, but this always appeared weaker when compared to the PG cells (internal control, n=10).

In all investigated ring glands taken from *obst-A* mutant larvae (n=10), normal FasII staining was detected in the CC, but the CA was not detected (Fig. 3.3.11 G, H, I). The absence of the CA was concluded from the missing FasII staining, where the CA is supposed to be, as well as from the uniform cell size in the small lobe of large cells, which corresponds to the PG. This is in line with the results from the EcR-DAPI costaining shown in Fig. 3.3.10 in which ring gland structure was obscure and small CA cells could not be distinguished from large PG cells as only cells of uniform size were present.

As an internal control for antibody specificity, Obst-A staining was investigated in the *obst-A* null mutants, confirming the absence of staining in the null mutant as only a weak background signal was detected in the brain.

The size of the ring gland in *obst-A* mutants was relatively variable, but in all cases it was much smaller than in wild type larvae of the same age (compare Fig. 3.3.11 F and I). There was only one lobe of the PG present, which was enormously reduced in size when compared to PG size in wild type larvae and the number of cells appeared smaller.

3.3.5 - Tissue specific knockdown reveals that *obstructor-A* function in the prothoracic gland is essential for larval molting

All the results described above indicate disturbed ecdysone production and signaling in the *obst-A* mutant probably caused by defective ring gland morphology. This raised the question if Obst-A regulates the ecdysone pathway directly by controlling ring gland cells or by a peripheral, cell non-autonomous signal, such as from the epidermis. In both the epidermis as well as the tracheal system Obst-A function is associated with chitin organization. However, chitin was not detected in the ring gland (data not shown). Therefore systematic knockdown of *obst-A* function in different organs was performed, including cuticle forming tissues, the ring gland and the Inka cells, and defects caused by the knockdown were compared. This was achieved by combining the UAS-GAL4 and the RNAi technology and using the ectodermal 69B Gal4 and ring gland or Inka cell specific driver lines. Lethality of animals was monitored using survival assays (Fig. 3.3.12).

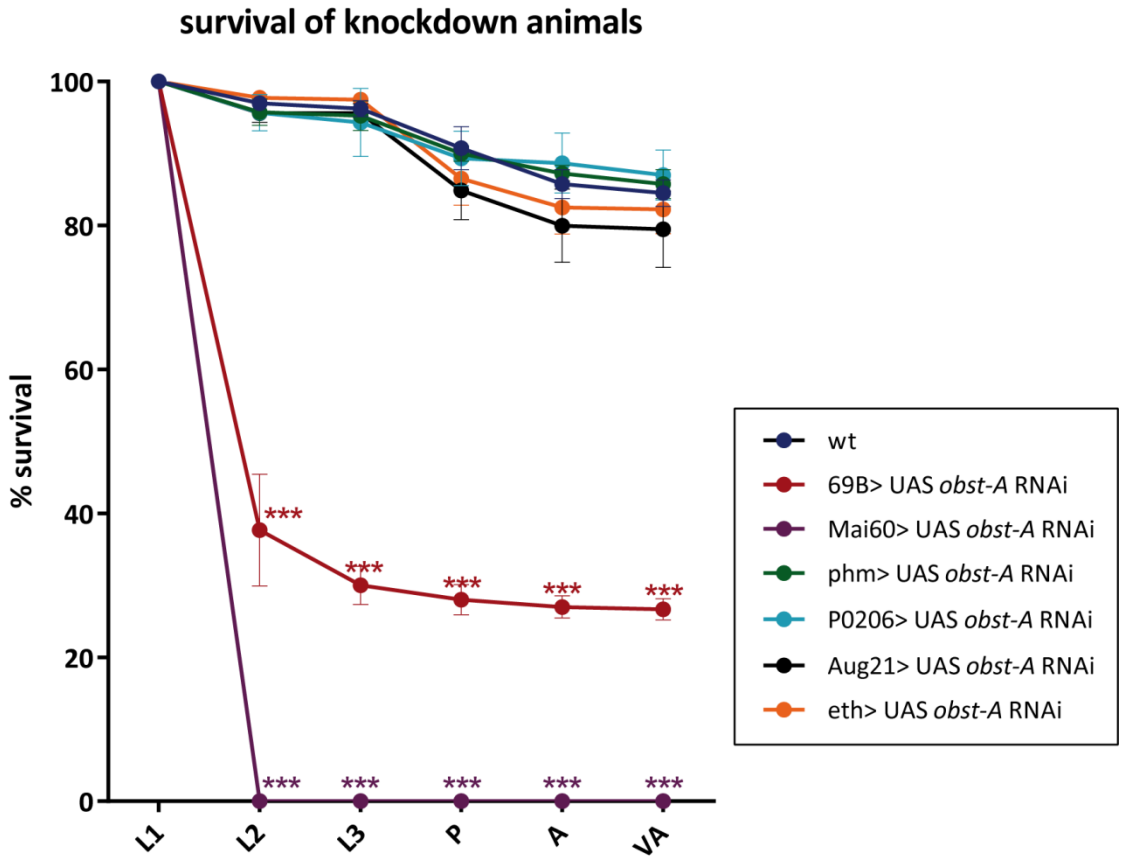

Fig. 3.3.12 - Survival profile for tissue specific knockdown of *obst-A* using different Gal4 driver lines. y-axis: % of animals surviving. x-axis: developmental stage. Freshly eclosed first instar larvae were transfered on apple juice plates with yeast and survival was monitored throughout the different stages: L1 (first instar), L2 (second instar), L3 (third instar), P (pupa), A (adult), VA (viable adult, meaning that flies survived for at least 24 h after eclosion). Normal survival to adulthood is seen in the wild type control (wt, dark blue), phm Gal4> UAS *obst-A* RNAi (light green; knockdown in PG), Aug21 Gal4> UAS *obst-A* RNAi (black; knockdown in CA), P0206 Gal4> UAS *obst-A* RNAi (light blue; weak knockdown in PG and CA), and eth Gal4> UAS *obst-A* RNAi (orange; knockdown in Inka cells). Complete lethality before reaching second instar stage was observed for Mai60 Gal4> *obst-A* RNAi animals (purple, strong knockdown in PG and salivary glands. Note that Obst-A is not endogenously expressed in the salivary glands). Many of the Mai60 *obst-A* knockdown larvae died upon molting, thus completely mimicking the null mutant phenotype. For 69B Gal4> *obst-A* RNAi larvae (dark red; knockdown in whole ectoderm including epidermis, trachea, gut, PG) less than 40 % survival to L2 and less than 30 % survival to adulthood was observed and most larvae died during the two larval molts. n≥3 for each survival assay (comprising 100 L1 larvae per n), significance was tested using Student's t-test (Microsoft Excel). *p<0.05; **p<0.01; ***p<0.001. Error bars indicate SEM.

A summary of the expression pattern of the different driver lines can be found in table 3.2.

	cuticle forming organs	*Inka cells*	*PG*	*CA*	*salivary glands*
endogenous Obst-A expression	+	+	+	(+)	-
69B Gal4	+	+	+	(+)	-
Mai60 Gal4	-	-	+	(+)	+
phm Gal4	-	-	+	-	-
P0206 Gal4	-	-	+	+	-
Aug21 Gal4	-	-	-	+	-
eth Gal4	-	+	-	-	-

Table 3.2 - Expression pattern of the different driver lines used for the survival assays and endogenous Obst-A expression. Faint expression is indicated by brackets.

Under the given experimental conditions about 85 % of wild type larvae survived to adulthood (Fig. 3.3.12). The 69B Gal4 driver line (Brand & Perrimon, 1993; Huang et al., 2005) leads to Gal4 expression in many ectodermal tissues, including the epidermis, the tracheal system, the gut, imaginal discs and, noticeably, the PG. Therefore, the expression pattern of 69B Gal4 strongly resembles the expression pattern of Obst-A. For the 69B Gal4> UAS *obst-A* RNAi knockdown that leads to 63 % reduction of *obst-A* mRNA levels (Supplementary Fig. S4) a high lethality rate was observed at the transition from first to second instar stage resulting in less than 40 % of the animals surviving to L2. Many of the surviving escapers died during the next molt to L3 due to failure in cuticle shedding. Those larvae that endured the two molts also survived to adulthood. Note that 69B Gal4> UAS *obst-A* RNAi knockdown larvae also showed epidermal and tracheal defects.

Knockdown of *obst-A* in the Inka cells using the eth Gal4 driver line (Diao et al., 2015) did not result in any lethality. Knockdown of *obst-A* in the PG using the phm Gal4 driver (Mirth et al., 2005) also did not cause death at any developmental stage. The Aug21 Gal4 driver line is specific for the CA (Siegmund & Korge, 2001). 80 % of Aug21 Gal4> *obst-A* RNAi knockdown animals survived to adult stage, which is less than for the wild type, but does not constitute a significant difference. Despite of the high survival rates, many larvae of the genotypes phm Gal4> UAS *obst-A* RNAi, Aug21 Gal4> UAS *obst-A* RNAi and P0206 Gal4> UAS *obst-A* RNAi had difficulties to shed their cuticle at the molt to third instar stage (Supplementary Fig. S5). Nevertheless, they pupariated normally and showed survival rates similar to the wild type

control. Even though knockdown of *obst-A* in the whole ring gland using the P0206 driver line (Mirth et al., 2005) resulted in 50 % reduction of whole-larva *obst-A* mRNA levels (Supplementary Fig. S4), which is immense as the ring gland is so small, no significant lethality was observed for P0206 Gal4> *obst-A* RNAi animals. However, many P0206 Gal4> *obst-A* RNAi larvae exhibited molting problems at the second to third instar transition, especially at 29 °C. Importantly, when P0206 Gal4> *obst-A* RNAi larvae were reared at 25 °C corresponding to partial activation of the Gal4-UAS system, the presence of the corpus allatum corresponded with the degree of Obst-A expression. The larvae that successfully molted to L3 had a normal ring gland with nearly normal Obst-A expression, whereas in the larvae with molting problems a defective ring gland with a degenerated corpus allatum was found. Obst-A staining was nearly absent in these ring glands proving efficient *obst-A* knockdown (Supplementary Fig. S6).

The strongest effect was detected for the Mai60 Gal4 driver line that results in strong Gal4 expression in both the PG and the salivary gland (Walker et al., 2013). As Obst-A is not expressed in the salivary glands, the defects in the Mai60 Gal4> UAS *obst-A* RNAi knockdown can solely originate from *obst-A* knockdown in the PG. Mai60 Gal4> UAS *obst-A* RNAi larvae bear a strong resemblance to the *obst-A* null mutants as both suffer from growth defects and a high lethality at the first larval molt, exhibiting the double mouth hook phenotype and incomplete cuticle shedding. As for the null mutant, no Mai60 Gal4> UAS *obst-A* RNAi larvae were capable of reaching second instar stage. Thus, *obst-A* knockdown in the PG completely mimicks the molting phenotype and lethality of the null mutant.

The efficiency of the different driver lines that lead to Gal4 expression in the ring gland was tested beforehand by crossing driver flies to UAS *EcR*-A^{F645A} flies (Brown et al., 2006) leading to overexpression of a dominant negative ecdysone receptor in the offspring. For all ring gland-specific driver lines, this led to full lethality during larval and pupal stages (data not shown).

As knockdown of *obst-A* with the 69B Gal4 driver line, which leads to *obst-A* reduction in basically all tissues in which Obst-A is normally present, and the Mai60 driver line, which causes *obst-A* knockdown in the prothoracic gland, led to severe lethality, 69B Gal4> UAS *obst-A* RNAi and Mai60 Gal4> UAS *obst-A* RNAi larvae were further investigated. Knockdown larvae of both genotypes showed severe molting defects and a reduced growth rate (Fig. 3.3.13).

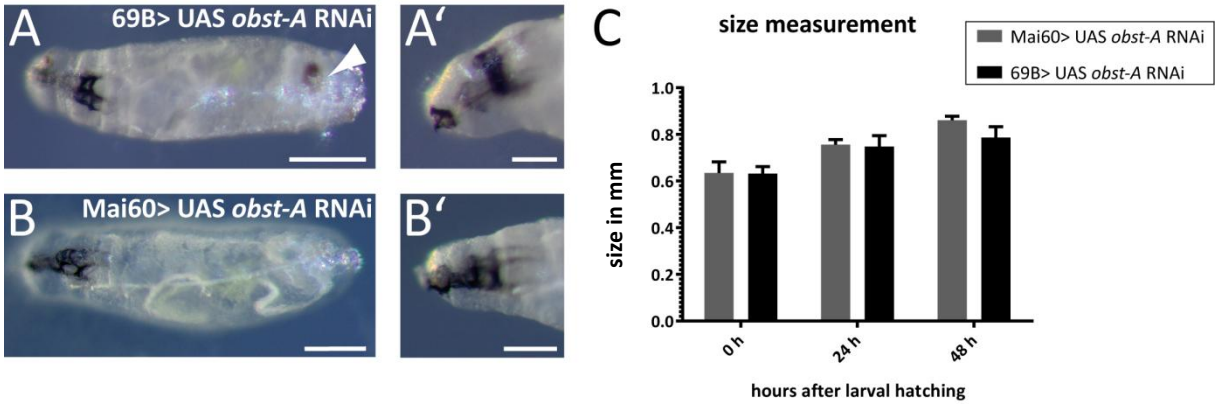

Fig. 3.3.13 - 69B Gal4> UAS *obst-A* RNAi and Mai60 Gal4> UAS *obst-A* RNAi knockdown larvae have an *obst-A* mutant like phenotype. A, A': 69B Gal4> UAS *obst-A* RNAi larva 26 h after larval hatching, which corresponds to early second instar stage in the wild type. The knockdown larvae are arrested in L1. A melanized spot in the cuticle is indicated by the arrowhead in A. B, B': Mai60 Gal4> UAS *obst-A* RNAi larva 26 h after larval hatching. Both show unusual double mouth hooks. Scale bars indicate 200 µm. C: Size measurement in 69B Gal4> UAS *obst-A* RNAi and Mai60 Gal4> UAS *obst-A* RNAi knockdown larvae reveals their inability to increase body size. Wild type size is depicted in Fig. 3.2.1 for comparison.

Both 69B Gal4> UAS *obst-A* RNAi and Mai60 Gal4> UAS *obst-A* RNAi larvae exhibited the inability to increase body size (Fig. 3.3.13 B; compare Fig. 3.2.1 for size measurement of the *obst-A* null mutant, which is comparable, and the wild type, which reaches much larger body size). They had double mouth hooks at the time point when wild type larvae just finished molting to second instar stage (Fig. 3.3.13 A). The knockdown larvae, however, were arrested in first instar stage. Thus, both genotypes of knockdown larvae had a phenotype highly similar to *obst-A*^{d03} null mutants.

A lethality profile of Mai60 Gal4> UAS *obst-A* RNAi larvae compared to *obst-A* null mutants is depicted in Supplementary Fig. S7 showing that the knockdown larvae are also completely lethal before reaching second instar stage and that a comparable percentage of larvae exhibits first signs of molting in the null mutant and in the PG-specific knockdown.

A wounding assay was performed in order to analyze knockdown larvae for cuticle defects (Supplementary Fig. S8). As expected, epidermal knockdown of *obst-A* with the 69B Gal4 driver line led to instability of the cuticle and death upon wounding. Also Mai60 Gal4> UAS obst-A RNAi larvae showed cuticle integrity defects. Even though these were not as severe as in the null mutant or in 69B Gal4> UAS *obst-A* RNAi larvae, this opened up the question if the Mai60 driver could be less specific than published in Walker et al., 2013, and if it could drive Gal4 expression in other tissues such as the epidermis.

In course of this thesis, a UAS *obst-A GFP* construct was cloned to generate UAS Obst-A GFP reporter flies, which express a Gal4-inducible Obst-A GFP fusion protein. Both 69B Gal4 and Mai60 driver flies were crossed with UAS Obst-A GFP flies, enabling in the offspring at the same time the verification of the driver expression patterns and analysis of the effects of *obst-A* overexpression (Fig. 3.3.14).

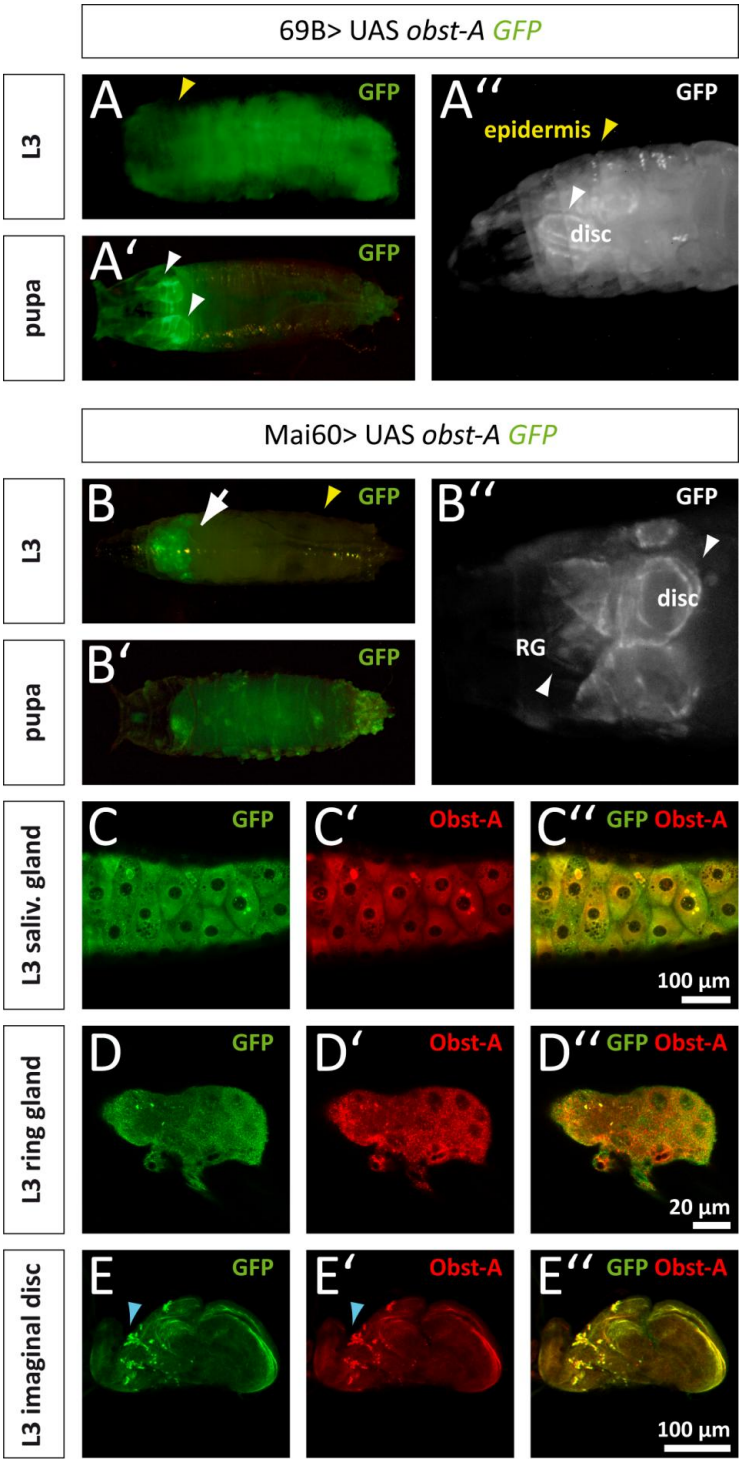

Fig. 3.3.14

Fig. 3.3.14 - Expression of UAS-*obst-A GFP* under control of the 69B and Mai60 driver lines. A-B' show fluorescent microscopy images of GFP expression, C-E'' show confocal images of immunostainings using anti-GFP and anti-Obst-A antibodies. In A-A' and B-B' the merge of GFP signal (green) with the brightfield image (weak, for visualization of body shape) is depicted. In A'' and B'' the single channel image of GFP is shown A-A'': GFP signal in 69B Gal4> UAS *obst-A GFP* animals. A: Third instar larval epidermis shows strong GFP signal as indicated by the yellow arrowhead. A': In the pupal stage GFP expression in the epidermis is weaker, instead strong GFP signal can be detected in imaginal discs (see white arrowheads) and at the posterior spiracles. A'': Head of a third instar larva shows strong GFP expression in the epidermis as illustrated by yellow arrowhead. The white arrowhead points at GFP expression in the imaginal discs. B-B'': GFP signal in Mai60 Gal4> UAS *obst-A GFP* animals. B: GFP signal is detected in the anterior part of a third instar larva (arrow), namely in the imaginal discs and the ring gland. B': In the pupal stage GFP expression is broader, but still enriched in the anterior part of the body. B'': Close-up showing GFP expression in the head region of a third instar larva. GFP signal is seen in the ring gland and the imaginal discs as indicated by the arrowheads. C-F'': Immunostaining of Mai60 Gal4> UAS *obst-A GFP* third instar larvae labeling GFP (green) and Obst-A (red). C-C'': In Mai60 Gal4> UAS *obst-A GFP* larvae strong GFP expression (C') can be detected in the salivary glands, which colocalizes with Obst-A signal (C', merge in C''). D-D'': GFP (D) and Obst-A (D') signal in the prothoracic gland of Mai60 Gal4> UAS *obst-A GFP* larvae. Merge is depicted in D''. Both GFP and Obst-A signal are enriched in the cytoplasm of prothoracic gland cells. Only weak signal is seen in the corpus allatum. E-E'': GFP (E) and Obst-A (E') signal is weakly detected in imaginal discs of Mai60 Gal4> UAS *obst-A GFP* larvae, but found strongly enriched in distinct cell clusters. Merge is depicted in E''. Size of scale bars is indicated in the respective images.

Overexpression of an Obst-A GFP fusion protein was not lethal in neither 69B Gal4> UAS *obst-A GFP* nor Mai60 Gal4> UAS *obst-A GFP* animals as they normally reached pupal (Fig. 3.3.14 A', B') and adult stage without any developmental defects. The endogenous expression pattern of Obst-A is depicted in Fig. 3.2.4. In 69B Gal4> UAS *obst-A GFP* larvae, GFP expression was detected strongly in the epidermis and the imaginal discs, whereas in Mai60 Gal4> UAS *obst-A GFP* larvae no signal was present in the epidermis (Fig. 3.3.14 B). Instead, strong staining in the salivary gland, the prothoracic gland and single cell clusters in the imaginal discs was seen (Fig. 3.3.14 B''-E''). In the wild type Obst-A is not detected in the salivary glands. In the imaginal discs Obst-A function in the distinct cell clusters (also see Fig. 3.2.4) is not analyzed yet.

These results imply that the molting defect in the Mai60-knockdown is not caused by *obst-A* deficiency in the epidermis, but most likely in the ring gland, because only the ring gland and a few Obst-A expressing cells in the imaginal discs are affected by Mai60 Gal4> UAS *obst-A* RNAi mediated knockdown.

A genetic rescue experiment was performed in which *obst-A* was tissue-specifically re-expressed in the null mutant background using both the Mai60 and the 69B Gal4 driver lines. As shown in Supplementary Fig. S9, successful outcome of this genetic rescue would be the survival of male flies with normal eyes (not heart-shaped Bar eyes) since they represent hemizygous mutants in which *obst-A* is re-introduced by the Gal4-UAS system. Indeed, when re-expressing *obst-A* using the 69B Gal4 driver line, which leads to obst-A expression in cuticle forming organs and the ring gland, viable normal eyed males hatched. In contrast, the rescue with the PG-specific Mai60 Gal4 driver line did not result in any normal eyed male flies and therefore was not successful.
In summary, this shows that one the one hand the function of Obst-A in the ring gland is essential for larval survival, but on the other hand Obst-A expression in the ring gland alone is not sufficient for survival due to the important role of Obst-A in the epidermis and the tracheal system.

3.3.6 - Feeding of ecdysone biosynthesis intermediates and 20-hydroxyecdysone partly rescues the phenotype of *obstructor-A* null mutants and knockdown larvae

A very common experiment that is performed with mutants suffering from ecdysone insufficiency is the feeding of ecdysone precursors and the active molting hormone 20-hydroxyecdysone. If the defect in the mutant is caused by improper ecdysteroid production, further developmental stages are reached upon sterol administration (Yoshiyama et al., 2006; Niwa et al., 2010; Danielsen et al., 2014). However, if the defect is caused by impaired ecdysone signaling instead of reduced production, no rescue is obtained (Gates et al., 2004).
Here, sterol feeding experiments were performed using *obst-A* null mutants and 69B Gal4> UAS *obst-A* RNAi knockdown larvae, which show some residual *obst-A* expression.

3.3.6.1 - *Obstructor-A* null mutants reach further developmental stages upon sterol feeding

Obst-A^{d03} mutants were fed with the different sterols cholesterol and 7-dehydrocholesterol, which both are substrates in the ecdysone biosynthesis pathway as well as with active 20-hydroxyecdysone in two different concentrations. The survival of larvae was monitored and

upon their death they were categorized into different stages (Fig. 3.3.15), namely the larvae dying before any signs of molt (blue), the larvae dying showing first signs of molt (double mouth hooks; red), larvae dying after partial molt (incomplete cuticle shedding; green) and larvae reaching L2 (yellow) and L3 (pink) stage.

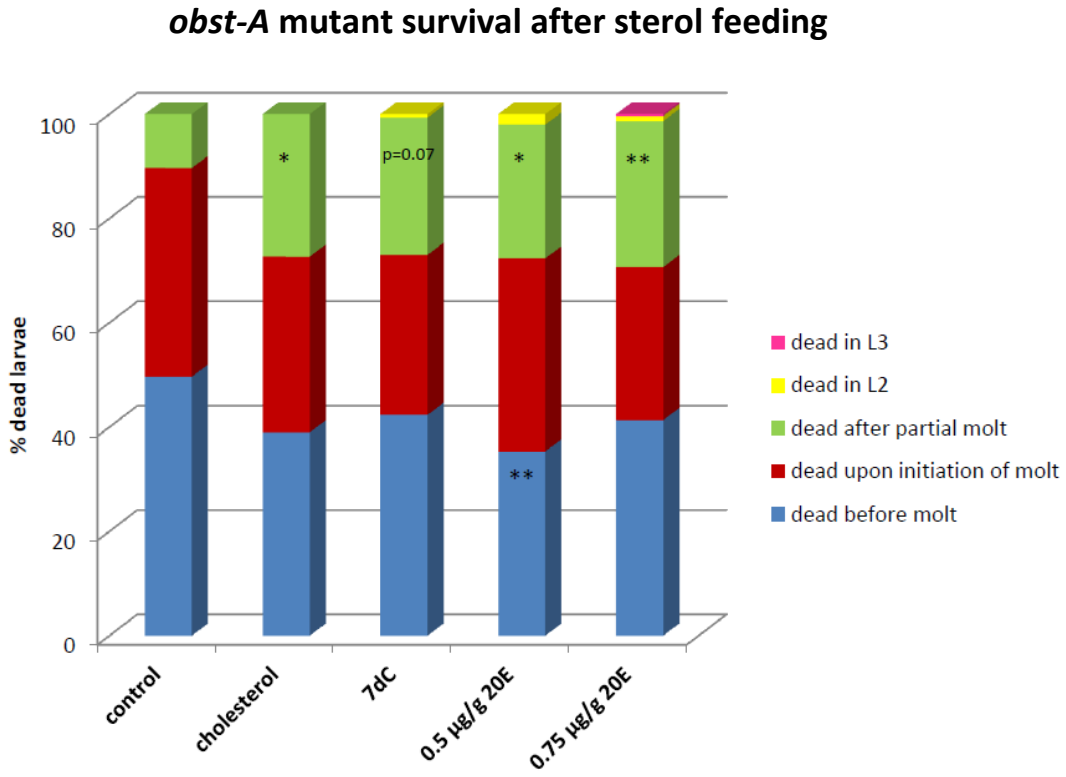

Fig. 3.3.15 - Sterol rescue partially rescues *obst-A*^{d03} null mutants to further developmental stages. y-axis: % of larvae dying in the particular developmental stage. pink: dead in L3; yellow: dead in L2; green: dead after partial molt (incomplete cuticle shedding); red: dead upon initiation of molt (double mouth hooks but no cuticle shedding); blue: dead before molt (no signs of molt). x-axis: feeding of sterol, control condition (meaning that larvae were not fed with sterols); 1 µg/g cholesterol; 1 µg/g 7-dehydrocholesterol (7dC); 0.5 µg/g 20-hydroxyecdysone (20E); 0.75 µg/g 20-hydroxyecdysone (20E). Note that upon sterol feeding less larvae died before showing signs of molting and more larvae died after partial molt. When feeding 7dC and 20E, a small percentage of mutants is able to reach L2 stage. For high 20E concentrations even a few escapers to L3 are observed. n=3 for each condition, each n comprising 100 larvae. The mean of the three experiments is depicted. Statistical analysis was performed with Student's t-test (Microsoft Excel), *p<0.05; **p<0.01. The experiment was conducted with help of Bachelor student Michelle Dassen.

Sterol feeding was able to partially, but not completely, rescue *obst-A* mutants to further developmental stages. Under control conditions (no sterol supplementation) about 49.7 % of *obst-A* mutants died before showing any signs of molting, whereas 40 % of larvae died in the

double mouth hook stage and only 10.3 % died after partial cuticle shedding. None of the *obst-A* mutants was capable of reaching second or third instar stage.

Feeding with 1 µg cholesterol per gram yeast resulted in less mutants dying before molting (39 %) and less larvae dying with double mouth hooks (33.7 %), but significantly more larvae dying with partially shed cuticle (27.3 %). No cholesterol-fed mutants reached second or third instar stage.

When feeding *obst-A* mutants with 1 µg 7-dehydrocholesterol per gram yeast 42.3 % of larvae died before the molt, 30.7 % of mutants died in the double mouth hook stage and 26.3 % died after partial molting. About 1 % of mutant larvae were able to completely molt and reach second instar stage.

The rescue effect was stronger upon 20-hydroxyecdysone feeding. For 20E two different concentrations were chosen, which did not differ very much in their outcome on mutant survival. Supplementing the yeast with 0.5 µg/g 20E resulted in 35.3 % of mutant larvae dying before molt, which is significantly less than in the control. With 37 % of larvae dying with double mouth hooks, this number is relatively unchanged compared to the control. Significantly more larvae (25.7 %) were capable of partial molting and 2 % of larvae survived to second instar stage. Using the higher 20E concentration (0.75 µg/g yeast) 41.3 % of larvae died before showing signs of molt, 29.3 % died with double mouth hooks and 28 % with partially shed cuticle, which is nearly three times more than in the control. 1 % of larvae reached L2 stage and 0.3 % of larvae even survived to L3 stage. In all feeding situations larvae that were able to molt to second instar showed tracheal defects such as dorsal trunk breaks. Most of them died after a prolonged L2 stage (72 h- 96 h in L2) (data not shown).

In parallel, the same feeding experiments were also performed with wild type larvae as control showing high survival rates for all conditions (control without sterols: 88 % average survival to adulthood; cholesterol: 87 %; 7dC: 88 %; 0.5 µg/g 20E: 86 %; 0.75 µg/g 20E: 90 %) proving that the used sterol concentrations are not detrimental to larval development.

3.3.6.2 - More larvae with ectodermal *obstructor-A* knockdown reach adult stage when fed with sterols

Because of the intermediate phenotype (Fig. 3.3.12), 69B Gal4> UAS *obst-A* RNAi knockdown larvae were chosen for further sterol rescue studies. 69B Gal4> UAS *obst-A* RNAi knockdown larvae show 30 % residual *obst-A* expression (Supplementary Fig. S4), which is sufficient for

about 30 % of larvae to survive to adulthood (Fig. 3.3.12). The idea behind using these knockdown larvae that still have little *obst-A* expression was to at least partially overcome the tracheal and epidermal defects, which lead to early lethality in the null mutant, in order to see any effect of sterol feeding on later stage larvae with reduced *obst-A* expression. Indeed, 7-dehydrocholesterol and 20-hydroxyecdysone had a beneficial effect on survival of *obst-A* knockdown larvae, whereas no significant rescue effect was observed upon cholesterol feeding (Fig. 3.3.16).

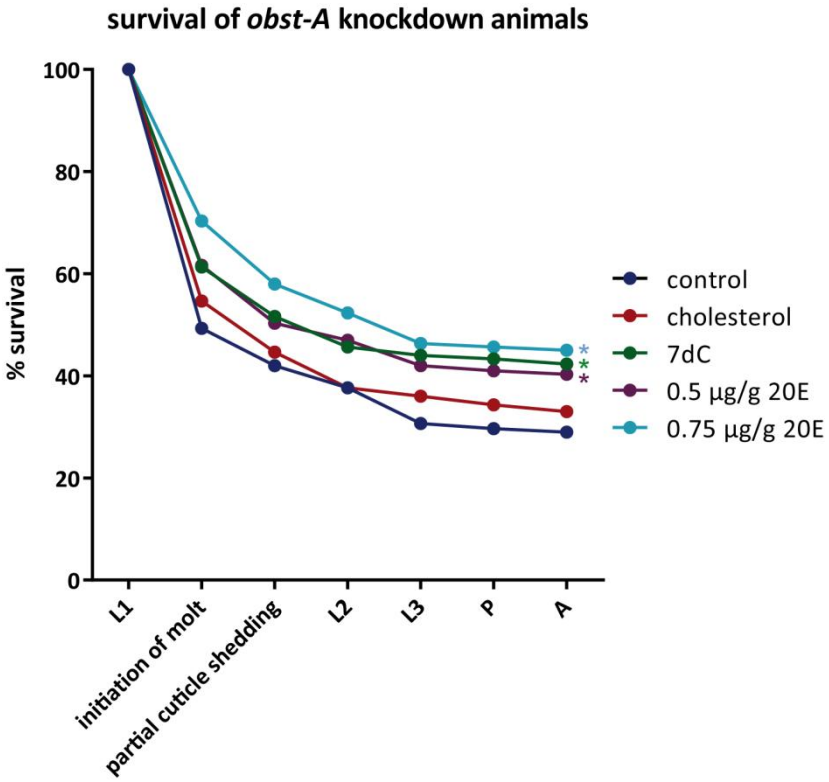

Fig. 3.3.16 - Survival of 69B Gal4> UAS *obst-A* RNAi knockdown larvae after sterol administration. y-axis: % of 69B Gal4> UAS *obst-A* RNAi larvae surviving to particular developmental stage. x-axis: developmental stage; L1: first instar before showing any signs of molting; initiation of molt: double mouth hooks; partial cuticle shedding; L2: second instar; L3: third instar; P: pupa; A: adult. Dark blue line: control (69B Gal4> UAS *obst-A* RNAi fed with control yeast, no sterols added); red line: 1 µg/g yeast cholesterol; green line: 1 µg/g yeast 7-dehydrocholesterol (7dC); purple line: 0.5 µg/g yeast 20-hydroxyecdysone (20E); light blue line: 0.75 µg/g yeast 20-hydroxyecdysone (20E). For all conditions high lethality during the first molt is observed. Feeding of sterols results in less larvae dying during the first molt and more animals reaching adulthood. n=3 for each condition, each n includes 100 larvae. The mean of the three experiments is depicted. Statistical analysis was performed with Student's t-test (Microsoft Excel). * represents $p<0.05$ compared to the control condition meaning that the rescue is significant for treatment with 7dC and both concentrations of 20 E.

Feeding of sterols had a beneficial effect on survival of 69B Gal4> UAS *obst-A* RNAi knockdown larvae. The survival was lowest for the control condition (no sterols) with 29 % of larvae reaching adulthood. The more downstream the fed compound was in the ecdysone biosynthesis cascade, the better rescue effect was reached. Cholesterol feeding resulted in 33 % of larvae reaching adult stage, which is no significant effect. The rescue was significant for feeding with 7-dehydrocholesterol (42.3 % of larvae developed to adults), 0.5 µg/g 20-hydroxyecdysone (40.3 % of larvae developed to adults) and 0.75 µg/g 20-hydroxyecdysone (45 % of larvae developed to adults). Comparing the percentage of larvae reaching the first phase of molting (double mouth hook stage), the effect of feeding 20E was very strong. Under control conditions only 49 % of knockdown larvae survived to the double mouth hook stage, whereas 61.7 % of larvae fed with 0.5 µg/g 20E and even 70 % of larvae fed with 0.75 µg/g 20E reached this stage. Thus, the partial rescue seen by feeding of sterols in *obst-A* null mutants and knockdown larvae proves the ecdysteroid deficiency that is caused by the loss of *obst-A*. The rescue is significant, but not complete as larvae lacking *obst-A* also suffer from severe tracheal and epidermal defects (Petkau et al., 2012; chapter 3.2).

Summing up all the results of the studies of the role of Obst-A in ecdysone production, it was clearly shown that loss of *obst-A* leads to defects in ecdysone biosynthesis and signaling, including misregulation of the *Halloween* genes and downstream effectors. The *E74A* gene, which is a sensitive indicator of ecdysone responses (Thummel et al., 1990; Karim & Thummel, 1991; Gates et al., 2004; Gündner et al., 2014), is not induced at all in *obst-A* mutants demonstrating the lack of edysone signaling in the mutant. *Obst-A* null mutants show severe malformation of the ring gland affecting both the ecdysone-producing prothoracic gland, which is strongly reduced in size in the mutant, and the Juvenile Hormone-producing corpus allatum, which is completely absent in the mutant. Since the function of the prothoracic gland also requires the function of the corpus allatum (Dai & Gilbert, 1991), this can explain the ecdysone insufficiency in the *obst-A* mutants. As a consequence, the molting hormones ETH and EH are misregulated and molting cannot be performed. Tissue-specific knockdown of *obst-A* in the ecdysone-producing prothoracic gland completely phenocopies the molting defects of the null mutant. Feeding larvae lacking *obst-A* with sterols from the ecdysone biosynthesis pathway partially rescued the larvae so that they were able to reach later developmental stages. This shows for the first time that a chitin-binding protein influences the hormonal control of molting in *Drosophila*.

4 - Discussion and Outlook

4.1 - The epidermal cuticle is crucial for insect development and survival

Just as the mammalian epidermis, the insect cuticle has a stratified architecture (Moussian & Uv, 2005). The mammalian epidermis is made up by a multilayered epithelium, while the insect cuticle comprises one cell monolayer and distinct layers of extracellular matrix (Fig. 4.1).

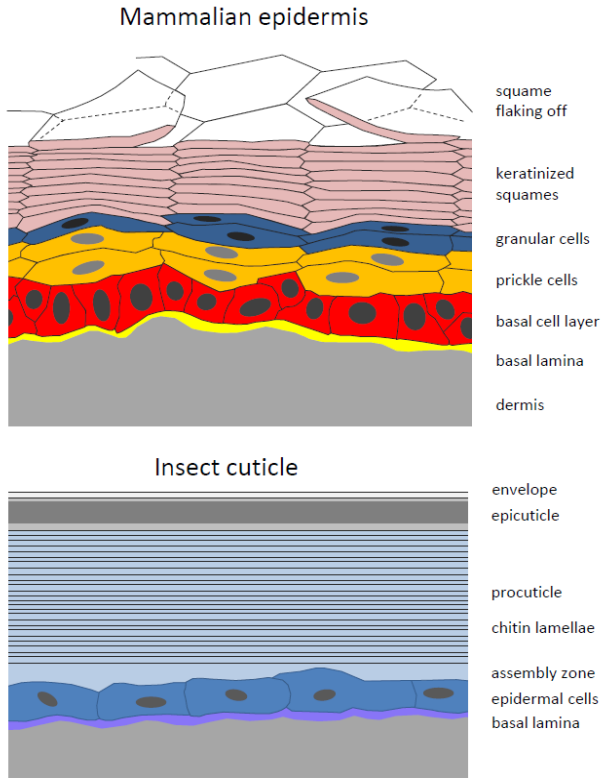

Fig. 4.1 - Multilayered architecture of the mammalian and insect epidermis. The mammalian epidermis is made up by several cell layers (see description on the right) on top of the basal lamina that separates the dermis from the epidermis. In the insect epidermal cuticle, distinct extracellular matrix layers (see description on the side) are found above a cell monolayer. Upper part based on Alberts, Molecular Biology of the Cell, 5th edition.

In mammals the uppermost layer of the epidermis, the stratum corneum, forms the cornified envelope providing the first outer barrier against water loss (Matsui & Amagai, 2015; Darido et al., 2016; van Smeden & Bouwstra, 2016). In addition, a transepithelial barrier in the granular cell layer beneath the stratum corneum is established by tight junctions (Bäsler et al., 2016).

This function is accomplished in the insect epidermal cuticle by the envelope layer that is rich in lipids and waxes and thereby mediates waterproofness (Beament, 1968; Parvy et al., 2012; Jaspers et al., 2014; Moussian, 2013a). In addition, both the mammalian and the insect epidermis act as a "first line of defense" to prevent the invasion of pathogens (Moussian et al., 2006a; Moussian, 2010; van Smeden & Bouwstra, 2016). Loss of the barrier function of the cornified envelope is associated with various skin diseases in humans such as atopic

dermatitis, which affects about 20 % of people during their lifetime (Thomsen, 2014; Sahle et al., 2015; van Smeden & Bouwstra, 2016).

The mammalian epidermis consists of several cell layers, to be precise, the granular cells, the prickle cells (also called spinous layer) and the basal cell layer (Moussian & Uv, 2005; Darido et al., 2016). In contrast the insect cuticle has only one cell layer and the stratification is achieved by distinct extracellular matrix layers, the envelope, the protein-rich epicuticle and the large procuticle made up by chitin lamellae and interspersed proteins (Moussian, 2010; Moussian, 2013a).

Importantly, the chitin-matrix layers need to provide both stability and flexibility since they act as an exoskeleton, but also enable locomotion (Moussian et al., 2006a). Depending on the respective organ, chitin-matrices show divergent organization to fulfill the individual requirements, e.g. flexibility for airways compared to stability for the epidermis. Nevertheless, all chitin-matrices need to undergo repetitive and synchronous processes of molting, by which means at the time when the rigidity of the cuticle restricts further body growth the old cuticle is degraded while a completely new cuticle is established at the same time (Locke & Huie, 1979; Chaudhari et al., 2011). If biosynthesis, formation or regular molting of the cuticle is defective this will result in inevitable death of insects during larval or pupal development.

Altogether, this implies that the synthesis of the ECM material by the epidermal cells needs to be strictly genetically coordinated and that its assembly also needs to be tightly controlled. Yet, not much is known how exactly cuticle components are organized into a highly ordered matrix (Moussian, 2010). Cuticle assembly occurs in the assembly zone that was molecularly characterized in the course of this PhD thesis.

4.2 - The molecular characterization of assembly zone markers sheds new light on the mechanisms of epidermal cuticle formation

The cuticle assembly zone has already been characterized in the 1970's and 1980's (Delbecque et al., 1978; Wolfgang et al., 1986; Wolfgang et al., 1987) as the cuticle region in between the epidermal cells and the lamellar procuticle. The assembly zone most likely is the site where integration of newly secreted chitin fibrils and proteins into the pre-existing

stratified cuticle occurs. However, the molecular mechanism of how exactly this is achieved is not yet understood.

In the present study the first molecular identification of factors localizing to the assembly zone was achieved. The scaffold protein Obst-A as well as the chitin deacetylases Serp and Verm and the potentially chitinolytic Chitinase 2 were found to predominantly localize to the assembly zone (chapters 3.1.2, 3.2.3, 3.2.4). Previously, it was only known that some factors are present the assembly zone, but they have not been identified or characterized yet (Wolfgang et al., 1987; Locke et al., 1994).

Strikingly, one of the few studies focusing on the cuticle assembly zone describes antigens that are constantly localized in the assembly zone and are especially abundant when molting occurs (Locke et al., 1994). This matches the results of the present study, which shows that the three assembly zone markers *obst-A*, *serp* and *verm* are strongly upregulated upon molting (Fig. 3.2.9, 3.3.1).

It is of outstanding interest that the presence of Obstructor proteins in the cuticle assembly zone was already hypothesized before the characterization of Obst-A function occurred (Moussian, 2010). In the rather speculative, but very interesting interpretation by Moussian, proteins such as the Obstructor family line up at the assembly zone to organize the specific site at which newly secreted cuticle components are integrated. The results of the present thesis are completely in line with this hypothesis.

As the study of Wolfgang et al. described, an assembly zone antigen was detected also in the molting fluid (Wolfgang et al., 1987). Thus, we wondered whether this could mean that also chitinolytic proteins might be part of an Obst-A-mediated machinery regulating chitin-formation at the apical cell surface. We therefore investigated the Glyco18 domain family by functional analysis and found out that Cht2 is required for cuticle thickening (chapter 3.1.1). In the next step we decided to analyze Cht2 localization in detail by generating an anti-Cht2 specific antibody. Indeed, immunofluorescent analysis showed enrichment of Cht2 in the epidermal cuticle assembly zone (Fig. 3.1.4) suggesting a function of Cht2 in cuticle assembly.

Because several of the other Chitinases are essential for proper epidermal cuticle formation and organization as well as for larval survival (Pesch et al., 2016a), it is necessary to analyze whether the other Chitinases are also localized in the assembly zone. For this, the generation of antibodies against the different Chts as well as expression of fluorescent protein-tagged

fusion proteins for *in vivo* characterization will be indispensable in the future to unravel the function of individual Chts in organizing cuticle dynamics.
In summary, my work on the identification of the assembly zone and its cuticle core complex proteins Obst-A, Serp, Verm and Cht2 sheds new light on the process of cuticle formation and organization.

4.3 - Chitinases and Idgfs are non-redundant regulators of cuticle assembly

Previously, not much was known about the role of Glyco18 domain proteins in the epidermal cuticle (chapter 1.5.3). Only few knockdown studies have been performed in *Tribolium castaneum* and the brown plant hopper *Nilaparvata lugens* (Zhu et al., 2008b; Xi et al., 2015), which demonstrated lethality and molting defects upon injection of siRNA directed against certain *Chitinases* and *Imaginal disc growth factors*.
Some but not all Chts were shown to hydrolyze chitin fibrils into fragments of smaller sugar chain length. For those Chts that do not possess a chitin binding domain, a function in cuticle remodeling was hypothesized (Zhu et al., 2004). For the Idgfs it is known that they are not enzymatically active due to a point mutation in the active site. As their name suggests, they act as "Imaginal Disc Growth Factors" promoting growth and polarization of imaginal disc cells (Kawamura et al., 1999; Zhu et al., 2008a).
The function of the *Glyco18* family in *Drosophila* remained completely unaddressed. The first systematic analysis of *Chts* and *idgfs* was performed by Dr. Matthias Behr and Kapil Patil. In a RNAi-mediated knockdown screen individual *Chts* and *idgfs* were depleted in cuticle forming tissues using the Gal4-UAS system and the 69B Gal4 driver line (Brand & Perrimon, 1993; Dietzl et al., 2007). This revealed a surprising role of *Drosophila* Chts and Idgfs in cuticle integrity since many *Cht* and *idgf* knockdown larvae did not withstand gentle injury, but died due to severe organ spill out. The analysis of *Cht* and *idgf* knockdown larvae was continued during my master thesis and my PhD thesis by investigation of cuticle ultrastructure (Pesch et al., 2016a; Pesch et al., 2016b). Upon knockdown of *Cht2, 5, 7, 9, 12* and *idgf1, 3, 4, 5, 6* genes defects in chitin-matrix structure were observed such as a narrowed procuticle in *Cht2* and *idgf6* knockdown larvae, a thickened structurally altered procuticle in *Cht9* knockdown larvae or unusual blister-like structures in *Cht7* knockdown larvae (Pesch et al., 2016a). In

summary, the results of this screen revealed that several Chts and Idgfs are crucial for cuticle organization and integrity.

These distinct chitin-matrix structure phenotypes might originate from different roles of the individual Chts and Idgfs in the cuticle. Some might be implicated in chitin hydrolysis to enable the packaging of appropriately sized chitin fragments into the cuticle and some could be involved in the organization of chitin fibrils into the regular, stacked lamellae.

The diverse cuticle structure defects in the individual *Glyco18* knockdown larvae and their enhanced larval lethality suggest non-redundant functions in cuticle assembly. One indication for this could be the diversity in domain structure of the different *Glyco18* family members (Fig. 1.5) (Zhu et al., 2004; Zhu et al., 2008a). Considering the enzymatic function of the Chitinases, they differ in their pH optima (Kramer & Muthukrishnan, 1997; Lu et al., 2002) and their substrate chain length specificity (Merzendorfer & Zimoch, 2003). All this indicates functional diversity among the distinct Glyco18 family members.

The reason for lethality upon knockdown of some but not all *Glyco18* genes remains unclear, since all gene knockdowns were very efficient as tested by qRT-PCR (Pesch et al., 2016a). Differences in genes expression patterns as well as in individual domain arrangements of predicted proteins (chapter 1.5.3; Pesch et al., 2016a) suggest individual requirement of different Glyco18 members for cuticle formation.

Strongest defects were observed in *Cht2* knockdown animals as they were completely lethal mostly during late larval and pupal stage and only few adults hatched that were not viable. *Cht2* knockdown larvae exhibited molting as well as strong epidermal integrity defects and showed a severely narrowed cuticle in ultrastructure analysis (Pesch et al., 2016a). For this reason the function of Cht2 in cuticle matrix formation was further analyzed.

4.4 - Chitinase 2 is essential for cuticle thickening in larvae

As *Cht2* knockdown resulted in strong lethality particularly during second and third instar larval stage (Pesch et al., 2016a), the function of Cht2 cuticle formation was investigated in these stages by immunofluorescent and electron microscopy techniques. Confocal studies showed that epidermal cuticle thickness is constant in the second instar stage but massively increases during third instar stage in control animals. In *Cht2* knockdown third instar larvae however, cuticle thickening does not occur (Supplementary Fig. S2). The maximum cuticle

thickness observed in late third instar 69B Gal4> UAS *Cht2* RNAi knockdown larvae was 2 µm, whereas in wild type third instar larvae the measured average cuticle thickness was 10 µm (Fig. 3.1.1).

This confocal microscopy data confirmed electron microscopy analysis (Supplementary Fig. S2) by Dietmar Riedel, Max Planck Institute for Biophysical Chemistry, Göttingen. The number of chitin lamellae was strongly reduced, which in wild type third instar larvae can go up to 50 due to massive cuticle synthesis as one new lamella is added each hour (Mitchell et al., 1971; Kaznowski et al., 1985). In *Cht2* knockdown larvae the number of lamellae did not increase at all during the third instar stage. Of great importance, the cuticle assembly zone that is usually detected as a distinct zone above the apical epidermal cell surface was strongly reduced or even not detected at all in *Cht2* knockdown larvae. Furthermore, distinct chitin lamellae in third instar *Cht2* knockdown larvae were irregularly spaced, fitting well to my observation that chitin-matrix structure is defective in the knockdown animals. In summary, our data suggest the requirement of *Cht2* gene function for the assembly zone, which in turn could be essential for proper chitin-matrix formation by increasing the amount of chitin-lamellae and thereby contributing to cuticle thickness.

To unravel possible underlying molecular events, it was addressed if maturation and protection of the newly synthesized chitin-matrix is affected in *Cht2* knockdown larvae. As the assembly zone is missing, the important cuticle regulatory factors Obst-A, Serp and Verm, which are normally enriched in the assembly zone (Fig. 3.2.5, 3.2.7 and Supplementary Fig. S3), were mislocalized. This most likely causes structural defects in the cuticle, because Obst-A was shown to have a scaffold function for cuticle assembly by binding chitin fibrils in the assembly zone. Additionally, Obst-A is essential for the proper localization of the chitin deacetylases Serp and Verm that play a role in the structural maturation and stabilization of the chitin-matrix (chapter 1.5.2). In contrast to Obst-A and the deacetylases, the localization of the chitin protector Knk was not affected in *Cht2* knockdown larvae (Supplementary Fig. S1) suggesting a function of Cht2 in assisting cuticle assembly and organization.

In this line of evidence, polyclonal antibodies raised against Cht2 were generated in rabbits and guinea pigs (chapters 2.2.3.4, 3.1.2). Immunostaining in the epidermis showed that Cht2 was indeed enriched in the cuticle assembly zone (Fig. 3.1.4), but was also found at the chitin-lamellae. Interestingly, not only functional data suggest the importance of Cht2 action

in the protein core complex in the chitin-matrix that is controlled by Obst-A, but additionally Cht2 is localized similar to Obst-A in the epidermal cuticle (Fig. 3.2.5). Thus, my studies support a molecular model for Cht2 function in cuticle thickening as summarized in Fig. 4.2. The function of Cht2 in the assembly zone for determining the size of the lamellar procuticle could be the enzymatic modification of nascent chitin fibrils into fragments of a certain length, which are subsequently bound by the Obst-A scaffold for packaging into stable lamellae and modified by Serp and Verm for their stabilization. Alternatively, Cht2 could inhibit premature assembly of chitin fibrils into lamellae or could assist in ordering and organizing chitin fibrils. These scenarios could all cause the absence of the assembly zone resulting in a cuticle with a reduced number of structurally altered lamellae and thus, might lead to epidermal integrity defects and lethality.

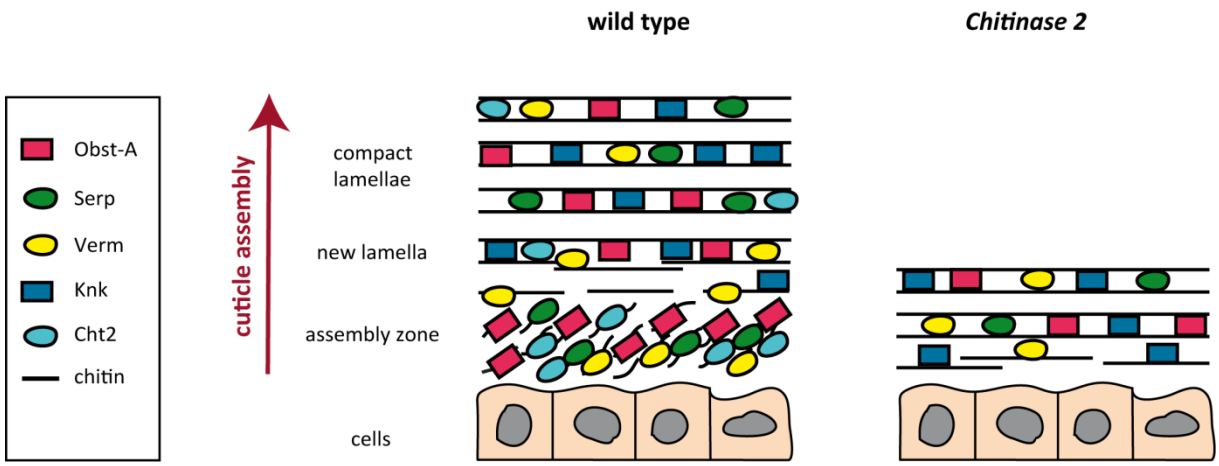

Fig. 4.2 - Chitinase 2 is necessary for lamellar cuticle thickening. Schematic model of Cht2 function in the epidermal cuticle. The direction of cuticle assembly is indicated by the red arrow. In the wild type (left) cells secrete chitin fibrils into the assembly zone where they are bound by the Obst-A scaffold protein and modified by the chitin deacetylases Serp and Verm. This enables the formation of new chitin lamellae and the integration into the compact lamellar chitin-matrix. Cht2 is primarily enriched in the assembly zone and crucial for the localization of Obst-A, Serp and Verm. When Cht2 is not present (right), the assembly zone is absent and the important factors Obst-A, Serp and Verm are mislocalized. This leads to reduction of the number of chitin lamellae, defects in lamellar structure and hence to impaired cuticle integrity.

As cuticle assembly zone is essential for organizing the chitin-matrix and Cht2 is required for assembly zone function, we expected that also outer cuticle layers could be affected by loss of the assembly zone. Indeed, electron microscopy analysis by Dietmar Riedel, Göttingen, also revealed misdistribution of pore canals in the cuticle of *Cht2* knockdown larvae (Pesch

et al., 2016b). Pore canals are connected to the epidermal cells and most likely transport lipids and waxes to the outermost envelope layer of the cuticle (Locke, 1961). In third instar wild type larvae pore canals can be detected in the outer parts of the procuticle reaching to the envelope, whereas upon *Cht2* knockdown deformed pore canal-like structures were found throughout the entire procuticle (Pesch et al., 2016b). It is hypothesized that correct localization of pore canals is dependent on chitin-matrix structure (Noh et al., 2014). Thus, the misdistribution of pore canals in *Cht2* knockdown larvae could be explained by the defective chitin-matrix.

4.5 - Chitinase 2 is expressed in chitin-synthesizing organs for cuticle organization.

Protein expression pattern and subcellular localization was left unknown for Cht2 in insects. My studies showed Cht2 expression during embryonic stage 14 and 15 in the salivary glands and the tracheal system. In late embryos additional Cht2 staining was found in the epidermis, the proventriculus, the hindgut, the anterior and posterior spiracles (Fig. 3.1.3). This is in line with in situ hybridization data in late embryos in which Cht2 expression was detected in the epidermis, the tracheal system, the foregut and the posterior spiracles (Pesch et al., 2016a).

In third instar larvae Cht2 staining was found in the epidermis where it was enriched in the cuticle assembly zone (see above), the trachea, salivary glands, anterior midgut (including the proventriculus), imaginal discs and the posterior spiracles (Fig. 3.1.4). These tissues mainly constitute sites of chitin production (Richards & Richards, 1977; Lehane, 1997; Tonning et al., 2005; Moussian et al., 2006a). In chitin-producing tissues Cht2 was found both intra- and extracellulary. The described expression pattern can explain the phenotypes observed upon knockdown of *Cht2* including the epidermal integrity phenotype and the molting defects affecting mouth hooks and spiracles (Pesch et al., 2016a). The localization of Cht2 in the cuticle assembly zone (Fig. 3.1.4) can explain the deficiency of Cht2 knockdown larvae to establish new cuticle lamellae (Fig. 3.1.1) as discussed above.

The expression of Cht2 in both cuticle-producing and non-chitinous organs such as the secretory active salivary glands suggests that Cht2 is a target of secretion. This might occur both in the cuticle-producing organs where Cht2 acts extracellularly in the chitin-matrix as

well as probably in non-chitinous organs, probably leading to Cht2 distribution via the hemolymph. Furthermore, the expression of Cht2 in several chitinous organs might indicate the function of Cht2 in chitin-matrices at distinct sites.

In the midgut Cht2 may either play a role in the digestion of chitin containing food or be involved in organization of the peritrophic matrix (Lehane, 1997). The epidermal expression of Cht2 from late embryogenesis onwards can be explained by the constant requirement of reorganization as the epidermal cuticle needs to be constantly renewed and extended during larval development, e.g. upon wounding, molting and body growth (Moussian, 2010).

4.6 - Obstructor-A is required for larval survival and epidermal cuticle assembly

Obst-A is a chitin-binding protein that is expressed in diverse tissues of ectodermal origin (Fig. 3.2.4), such as the epidermis, the tracheal system, the proventriculus, imaginal discs and the ring gland.

The function of Obst-A in the tracheal cuticle was molecularly characterized in Petkau et al., 2012. In this thesis the function of Obst-A in the epidermis and the endocrine ring gland was addressed (chapters 3.2 and 3.3). Loss of *obst-A* leads to full lethality before reaching second instar stage and to severe cuticle integrity defects (Fig. 3.2.2, 3.3.15; Petkau et al., 2012). This indicates a function of Obst-A in the epidermal cuticle. Indeed, Obst-A was found to be a crucial scaffold for cuticle assembly. The mechanism of Obst-A mediated cuticle formation was published in Pesch et al., 2015, and is discussed below.

Analysis of cuticle ultrastructure in JB-4 sections of *obst-A* mutants revealed normal chitin levels (Fig. 3.2.3) excluding a role of Obst-A in chitin formation. Nevertheless, the procuticle was structurally highly defective. About half of the larvae showed an immensely wrinkled cuticle representing an unique phenotype that has never been published before. The furrowed cuticle of *obst-A* mutants was also seen in cryosections (data not shown) excluding a dehydration artifact caused by the harsh treatment that is needed for generating JB-4 sections. The wrinkle phenotype was also frequently observed in transheterozygous *obst-A/+;knk/+* larvae (Fig. 3.2.14).

Additionally, detachment of the chitinous cuticle from the epidermal cells occurred in about 30 % of *obst-A* mutants (Fig. 3.2.3). A similar detachment phenotype was observed in

mutants lacking the zona pellucida protein Piopio and the large ECM protein Dumpy, which attach the cuticle to epithelial cells (Wilkin et al., 2000; Jaźwińska et al., 2003; Bökel et al., 2005). Furthermore, cuticle detachment was seen in *kkv*/*chitin synthase-1* mutants (Ostrowski et al., 2002) and in *alas* mutants (Shaik et al., 2012). Alas (aminolevulinate synthase) is implicated in protection of the cuticle against dehydration (Shaik et al., 2012). In addition to *obst-A* null mutants, detachment was frequently seen in *serp* knockdown larvae and transheterozygous *obst-A/+;serp,verm/+* mutants (Fig. 3.2.12, Fig. 3.2.14). As Obst-A was found to be implicated in cuticle organization and the assembly zone was missing in *obst-A* deficient larvae (chapter 3.2.3), these results suggest that proper cuticle formation in the assembly zone is a prerequisite for tight adhesion of the cuticle to the epidermal cells.

The apical cell surface of the epidermal cells most probably represents the site at which first chitin-organization takes place (Moussian, 2013b) whilst in the cuticle assembly zone directly above the apical cell surface the integration of chitin fibrils into the lamellar matrix is thought to occur (Wolfgang et al., 1987; Locke et al., 1994).

Throughout all larval stages Obst-A was always detected at the sites of cuticle assembly, being enriched in the assembly zone from first instar stage onwards and present in high levels in the newly synthesized cuticle upon molting (Fig. 3.2.5). In addition, Obst-A was also found in the procuticle where it localized to the distinct chitin lamellae (Fig. 3.2.6). This is in line with biochemical assays that prove the capability of Obst-A to bind chitin (Petkau et al., 2012; unpublished data Matthias Behr). Supportive electron microscopy data by Dietmar Riedel (Supplementary Fig. S3) show that the cuticle assembly zone is absent in *obst-A* mutants, normal lamellar chitin architecture is disturbed and the cuticle is unusually wrinkled. Thus, Obst-A is not only localized in the assembly zone, but it is also essential for its presence.

In the tracheal system Obst-A controls a core complex of proteins and chitin for chitin-matrix maturation and protection. Obst-A binds chitin and recruits the chitin deacetylase Serp and the chitin protector Knk to the matrix (Petkau et al., 2012). However, the tracheal chitin-matrix is is rather viscous and elastic when compared to the compact and lamellar epidermal chitin-matrix. Furthermore, the tracheal matrix is very thin and hence problematic for a detailed localization study of chitin-matrix proteins. By contrast, the epidermal chitin-matrix is much thicker and even massively increases its size. As the epidermal body wall cuticle needs to be very stable against environmental stresses, we decided to test whether Obst-A

may have similar roles there or wether the massive epidermal cuticle formation involves different sets of proteins. The latter is thinkable since the *obstructor* family comprises at least four genes strongly related to Obst-A and it could be possible that there is redundancy (Tiklová et al., 2013) in organizing the cuticle.

Thus, the tracheal interaction partners of Obst-A were investigated in the epidermal cuticle. In *obst-A* null mutants, Serp and Verm (Luschnig et al., 2006; Wang et al., 2006), which are found to be enriched in the assembly zone in wild type larvae (Fig. 3.2.7), were misdistribited throughout the entire cuticle (Fig. 3.2.8). Furthermore, on the mRNA expression level *serp* and *verm* were reduced in *obst-A* mutants particularly at the stage when in the wild type molting to second instar stage occurs, which is hindered in the mutants (Fig. 3.2.9).

We next asked whether cuticle protection is affected in *obst-A* mutants. The chitin protector Knk (Moussian et al., 2006b; Chaudhari et al., 2011) can be found throughout the procuticle of wildtype larvae in strong colocalization with chitin (Fig. 3.2.7). Although in the *obst-A* mutant the cuticle structure was clearly disturbed, Knk was still properly localized, *knk* mRNA expression was upregulated in *obst-A* mutants shortly before their death (Fig. 3.2.10) most probably representing a mechanism to enhance protection of the defective cuticle.

However, localization data indicates that Obst-A is not restricted to the assembly zone but can also be observed in the chitin-lamellae where Knk appears as well. Moreover, analysis of transheterozygous *obst-A*/+;*knk*/+ mutant larvae clearly showed the most severe cuticle phenotype as they exhibited a wrinkled and therefore instable body wall cuticle. In addition these mutants are extremely lethal, altogether strongly indicating a genetic interaction of both proteins for protecting newly synthesized chitin-matrix as found in trachea.

In summary, our data imply that tracheal and epidermal chitin-matrix formation requires the same protein core complex, due to amino acid sequence conservation most likely representing an evolutionarily conserved mechanism in insects (Pesch et al., 2015). Nevertheless, these results do not exclude that other Knk-related proteins or other yet unidentified chitin protectors are affected in *obst-A* mutants. In *Tribolium castaneum* the *knk* family comprises three distinct genes and also in *Drosophila* the existence of three distinct *knk* members was predicted (Chaudhari et al., 2014).

In transheterozygous *obst-A*/+;*serp*, *verm*/+ larvae, frequent detachment of the cuticle from the epidermal cells was detected and Obst-A, Serp and Verm were restricted to the epidermal cells and not distributed within the thinned chitin-matrix (Fig. 3.2.14). These

findings provide evidence that *obst-A* interacts at least genetically with *serp* and *verm* for organizing the chitin-matrix formation and maturation within the assembly zone at the apical cell surface. This molecular mechanisms is not limited to one specific organ but likely is rather general for cuticle formation.

Taken together, our data indicate that Obst-A is a crucial factor for cuticle assembly. As it binds lamellar chitin (Fig. 3.2.6), is highly enriched in the assembly zone and colocalizes with the lowest and therefore newest chitin lamella (Fig. 3.2.5) Obst-A could assist in packaging of newly secreted chitin fibrils into the stratified procuticle. This might occur particularly in the cuticle assembly zone for *de novo* assembly of lamellae, but also in the lamellar procuticle for reorganization and stabilization of the chitin-matrix. Additionally, Obst-A is required for the localization of Serp and Verm in the assembly zone where they can directly modify newly secreted chitin into the more stable chitosan (Luschnig et al., 2006; Tsigos et al., 2000; Yang et al., 2011; Hsiao et al., 2013). A model of Obst-A function is illustrated in Fig. 4.3.

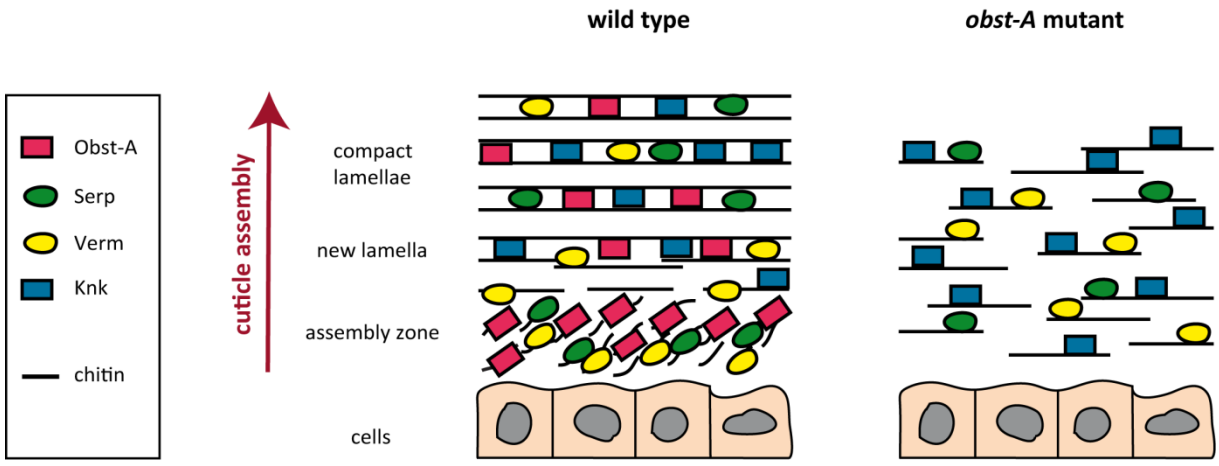

Fig. 4.3 - The Obst-A-mediated scaffold is required for chitin-matrix formation and localization of maturation enzymes within the cuticle. Schematic model of Obst-A function. The direction of cuticle assembly is indicated by the red arrow. In the wildtype (left) the epidermal cells secrete chitin fibrils and proteins into the assembly zone. This is the place where those components are integrated into the preexisting lamellar structure. Obst-A can be found enriched in the assembly zone where it builds a scaffold for correct cuticle assembly. We could show that it binds to lamellar chitin and that it is necessary for the proper localization of the chitin deacetylases Serp and Verm. These are also enriched in the assembly zone and contribute to cuticle formation by modifying chitin into the more stable chitosan enhancing cuticle integrity. In *obst-A* mutants (right) this important scaffold for cuticle assembly is lost. Chitin and other components are secreted by the epidermal cells, but they cannot be assembled into a stable, organized structure. The deacetylases cannot properly modify chitin and consequently, chitin does not form a dense lamellar structure leading to heavily compromised cuticle stability.

As Obst-A acts as scaffold for chitin-matrix formation and maturation, this explains the severe cuticle integrity defects in *obst-A* deficient larvae. It still remains elusive if Obst-A prevents the premature, unorganized assembly of chitin fibrils or if it directly orders chitin. The Obst-A protein structure consisting of three regularly spaced chitin binding domains (Behr & Hoch, 2005) and the loss of the assembly zone in *obst-A* mutants are arguments for the second hypothesis.

It was argued that the high number of genes encoding for different chitin-binding proteins might ensure cuticle stability even if one factor is lost because of a genetic defect (Moussian, 2010). However, for *obst-A* this does not hold true as mutants are completely lethal before reaching second instar stage (Petkau et al., 2012; chapter 3.3). The tremendous cuticle defects observed in the mutants suggest a function of Obst-A as "master regulator" of cuticle assembly.

To investigate the function of Obst-A in the digestive system and in the imaginal discs was beyond the scope of this thesis. In the chitin-forming parts of the gut to which the proventriculus belongs (Lehane, 1997), Obst-A could have a role in chitin-matrix assembly in the peritrophic matrix. The chitinous peritrophic matrix of the midgut provides stability to the digestive system and exerts a barrier function to avoid damage caused by the passage of food or by invading pathogens (Lehane, 1997). In the imaginal discs Obst-A is strongly expressed in single cell clusters (Fig. 3.2.4), which possibly represent sensory organ precursors. These develop as single cell clusters in the imaginal disc to form adult sensory organs such as bristles. Cuticle formation also plays a role in the differentiation of imaginal sensory organ precursors during metamorphosis (Hartenstein & Posakony, 1989; Bang et al., 1995).

The Obstructor family of chitin-binding proteins is highly conserved among invertebrates (Behr & Hoch, 2005; Petkau et al., 2012; Jasrapuria et al., 2012) indicating that the Obst-A mediated scaffold for chitin-matrix organization could be a mechanism present in many different species. The function of the other Obstructor family members in *Drosophila* also still needs to be characterized. Due to the presence of chitin binding domains and their expression in cuticle-forming tissues (Behr & Hoch, 2005) it could be possible that other Obstructor members have functions in cuticle assembly in the chitin-matrix of epidermis, trachea and/or digestive system. For Obst-C/Gasp it was shown that it is implicated in tracheal tube dilatation and that it is also required for epidermal cuticle integrity and larval

growth (Tiklová et al., 2013). Also the Obst-C/Gasp homolog of the spruce budworm *Choristoneura fumiferana* plays a role in cuticle assembly (Nisole et al., 2010). *Choristoneura fumiferana* is the major pest destroying coniferous forests in North America opening up the question if the Obst-C/Gasp homolog could be a possible target for pest control (Zhang et al., 2014; P. Bhagat Kumar et al., 2016).

Obstructor subgroup 2 proteins, in which the chitin binding domains are not evenly spaced, are expressed in chitin-producing parts of the digestive system where they could possibly assist formation and organization of the peritrophic matrix that is less organized than the stratified epidermal chitin-matrix (Lehane, 1997; Behr & Hoch, 2005).

In the future it will be important to study the putative function of the different Obstructor proteins in the cuticle to identify molecular mechanisms of chitin-matrix assembly, which may potentially lead to the development of new pest control strategies.

4.7 - Obstructor-A has similar but divergent roles in the epidermal and the tracheal cuticle

It was previously shown that Obst-A has a crucial role for cuticle maintenance in the tracheal system (Petkau et al., 2012) in which Obst-A is apically secreted and builds a ternary complex at the chitin lamellae together with Serp and Knk, preventing chitin from its premature degradation by chitinolytic enzymes. Thereby, Obst-A is essential for cuticle integrity. In late embryogenesis chitin in the tube lumina is eventually degraded by chitinolytic enzymes and cleared by clathrin-mediated endocytosis (Tonning et al., 2005; Behr et al., 2007; Stümpges & Behr, 2011).

The present study intended to investigate the function of Obst-A in the epidermal cuticle. Indeed, in the epidermis Obst-A also has an important function in cuticle integrity and is also found within the chitinous procuticle (Fig. 3.2.6). However, the strongest accumulation of Obst-A can be seen at the apical cell surface of the epidermal cells in the cuticle assembly zone (Fig. 3.2.5). This is different from the trachea where Obst-A is primarily found colocalizing with chitin at the fibrils (Petkau et al., 2012).

In the epidermis Obst-A also colocalizes with Serp in the assembly zone (Fig. 3.2.7). Knk, however, was found to be distributed at the chitin lamellae of the entire procuticle, mostly colocalizing with chitin (Fig. 3.2.7). This is in line with the studies from Chaudhari et al., 2011,

in the red flour beetle *Tribolium castaneum* where it was also shown that Knk is localized within the chitinous procuticle. Obst-A was also detected at the chitin lamellae in colocalization with chitin (Fig. 3.2.6).

In contrast to the tracheal system, the ternary complex of Obst-A, Serp and Knk at the chitin fibrils does not form. On the contrary, Obst-A and the deacetylases Serp and Verm are enriched at the assembly zone. Upon loss of *obst-A*, Serp and Verm are mislocalized within the epidermis showing that proper Obst-A function is needed for the placement of the cuticle maturation enzymes. This reveals two connected functions of Obst-A in the epidermal cuticle: First of all, its scaffold function as chitin-binding protein aids in the proper integration of newly synthesized chitin into the nascent lamellar matrix. Second, Obst-A has a role in the stabilization of chitin by its maturation through localization of the deacetylases Serp and Verm. This is more multifaceted than in the trachea where the primary function of Obst-A is the protection of chitin against its premature degradation.

It was shown that in the epidermis *obst-A* genetically interacts with *serp*, *verm* and *knk* (chapter 3.2.4.5). In the trachea, direct protein interaction of Obst-A was observed with Serp, Knk, but not with Verm, and genetic interaction of *obst-A* with *serp* and *knk* was proven (Petkau et al., 2012). Both in the tracheal system and in the epidermis, Obst-A is necessary for the proper localization of Serp. Verm, however, only seems to play a functional role in the epidermal cuticle as no interaction of Obst-A and Verm was proven in the tracheal cuticle (Petkau et al., 2012).

4.8 - Obstructor-A is upregulated upon larval molting and is targeted by ecdysone signaling

Both Obst-A protein (Fig. 3.2.5) as well as mRNA levels (Fig. 3.3.1) were found to be strongly enriched upon larval molting. During the first molt *obst-A* mRNA is 25-fold upregulated and during the second molt more than 30-fold.

Expression analysis of other *obst* family members (*obst-B, -C, -D, -E*) showed a similar pattern being upregulated at times of molting, too (data not shown). Comparable upregulation during molting was already published before for Gasp (Obst-C) in the spruce budworm *Choristoneura fumiferana* (Nisole et al., 2010). In the mosquito *Anopheles gambiae* genes related to the *obstructor* family were found to be strongly elevated in their expression upon

molting (Vannini et al., 2015). Both *Choristoneura fumiferana* and *Anopheles gambiae* constitute major pests, the first by defoliating forests and the latter by transmitting malaria (Zhang et al., 2014; Swale et al., 2016). If the upregulation of *obstructor*-related genes during molting is crucial for larval survival or the exertion of the molt, this could potentially lead to the development of new pest control strategies.

In insects molting is controlled by the steroid hormone ecdysone, which binds to a nuclear receptor complex and induces a cascade of target genes that in the end leads to accomplishment of the developmental transition (Thummel, 2002). A microarray analysis by the Thummel lab found that *obst-A* is direct target gene of ecdysone responses and that its expression is dependent on the ecdysone receptor (Beckstead et al., 2005). To further analyze which transcription factors that are induced by ecdysone control *obst-A* expression, transcription factor binding site analyses using the *obst-A* sequence and its putative promotor were conducted (chapter 3.3.1.2). The outcome was that in the analyzed sequence a multitude of binding sites of ecdysone-related transcription factors are present, many of which also showed high probability to be functional *in vivo*. The predicted major regulatory factors influencing *obst-A* expression are the broad complex (Karim et al., 1993; Crossgrove et al., 1996), E74A (Karim & Thummel, 1991) and Vvl (Danielsen et al., 2013). The binding of major ecdysone-related transcription factors responsible for exerting the "molting gene expression program" can explain the upregulation of *obst-A* when molting occurs.

It might be of great biological relevance that a chitin binding cuticle-matrix scaffold protein like Obst-A is strongly enriched during molting. We could show that Obst-A is localized everywhere where new cuticle material is deposited (Fig. 3.2.5). For example, during molting events Obst-A is strongly enriched in the new cuticle that is being synthesized, whereas it is only weakly detected in the old cuticle that is being degraded.

Upon molting a new complete cuticle is synthesized within a short period of time, which requires a stringent regulation of cuticle formation and organization. As the degradation of the old cuticle occurs in parallel, the new cuticle must be stable enough to withstand the chitinolytic and proteolytic enzymes in the molting fluid. This also involves protective mechanisms (Chaudhari et al., 2011). The scaffold function of Obst-A as chitin-binding protein required for cuticle assembly and maturation makes it absolutely crucial for proper cuticle assembly in periods in which the epidermal chitin-matrix is reorganized.

Since during molting rapid secretion of chitin-fibrils by the epidermal cells and extensive cuticle remodeling takes place, the upregulation of *obst-A* as "master organizer" of chitin-matrix formation and maturation is explainable.

4.9 - Obstructor-A mutants suffer from ecdysone deficiency

It was previously thought that the structural defects of the tracheal and epidermal cuticles in *obst-A* mutants led to their insufficiency to molt (Petkau et al., 2012). Nevertheless, this does not fully explain their tremendous growth defect and their capability to synthesize a second instar cuticle (chapters 3.2.1.1, 3.3.2). If only the function of Obst-A in organizing cuticle assembly played a role, this would not explain the death after synthesizing the second instar cuticle, but before shedding the old first instar cuticle. Also upon knockdown of certain *Chitinases* and *idgfs* double mouth hooks or spiracles can be observed (Pesch et al., 2016a), but despite of the lethality observed in the knockdown larvae, these molting defects are mostly transient and many knockdown larvae develop to third instar stage, in contrast to the *obst-A* mutants, which cannot enter the second instar stage at all. However, it should be noted that the knockdown larvae show about 10 % residual *Cht* and *idgf* expression. Therefore, the generation of transcript null mutants would be important to determine if and how Cht and Idgf function is required for molting.

Obst-A mutants show the typical phenotype of mutants suffering from deficiency of the molting hormones ecdysone or ETH. Just as *obst-A* mutants, *eth* mutants are unable to molt to second instar stage showing incomplete cuticle shedding, the presence of double mouth hooks and 98% lethality upon molting (Park et al., 2002). This is nearly identical to the *obst-A* mutant phenotype showing 100 % lethality before completing the molt from L1 to L2. Furthermore, the behavioral sequence upon ecdysis is changed both in *eth* mutants (Park et al., 2002) and *obst-A* mutants. Just as *eth* mutants, *Obst-A* deficient larvae do not exhibit the "forward thrust" of ecdysis behavior, which would normally result in shedding of the old mouth hooks. As a consequence, only the posterior part of the cuticle is discarded in mutants that survive until this stage.

The expression of *eth* as well as the related *eh* (Zitnan et al., 1999; Park et al., 2002), which are responsible for the behavioral sequence that leads to cuticle shedding, were found to be reduced in *obst-A* mutants (Fig. 3.3.3). However, as *eth* is a direct target of ecdysone and *eh*

is controlled by *eth* (Zitnan et al., 1999; Krüger et al., 2015), the reduced levels of *eth* and *eh* in *obst-A* mutants might also be caused by impaired ecdysone production.

Several mutants of the ecdysone pathway show a phenotype similar to the molting defects seen in *obst-A* mutants. Defects in the ecdysone pathway either lead to developmental arrest at a certain stage (Karim et al., 1993; Fletcher & Thummel, 1995; Neubueser et al., 2005) or to the presence of a double cuticle that is visible at the mouth hooks and spiracles as the larvae are able to synthesize a new cuticle, but cannot shed their old cuticle (Perrimon et al., 1985; Oro et al., 1992; Bender et al., 1997; Schubiger et al., 1998; Hall & Thummel, 1998; Freeman et al., 1999; Li & Bender, 2000; Yamada et al., 2000; Bialecki et al., 2002; Oron et al., 2002; Gates et al., 2004; Gaziova et al., 2004; Ou et al., 2016). The mutations causing this so called "ultraspiracle" phenotype (Perrimon et al., 1985; Oro et al., 1992; Gates et al., 2004) affect either genes that are important for the production and release of ecdysone or nuclear receptors including early response genes.

As the molting defect of *obst-A* mutants is identical to the "ultraspiracle" phenotype, the obvious next step was to test for ecdysone production in the *obst-A* mutant. A commonly used read out for quantifying ecdysone production is the expression of the early response gene *E74A* (Thummel et al., 1990; Karim & Thummel, 1991; Fletcher & Thummel, 1995; Gates et al., 2004; Gündner et al., 2014), which is described to be a sensitive indicator of ecdysone responses.

qRT-PCR analysis of *E74A* expression revealed a severe ecdysone deficiency in *obst-A* mutants (Fig. 3.3.5). In the wild type *E74A* is 150-fold upregulated during molting, whereas only a minor rise in expression was detected in *obst-A* mutants shortly before their death, which constituted only a small fraction of the normal peak amplitude at molting.

In the mutant lacking the ecdysone receptor cofactor *rigor mortis* (Gates et al., 2004) also no induction of *E74A* was detected just as in *obst-A* mutants. Similar to *obst-A* mutants, larvae lacking *rigor mortis* show severely disturbed ecdysone signaling and lethality upon molting.

E74A is an important factor inducing stage- and tissue-specific ecdysone secondary response genes, in the epidermis, the imaginal discs and the fat body. Therefore it is absolutely necessary for developmental progression (Fletcher & Thummel, 1995). Thus, the lack of *E74A* induction alone would explain the inability of *obst-A* mutants to molt. Nevertheless, the ecdysteroid insuficiency in *obst-A* mutants was further analyzed to find out if and how Obst-A can influence molting on a hormonal level.

The impaired ecdysone response in the *obst-A* mutant gave rise to two hypotheses. First, ecdysone biosynthesis is so strongly reduced that ecdysone responses cannot be established and in the end the ecdysteroid amount produced is not sufficient to reach the next larval stage; or second, ecdysone signaling downstream of the receptor is heavily disturbed.

4.10 - Obstructor-A influences the hormonal control of molting

To prove one of the hypotheses, the expression of several genes controlling ecdysone production were tested. These included *ptth*, which is the main upstream regulator of ecdysone biosynthesis (Kawamaki et al., 1999; Gilbert et al., 2002; McBrayer et al., 2007), the *Halloween* genes (Warren et al., 2002; Gilbert et al., 2004; Rewitz et al., 2006; Petryk et al., 2003), the receptor complex (Perrimon et al., 1985; Oro et al., 1990; Schubiger et al., 1998; Schubiger & Truman, 2000; Gates et al., 2004), the substrate import and ecdysone degradation machinery (Huang et al., 2005; Rewitz et al., 2010; Rewitz et al., 2013), important transcription factors positively influencing ecdysone production (Wismar et al., 2000; Warren et al., 2001; Jin et al., 2005; Neubueser et al., 2005; Danielsen et al., 2014) and ecdysone target genes such as the *broad* complex (Karim et al., 1993; Riddiford et al., 2003).
Based on the finding that expression of the primary response gene *E74A* is not induced in the *obst-A* mutant, it was not surprising that also the expression of *broad* isoforms and *Ftz-f1* was downregulated in the mutant (Fig. 3.3.5).
Unexpectedly, already the most upstream factor regulating ecdysteroidogenesis, namely *ptth*, was found to be transcriptionally reduced in *obst-A* mutants (Fig. 3.3.4). PTTH is a neuropeptide hormone that is secreted by a lateral pair of neurons in each brain hemisphere (Siegmund & Korge, 2001) and stimulates ecdysone production in the prothoracic gland (Gilbert et al., 2002; McBrayer et al., 2007). The reduced *ptth* levels in *obst-A* mutants could have several reasons. Even though the regulation of *ptth* levels is not completely understood, it is known that they are influenced by the nutritional status of the larvae, the circadian clock and ecdysone levels (Mirth et al., 2005; McBrayer et al., 2007; Young et al., 2012). An influence of the circadian clock can be ruled out as larvae for all experiments larvae were reared in an incubator with a constant light/dark cycle (12 h/12 h) and mutant and wild type control larvae were always let grown and collected in parallel. Additionally, the

expression of genes that are implicated in regulation of the circadian rhythm were unaltered in *obst-A* mutants (data not shown).

PTTH is also influenced by nutritional status, such as the TAG levels, which were strongly reduced in *obst-A* mutants (Fig. 3.3.4 B), even though they take up food normally (data feeding assay Matthias Behr). Albeit TAG levels were lowered in *obst-A* mutants, they did not suffer from severe starvation. The expression of *lipase 3*, which is normally strongly upregulated upon starvation, was unaltered in *obst-A* mutants compared to wild type control larvae (data not shown). Additionally, target genes of TOR and Insulin signaling, which would indicate starvation responses, were not significantly affected in *obst-A* mutants (data internship Michelle Dassen). Yet it is possible that the double mouth hooks prevent the mutants to take up nutrition (Chadfield & Sparrow, 1985) resulting in mobilization of storage fat represented by lowered TAG levels. A weak starvation response was seen in late stage *obst-A* mutants exhibiting the double mouth hook phenotype (data internship Michelle Dassen). Thus, the nutritional status of *obst-A* mutants can negatively influence *ptth* expression, but the regulation of *ptth* levels by ecdysone needs to be taken into account.

PTTH is implicated in a positive feedback loop with the active molting hormone 20E (Young et al., 2012; Yamanaka et al., 2013). This means that the reduced *ptth* levels in the *obst-A* mutants can also be caused by improper ecdysone production, which as a consequence further shuts down ecdysone biosynthesis and signaling leading to even less *ptth* expression in a vicious cycle.

Ecdysone biosynthesis begins with cholesterol that is taken up with the food and imported into cells of the prothoracic gland. The Neverland dehydrogenase (Gilbert et al., 2002; Yoshiyama et al., 2006) and the Halloween enzymes Spookier, Shroud, Phantom, Disembodied and Shadow mediate the stepwise conversion of cholesterol into ecdysone (Chávez et al., 2000; Warren et al., 2002; Warren et al., 2004; Niwa et al., 2004; Namiki et al., 2005). In *obst-A* mutants the expression of *neverland*, *spookier*, *shroud* and *phantom* was found to be markedly reduced (Fig. 3.3.6) indicating a defect in ecdysone biosynthesis. The expression of the late biosynthesis genes *disembodied* and *shadow* in contrast was found to be higher in the *obst-A* mutants in late stages when normally molting would occur (Fig. 3.3.6). This finding could hint at a feedback mechanism with the function to stimulate ecdysone production.

In addition, *obst-A* mutants exhibited lowered expression levels of the transcription factors *kni*, *vvl* and *woc* (Fig. 3.3.8), which are responsible for the induction of the *Halloween* genes (Wismar et al., 2000; Warren et al., 2001; Jin et al., 2005; Danielsen et al., 2014). This might also explain the misregulation of the *Halloween* genes in larvae lacking *obst-A*. The misregulation of the above mentioned transcription factors and the *Halloween* genes is another indication of a complicated feedback mechanism taking place in which Obst-A positively influences ecdysone production. The exact regulation of ecdysone production and the complicated feedback mechanisms that are involved are not yet understood (Yamanaka et al., 2013; Ou et al., 2016). The involvement of many different pathways in ecdysone signaling (Mirth et al., 2005; Layalle et al., 2008; Gibbens et al., 2011; Johnston et al., 2011; Shimada-Niwa & Niwa, 2014; Colombani et al., 2015) and the discovery of more and more transcription factors that specifically regulate the expression of certain ecdysone-related genes (Neubueser et al., 2005; Warren et al., 2001; Danielsen et al., 2014; Komura-Kawa et al., 2015) suggests the presence of yet undiscovered regulatory factors and underlines the complexity of the ecdysone pathway. Recent results also show that epigenetic regulation plays an important role in fine-tuning ecdysone responses (Pankotai et al., 2010; Bodai et al., 2012; Borsos et al., 2015; Pahi et al., 2015) adding an additional level of complexity.
The misregulation of so many genes involved in different steps of ecdysone signaling, reception and downstream signaling in *obst-A* mutants points towards a crucial role of Obst-A in the hormonal control of molting.

4.11 - The ecdysone receptor complex might be disturbed in *obstructor-A* mutants

When ecdysone is released from the cells of the prothoracic gland the hydroxylase Shade mediates its conversion into the active molting hormone 20-hydroxyecdysone that is able to bind to the ecdysone receptor complex (Petryk et al., 2003). In the wild type the ecdysone receptor (*EcR*) shows upregulation upon molting, further amplifying ecdysone signaling in a positive feedback loop (Koelle et al., 1991) (Fig. 3.3.7). The upregulation of *shade* and *EcR*, which is normally seen when molting occurs, is absent in *obst-A* mutants. This of course is a consequence of the reduced ecdysone production, but further shuts down ecdysone signaling.

In *obst-A* mutants the EcR was detected predominantly in the nuclei with no difference seen between mutant and control animals (Fig. 3.3.10). However, this does not necessarily mean that there is full EcR-mediated target gene induction, which would be in strong contrast to the results of qRT-PCRs showing that ecdysone target genes are not induced in *obst-A* mutants (chapter 3.3.3). First of all, EcR can enter the nucleus without ecdysone binding and also independent of Usp (Cronauer et al., 2007). Furthermore, the unliganded EcR/Usp heterodimer can act as repressor changing its function upon ecdysone binding (Schubiger & Truman, 2000). Additionally, a multitude of co-factors are needed for EcR function (Yamanaka et al., 2013).

The EcR cofactor *rigor mortis* (Gates et al., 2004) was shown to be strongly misregulated in *obst-A* mutants (Fig. 3.3.8), thereby possibly disturbing ecdysone signaling. Rigor mortis binds to the EcR/Usp complex and is essential for the progression during molting and pupariation (Gates et al., 2004). In *obst-A* mutants *rig* is 20-fold upregulated at most investigated time points. This could severely disturb the stochiometry of the receptor complex and hinder binding to ecdysone responsive DNA elements, thereby blocking target gene induction. Strikingly, the phenotype of *rig* mutants strongly resembles the defects seen in *obst-A* mutants as many *rig* mutants die while trying to shed their cuticle (Gates et al., 2004). Biochemical assays showed the interaction of *rig* with the nuclear receptors EcR, Usp, DHR3 and β-Ftz-f1, which are all indispensable for ecdysone signaling (Gates et al., 2004). By this means, the upregulation of *rig* in the *obst-A* mutants might disturb the complex regulatory cascade of ecdysone responses in which DHR3 and β-Ftz-f1 play key roles (Yamada et al., 2000; Parvy et al., 2014).

As rig acts downstream of the ecdysone receptor, the mutant phenotype cannot be rescued by administration of sterols (Gates et al., 2004). It is possible that the strong misregulation of rig also renders *obst-A* mutants insensitive to sterols, thereby limiting the rescue effects of sterol feeding.

Even after the described analyses the question if Obst-A acts upstream or downstream of the ecdysone receptor complex could not be completely answered. The two hypotheses of Obst-A function mentioned above both remain plausible.

The first hypothesis is that loss of *obst-A* results in insufficient ecdysone production, leading to the absence of a clear ecdysone peak and consequently block of molting. An argument for this is the misregulation of *ptth,* the *Halloween* genes and the transcription factors *vvl*, *kni*

and *woc* (Fig. 3.3.4, 3.3.6, 3.3.8). Additionally, the partial rescue effect of sterol feeding on larvae lacking *obst-A* (Fig. 3.3.15) speaks for an ecdysone insufficiency as supplementing the food with sterols is the only way to rescue *obst-A* mutants to second instar stage. If ecdysone levels never reach a certain threshold, molting cannot be completed. The upregulation of the cholesterol importer *npc1a* (Huang et al., 2005) and the lack of induction of the ecdysone degrading enzyme *cyp18a* (Rewitz et al., 2010) (Fig. 3.3.9) also speaks for reduced ecdysone levels in the *obst-A* mutants since increasing substrate availability for ecdysone production and decreasing ecdysone degradation most likely represents a feedback response in order to try to elevate ecdysone levels.

The second hypothesis is that Obst-A disturbs signaling downstream of the EcR. Arguments for this would be that the expression level of the *Halloween* genes is altered, but not completely down to zero, meaning that at least minor ecdysteroid production must take place in *obst-A* mutants. Nevertheless, the normal *E74A* response is not just delayed or slightly reduced in its amplitude, but almost completely missing, which indicates severe defects in ecdysone signaling (Fletcher & Thummel, 1995; Gates et al., 2004) (Fig. 3.3.5).

The complete absence of an *E74A* induction was also seen in larvae lacking the EcR cofactor *rigor mortis* (Gates et al., 2004). A further investigation of other EcR-cofactors such as Taiman (Nakagawa & Henrich, 2009) in *obst-A* mutants is obligatory to investigate if the functionality of the EcR-receptor complex is disturbed in the mutants. Additionally, an EcR-ligand binding reporter line from the Thummel lab is available that I have started to cross into the *obst-A* mutant background. This should soon result in a fly line in which *obst-A* mutant offspring can be tested for 20E binding to the EcR by LacZ staining.

Exact quantification of ecdysteroid levels are possible by radioimmunoassay (RIA) or ELISA, which is extremely laborious when using first instar larvae (Kim Rewitz, personal communication), and by mass spec analysis using a special new LC-MS/MS method that is currently only available in the Shevchenko lab (Lavrynenko et al., 2015). The latter has the advantage that it can discriminate between the different sterols, whereas the RIA/ELISA method cannot differentiate between the levels of ecdysone and the modified, active 20-hydroxyecdysone (Shiotsuki et al., 2005; Lavrynenko et al., 2015).

Ecdysone pulses precede each developmental transition in *Drosophila* (Kozlova & Thummel, 2000). It was shown that a severe reduction of embryonic 20E levels leads to developmental defects such as defective head involution and germ band retraction and arrest in tracheal

tube branching preventing late embryos from hatching to first instar larvae (Kozlova & Thummel, 2003; Chavoshi et al., 2010). As *obst-A* mutants only show about 15-20% embryonic lethality (Petkau et al., 2012), a severe general ecdysteroid deficiency in embryos upon loss of *obst-A* can be excluded.

However, recent LC-MS/MS results (Lavrynenko et al., 2015) indicate that the levels of 20E during embryonic development are much lower than the previously published values that were measured by RIA (Kozlova & Thummel, 2000). In contrast, the levels of the steroid 24(28)-dehydromakisterone (dhMaA) are very high in embryos. dhMaA was shown to be a functional ecdysteroid as larvae which were only capable of producing dhMaA, but no other ecdysteroids, developed into pupal stage (Lavrynenko et al., 2015).

This might explain why the majority of *obst-A* mutant embryos are still capable of undergoing hatching. If dhMaA production in the mutant embryos is not or only slightly impaired, this might overcome the effect of reduced 20E production and as a consequence *obst-A* mutant embryos can still hatch. At the first molt when dhMaA levels are low (Lavrynenko et al., 2015) *obst-A* mutants are most likely arrested due to reduced 20E levels, because dhMaA levels at this stage are most probably not sufficient to induce molting.

4.12 - Obstructor-A in the prothoracic gland is necessary for maintenance of the corpus allatum

The most surprising finding of this thesis was that *obst-A* mutants show severe structural defects of the ring gland (Fig. 3.3.10, 3.3.11). Even though ring gland size was relatively variable in *obst-A* mutants, in all investigated larvae the prothoracic gland (PG) that is responsible for ecdysone production (Chino et al., 1974; King et al., 1974) was very small compared to the stage-matched wild type control. Most importantly, the lobe architecture of the ring gland was found to be heavily disturbed in the mutant as in all investigated larvae only one lobe of the PG was present and the corpus allatum (CA) was completely missing. The CA is the source of the Juvenile Hormone (JH) that determines the architecture of the molt. When JH levels are high, the animals are retained in a larval state leading to larval molts upon ecdysone peaks, but when JH levels drop shortly before pupariation, the pupal molt is induced as soon as the next ecdysone peak is reached and metamorphosis begins (Riddiford, 1980; Wolfgang & Riddiford, 1986).

Loss of the CA causes defects upon pupariation leading to lethality at head eversion (Riddiford et al., 2010; Mirth et al., 2014), but the authors of this study cannot exclude the presence of remaining CA cells during first and second instar larval stage, which might lead to residual JH expression. Thus, full functional knockdown of CA is only achieved by blocking JH synthesis (Jones et al., 2010). Larvae with completely blocked JH synthesis show lethality upon first to second or second to third instar molt, exhibiting a double mouth hook and incomplete cuticle shedding phenotype. Knockdown of the JH-biosynthesis enzyme *HMGCR* leads to larval arrest at molting and incomplete cuticle shedding, just as in the *obst-A* mutant. *HMGCR* deficient larvae could be completely rescued by administration of the JH-related compound farnesol (Jones et al., 2010).

Feeding of *obst-A* mutants with yeast supplemented with different concentrations of farnesol had no rescue effect as the larvae strongly avoided the yeast and starved to death even when very low concentrations were used (5 µM compared to 50 µM in the literature (Bendena et al., 2011)). Farnesol-treated wild type control larvae showed the expected effect of being treated with a JH-related compound as they were delayed in pupariation in a concentration-dependent manner (5 µM JH: six hours; 100 µM JH: two days; data not shown), but this delay can also result from the larvae avoiding the yeast. The higher the JH concentration, the less yeast was consumed by the larvae, which remained small and were most probably delayed in reaching the critical weight that is required for pupariation (Mirth et al, 2005). The rescue experiment should be repeated using even lower farnesol concentrations or different types of JH-analogs as a multitude of factors mimicking JH activity are available (Jindra et al., 2015).

The absence of the CA in *obst-A* mutants and the severely reduced size of the PG means that most probably the ecdysone deficiency in the mutants is not primarily caused by a secondary effect from the defective cuticle, potentially blocking ecdysone production and thereby developmental progression. On the contrary, the defects in *obst-A* mutants originate from defective ring gland architecture, which likely influences the whole ecdysone biosynthesis and signaling machinery.

How can the absence of the CA and the size reduction of the PG in *obst-A* mutants be explained? Strong Obst-A staining in the PG cells and weak staining in the CA was detected throughout larval stages (Fig. 3.3.11). Strikingly, the Obst-A staining in the PG was solely cytoplasmic. This is in contrast to the Obst-A staining in the epidermis and the trachea in

which a significant apical extracellular staining is detected (Petkau et al., 2012; Fig. 3.2.5, 3.2.6). In both the epidermis (this thesis, chapter 3.2) and the tracheal system (Petkau et al., 2012) the main function of Obst-A is being a chitin-binding scaffold protein at the apical cell surface. In the ring gland no chitin is detected except for in the small tracheal branches that terminate in proximity of the ring gland cells (data not shown). This excludes a function for Obst-A in chitin organization in the ring gland. For further functional analysis it is necessary to determine the subcellular localization of Obst-A in the ring gland cells. The vesicle-like staining pattern suggests the presence of Obst-A in the ER of PG cells, which is also the site of ecdysone production (King et al., 1966; Dai & Gilbert, 1991).

Even though only cytoplasmic Obst-A staining was detected in the ring gland it cannot be excluded that also in this organ partial secretion of Obst-A occurs. By secretion from the ring gland, Obst-A would be released into the hemolymph, which would make it very difficult to detect. By analyzing mutants with defective secretion, such as mutants lacking *gartenzwerg* (Wang et al., 2012a) or *dSec10*, an exocyst-complex component specifically regulating exocytosis in the ring gland (Andrews et al., 2002), or by generating Obst-A variants lacking the signal peptide it should be possible to determine if Obst-A is secreted from the ring gland.

The Obst-A staining in the PG and the strong ring gland defects that are caused by the lack of *obst-A* suggest a direct function of Obst-A in the ring gland is essential for the development or maintenance of the CA and for proper ecdysone production by the PG.

During metamorphosis, when JH titers drop down to a minimal level, the apoptotic degradation of the PG is triggered and the CA detaches from the ring gland to become a separate gland for JH production in the adult fly (Dai & Gilbert, 1991). This could imply that in the *obst-A* mutant, in which JH synthesis is compromised or abolished due to lack of the CA, premature degradation of the ring gland occurs leading to a misshaped, small PG that is not capable of producing enough ecdysteroids for molting. This might explain the size reduction of the prothoracic gland and the defective ecdysone signaling in *obst-A* mutants. An argument for apoptosis in the ring gland is that its size is not uniform in the mutants, but is in general strongly reduced when compared to wild type larvae. The presence of apoptosis can be tested by several methods including annexin V/propidium iodide staining (Rieger et al., 2011).

If progressive apoptotic degradation took place, the ring gland could be still functional in the embryo leading to ecdysone production sufficient for embryonic hatching. Therefore, it is absolutely crucial to analyze ring gland formation in *obst-A* mutant embryos to prove whether CA formation or maintenance is disturbed.

During embryonic development the PG, the CA and the trachea originate from the same ectodermal precursor, but develop in distinct embryonic segments. All three share expression of the transcription factor *vvl*, which is necessary for specification of the three developing cell types. The cells of the developing PG and CA undergo an epithelial to mesenchymal transition and migrate over a long range until they finally fuse with the mesodermally-derived corpora cardiaca to form the tripartite ring gland that is attached to the brain and encircles the aorta (Sánchez-Higueras et al., 2014; Sánchez-Higueras & Hombría, 2016).

There are several possibilities that would explain the ring gland defects in *obst-A* mutants. First, specification of the cell types during embryogenesis could be affected. The disturbed *vvl* expression in the *obst-A* mutant (Fig. 3.3.8) might be of great importance to find an explanation for the abnormal ring gland architecture. Altered *vvl* expression could also have an impact on the trachea, which also show severe defects in *obst-A* mutants (Petkau et al., 2012). Second, the embryonic migration of the different developing parts of the ring gland could be affected. However, it should be noted that Obst-A is only expressed from embryonic stage 13 onwards (data Matthias Behr), whereas the migration takes place from stage 11 onwards until stage 16. As fusion of the ring gland lobes occurs in stage 14, this could be a process where Obst-A plays a role (Sánchez-Higueras et al., 2014; Sánchez-Higueras & Hombría, 2016). Third, a functional ring gland including all three parts could be specified in *obst-A* mutant embryos, but the corpus allatum could be lost soon thereafter.

The question could be addressed by closely monitoring ring gland development in *obst-A* mutant embryos by staining for different markers of the developing ring gland lobes, such as Vvl for the PG and the CA, FasII for the CA and the CC (Fig. 3.3.11), svp for the CA and sal for the PG (Sánchez-Higueras et al., 2014; Sánchez-Higueras & Hombría, 2016).

Preliminary data reveals that upon knockdown of *obst-A* using the weak P0206 driver that leads to reduction of *obst-A* levels in the ring gland, the presence of the CA correlates with *obst-A* levels. P0206 Gal4> *obst-A* RNAi larvae raised at 25 °C, which is sufficient enough for activating the Gal4-UAS system, but does not cause its full activation (Brand & Perrimon,

1993), had a mixed phenotype. Most larvae did not exhibit any defects at all, whereas some larvae showed impeded growth and difficulties to shed their cuticle at the molt from second to third instar stage. Strikingly, the larvae that did not have any phenotype had a normally built ring gland with visible Obst-A staining in the PG and normal presence of the CA. In contrast, the larvae displaying the molting defects had small ring glands lacking Obst-A staining and, more importantly, had degenerated corpora allata that were barely present (Supplementary Fig. S6). This suggests that Obst-A expression in the PG is crucial for maintenance of the CA.

4.13 - Tissue specific knockdown of *obstructor-A* in the prothoracic gland fully recapitulates the molting phenotype

In order to analyze the function of Obst-A in the ring gland, tissue specific knockdown of *obst-A* via the Gal4-UAS system (Brand & Perrimon, 1993) was performed using different driver lines.

Obst-A staining was detected in the PG and in weak levels in the CA of the ring gland (Fig. 3.3.11). Knockdown with the 69B Gal4 line, driving Gal4 expression in all ectodermal tissues such as the epidermis, the trachea, the gut and, notably, the PG (Brand & Perrimon, 1993; Huang et al., 2005) resulted in strong reduction of *obst-A* levels (Supplementary Fig. S4). 69B Gal4> UAS *obst-A* RNAi animals resemble *obst-A null* mutants as they were reduced in size and showed severe molting defects. The main lethal phases of the knockdown larvae were during the first and second molt (Fig. 3.3.16).

For addressing the different lobes of the ring gland, several driver lines were tested. Even though the phm Gal4 line is described to lead to strong Gal4 expression in the PG, whereas P0206 was published to be a relatively weak driver line (Mirth et al., 2005; Moeller et al., 2013), *obst-A* knockdown efficiency was higher when using the P0206 line (Supplementary Fig. S4). Furthermore, no lethality was observed in the phm Gal4> UAS *obst-A* RNAi knockdown, whereas knockdown of *obst-A* using the strong PG driver line Mai60 Gal4 (Walker et al., 2013) was completely lethal before reaching the second instar stage (Fig. 3.3.12). When expressing a UAS-GFP construct under control of the different driver lines (data not shown), the GFP expression in the ring gland was lowest with the phm Gal4 driver concluding that the phm driver line used for this study only weakly expresses Gal4.

Knockdown of *obst-A* in the CA by the strong Aug21 Gal4 line did not cause any lethality phenotype (Fig. 3.3.12). A fraction of Aug21 Gal4> UAS *obst-A* RNAi, phm Gal4> UAS *obst-A* RNAi and P0206 Gal4> UAS *obst-A* RNAi larvae exhibited molting defects at the transition from second to third instar stage, but all were capable of developing into adult flies (Fig. 3.3.12).

Knockdown of *obst-A* in the PG with the PG driver line Mai60 Gal4 completely mimicked the molting phenotype of the null mutant as Mai60 Gal4> UAS *obst-A* RNAi larvae died before reaching the second instar stage and displayed double mouth hooks and incomplete cuticle shedding (Fig. 3.3.12, 3.3.13). For the Mai60 Gal4 line, in addition to the expression in the PG and the salivary glands (Walker et al., 2013), expression in the imaginal discs was detected (Fig. 3.3.14). Obst-A is not expressed in the salivary glands and it is very unlikely that the complete lethality and the strong molting defects of Mai60 Gal4> UAS *obst-A* RNAi larvae, which indicate ecdysteroid deficiency, originate from knockdown of *obst-A* in the imaginal discs that show Obst-A expression in single cell clusters (Fig. 3.2.4).

Overall, the results indicate that even though the CA is mostly affected by the loss of *obst-A*, the function of Obst-A in the ring gland is in the PG cells. The exact function of Obst-A in the PG remains to be clarified.

4.14 - Sterol feeding is beneficial, but not sufficient for *obstructor-A* mutant survival

Survival assays in which *obst-A* mutant, knockdown and control larvae were fed with yeast supplemented with sterols showed enhanced developmental progression of *obst-A* mutant and knockdown larvae. Larvae were fed with either cholesterol (C), 7-dehydrocholesterol (7dC) or 20-hydroxyecdysone (20E) and their survival was monitored closely (chapter 3.3.6).

As described in chapter 1.6.1, all three sterols are components of the ecdysone biosynthesis pathway. 20-hydroxyecdysone is the active molting hormone (Petryk et al., 2003) and should therefore lead to a stronger rescue of the *obst-A* molting phenotype than the biosynthesis intermediates C and 7dC (Yoshiyama et al., 2006).

Even upon sterol feeding, *obst-A* null mutants are completely larval lethal. Nevertheless, it was observed that they progress further in larval development when fed with sterols, particularly with 20E (Fig. 3.3.15). Because of their complete lethality, which occurs mostly

upon the L1/L2 transition, *obst-A* mutants were classified into their lethal developmental stage, namely into larvae that died before showing first signs of molting; larvae that died with double mouth hooks, but without partially shed cuticle; larvae that were capable of shedding parts of their cuticle; and larvae that could completely discard their L1 cuticle and enter L2 stage.

Our results show that C as well as 7dC and 20E feeding leads to a lower percentage of mutants that die before showing any signs of initiation of molting. In case of 20E feeding, this was statistically strongly significant. The percentage of larvae dying in the double mouth hook stage before trying to shed their cuticle was unaltered upon C, 7dC and 20E feeding. Feeding with all three sterols increased the percentage of mutants that died after partly shedding their cuticle.

Without sterol feeding and also after cholesterol feeding, *obst-A* mutants cannot reach second instar larval stage as they fail to molt. Upon 7dC feeding, few larvae could progress to second instar stage. When feeding 20E, the number of L2 escapers was higher. This makes sense as 7dC is downstream of C and 20E is the most downstream component of ecdysone biosynthesis and represents the active molting hormone. Both C as well as 7dC first have to enter the ring gland before they can be further modified by the ecdysteroidogenesis enzymes, which are misexpressed in *obst-A* mutants (Fig. 3.3.6). Feeding of 20E, on the other hand, directly provides the active molting hormone and should thereby directly exert its effect on target tissues in the mutant larvae, circumventing uptake in the defective PG and enzymatic modification by the impaired ecdysteroidogenesis machinery.

20E feeding was conducted using two different concentrations. No major differences in mutant survival were seen upon comparison of the two concentrations, but only upon feeding of 0.75 µg/g 20E single *obst-A* mutants were capable of reaching third instar stage, however with severe tracheal abnormalities. An even higher concentration was not tested because of the high costs of 20E.

All *obst-A* mutants that reached second or third instar larval stage because of the sterol supplementation were arrested for several days in the respective stage before eventually dying. They all displayed convoluted tracheal tubes as well as gas filling defects, which might in the end be the cause of their death and can be contributed to the function of Obst-A in the tracheal cuticle (Petkau et al., 2012). The long developmental arrest is a typical sign of

ecdysone deficiency (Karim et al., 1993; Fletcher & Thummel, 1995; Neubueser et al., 2005) and could potentially be overcome by feeding an even higher 20E concentration.

The partial rescue of *obst-A* null mutants by feeding sterols proves that they indeed suffer from ecdysteroid deficiency. The experimental concentrations were chosen so that they do not influence the survival or developmental timing of control larvae, which have normal ecdysteroid titers.

Obst-A knockdown larvae were also subjected to sterol feeding experiments because of their milder phenotype compared to null mutants. A stronger rescue effect of the sterols was expected for 69B Gal4> *obst-A* RNAi larvae since they still show about 40 % residual *obst-A* mRNA expression (Supplementary Fig. S4) and about 30 % of animals reach the adult stage (Fig. 3.3.16). This should at least partially overcome the influence of the fatal tracheal and epidermal cuticle phenotypes caused by loss of *obst-A*. Indeed, a strong beneficial effect of sterol feeding was seen in 69B Gal4> *obst-A* RNAi larvae. Even though most knockdown larvae still died during the molts from first to second and second to third instar, more survivors were seen upon sterol feeding. The rescue by cholesterol feeding was minimal and a stronger effect was seen when feeding 7dC as well as 0.5 µg/g 20E and 0.75 µg/g 20E. This represents the expected gradual increase in rescue potential by the different feeding strategies.

Even though ecdysteroid feeding was shown to have a beneficial influence on survival of *obst-A* mutant larvae and lets them progress further during their development, no complete rescue of the mutants can be achieved as is frequently seen in ecdysteroidogenesis-defective larvae (Yoshiyama et al., 2006; Niwa et al., 2010; Danielsen et al., 2014). The main difference is that these mutants, which can be completely rescued by sterol feeding, have their only defects in ecdysteroidogenesis. This is in stark contrast to the *obst-A* mutants, that in addition to the obvious molting phenotype also have a severe tracheal and epidermal phenotype (Petkau et al., 2012; this thesis). In the present study it was shown that Obst-A is crucial for epidermal cuticle assembly and integrity (chapter 3.2). Even collisions of larvae while crawling on the apple juice plates can be fatal for *obst-A* mutants because of their fragile cuticle. In addition, the impaired barrier function of the cuticle renders *obst-A* mutants susceptible to infections. Even when mutant larvae are optimally fed with ecdysteroids, the cuticle defects in the trachea and epidermis can still restrict larval growth and disable developmental progression.

In summary, the results show that *obst-A* mutants suffer from ecdysteroid deficiency, but also underline that *obst-A* has other functions apart from its implication in ecdysteroid production. Even when they are fed with ecdysteroids, *obst-A* mutants still most frequently die during the molt from first to second instar larval stage (Fig. 3.3.15). This shows that the sterol concentration used in the feeding experiments could have been too low even though the used concentrations are based on the literature (Huang et al., 2005). A higher 20E concentration was used in Yoshiyama et al., 2006, leading to complete rescue of the *neverland* mutant phenotype, and in the studies by Pankotai et al., 2010, and Parvy et al., 2014. A different possible explanation is that Obst-A is needed in high concentrations in the epidermal cuticle upon molting, acting as a scaffold to organize the rapid assembly of chitin fibrils into a strong, lamellar matrix.

Mutants that have defects in ecdysone signaling downstream of the ecdysone receptor cannot be rescued by sterol feeding with one example being the mutant lacking the ecdysone receptor cofactor *rigor mortis* (Gates et al., 2004). Here it was shown that *rigor mortis* is immensely upregulated in *obst-A* mutants, which might heavily disturb downstream receptor signaling, thereby limiting the rescue effect of sterol feeding.

The sterol feeding assay needs to be repeated with Mai60 Gal4> UAS *obst-A* RNAi knockdown larvae as this represents a tissue specific knockdown in the PG and circumvents the defects caused by epidermal and tracheal reduction of Obst-A.

A possible future direction would be the use of the inducible Gal80ts TARGET system (Zeidler et al., 2004) for stage-specific knockdown of *obst-A* in either the PG or the whole ectoderm. For this Mai60 Gal80ts (PG) and 69B Gal80ts (whole ectoderm) need to be generated. Starting knockdown of *obst-A* in the second instar stage would skip the main lethal phase at the L1/L2 molt and would enable the analysis of potential defects at the L2/L3 molt or at the pupal molt. The phenotypic analysis should be combined with sterol feeding to find out exactly at which developmental stage transitions Obst-A is required for proper molting and if putative *obst-A* mediated molting phenotypes at later stages can be rescued by sterol application as well.

4.15 - Necessity of ecdysone signaling for cuticle formation

Ecdysone signaling has a great impact on cuticle formation (Moussian et al., 2010). First, the exposure to a certain amount of ecdysone, close to the concentration at ecdysone peak secretion, is necessary for cuticle formation in all cuticle-producing tissues (Oberlander, 1976; Riddiford, 1980).

Strikingly, mutants of the *Halloween* gene family, which is responsible for synthesis of the molting hormone ecdysone, fail to establish a proper embryonic cuticle (Nüsslein-Volhard et al., 1984; Jürgens et al., 1984; Wieschaus et al., 1984; Chávez et al., 2000; Warren et al., 2002; Petryk et al., 2003). This implies that ecdysone production regulates embryonic chitin synthesis (Gilbert, 2004; Gangishetti et al., 2012). Recent data show that expression of Chitin synthases during larval stages is induced by 20E and JH (Shi et al., 2016a).

Additionally, many important factors for pupal cuticle remodeling are ecdysone target genes such as the *glucose dehydrogenase* (Cox-Foster et al., 1989), *Edg84A* (Kayashima et al., 2005) and *Edg78E* (Kawasaki et al., 2002). Certain genes that are necessary for integrity of the adult cuticle are regulated by ecdysone responses as well (Kozlova et al., 2009; Cui et al., 2009).

Also *obstructor-A* was shown to be an ecdysone target gene that is regulated by transcription factors of the ecdysone machinery (Beckstead et al., 2005) and is upregulated upon molting (chapter 3.3.1). Noticeably, ring gland-specific Mai60 Gal4> UAS *obst-A* RNAi knockdown larvae exhibited cuticle integrity defects, showing that proper ecdysone signaling is a prerequisite for cuticle stability (Supplementary Fig. S8).

Chitinases are implicated in chitin degradation, but were also proven to be crucial for epidermal cuticle integrity (this thesis; Pesch et al., 2016a). Chitinases show a periodical fluctuating expression pattern associated with molting and might be under transcriptional regulation by the molting hormone ecdysone (Arakane & Muthukrishnan, 2010; Xi et al., 2015). Genes that are related to *verm* have been identified in crustaceans, undergoing molting-cycle-specific regulation in mRNA expression (Kuballa et al., 2007).

It was shown that the well-described ecdysone-induced transcription factors broad and E74A are implicated in cuticle differentiation (Karim et al., 1993; Fletcher & Thummel, 1995; Crossgrove et al., 1996; Zhou & Riddiford, 2002), most probably by mediating induction of cuticle-specific target genes.

Both *broad* as well as *E74A* transcript levels are downregulated in *obst-A* null mutants (Fig. 3.3.5), which might contribute to the impaired cuticle integrity in the *obst-A* mutant by affecting other cuticle regulators in addition to the described function of Obst-A itself in cuticle organization.

4.16 - Cuticle proteins and molting as potential pest control targets

Many harmful insect species evoke world-wide problems by destroying crops and forests or by transmitting diseases (Chandler et al., 2011; Zhang et al., 2014; Khandelwal et al., 2016; Swale et al., 2016). Each year mosquitoes transmitting disease vectors such as malaria, dengue or yellow fewer cause more than 500,000 deaths, mostly in the developing world. The recent outbreak of the mosquito-borne Zika virus, which is linked to microcephaly in newborns, opened up a new discussion about pest control (Swale et al., 2016). Developing resistance of harmful species against insecticides poses a major problem in pest management (Swale et al., 2016).

The two main topics of this thesis - epidermal cuticle assembly and hormonal control of molting - offer many possibilities for the development of insecticides as both processes are highly conserved among insects and crucial for their development and survival (Gilbert et al., 2002; Moussian, 2010).

Inhibiting chitin synthesis is a potential pest control strategy as Chitin synthase inhibitors are used as pesticides and fungicides (Dähn et al., 1976; Kramer & Muthukrishnan, 1997; Merzendorfer & Zimoch, 2003). The chitin synthesis inhibitor nikkomycin was successful in the treatment of coccidioidomycosis (valley fever) in animal experiments (Shubitz et al., 2014). Benzoylphenyl urea derivatives, which inhibit chitin synthesis, are frequently used insecticides due to their low toxicity in non-target organisms (Sun & Zhou, 2015). In many different insect species such as *Tribolium castaneum* (Arakane et al., 2008) and the lepidopteran crop pest *Spodoptera exigua* (Tian et al., 2009), injection or nutritional uptake of RNAi directed against *Chitin synthases* led to reduced larval growth, molting defects, hindered eclosion from pupal cases and reduced fecundity of adults. Importantly, RNAi-based chitin synthesis inhibition was successful in the potato beetle *Leptinotarsa decemlineata* and the brown planthopper *Nilaparvata lugens*, which are major pests destroying potato or rice plants, respectively (Wang et al., 2012b; Shi et al., 2016b).

Furthermore, molting defects and impaired oogenesis was introduced by RNAi targeting the single *Chitin synthase* in *Rhodnius prolixus*, the vector transmitting the potentially lethal Chargas disease that affects the heart, the digestive and the nervous system (Mansur et al., 2014).

As RNAi-mediated knockdown of *obst-A* and several *Chts*, especially *Cht2*, led to strong lethality mostly during larval stages (chapter 3.3.5, Pesch et al., 2016a), these genes are promising targets for RNAi-based pest control strategies. Glyco18 domain proteins, which are discussed in this thesis, thereby also are potential pest control targets. Glyco18 homologs are found in pests such as mosquitoes, lice and spotted wing *Drosophila* (Zhang et al., 2011c; Eichner et al., 2015; Fan et al., 2015). Inhibitors of Chitinases feature carbohydrate substrate analogs or substances that mimick the intermediate state of catalysis but cannot be hydrolytically processed. The Cht inhibitor allosamidin can be used to inhibit *plasmodium falciparum* Cht activity, thereby blocking the penetration of the peritrophic matrix of the mosquito host (Vinetz et al., 2000). However, allosamidin synthesis is expensive showing the need for the generation of new Cht inhibitors. Blocking Cht function could be a promising pest control strategy as several other parasites such as *Leishmania mexicana* also use Chts for the invasion of the host (Merzendorfer & Zimoch, 2003).

Our study identified Cht2 as factor crucial for cuticle barrier function as knockdown resulted in a thinned cuticle with defective chitin-matrix as well as lethality mostly during larval stages (chapter 3.1; Pesch et al., 2016a). Strikingly, Cht2 is highly conserved except for certain variable sequence stretches in the C-terminus (Pesch et al., 2016a) allowing the search for species-specific inhibitors of Cht2.

Many frequently used insecticides target the molting process (Dhadialla et al., 1998). Diacylhydrazines such as methoxyfenozide and halofenozide act as ecdysone agonists, binding to the EcR with high insect selectivity, thereby inducing premature molting and larval death (Dhadialla et al., 1998; Farinós et al., 1999; Smagghe et al., 2001). A wide range of synthetic JH mimics including methoprene and pyriproxifen is often used as insecticides, also causing death by inhibiting metamorphosis (Dhadialla et al., 1998; King-Jones & Thummel, 2005; Jindra et al., 2013). A recent study by P. Bhagat Kumar et al., 2016, shows that ETH in the spruce budworm *Choristoneura fumiferana*, which is the main pest destroying coniferous forests in North America, is a target for pest control. A different study on *Choristoneura fumiferana* proves that its Obst-C/Gasp homolog is implicated in epidermal cuticle-matrix

formation, likely opening up another possibility for the development of an insecticide against this harmful species (Nisole et al., 2010). *Choristoneura fumiferana* is a major pest in North America raising the question if the Obst-C/Gasp homolog could be a potential target for pest control.

As shown in this study, Obst-A plays important roles both in epidermal cuticle formation (chapter 3.2) and the hormonal control of molting (chapter 3.3). Loss of *obst-A* is lethal in early larval development and it is highly conserved among all invertebrates (Petkau et al., 2012), making it an excellent target for pest control. A species-specific insecticide directed against Obst-A should target a non-conserved protein region to circumvent the killing of beneficial insects and negative effects to the ecosystem.

In summary, both factors that were moleculary characterized in course of this thesis - Cht2 and Obst-A - constitute new promising targets for pest control. Due to the high lethality upon loss of *Cht2* and *obst-A*, by blocking one of these two factors development of the harmful species can already be interrupted during larval stages, thereby preventing the growth of the next generations.

4.17 - Open questions concerning Obstructor-A function

This thesis primarily focused on the function of Obst-A in epidermal cuticle assembly and the hormonal control of molting. The mechanism of Obst-A mediated epidermal cuticle assembly was described and as most probable reason for ecdysteroid deficiency in *obst-A* mutants structural defects in the molting hormone-producing ring gland were revealed.

Nevertheless, a few open questions remain. The molecular mechanism how Obst-A regulates ring gland formation and/or maintenance is still elusive, but can be investigated by analysis of ring gland development in *obst-A* mutant and wild type embryos and by checking for apoptosis in the ring gland of late embryos and larvae. It is also still elusive if only the ring gland malformation in *obst-A* mutants causes their ecdysteroid deficiency or if other mechanisms play a role. One possibility could be the secretion of Obst-A from the ring gland into the hemolymph and a peripheral yet unidentified function in controlling ecdysone signaling. No clear interaction partner of Obst-A in the ecdysone machinery has been identified yet. However, the strong upregulation of the EcR cofactor *rigor mortis* (Gates et

al., 2004) in *obst-A* mutants is a promising starting point for the further analysis of Obst-A function in ecdysone signaling.

Mass Spec analysis was performed by Matthias Behr to identify proteins interacting with Obst-A, but the candidate proteins have not yet been analyzed. One binding partner that was confirmed for Obst-A is the Wurst protein that is a key factor of clathrin-mediated endocytosis (Behr et al., 2007; Behr, unpublished data). The analysis of the Obst-A-Wurst interaction could lead to new insights in both clathrin-mediated endocytosis and cuticle remodeling. The analysis of Wurst-mediated endocytosis also constitutes a starting point to investigate a putative feedback mechanism in the ring gland that could require both Obst-A secretion and endocytic internalization.

4.18 - The dual function of Obstructor-A in cuticle assembly and ecdysone signaling

In the present study it was shown that the chitin-binding protein Obst-A has a dual function as it is crucial for both epidermal cuticle formation and for the structure of the endocrine ring gland, thereby influencing ecdysone signaling.

These two functions could also influence each other, as if ecdysone production is inhibited this can lead to defects in cuticle development (Oberlander, 1976; Riddiford, 1980). It is not yet known if there is any mechanism by which the presence of a defective cuticle can inhibit ecdysteroidogenesis and thus block developmental progression. Due to its dual expression in both the epidermal cuticle and the ring gland, Obst-A could be such an "integrating factor", which transmits a signal that the cuticle is defective to the ring gland and in that way regulates ecdysone production. However, this hypothesis is highly speculative.

The results that Obst-A is essential for proper ring gland function suggest that it acts a modulator, not mediator of ecdysone responses. The function of Obst-A in the ring gland was proven to be necessary but not sufficient for larval survival as a rescue experiment with the PG driver line Mai60 Gal4 (Walker et al., 2013) failed. In contrast very successful rescue was achieved by the ectodermal driver line 69B Gal4 (Brand & Perrimon, 1993) with expression in all tissues in which Obst-A has an important function, namely the tracheal system, the epidermis and the prothoracic gland.

In the epidermal cuticle Obst-A was shown to build a scaffold for organizing newly synthesized chitin fibrils and for placing the chitin modifiers Serp and Verm, thereby mediating lamellar organization of the cuticle and stabilization of the chitin-matrix.

The strong molting defects in Mai60 Gal4> UAS *obst-A* RNAi larvae, which can also be observed in 69B Gal4> UAS *obst-A* RNAi larvae (Fig. 3.3.13) indicate that Obst-A in the ring gland is necessary for correct molting. In cuticle forming tissues, however, Obst-A mediates chitin-matrix formation, suggesting a dual function of Obst-A that is absolutely crucial for larval survival and probably hinting at a yet uncharacterized feedback mechanism between the tissues. The different yet linked functions of Obst-A that were characterized in this thesis are depicted in Fig. 4.4.

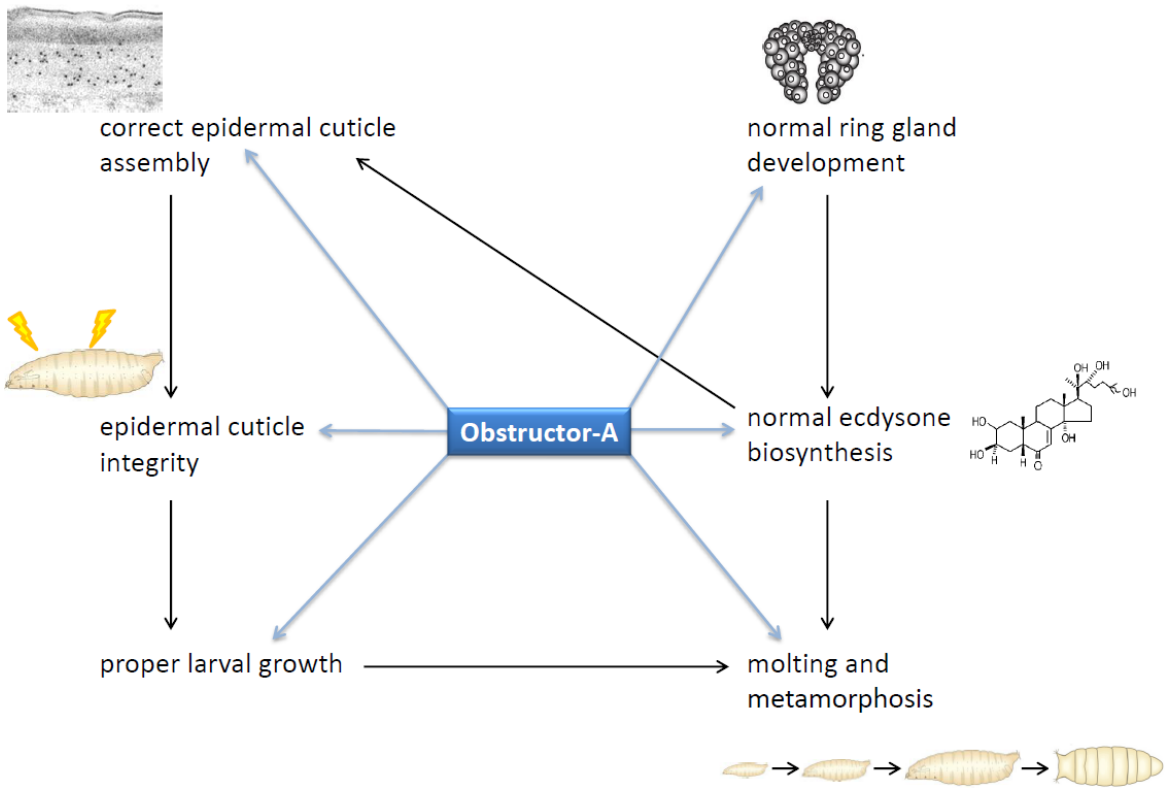

Fig. 4.4

Fig. 4.4 - Schematic model of Obstructor-A function. This model only takes into account data obtained during the work on this thesis. The function of Obst-A in the tracheal system was characterized in Petkau et al., 2012. Correct assembly of the epidermal cuticle is a prerequisite for epidermal cuticle integrity, protecting the larva against wounding, infection and other kinds of damage. Only if the epidermal cuticle is stable, proper larval growth is ensured, which enables developmental progression through molting and metamorphosis. Normal development and structure of the ring gland is required for synthesis of the molting hormone ecdysone, which triggers molting and metamorphosis. Ecdysone also influences epidermal cuticle assembly by inducing certain target genes required for cuticle formation. Obst-A is a central mediator influencing all of these processes. First, Obst-A plays a crucial role in epidermal cuticle organization via acting as a scaffold for chitin-matrix formation and recruiting of the chitin modifiers Serp and Verm. Thereby, Obst-A is required for epidermal cuticle integrity and influences larval growth. Second, Obst-A is necessary for proper ring gland architecture and has a strong impact on ecdysone production. Ecdysone biosynthesis and signaling is disturbed in *obst-A* mutants leading to the inability to molt. Both by influencing the ecdysone pathway and by being a key mediator of cuticle assembly, Obst-A ensures proper developmental progression through molting.

In summary, our data show that Obst-A is a crucial regulator of developmental progression in *Drosophila* larvae by ensuring proper larval growth and molting, both by regulating epidermal cuticle assembly and by influencing ring gland structure.

5 - Summary

The insect epidermal cuticle confers exoskeletal stability and protection against wounding, desiccation, invading pathogens and other potential stresses. In order to adapt to increasing body growth, insects periodically shed their cuticle in a molting process, which is initiated by peak synthesis of the ecdysteroid hormone ecdysone. Body growth, molting and wounding requires organized cuticle rearrangement. However, how exactly the complex architecture of the cuticle is arranged and reorganized, is not completely understood.

In this thesis, the molecular mechanism how the *Drosophila* chitin-binding protein Obstructor-A (Obst-A) regulates epidermal cuticle assembly and maturation was investigated. Obst-A mediates matrix assembly at the apical epidermal cell surface where it provides a scaffold for organizing a core complex of enzymes and proteins involved in the formation and protection of chitinous structures.

For cuticle organization Chitinases process chitin-fibrils into fragments of different lengths. Surprisingly, the Chitinase 2 is necessary for lamellar organization and for proper function of Obst-A at the apical cell surface. All molecular mechanisms of cuticle formation are primarily concentrated at the apical cell surface in a so far completely uncharacterized region - the cuticle assembly zone, which is the center of cuticle organization. Due to protein sequence conservations the discovered mechanisms may hold true for insects and most chitinous invertebrates.

In addition to the role of Obst-A in chitin-matrix organization, it was investigated how the chitin-binding protein Obst-A controls production of the molting hormone 20-hydroxyecdysone (20E). First, loss of *obst-A* results in characteristic phenotypes known from mutants affecting 20E production, such as impaired body growth, lethality at larval molting and failure in shedding the old cuticle. 20E feeding partly rescues these phenotypes. Second, genes involved in ecdysone synthesis are downregulated and ecdysone target genes are not induced in *obst-A* mutant larvae. Third, Obst-A is expressed in the ecdysone-producing cells of the ring gland and loss of *obst-A* results in severe malformation of the ring gland. In summary, the findings strongly indicate that Obst-A affects hormone production probably either by organizing ring gland maintenance and/or by providing a feedback mechanism to control growth, timing and molting in larval development.

6 - Appendix

6.1 - Supplementary figures

Supplementary figure S1

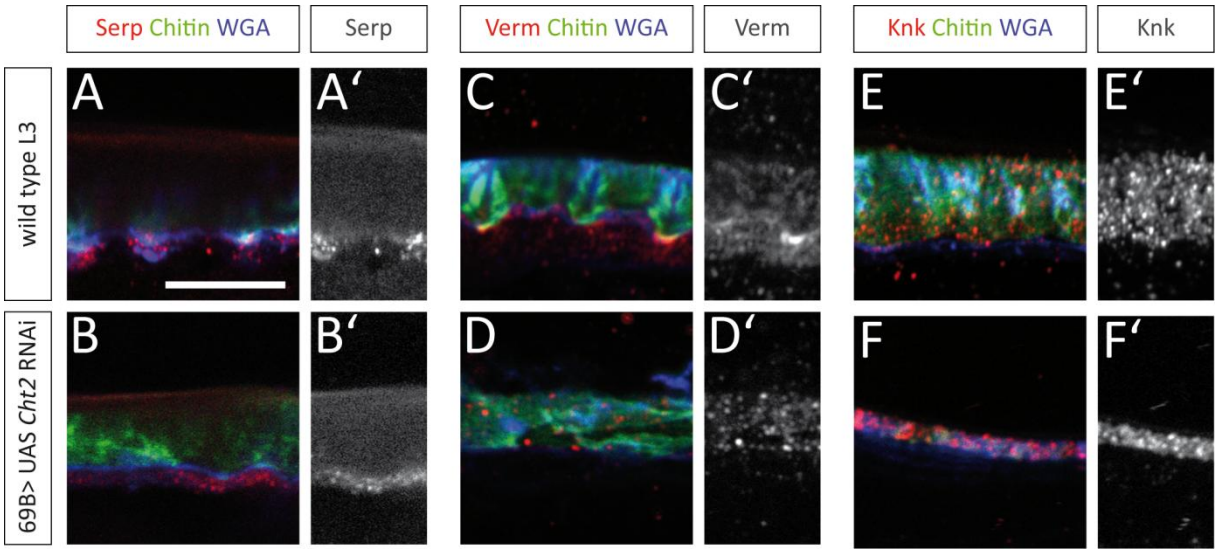

Fig. S1 - Serp and Verm localization is altered in *Cht2* knockdown larvae, but Knk is not affected. Representative immunostaining of JB-4 sections generated from wild type (A-A'; C-C'; E-E') and 69B Gal4> UAS *Cht2* RNAi knockdown (B-B'; D-D'; F-F') third instar larvae. Chitin staining (CBP, green) and WGA staining (blue) is shown together with Serp (red; A, B), Verm (red; C, D) and Knk (red; E, F) staining. Single channel signals of Serp (A', B') Verm (C', D') and Knk (E', F') are shown in grey. In the wild type Serp (A, A') and Verm (C, C') can be found enriched in the cuticle assembly zone. In *Cht2* knockdown larvae, in contrast, Serp (B, B') and Verm (D, D') are diffusely localized in the entire procuticle. Knk localizes to the chitinous procuticle in both wild type (E, E') and *Cht2* knockdown larvae (F, F'). Scale bar represents 10 µm. Adapted from Pesch et al., 2016a.

Supplementary figure S2

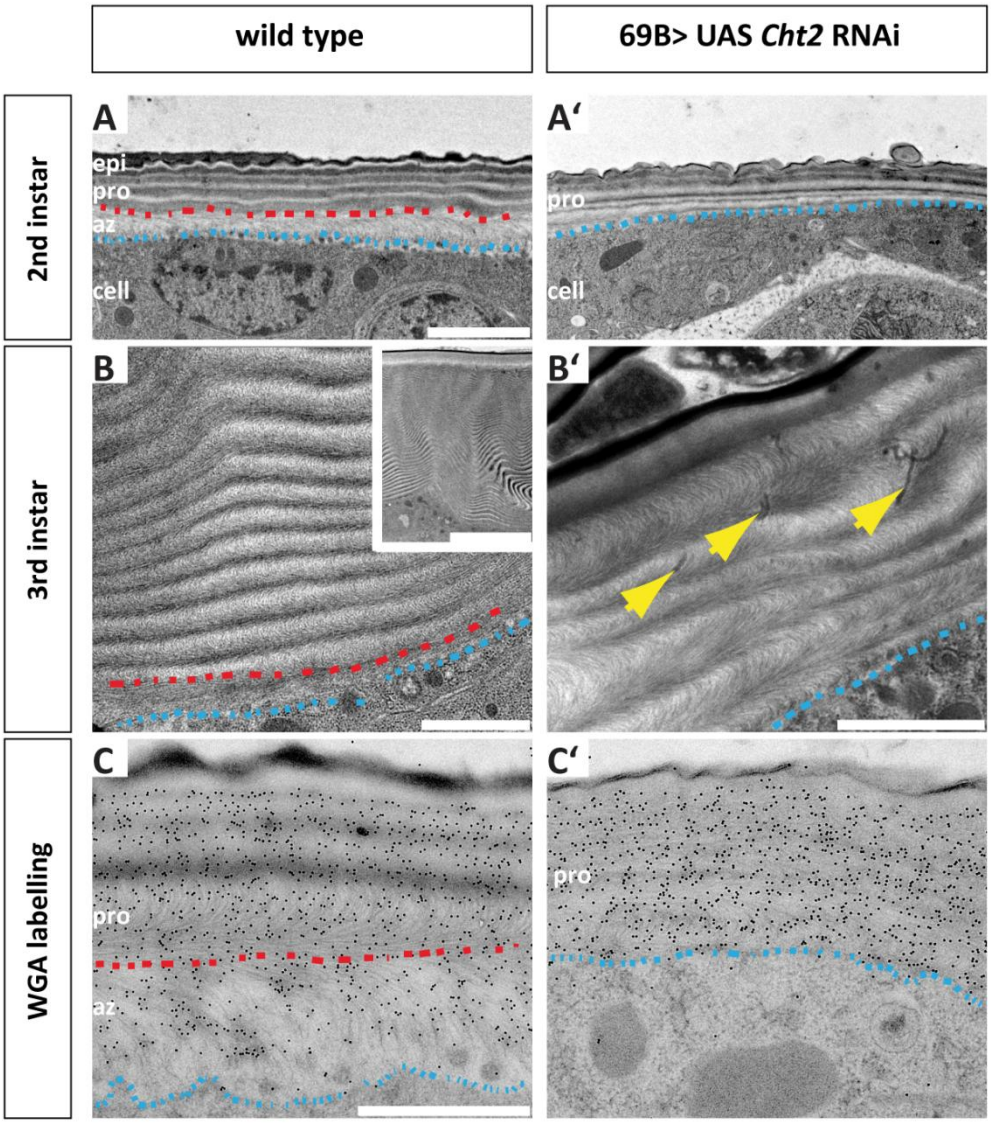

Fig. S2 - The number of chitin lamellae is reduced in *Chitinase 2* knockdown larvae. Transmission electron microscopy performed by Dietmar Riedel, Max Planck Institute for Biophysical Chemistry, Göttingen. Representative images are shown. A, B, C: wild type; A', B', C': 69B Gal4> UAS *Cht2* RNAi larvae. Blue dashes illustrate the apical cell surface and red dashes illustrate the interface between the non-lamellar assembly zone and the lamellar procuticle. In the second instar wild type cuticle (A) above the apical epidermal cell surface the assembly zone (az) can be detected, followed by the lamellar procuticle (pro) and the electron dense epicuticle (epi). In the *Cht2* knockdown (A') the assembly zone is not present. In comparison to the wild type chitin lamellae appeared irregular. In the third instar stage in the wild type (B) many more lamellae are present (see inset), but in the *Cht2* knockdown (B') no increase in the number of lamellae is detected. Lamellar chitin architecture is disturbed as indicated by the yellow arrow. The assembly zone is absent. C, C': Immunogold labeling using WGA stains lamellar chitin. In the wild type (C) strong immunogold WGA staining is found within the lamellar procuticle (pro) and staining intensity is weaker in the assembly zone (az). In the *Cht2* knockdown (C') uniform immunogold WGA staining is seen in the procuticle down to the apical cell surface, indicating the absence of the assembly zone. Scale bars represent 1 µm and 2 µm in the inset in B. Adapted from Pesch et al., 2016a.

Supplementary figure S3

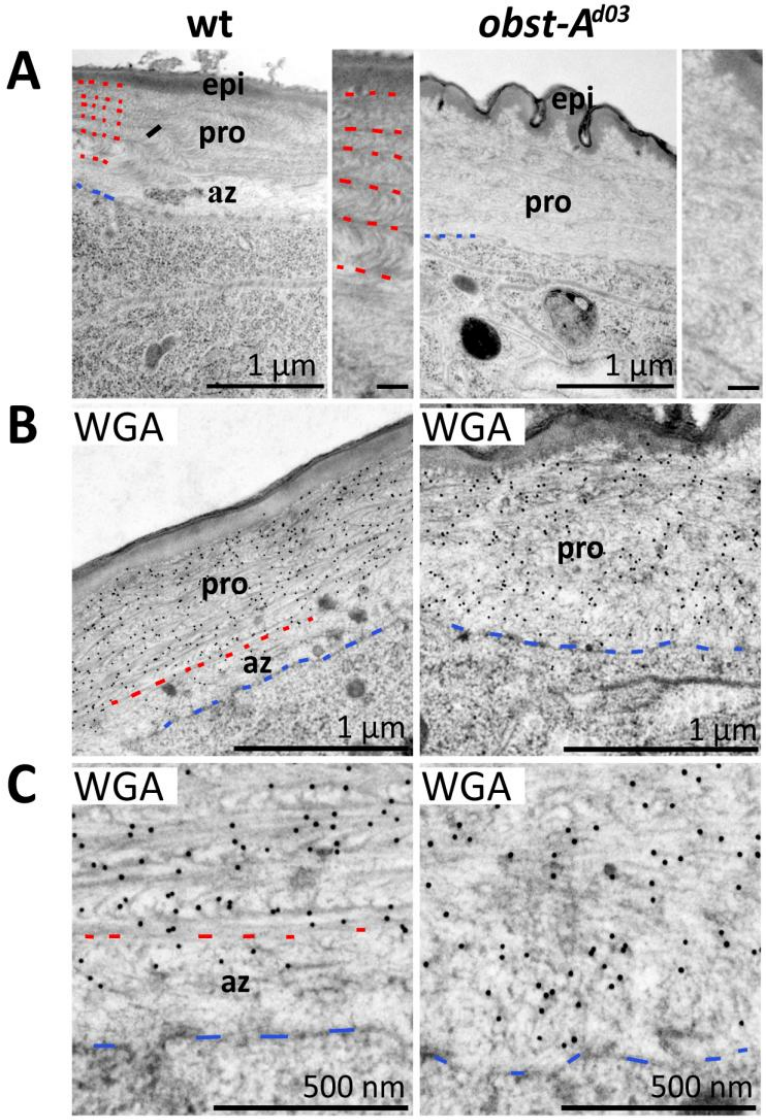

Fig. S3 - The cuticle assembly zone is absent and lamellar chitin architecture is disturbed in *obst-A*^{d03} mutants. Transmission electron microscopy performed by Dietmar Riedel, Max Planck Institute for Biophysical Chemistry, Göttingen. Representative images are shown. The wild type (wt) is shown in the left panel and the *obst-A*^{d03} mutant is shown in the right panel. A: In the wild type first instar stage the electron dense epicuticle (epi) is detected as uppermost layer of the cuticle, followed by the lamellar procuticle (pro) and the less electron dense assembly zone (az), which is located in between the chitin lamellae and the apical cell surface. Blue dashes indicate the apical cell surface and red dashes label the distinct chitin lamellae. In the *obst-A*^{d03} mutant the cuticle appears wrinkled, the lamellae are not as pronounced and the assembly zone as distinct zone is not detected. B, closeup in C: WGA immunogold labeling stains the chitinous procuticle. Blue dashes mark the apical cell surface and red dashes label the lowest chitin lamella at the border of the cuticle assembly zone. In the wild type, immunogold particles are mainly detected in the lamellar procuticle, whereas in the *obst-A* mutant uniform staining reaches down to the apical cell surface showing that the assembly zone is absent.Note the disturbed chitin architecture in the *obst-A* mutant. Size of scale bars is indicated in the respective images. Adapted from Pesch et al., 2015.

Supplementary figure S4

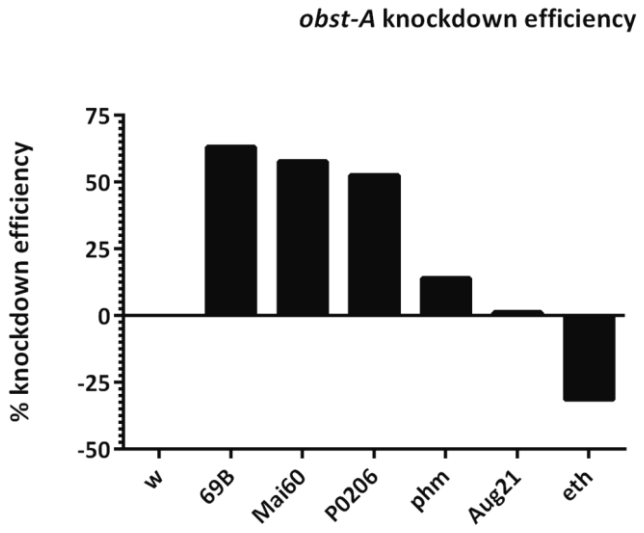

Fig. S4 - Efficiency of *obst-A* knockdown using different Gal4 driver lines. qRT-PCR analysis. n=2 for each condition, the mean is depicted. Stage-matched early first instar larvae were used for the experiment. y-axis: efficiency of *obst-A* knockdown, meaning reduction in *obst-A* mRNA level in % (*obst-A* expression was normalized to the housekeeping gene *rp49*). x-axis: different tested genotypes. The genotype of the analyzed animals was the following: w: w> UAS *obst-A* RNAi (no knockdown expected); 69B: 69B Gal4> UAS *obst-A* RNAi (knockdown in whole ectoderm);); Mai60: Mai60 Gal4> UAS *obst-A* RNAi (strong knockdown in prothoracic gland); P0206: P0206 Gal4> UAS *obst-A* RNAi (knockdown in PG and CA); phm: phm Gal4> UAS *obst-A* RNAi (knockdown in PG); Aug21: Aug21 Gal4> UAS *obst-A* RNAi (knockdown in CA); eth: eth Gal4> UAS *obst-A* RNAi (knockdown in Inka cells). No knockdown of *obst-A* expression was observed in the control (w) as expected. Strong knockdown was seen when using the 69B Gal4, the Mai60 Gal4 and the P0206 Gal4 line, whereas weak or no knockdown was observed with the Aug21 Gal4 and the phm Gal4 line. Surprisingly, *obst-A* levels were elevated in eth Gal4> UAS *obst-A* RNAi animals.

Supplementary figure S5

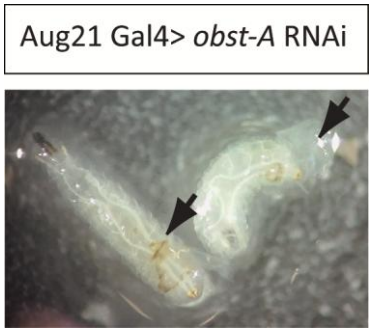

Fig. S5 - Molting defects of Aug21 Gal4> *obst-A* RNAi larvae at the L2/L3 transition. Many Aug21 Gal4> *obst-A* RNAi knockdown larvae show incomplete cuticle shedding at the L2/L3 molt and melanized spots where parts of the second instar cuticle remain attached (see black arrows).

Supplementary figure S6

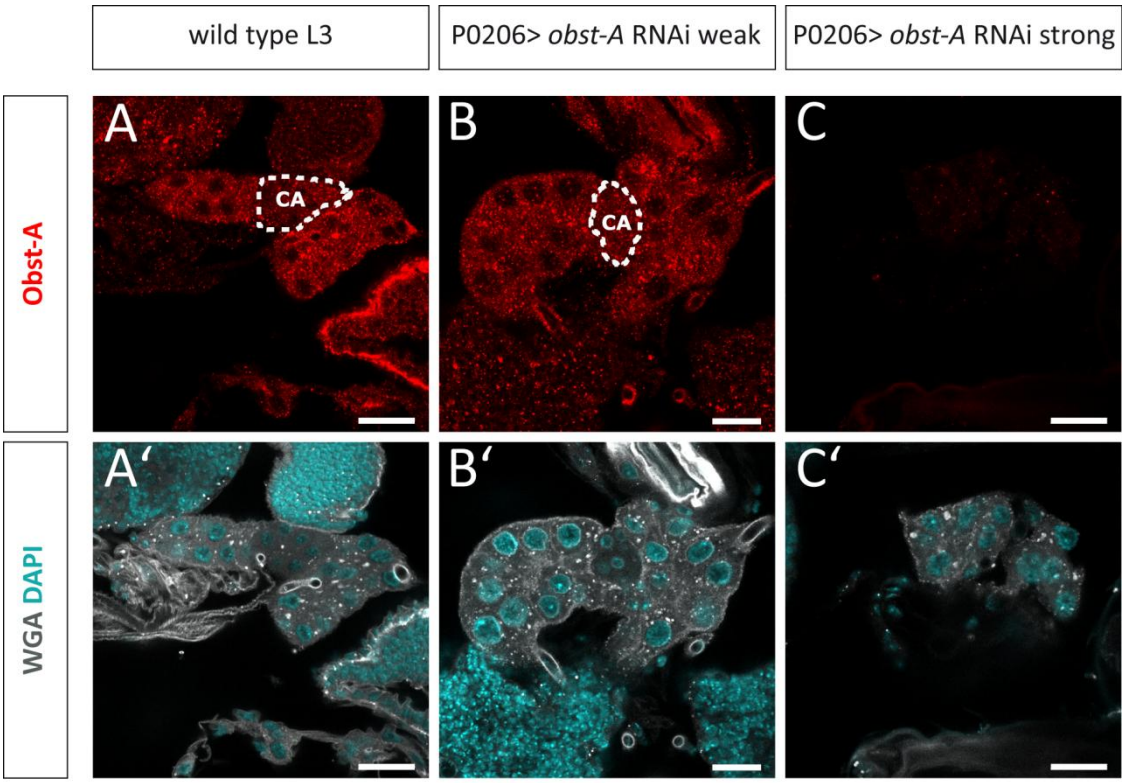

Fig. S6 - Presence of the corpus allatum correlates with Obst-A levels. Immunostaining (n=2 with >10 ring glands per condition) of third instar wild type (A, A') and P0206> *obst-A* RNAi larvae (B, B' - weak knockdown; C, C' - strong knockdown). A-C: Single channel Obst-A staining is depicted in red. A'-C': WGA staining (grey) and DAPI staining (cyan), labeling cell surfaces and nuclei, respectively. In the wild type (A, A') strong Obst-A staining can be detected in the prothoracic gland (A). The CA (indicated by white dashes in A) is distinguishable due to weaker Obst-A staining and due to differences in WGA staining and smaller size of nuclei (A'). At 25 °C when the Gal4-UAS system is not fully activated P0206> *obst-A* RNAi knockdown larvae can be subdivided into larvae without any developmental defects (B, B') and larvae with molting defects at the L2/L3 transition (C, C'). In the normal appearing larvae the prothoracic gland shows intense Obst-A staining (red) and the CA (indicated by dashes in B) is detected (B; also seen by reduction of WGA staining and nuclei size in B'). This implies that in the larvae without any defects *obst-A* knockdown efficiency is weak and hence, no defects can be observed. In the larvae with molting defects (C, C') however, Obst-A staining (C) is weak and the ring gland is small (C') A corpus allatum is not detected (C'). This shows that presence of the corpus allatum and ring gland size correlates with Obst-A protein levels. Scale bars indicate 20 µm.

Supplementary figure S7

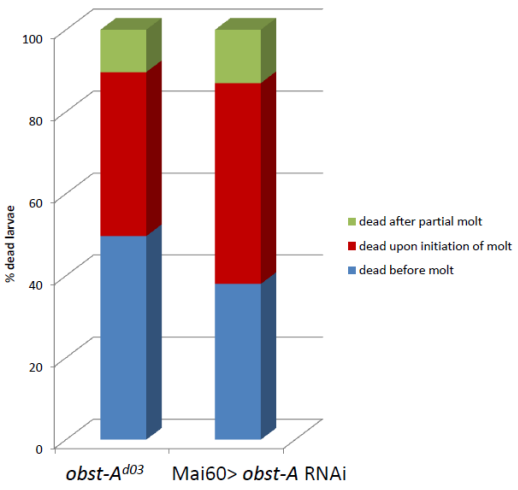

Fig. S7 - Lethality profile of *obst-A*^{d03} and Mai60 Gal4> UAS *obst-A* RNAi larvae. y-axis: % dead larvae. x-axis: genotype. Both genotypes are completely lethal before reaching second instar stage. Larvae are classified into larvae that die before molt (blue), larvae that die upon initiation of molt (double mouth hook stage; red) and larvae that die after partial molt (partial cuticle shedding; green). n=3, each n equals 100 larvae per genotype.

Supplementary figure S8

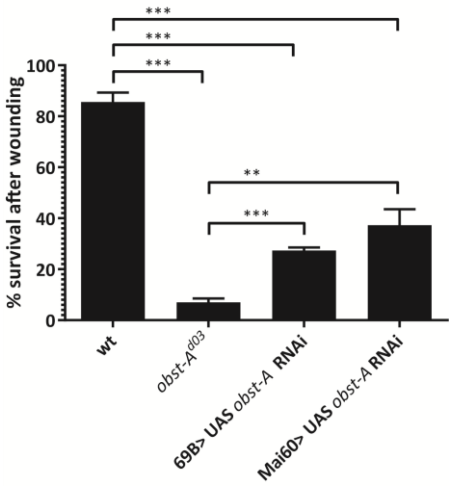

Fig. S8 - Quantification of survival after wounding in 69B Gal4 and Mai60 Gal4 *obst-A* knockdown larvae. y-axis: % survival of animals after gentle lateral pricking with a thin glass needle. x-axis: analyzed genotype**.** The cuticle integrity test was performed in early first instar wild type control larvae (wt), *obst-A*^{d03} null mutant larvae, 69B Gal4> UAS *obst-A* RNAi and Mai60 Gal4> UAS *obst-A* RNAi. n≥30 larvae for each condition. Error bars represent SEM. **p<0.01; ***p<0.001.

Supplementary figure S9

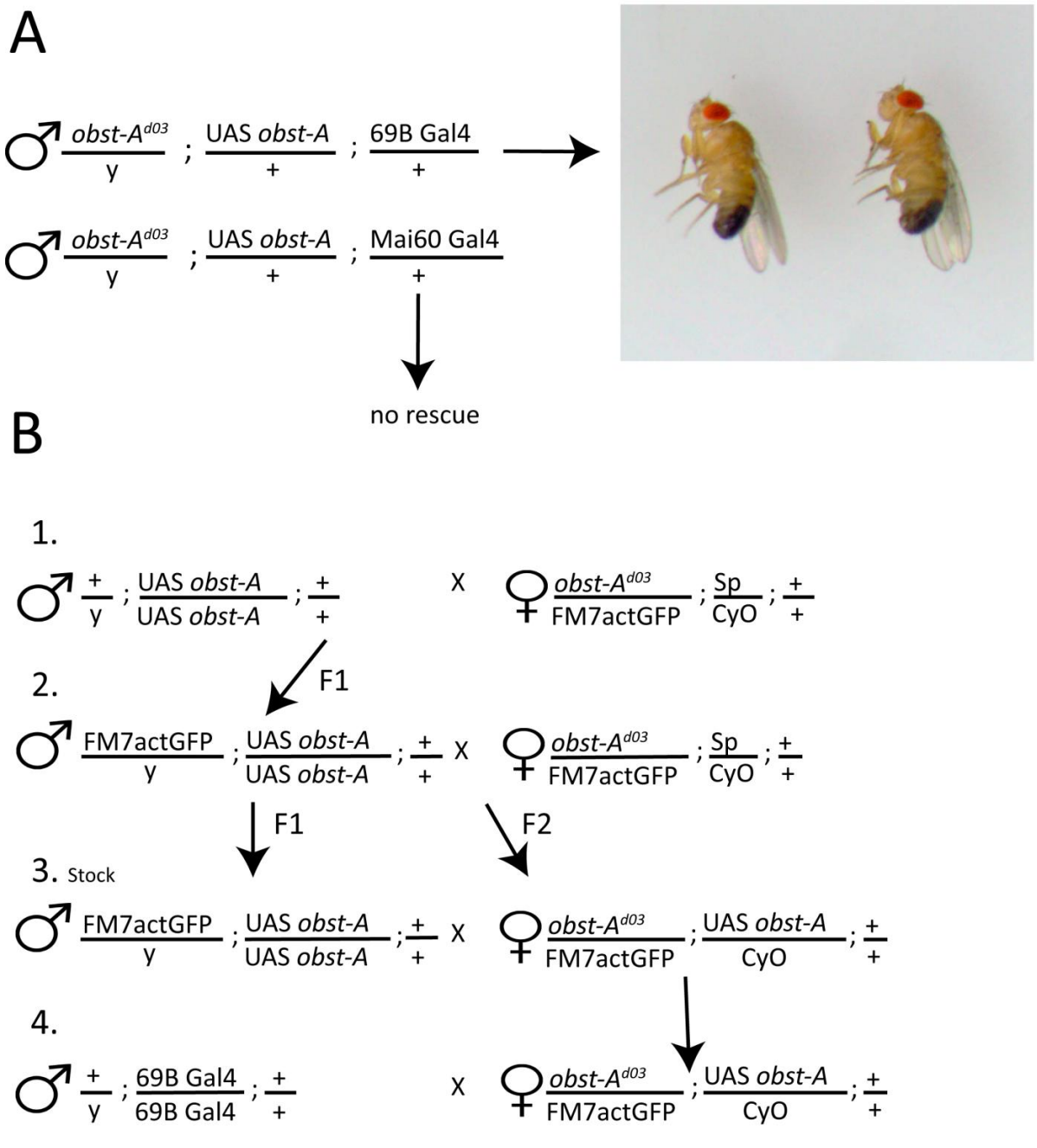

Fig. S9 - Genetic rescue of *obst-A* mutants. A: genotype of *obst-A* rescue animals. As *obst-A* is located on the X-chromosome, rescued animals were male mutants with normal eyes (not heart-shaped eyes as in the heterozygous mutant balanced with FM7actGFP) in which *obst-A* was re-introduced by Gal4-mediated expression of a UAS *obst-A* construct. The rescue was successful with the ectoderm-driver line 69B Gal4 (male normal-eyed adult flies shown on the right), but not with the prothoracic gland-driver Mai60 Gal4. B: Crossing scheme for the generation of rescue flies. Heterozygous *obst-A* mutant females were crossed with UAS *obst-A* flies. Offspring males were crossed with heterozygous *obst-A* mutant females and then with heterozygous offsping females as indicated in the scheme. Females from the established stock were then crossed with male driver line flies for the rescue crossing.

6.2 - List of abbreviations

°C	degrees Celsius	Domon	dopamine monooxygenase
µ	micro	DS	donkey serum
20E	20-hydroxy ecdysone	E	ecdysone
7dC	7-dehydro cholesterol	*E. coli*	Escherichia coli
A	Adult stage	ECM	Extracellular matrix
A488	Alexa488 fluorophore	EcR	ecdysone receptor
A633	Alexa633 fluorophore	Edg	ecdysone-dependent gene
A647	Alexa647 fluorophore	EDTA	ethylenediaminetetraacetic acid
act	actin	eh	eclosion hormone
aECM	apical extracellular matrix	ELISA	Enzyme linked immunosorbent assay
AKH	Adipokinetic Hormone	env	envelope
alas	Aminolevulinate synthase	epi	epicuticle
APS	ammoniumpersulfate	ER	endoplasmic reticulum
az	assembly zone	eth	ecdysis triggering hormone
BCA	Bicinchoninic acid	FasII	Fasciclin II
bf	brightfield	FM7	balancer chromosome
br-Z	isoform of broad complex	ftz	fushi tarazu
C	cholesterol	g	gram
C. elegans	Caenorrhabditis elegans	Gal4	yeast transcription factor
CA	corpus allatum	Gce	Germ cell expressed
CBD2	Chitin binding domain type 2	GFP	green fluorescent protein
CBP	Chitin Binding Probe	GlcNAc	N-acetyl-β-D-glucosamine
CC	corpora cardiaca	Glyco18	Glycosylhydrolase Family 18
CCAP	Crustacean Cardioactive Peptide	GPI	Glycosyl phosphatidyl inositol
cDNA	copy DNA	GTPase	guanosine triphosphate hydrolase
CG	cytosine guanine	h	hour
Cht	Chitinase	Hu	Humeral
CNS	central nervous system	Idgf	Imaginal disc growth factor
CPAPs	Cuticle Proteins Analogous to Peritrophins	if	irregular facets
cy	cytoplasm	JB-4	Glycol methacrylate resin
Cy3	cyanine3 fluorophore	JH	Juvenile Hormone
CyO	balancer chromosome	kDa	kilodalton
cyp18a	cyclophilin 18a	Kkv	Krotzkopf verkehrt
DAPI	4',6-diamidino-2-phenylindole	Kni	Knirps
ddH2O	double distilled water	Knk	Knickkopf
dhMaA	24(28)-dehydromakisterone	l	liter
DHR	Drosophila Hormone Receptor	L1	first instar larva
dib	disembodied	L2	second instar larva
DIC	Differential interference contrast	L3	third instar larva
DNA	Desoxyribonucleic acid	LC-MS/MS	Liquid-Chromatography-Mass Spectrometry/Mass Spectrometry

LSM	laser scanning microscope	Rtv	Retroactive
m	Milli	s	second
M	molar	sad	shadow
MAPK	MAP Kinase	sal	spalt
Met	Methoprene tolerant	sb	stubble
min	minute	SDS	sodium dodecyl sulfate
MKRS	balancer chromosome	SDS-PAGE	Sodium Dodecyl Sulfate Polyacrylamide Gel Electrophoresis
Mld	Molting defective	SEM	standard error of the mean
mRNA	messenger RNA	Ser	serrate
n	nano	Serp	Serpentine
npc1a	Niemann-Pick type C 1a	SF-1	steroidogenic factor 1
nvd	Neverland	shd	shade
Obst	Obstructor	SMRTR	SMRT-related and ecdysone receptor interacting factor
Obst-A	Obstructor-A	Sp	sternopleural
Ouib	ouija board	Spec	Spectrin
p	pico	spok	spookier
p	p-value (probability value)	sro	shroud
P	pupal stage	svp	seven up
PBS	phosphate buffered saline	TAG	triacylglycerol
PCR	polymerase chain reaction	Tb	tubby
P-element	mobile genetic element	TELT	Tris EDTA LiCl Triton
PG	prothoracic gland	TEMED	N,N,N',N'-Tetramethylethane-1,2-diamine
pH	pondus hydrogenii	TGF	transforming growth factor
phm	phantom	phantom	balancer chromosome
pro	procuticle	TM6	balancer chromosome
PTTH	prothoracicotropic hormone	TOR	target of rapamycin
PVDF	Polyvinylidene difluoride	Tris	tris(hydroxymethyl)aminomethane
qRT-PCR	quantitative real time PCR	UAS	upstream activating sequence
R & R	Rebers & Riddiford Domain	UDP-GlcNAc	Uridine-diphosphate–N-acetyl-D-glucosamine
Ras	Rat sarcoma GTPase	usp	ultraspiracle
RG	ring gland	V	Volt
RIA	Radioimmunoassay	VA	viable adult
rig	rigor mortis	v/v	volume per volume
RIPA	Radioimmunoprecipitation assay buffer	Verm	Vermiform
RNA	ribonucleic acid	Vvl	ventral veins lacking
RNAi	RNA interference	w/v	weight per volume
rp49	ribosomal protein L32, housekeeping gene	WGA	Wheat germ agglutinin
rpm	rotations per minute	Woc	Without children
RT	Reverse Transcriptase	wt	Wild type

6.3 - List of references

Abdou MA, He Q, Wen D, Zyaan O, Wang J, Xu J, Baumann AA, Joseph J, Wilson TG, Li S, Wang J (2011) Drosophila Met and Gce are partially redundant in transducing juvenile hormone action. Insect Biochem Mol Biol 41(12):938-945.

Alberts B, Johnson A, Lewis J, Raff M, Roberts K, Walter P (2008) Molecular Biology of the Cell. Garland Science. 5th edition:1419-1420.

Andersen DS, Colombani J, Léopold P (2013) Coordination of organ growth: principles and outstanding questions from the world of insects. Trends Cell Biol 23(7):336-344.

Andres AJ, Thummel CS (1992) Hormones, puffs and flies: the molecular control of metamorphosis by ecdysone. Trends Genet 8(4):132-138.

Andrews HK, Zhang YQ, Trotta N, Broadie K (2002) Drosophila sec10 is required for hormone secretion but not general exocytosis or neurotransmission. Traffic 3(12):906-921.

Aguinaldo AM, Turbeville JM, Linford LS, Rivera MC, Garey JR, Raff RA, Lake JA (1997) Evidence for a clade of nematodes, arthropods and other moulting animals. Nature 387(6632):489-493.

Arakane Y, Muthukrishnan S, Beeman RW, Kanost MR, Kramer KJ (2005) Laccase 2 is the phenoloxidase gene required for beetle cuticle tanning. Proc Natl Acad Sci U S A 102(32):11337-11342.

Arakane Y, Specht CA, Kramer KJ, Muthukrishnan S, Beeman RW (2008) Chitin synthases are required for survival, fecundity and egg hatch in the red flour beetle, Tribolium castaneum. Insect Biochem Mol Biol 38(10):959-962.

Arakane Y, Muthukrishnan S (2010) Insect chitinase and chitinase-like proteins. Cell Mol Life Sci 67(2):201-216.

Araújo SJ, Aslam H, Tear G, Casanova J (2005) mummy/cystic encodes an enzyme required for chitin and glycan synthesis, involved in trachea, embryonic cuticle and CNS development--analysis of its role in Drosophila tracheal morphogenesis. Dev Biol 288(1):179-193.

Ashburner M (1971) Induction of puffs in polytene chromosomes of in vitro cultured salivary glands of Drosophila melanogaster by ecdysone and echysone analogues. Nat New Biol 230(15):222-224.

Bai J, Uehara Y, Montell DJ (2000) Regulation of invasive cell behavior by taiman, a Drosophila protein related to AIB1, a steroid receptor coactivator amplified in breast cancer. Cell 103(7):1047-1058.

Bang AG, Bailey AM, Posakony JW (1995) Hairless promotes stable commitment to the sensory organ precursor cell fate by negatively regulating the activity of the Notch signaling pathway. Dev Biol 172(2):479-494.

Barbakadze N, Enders S, Gorb S, Arzt E (2006) Local mechanical properties of the head articulation cuticle in the beetle Pachnoda marginata (Coleoptera, Scarabaeidae). J Exp Biol 209(Pt 4ag), 722-730.

Barry MK, Triplett AA, Christensen AC (1999) A peritrophin-like protein expressed in the embryonic tracheae of Drosophila melanogaster. Insect Biochem Mol Biol 29(4):319-327.

Bäsler K, Bergmann S, Heisig M, Naegel A, Zorn-Kruppa M, Brandner JM (2016) The role of tight junctions in skin barrier function and dermal absorption. J Control Release 242:105-118.

Beament JW (1968) The insect cuticle and membrane structure. Br Med Bull 24(2):130-134.

Beckstead R, Ortiz JA, Sanchez C, Prokopenko SN, Chambon P, Losson R, Bellen HJ (2001) Bonus, a Drosophila homolog of TIF1 proteins, interacts with nuclear receptors and can inhibit betaFTZ-F1-dependent transcription. Mol Cell 7(4):753-765.

Beckstead RB, Lam G, Thummel CS (2005) The genomic response to 20-hydroxyecdysone at the onset of Drosophila metamorphosis. Genome Biol 6(12):R99.

Beckstead RB, Lam G, Thummel CS (2007) Specific transcriptional responses to juvenile hormone and ecdysone in Drosophila. Insect Biochem Mol Biol 37(6):570-578.

Behr M, Riedel D, Schuh R (2003) The claudin-like megatrachea is essential in septate junctions for the epithelial barrier function in Drosophila. Dev Cell 5(4):611-620.

Behr M, Hoch M (2005) Identification of the novel evolutionary conserved obstructor multigene family in invertebrates. FEBS Lett 579(30):6827-6833.

Behr M, Wingen C, Wolf C, Schuh R, Hoch M (2007) Wurst is essential for airway clearance and respiratory-tube size control. Nat Cell Biol 9(7):847-853.

Beitel GJ, Krasnow MA (2000) Genetic control of epithelial tube size in the Drosophila tracheal system. Development 127(15):3271-3282.

Bendena WG, Zhang J, Burtenshaw SM, Tobe SS (2011) Evidence for differential biosynthesis of juvenile hormone (and related) sesquiterpenoids in Drosophila melanogaster. Gen Comp Endocrinol 172(1):56-61.

Bender M, Imam FB, Talbot WS, Ganetzky B, Hogness DS (1997) Drosophila ecdysone receptor mutations reveal functional differences among receptor isoforms. Cell 1997 91(6):777-788.

Bialecki M, Shilton A, Fichtenberg C, Segraves WA, Thummel CS (2002) Loss of the ecdysteroid-inducible E75A orphan nuclear receptor uncouples molting from metamorphosis in Drosophila. Dev Cell 3(2):209-220.

Bodai L, Zsindely N, Gáspár R, Kristó I, Komonyi O, Boros IM (2012) Ecdysone induced gene expression is associated with acetylation of histone H3 lysine 23 in Drosophila melanogaster. PLoS One 7(7):e40565.

Bökel C, Prokop A, Brown NH (2005) Papillote and Piopio: Drosophila ZP-domain proteins required for cell adhesion to the apical extracellular matrix and microtubule organization. J Cell Sci 118(Pt 3):633-642.

Borsos BN, Pankotai T, Kovács D, Popescu C, Páhi Z, Boros IM (2015). Acetylations of Ftz-F1 and histone H4K5 are required for the fine-tuning of ecdysone biosynthesis during Drosophila metamorphosis. Dev Biol 404(1):80-87.

Brand AH, Perrimon N (1993) Targeted gene expression as a means of altering cell fates and generating dominant phenotypes. Development 118(2):401–415.

Broadus J, McCabe JR, Endrizzi B, Thummel CS, Woodard CT (1999) The Drosophila beta FTZ-F1 orphan nuclear receptor provides competence for stage-specific responses to the steroid hormone ecdysone. Mol Cell 3(2):143-149.

Broughton SJ, Piper MD, Ikeya T, Bass TM, Jacobson J, Driege Y, Martinez P, Hafen E, Withers DJ, Leevers SJ, Partridge L (2005) Longer lifespan, altered metabolism, and stress resistance in Drosophila from ablation of cells making insulin-like ligands. Proc Natl Acad Sci U S A 102(8):3105-31010.

Brown HL, Cherbas L, Cherbas P, Truman JW (2006) Use of time-lapse imaging and dominant negative receptors to dissect the steroid receptor control of neuronal remodeling in Drosophila. Development 133(2):275-285.

Cáceres L, Necakov AS, Schwartz C, Kimber S, Roberts IJ, Krause HM (2011) Nitric oxide coordinates metabolism, growth, and development via the nuclear receptor E75. sGenes Dev 25(14):1476-1485.

Caldwell PE, Walkiewicz M, Stern M (2005) Ras activity in the Drosophila prothoracic gland regulates body size and developmental rate via ecdysone release. Curr Biol 15(20):1785-1795.

Campos-Ortega JA, Hartenstein V (1997) The embryonic development of Drosophila melanogaster. Springer, Berlin, 2nd edition.

Chadfield CG, Sparrow JC (1985) Pupation in Drosophila melanogaster and the Effect of the Lethalcryptocephal Mutation. Developmental Genetics 5:103-114.

Chandler D, Bailey AS, Tatchell GM, Davidson G, Greaves J, Grant WP (2011) The development, regulation and use of biopesticides for integrated pest management. Philos Trans R Soc Lond B Biol Sci 366(1573):1987-1998.

Chang ES (1993) Comparative endocrinology of molting and reproduction: insects and crustaceans. Annu Rev Entomol. 38:161-180.

Chaudhari SS, Arakane Y, Specht CA, Moussian B, Boyle DL, Park Y, Kramer KJ, Beeman RW, Muthukrishnan S. Knickkopf protein protects and organizes chitin in the newly synthesized insect exoskeleton (2011) Proc Natl Acad Sci U S A 108(41):17028-17033.

Chaudhari SS, Arakane Y, Specht CA, Moussian B, Kramer KJ, Muthukrishnan S, Beeman RW (2013) Retroactive maintains cuticle integrity by promoting the trafficking of Knickkopf into the procuticle of Tribolium castaneum. PLoS Genet. 9(1):e1003268.

Chaudhari SS, Moussian B, Specht CA, Arakane Y, Kramer KJ, Beeman RW, Muthukrishnan S (2014) Functional Specialization among Members of Knickkopf Family of Proteins in Insect Cuticle Organization. PLoS Genet 10(8):e1004537.

Chaudhari SS, Noh MY, Moussian B, Specht CA, Kramer KJ, Beeman RW, Arakane Y, Muthukrishnan S (2015) Knickkopf and retroactive proteins are required for formation of laminar serosal procuticle during embryonic development of Tribolium castaneum. Insect Biochem Mol Biol 60:1-6.

Chávez VM, Marqués G, Delbecque JP, Kobayashi K, Hollingsworth M, Burr J, Natzle JE, O'Connor MB (2000) The Drosophila disembodied gene controls late embryonic morphogenesis and codes for a cytochrome P450 enzyme that regulates embryonic ecdysone levels. Development 127(19):4115-4126.

Chavoshi TM, Moussian B, Uv A (2010) Tissue-autonomous EcR functions are required for concurrent organ morphogenesis in the Drosophila embryo. Mech Dev 127(5-6):308-319.

Chino H, Sakurai S, Ohtaki T, Ikekawa N, Miyazaki H, Ishibashi M, Abuki H (1974) Biosynthesis of α-Ecdysone by Prothoracic Glands in vitro. Science 183(4124):529-530.

Church RB, Robertson FW (1966) A biochemical study of the growth of Drosophila melanogaster. J Exp Zool 12:852-858.

Clark AC, del Campo ML, Ewer J (2004) Neuroendocrine control of larval ecdysis behavior in Drosophila: complex regulation by partially redundant neuropeptides. J Neurosci 24(17):4283-4292.

Colombani J, Bianchini L, Layalle S, Pondeville E, Dauphin-Villemant C, Antoniewski C, Carré C, Noselli S, Léopold P (2005) Antagonistic actions of ecdysone and insulins determine final size in Drosophila. Science 310(5748):667-670.

Colombani J, Andersen DS, Boulan L, Boone E, Romero N, Virolle V, Texada M, Léopold P (2015) Drosophila Lgr3 Couples Organ Growth with Maturation and Ensures Developmental Stability. Curr Biol 25(20):2723-2729.

Condoulis WV, Locke M (1966) The deposition of endocuticle in an insect, Calpodes Ethlius Stoll (Lepidoptera, Hesperiidae) J Insect Physiol 12:311-323.

Cox-Foster DL, Schonbaum CP, Murtha MT, Cavener DR (1989) Developmental expression of the glucose dehydrogenase gene in Drosophila melanogaster. Genetics 124(4):873-880.

Cronauer MV, Braun S, Tremmel Ch, Kröncke KD, Spindler-Barth M (2007) Nuclear localization and DNA binding of ecdysone receptor and ultraspiracle. Arch Insect Biochem Physiol 65(3):125-133.

Crossgrove K, Bayer CA, Fristrom JW, Guild GM (1996) The Drosophila Broad-Complex early gene directly regulates late gene transcription during the ecdysone-induced puffing cascade. Dev Biol 180(2):745-758.

Cui HY, Lestradet M, Bruey-Sedano N, Charles JP, Riddiford LM (2009) Elucidation of the regulation of an adult cuticle gene Acp65A by the transcription factor Broad. Insect Mol Biol 18(4):421-429.

Dähn U, Hagenmaier H, Höhne H, König WA, Wolf G, Zähner H (1976) Stoffwechselprodukte von Mikroorganismen. 154. Mitteilung. Nikkomycin, ein neuer Hemmstoff der Chitinsynthese bei Pilzen. Arch Microbiol 107(2):143-160.

Dai JD, Gilbert LI (1991) Metamorphosis of the corpus allatum and degeneration of the prothoracic glands during the larval-pupal-adult transformation of Drosophila melanogaster: a cytophysiological analysis of the ring gland. Dev Biol 144(2):309-326.

Danielsen ET, Moeller ME, Dorry E, Komura-Kawa T, Fujimoto Y, Troelsen JT, Herder R, O'Connor MB, Niwa R, Rewitz KF (2014) Transcriptional control of steroid biosynthesis genes in the Drosophila prothoracic gland by ventral veins lacking and knirps. PLoS Genet 10(6):e1004343.

Darido C, Georgy SR, Jane SM (2016) The role of barrier genes in epidermal malignancy. Oncogene 35(44):5705-5712.

Dawson MI, Xia Z (2012) The retinoid X receptors and their ligands. Biochim Biophys Acta 1821(1):21-56.

Delbecque JP, Hirn M, Delachambre J, De Regg M (1978) Cuticular cycle and molting hormone levels during the metamorphosis of Tenebrio molitor (Insecta Coleoptera). Dev Biol 64(1):11-30.

Dennel R (1944) Hardening and Darkening of the Insect Cuticle. Nature 154(3897):57-58.

Devine WP, Lubarsky B, Shaw K, Luschnig S, Messina L, Krasnow MA (2005) Requirement for chitin biosynthesis in epithelial tube morphogenesis. Proc Natl Acad Sci U S A 102(47):17014-17019.

Dhadialla TS, Carlson GR, Le DP (1998) New insecticides with ecdysteroidal and juvenile hormone activity. Annu Rev Entomol 43:545-569.

Diao F, Ironfield H, Luan H, Diao F, Shropshire WC, Ewer J, Marr E, Potter CJ, Landgraf M, White BH (2015) Plug-and-play genetic access to drosophila cell types using exchangeable exon cassettes. Cell Rep 10(8):1410-1421.

Di Cara F, King-Jones K (2013) How clocks and hormones act in concert to control the timing of insect development. Curr Top Dev Biol 105:1-36.

Dietzl G, Chen D, Schnorrer F, Su KC, Barinova Y, Fellner M, Gasser B, Kinsey K, Oppel S, Scheiblauer S, Couto A, Marra V, Keleman K, Dickson BJ (2007) A genome-wide transgenic RNAi library for conditional gene inactivation in Drosophila. Nature 448(7150), 151-156.

Dixit R, Arakane Y, Specht CA, Richard C, Kramer KJ, Beeman RW, Muthukrishnan S (2008) Domain organization and phylogenetic analysis of proteins from the chitin deacetylase gene family of Tribolium castaneum and three other species of insects. Insect Biochem Mol Biol 38(4):440-451.

Dong B, Miao G, Hayashi S (2014) A fat body-derived apical extracellular matrix enzyme is transported to the tracheal lumen and is required for tube morphogenesis in Drosophila. Development 141(21):4104-4109.

Dong B, Hayashi S (2015) Shaping of biological tubes by mechanical interaction of cell and extracellular matrix. Curr Opin Genet Dev 32:129-134.

Dressel U, Thormeyer D, Altincicek B, Paululat A, Eggert M, Schneider S, Tenbaum SP, Renkawitz R, Baniahmad A (1999) Alien, a highly conserved protein with characteristics of a corepressor for members of the nuclear hormone receptor superfamily. Mol Cell Bio 19(5):3383-3394.

Eichner C, Harasimczuk E, Nilsen F, Grotmol S, Dalvin S (2015) Molecular characterisation and functional analysis of LsChi2, a chitinase found in the salmon louse (Lepeophtheirus salmonis salmonis, Krøyer 1838). Exp Parasitol 151-152:39-48.

Ewer J (2005) How the ecdysozoan changed its coat. PLoS Biol 3(10):e349.

Fan XJ, Mi YX, Ren H, Zhang C, Li Y, Xian XX (2015) Cloning and functional expression of a chitinase cDNA from the apple leaf miner moth Lithocolletis ringoni. Biochemistry (Mosc) 80(2):242-250.

Farinós GP, Smagghe G, Tirry L, Castanera P (1999) Action and pharmacokinetics of a novel insect growth regulator, halofenozide, in adult beetles of aubeonymus mariaefranciscae and leptinotarsa decemlineata. Arch Insect Biochem Physiol 41(4):201-213.

Fletcher JC, Thummel CS (1995) The Drosophila E74 gene is required for the proper stage- and tissue-specific transcription of ecdysone-regulated genes at the onset of metamorphosis. Development 121(5):1411-1421.

Freeman MR, Dobritsa A, Gaines P, Segraves WA, Carlson JR (1999) The dare gene: steroid hormone production, olfactory behavior, and neural degeneration in Drosophila. Development 126(20):4591-4602.

Fresán U, Cuartero S, O'Connor MB, Espinàs ML (2015) The insulator protein CTCF regulates Drosophila steroidogenesis. Biol Open 4(7):852-857.

Fristrom JW (1965) Development of the morphological mutant cryptocephal of Drosophila Melanogaster. Genetics 52:297-318.

Galko MJ, Krasnow MA (2004) Cellular and genetic analysis of wound healing in Drosophila larvae. PLoS Biol 2(8): e239.

Gangishetti U, Veerkamp J, Bezdan D, Schwarz H, Lohmann I, Moussian B (2012) The transcription factor Grainy head and the steroid hormone ecdysone cooperate during differentiation of the skin of Drosophila melanogaster. Insect Mol Biol 21(3):283-295.

Gates J, Lam G, Ortiz JA, Losson R, Thummel CS (2004) rigor mortis encodes a novel nuclear receptor interacting protein required for ecdysone signaling during Drosophila larval development. Development 131(1):25-36.

Gauthier SA, Hewes RS (2006) Transcriptional regulation of neuropeptide and peptide hormone expression by the Drosophila dimmed and cryptocephal genes. J Exp Biol 209(Pt 10):1803-15.

Gaziova I, Bonnette PC, Henrich VC, Jindra M (2004) Cell-autonomous roles of the ecdysoneless gene in Drosophila development and oogenesis. Development 131(11):2715-2725.

Ghabrial A, Luschnig S, Metzstein MM, Krasnow MA (2003) Branching morphogenesis of the Drosophila tracheal system. Annu Rev Cell Dev Biol 19:623-647.

Ghildiyal M, Zamore PD (2009) Small silencing RNAs: an expanding universe. Nat Rev Genet 10(2), 94-108.

Gibbens YY, Warren JT, Gilbert LI, O'Connor MB (2011) Neuroendocrine regulation of Drosophila metamorphosis requires TGFbeta/Activin signaling. Development 138(13):2693-2703.

Gibbs A (1998) Water-proofing properties of cuticular lipids. Amer Zool 38:471-482.

Gibbs AG (2011) Thermodynamics of cuticular respiration. J Insect Physiol 57(8):1066-1069.

Gilbert LI, Granger NA, Roe RM (2000) The juvenile hormones: historical facts and speculations on future research directions. Insect Biochem Mol Biol 30(8-9):617-644.

Gilbert LI, Rybczynski R, Warren JT (2002) Control and biochemical nature of the ecdysteroidogenic pathway. Annu Rev Entomol 47:883-916.

Gilbert LI (2004) Halloween genes encode P450 enzymes that mediate steroid hormone biosynthesis in Drosophila melanogaster. Mol Cell Endocrinol 215(1-2):1-10.

Gu SH, Chow YS, Yin CM (1997) Involvement of juvenile hormone in regulation of prothoracicotropic hormone transduction during the early last larval instar of Bombyx mori. Mol Cell Endocrinol 127(1):109-116.

Gündner AL, Hahn I, Sendscheid O, Aberle H, Hoch M (2014) The PIKE homolog Centaurin gamma regulates developmental timing in Drosophila. PLoS One 9(5):e97332. doi: 10.1371/journal.pone.0097332.

Hall BL, Thummel CS (1998) The RXR homolog ultraspiracle is an essential component of the Drosophila ecdysone receptor. Development 125(23):4709-4717.

Halme A, Cheng M, Hariharan IK (2010) Retinoids regulate a developmental checkpoint for tissue regeneration in Drosophila. Curr Biol 20(5):458-463.

Hartenstein V, Posakony JW (1989) Development of adult sensilla on the wing and notum of Drosophila melanogaster. Development 107(2):389-405.

Hartenstein V (2006) The neuroendocrine system of invertebrates: a developmental and evolutionary perspective. J Endocrinol 190(3):555-570.

Hemphälä J, Uv A, Cantera R, Bray S, Samakovlis C (2003) Grainy head controls apical membrane growth and tube elongation in response to Branchless/FGF signalling. Development 130(2):249-258.

Hesterlee S, Morton DB (1996) Insect physiology: the emerging story of ecdysis. Curr Biol 6(6):648-650.

Hopkins TL, Kramer KJ (1992) Insect cuticle sclerotization. Annu Rev Entomol 37:273-302.

Horn DH, Middleton EJ, Wunderlich JA (1966) Identity of the Moulting Hormones of Insects and Crustaceans. Chemical Communications 11:339-341.

Huang X, Suyama K, Buchanan J, Zhu AJ, Scott MP (2005) A Drosophila model of the Niemann-Pick type C lysosome storage disease: dnpc1a is required for molting and sterol homeostasis. Development 132(22):5115-5124.

Hsiao YC, Chen CN, Chen YT, Yang TL (2013) Controlling branching structure formation of the salivary gland by the degree of chitosan deacetylation. Acta Biomater 9(9):8214-8223.

Jacinto A, Woolner S, Martin P (2012) Dynamic analysis of dorsal closure in Drosophila: from genetics to cell biology. Dev Cell 3(1):9-19.

Jasrapuria S, Arakane Y, Osman G, Kramer KJ, Beeman RW, Muthukrishnan S (2010) Genes encoding proteins with peritrophin A-type chitin-binding domains in Tribolium castaneum are grouped into three distinct families based on phylogeny, expression and function. Insect Biochem Mol Biol 40(3):214-227.

Jasrapuria S, Specht CA, Kramer KJ, Beeman RW, Muthukrishnan S (2012) Gene families of cuticular proteins analogous to peritrophins (CPAPs) in Tribolium castaneum have diverse functions. PLoS One 7(11):e49844.

Jaszczak JS, Wolpe JB, Bhandari R, Jaszczak RG, Halme A (2016) Growth Coordination During Drosophila melanogaster Imaginal Disc Regeneration Is Mediated by Signaling Through the Relaxin Receptor Lgr3 in the Prothoracic Gland. Genetics 204(2):703-709.

Jaspers MH, Pflanz R, Riedel D, Kawelke S, Feussner I, Schuh R (2014) The fatty acyl-CoA reductase Waterproof mediates airway clearance in Drosophila. Dev Biol 385(1):23-31.

Jaźwińska A, Ribeiro C, Affolter M (2003) Epithelial tube morphogenesis during Drosophila tracheal development requires Piopio, a luminal ZP protein. Nat Cell Biol 5(10):895-901.

Jin X, Sun X, Song Q (2005) Woc gene mutation causes 20E-dependent alpha-tubulin detyrosination in Drosophila melanogaster. Arch Insect Biochem Physiol 60(3):116-129.

Jindra M, Palli SR, Riddiford LM (2013) The juvenile hormone signaling pathway in insect development. Annu Rev Entomol 58:181-204.

Jindra M, Uhlirova M, Charles JP, Smykal V, Hill RJ (2015) Genetic Evidence for Function of the bHLH-PAS Protein Gce/Met As a Juvenile Hormone Receptor. PLoS Genet 11(7):e1005394.

Johnston DM, Sedkov Y, Petruk S, Riley KM, Fujioka M, Jaynes JB, Mazo A (2011) Ecdysone- and NO-mediated gene regulation by competing EcR/Usp and E75A nuclear receptors during Drosophila development. Mol Cell 44(1):51-61.

Jones G, Wozniak M, Chu Y, Dhar S, Jones D (2001) Juvenile hormone III-dependent conformational changes of the nuclear receptor ultraspiracle. Insect Biochem Mol Biol 32(1):33-49.

Jones D, Jones G, Teal P, Hammac C, Messmer L, Osborne K, Belgacem YH, Martin JR (2010) Suppressed production of methyl farnesoid hormones yields developmental defects and lethality in Drosophila larvae. Gen Comp Endocrinol 165(2):244-254.

Jürgens G, Wieschaus E, Nüsslein-Volhard C, Kluding H (1984) Mutations affecting the pattern of the larval cuticle in Drosophila melanogaster I. Zygotic loci on the third chromosome. Roux's Arch Dev Biol 193:283-295.

Karim FD, Thummel CS (1991) Ecdysone coordinates the timing and amounts of E74A and E74B transcription in Drosophila. Genes Dev 5(6):1067-1079.

Karim FD, Guild GM, Thummel CS (1993) The Drosophila Broad-Complex plays a key role in controlling ecdysone-regulated gene expression at the onset of metamorphosis. Development 118(3):977-988.

Karunakaran R, Mauchline TH, Hosie AH, Poole PS (2005) A family of promoter probe vectors incorporating autofluorescent and chromogenic reporter proteins for studying gene expression in Gram-negative bacteria. Microbiology 151(Pt 10):3249-3256.

Kawakami A, Kataoka H, Oka T, Mizoguchi A, Kimura-Kawakami M, Adachi T, Iwami M, Nagasawa H, Suzuki A, Ishizaki H (1990) Molecular cloning of the Bombyx mori prothoracicotropic hormone. Science 247(4948):1333-1335.

Kawamura K, Shibata T, Saget O, Peel D, Bryant PJ (1999) A new family of growth factors produced by the fat body and active on *Drosophila* imaginal disc cells. Development 126(2):211-219.

Kayashima Y, Hirose S, Ueda H (2005) Anterior epidermis-specific expression of the cuticle gene EDG84A is controlled by many cis-regulatory elements in Drosophila melanogaster. Dev Genes Evol 215(11):545-552.

Kawasaki H, Hirose S, Ueda H (2002) BetaFTZ-F1 dependent and independent activation of Edg78E, a pupal cuticle gene, during the early metamorphic period in Drosophila melanogaster. Dev Growth Differ 44(5):419-425.

Kaznowski CE, Schneiderman HA, Bryant PJ (1985) Cuticle secretion during larval growth in Drosophila melanogaster. J Insect Physiol 31(10):801-813.

Khandelwal N, Barbole RS, Banerjee SS, Chate GP, Biradar AV, Khandare JJ, Giri AP (2016) Budding trends in integrated pest management using advanced micro- and nano-materials: Challenges and perspectives. J Environ Manage 184(Pt 2):157-169.

Kibbe WA (2007) OligoCalc: an online oligonucleotide properties calculator. Nucleic Acids Res 35(Web Server issue):W43-46.

Kim SE, Cho JY, Kim KS, Lee SJ, Lee KH, Choi KY (2004) Drosophila PI3 kinase and Akt involved in insulin-stimulated proliferation and ERK pathway activation in Schneider cells. Cell Signal 16(11):1309-1317.

King RC, Aggarwal SK, Bodenstein D (1966) The comparative submicroscopic morphology of the ring gland of Drosophila melanogaster during the second and third larval instars. Zellforsch Mikrosk Anat 73(2):272-85.

King DS, Bollenbacher WE, Borst DW, Vedeckis WV, O'Connor JD, Ittycheriah PI, Gilbert LI (1974) The Secretion of alpha-Ecdysone by the Prothoracic Glands of Manduca sexta In Vitro. Proc Natl Acad Sci U S A 71(3):793-796.

King-Jones K, Thummel CS (2005) Nuclear receptors--a perspective from Drosophila. Nat Rev Genet 6(4):311-323.

Kirkpatrick RB, Matico RE, McNulty DE, Strickler JE, Rosenberg M (1995) An abundantly secreted glycoprotein from Drosophila melanogaster is related to mammalian secretory proteins produced in rheumatoid tissues and by activated macrophages. Gene 153(2):147-154.

Koelle MR, Talbot WS, Segraves WA, Bender MT, Cherbas P, Hogness DS (1991) The Drosophila EcR gene encodes an ecdysone receptor, a new member of the steroid receptor superfamily. Cell 67(1):59–77.

Komura-Kawa T, Hirota K, Shimada-Niwa Y, Yamauchi R, Shimell M, Shinoda T, Fukamizu A, O'Connor MB, Niwa R (2015) The Drosophila Zinc Finger Transcription Factor Ouija Board Controls Ecdysteroid Biosynthesis through Specific Regulation of spookier. PLoS Genet 11(12):e1005712.

Koyama T, Rodrigues MA, Athanasiadis A, Shingleton AW, Mirth CK (2014) Nutritional control of body size through FoxO-Ultraspiracle mediated ecdysone biosynthesis. eLife 3. doi: 10.7554/eLife.03091.

Kozlova T, Thummel CS (2000) Steroid regulation of postembryonic development and reproduction in Drosophila. Trends Endocrinol Metab 11(7):276-280.

Kozlova T, Thummel CS (2003) Essential roles for ecdysone signaling during Drosophila mid-embryonic development. Science 301(5641):1911-1914.

Kozlova T, Lam G, Thummel CS (2009) Drosophila DHR38 nuclear receptor is required for adult cuticle integrity at eclosion. Dev Dyn 238(3):701-707.

Kramer KJ, Muthukrishnan S (1997) Insect Chitinases: Molecular Biology and Potential Use as Biopesticides. Insect Biochem Mol Biol 27(11), 887-900.

Krüger E, Mena W, Lahr EC, Johnson EC, Ewer J (2015) Genetic analysis of Eclosion hormone action during Drosophila larval ecdysis. Development 142(24):4279-4287.

Kuballa AV, Merritt DJ, Elizur A (2007) Gene expression profiling of cuticular proteins across the moult cycle of the crab Portunus pelagicus. BMC Biol 5:45.

Laemmli UK (1970) Cleavage of structural proteins during the assembly of the head of bacteriophage T4. Nature 227(5259):680–685.

Lavrynenko O, Rodenfels J, Carvalho M, Dye NA, Lafont R, Eaton S, Shevchenko A (2015) The ecdysteroidome of Drosophila: influence of diet and development. Development 142(21):3758-3768.

Layalle S, Arquier N, Léopold P (2008) The TOR pathway couples nutrition and developmental timing in Drosophila. Dev Cell 15(4):568-577.

Lechner H, Josten F, Fuss B, Bauer R, Hoch M (2007) Cross regulation of intercellular gap junction communication and paracrine signaling pathways during organogenesis in Drosophila. Dev Biol 310(1):23-34.

Lehane MJ (1997) Peritrophic matrix structure and function. Annu Rev Entomol 42:525-550.

Lensky Y, Cohen C, Schneiderman HA (1970) The origin, distribution and fate of the molting fluid proteins of the cecropia silkworm. Biol Bull 139:277-295.

Li T, Bender M (2000) A conditional rescue system reveals essential functions for the ecdysone receptor (EcR) gene during molting and metamorphosis in Drosophila. Development 127(13):2897-2905.

Livak KJ, Schmittgen TD (2001) Analysis of Relative Gene Expression Data Using Real-Time Quantitative PCR and the 2-[Delta][Delta]CT Method. Methods 25(4):402-408.

Locke M (1961) Pore canals and related structures in insect cuticle. J Biophys Biochem Cytol 10:589–618.

Locke M, Huie P (1979) Apolysis and the turnover of plasma membrane plaques during cuticle formation in an insect. Tissue Cell 11(2), 277-291.

Locke M, Kiss A, Sass M (1994). The cuticular localization of integument peptides from particular routing categories. Tissue Cell 26(5):707-734.

Locke M (2001) The Wigglesworth Lecture: Insects for studying fundamental problems in biology. J Insect Physiol 47(4-5):495-507.

Loveall BJ, Deitcher DL (2010) The essential role of bursicon during Drosophila development. BMC Dev Biol 10:92.

Lu Y, Zen KC, Muthukrishnan S, Kramer KJ (2002) Site-directed mutagenesis and functional analysis of active site acidic amino acid residues D142, D144 and E146 in Manduca sexta (tobacco hornworm) chitinase. Insect Biochem Mol Biol 32(11):1369-1382.

Lubarsky B, Krasnow MA (2003) Tube Morphogenesis: Making and Shaping Biological Tubes. Cell 112(1):19-28.

Luschnig S, Bätz T, Armbruster K, Krasnow MA (2006) serpentine and vermiform encode matrix proteins with chitin binding and deacetylation domains that limit tracheal tube length in Drosophila. Curr Biol 16(2):186-194.

Mansur JF, Alvarenga ES, Figueira-Mansur J, Franco TA, Ramos IB, Masuda H, Melo AC, Moreira MF (2014) Effects of chitin synthase double-stranded RNA on molting and oogenesis in the Chagas disease vector Rhodnius prolixus. Insect Biochem Mol Biol 51:110-121.

Mathelier A, Zhao X, Zhang AW, Parcy F, Worsley-Hunt R, Arenillas DJ, Buchman S, Chen CY, Chou A, Ienasescu H, Lim J, Shyr C, Tan G, Zhou M, Lenhard B, Sandelin A, Wasserman WW (2014) JASPAR 2014: an extensively expanded and updated open-access database of transcription factor binding profiles. Nucleic Acids Res 42(Database issue):D142-147.

Matsui T, Amagai M (2015) Dissecting the formation, structure and barrier function of the stratum corneum. Int Immunol 27(6):269-280.

Maxeiner S, Dedek K, Janssen-Bienhold U, Ammermüller J, Brune H, Kirsch T, Pieper M, Degen J, Krüger O, Willecke K, Weiler R (2005) Deletion of connexin45 in mouse retinal neurons disrupts the rod/cone signaling pathway between AII amacrine and ON cone bipolar cells and leads to impaired visual transmission. J Neurosci 25(3):566-576.

McBrayer Z, Ono H, Shimell M, Parvy JP, Beckstead RB, Warren JT, Thummel CS, Dauphin-Villemant C, Gilbert LI, O'Connor MB (2007) Prothoracicotropic hormone regulates developmental timing and body size in Drosophila. Dev Cell 13(6):857-871.

Merzendorfer H, Zimoch L (2003) Chitin metabolism in insects: structure, function and regulation of chitin synthases and chitinases. The Journal of Experimental Biology 206:4393-4412.

Merzendorfer H (2006) Insect chitin synthases: a review. J Comp Physiol B 176:1–15.

Mirth C, Truman JW, Riddiford LM (2005) The role of the prothoracic gland in determining critical weight for metamorphosis in Drosophila melanogaster. Curr Biol 15(20):1796-1807.

Mirth CK, Riddiford LM (2007) Size assessment and growth control: how adult size is determined in insects. Bioessays 29(4):344-355.

Mirth CK, Tang HY, Makohon-Moore SC, Salhadar S, Gokhale RH, Warner RD, Koyama T, Riddiford LM, Shingleton AW (2014) Juvenile hormone regulates body size and perturbs insulin signaling in Drosophila. Proc Natl Acad Sci U S A. 2014 111(19):7018-7023.

Mitchell HK, Weber-Tracy UM, Schaar G (1971) Aspects of cuticle formation in Drosophila melanogaster. J Exp Zoo 176:429–444.

Moeller ME, Danielsen ET, Herder R, O'Connor MB, Rewitz KF (2013) Dynamic feedback circuits function as a switch for shaping a maturation-inducing steroid pulse in Drosophila. Development 140(23):4730-4739.

Montagne J, Lecerf C, Parvy JP, Bennion JM, Radimerski T, Ruhf ML, Zilbermann F, Vouilloz N, Stocker H, Hafen E, Kozma SC, Thomas G (2010) The nuclear receptor DHR3 modulates dS6 kinase-dependent growth in Drosophila. PLoS Genet 6(5):e1000937.

Moussian B, Söding J, Schwarz H, Nüsslein-Volhard C (2005a) Retroactive, a membrane-anchored extracellular protein related to vertebrate snake neurotoxin-like proteins, is required for cuticle organization in the larva of Drosophila melanogaster. Dev Dyn 233(3), 1056-1063.

Moussian B, Schwarz H, Bartoszewski S, Nüsslein-Volhard C (2005b) Involvement of Chitin in Exoskeleton Morphogenesis in Drosophila melanogaster. J Morphol 264(1), 117-130.

Moussian B, Uv AE (2005) An ancient control of epithelial barrier formation and wound healing. Bioessays 27(10):987-990.

Moussian B, Seifarth C, Müller U, Berger J, Schwarz H (2006a) Cuticle differentiation during Drosophila embryogenesis. Arthropod Struct Dev 35(3), 137-52.

Moussian B, Tång E, Tonning A, Helms S, Schwarz H, Nüsslein-Volhard C, Uv AE (2006b) Drosophila Knickkopf and Retroactive are needed for epithelial tube growth and cuticle differentiation through their specific requirement for chitin filament organization. Development 133(1):163-171.

Moussian B (2010) Recent advances in understanding mechanisms of insect cuticle differentiation. Insect Biochem Mol Biol 40(5):363-375.

Moussian B (2013a) The Arthropod Cuticle. Arthropod Biology and Evolution:171-196.

Moussian B (2013b) The apical plasma membrane of chitin-synthesising epithelia. Insect Sci 20(2):139-146.

Nakagawa Y, Henrich VC (2009) Arthropod nuclear receptors and their role in molting. FEBS J 276(21):6128-6157.

Namiki T, Niwa R, Sakudoh T, Shirai K, Takeuchi H, Kataoka H (2005) Cytochrome P450 CYP307A1/Spook: a regulator for ecdysone synthesis in insects. Biochem Biophys Res Commun 337(1):367-374.

Neubueser D, Warren JT, Gilbert LI, Cohen SM (2005) molting defective is required for ecdysone biosynthesis. Dev Biol 280(2):362-372.

Nisole A, Stewart D, Bowman S, Zhang D, Krell PJ, Doucet D, Cusson M (2010) Cloning and characterization of a Gasp homolog from the spruce budworm, Choristoneura fumiferana, and its putative role in cuticle formation. J Insect Physiol 56(10):1427-1435.

Niwa R, Matsuda T, Yoshiyama T, Namiki T, Mita K, Fujimoto Y, Kataoka H (2004) CYP306A1, a cytochrome P450 enzyme, is essential for ecdysteroid biosynthesis in the prothoracic glands of Bombyx and Drosophila. J Biol Chem 279(34):35942-35949.

Niwa R, Namiki T, Ito K, Shimada-Niwa Y, Kiuchi M, Kawaoka S, Kayukawa T, Banno Y, Fujimoto Y, Shigenobu S, Kobayashi S, Shimada T, Katsuma S, Shinoda T (2010) Non-molting glossy/shroud encodes a short-chain dehydrogenase/reductase that functions in the 'Black Box' of the ecdysteroid biosynthesis pathway. Development 137(12):1991-1999.

Niwa YS, Niwa R (2016) Transcriptional regulation of insect steroid hormone biosynthesis and its role in controlling timing of molting and metamorphosis. Dev Growth Differ 58(1):94-105.

Noh MY, Kramer KJ, Muthukrishnan S, Kanost MR, Beeman RW, Arakane Y (2014) Two major cuticular proteins are required for assembly of horizontal laminae and vertical pore canals in rigid cuticle of Tribolium castaneum. Insect Biochem Mol Biol 53:22-29.

Nüsslein-Volhard C, Wieschaus E, Kluding H (1984) Mutations affecting the pattern of the larval cuticle in Drosophila melanogaster I. Zygotic loci on the second chromosome. Roux's Arch Dev Biol 193(5):267–282.

Oberlander H (1976) Hormonal control of growth and differentiation of insect tissues cultured in vitro. In Vitro 12(3):225-235.

Odegaard F (2000) How many species of arthropods? Erwin's estimate revised. Biological Journal of the Linnean Society 71:583–597.

Odier A (1823) Mémoires sur la composition chimique des parties cornées des insectes. Mém Soc Hist Nat Paris 1:29-42.

Ohhara Y, Shimada-Niwa Y, Niwa R, Kayashima Y, Hayashi Y, Akagi K, Ueda H, Yamakawa-Kobayashi K, Kobayashi S (2014) Autocrine regulation of ecdysone synthesis by β3-octopamine receptor in the prothoracic gland is essential for Drosophila metamorphosis. Proc Natl Acad Sci U S A 112(5):1452-1457.

Ono H, Rewitz KF, Shinoda T, Itoyama K, Petryk A, Rybczynski R, Jarcho M, Warren JT, Marqués G, Shimell MJ, Gilbert LI, O'Connor MB (2006) Spook and Spookier code for stage-specific components of the ecdysone biosynthetic pathway in Diptera. Dev Biol 298(2):555-570.

Oro AE, McKeown M, Evans RM (1990) Relationship between the product of the Drosophila ultraspiracle locus and the vertebrate retinoid X receptor. Nature 347(6290):298-301.

Oron E, Mannervik M, Rencus S, Harari-Steinberg O, Neuman-Silberberg S, Segal D, Chamovitz DA (2002) COP9 signalosome subunits 4 and 5 regulate multiple pleiotropic pathways in Drosophila melanogaster. Development 129(19):4399-4409.

Ostrowski S, Dierick HA, Bejsovec A (2002) Genetic Control of Cuticle Formation During Embryonic Development of *Drosophila melanogaster*. Genetics 161(1):171-182.

Ou Q, Magico A, King-Jones K (2011) Nuclear receptor DHR4 controls the timing of steroid hormone pulses during Drosophila development. PLoS Biol 9(9):e1001160.

Ou Q, Zeng J, Yamanaka N, Brakken-Thal C, O'Connor MB, King-Jones K (2016) The Insect Prothoracic Gland as a Model for Steroid Hormone Biosynthesis and Regulation. Cell Rep 16(1):247-262.

Öztürk-Çolak A, Moussian B, Araújo SJ (2016) Drosophila chitinous aECM and its cellular interactions during tracheal development. Dev Dyn 245(3):259-267.

P Bhagat Kumar*, K Kasi Viswanath*, S Tuleshwori Devi*, R Sampath Kumar*, Doucet D, Retnakaran A, Krell PJ, Feng Q, Ampasala DR (2016) Molecular cloning and structural characterization of Ecdysis Triggering Hormone from Choristoneura fumiferana. Int J Biol Macromol 88:213-221.
(* last name was abbreviated and not specified, therefore first names are mentioned)

Pahi Z, Kiss Z, Komonyi O, Borsos BN, Tora L, Boros IM, Pankotai T (2015) dTAF10- and dTAF10b-Containing Complexes Are Required for Ecdysone-Driven Larval-Pupal Morphogenesis in Drosophila melanogaster. PLoS One 10(11):e0142226.

Pankotai T, Popescu C, Martín D, Grau B, Zsindely N, Bodai L, Tora L, Ferrús A, Boros I (2010) Genes of the ecdysone biosynthesis pathway are regulated by the dATAC histone acetyltransferase complex in Drosophila. Mol Cell Biol 30(17):4254-4266.

Papaioannou M, Melle C, Baniahmad A (2007) The coregulator Alien. Nucl Recept Signal 5:e008.

Park Y, Filippov V, Gill SS, Adams ME (2002) Deletion of the ecdysis-triggering hormone gene leads to lethal ecdysis deficiency. Development 129(2):493-503.

Parvy JP, Blais C, Bernard F, Warren JT, Petryk A, Gilbert LI, O'Connor MB, Dauphin-Villemant C (2005) A role for betaFTZ-F1 in regulating ecdysteroid titers during post-embryonic development in Drosophila melanogaster. Dev Biol 282(1):84-94.

Parvy JP, Napal L, Rubin T, Poidevin M, Perrin L, Wicker-Thomas C, Montagne J (2012) Drosophila melanogaster Acetyl-CoA-carboxylase sustains a fatty acid-dependent remote signal to waterproof the respiratory system. PLoS Genet 8(8):e1002925. doi: 10.1371/journal.pgen.1002925.

Parvy JP, Wang P, Garrido D, Maria A, Blais C, Poidevin M, Montagne J (2014) Forward and feedback regulation of cyclic steroid production in Drosophila melanogaster. Development 141(20):3955-3965.

Peters W, Latka I (1986) Electron microscopic localization of chitin using colloidal gold labelled with wheat germ agglutinin. Histochemistry 84(2):155-160.

Petkau G, Wingen C, Jussen LC, Radtke T, Behr M (2012) Obstructor-A is required for epithelial extracellular matrix dynamics, exoskeleton function, and tubulogenesis. J Biol Chem 287(25):21396-213405.

Petryk A, Warren JT, Marqués G, Jarcho MP, Gilbert LI, Kahler J, Parvy JP, Li Y, Dauphin-Villemant C, O'Connor MB (2003) Shade is the Drosophila P450 enzyme that mediates the hydroxylation of ecdysone to the steroid insect molting hormone 20-hydroxyecdysone. Proc Natl Acad Sci U S A 100(24):13773-13778.

Perrimon N, Engstrom L, Mahowald AP (1985) Developmental genetics of the 2C-D region of the Drosophila X chromosome. Genetics 111(1):23-41.

Pesch YY, Riedel D, Behr M (2015) Obstructor A organizes matrix assembly at the apical cell surface to promote enzymatic cuticle maturation in Drosophila. J Biol Chem 290(16):10071-10082.

Pesch YY, Riedel D, Patil KR, Loch G, Behr M (2016a) Chitinases and Imaginal disc growth factors organize the extracellular matrix formation at barrier tissues in insects. Sci Rep 6:18340.

Pesch YY, Riedel D, Behr M (2016b) Drosophila Chitinase 2 is expressed in chitin producing organs for cuticle formation. Arthropod Struct Dev. pii: S1467-8039(16)30172-30174.

Qin G, Lapidot S, Numata K, Hu X, Meirovitch S, Dekel M, Podoler I, Shoseyov O, Kaplan DL (2009) Expression, cross-linking, and characterization of recombinant chitin binding resilin. Biomacromolecules 10(12):3227-3234.

Rathore AS, Gupta RD (2015) Chitinases from Bacteria to Human: Properties, Applications, and Future Perspectives. Enzyme Res 2015:791907. doi: 10.1155/2015/791907.

Rebers JE, Riddiford LM (1988) Structure and expression of a Manduca sexta larval cuticle gene homologous to Drosophila cuticle genes. J Mol Biol 203(2):411-423.

Rebers JE, Willis JH (2001) A conserved domain in arthropod cuticular proteins binds chitin. Insect Biochem Mol Biol 31(11):1083-1093.

Rewitz KF, Rybczynski R, Warren JT, Gilbert LI (2006) The Halloween genes code for cytochrome P450 enzymes mediating synthesis of the insect moulting hormone. Biochem Soc Trans 34(Pt 6):1256-1260.

Rewitz KF, Yamanaka N, Gilbert LI, O'Connor MB (2009) The insect neuropeptide PTTH activates receptor tyrosine kinase torso to initiate metamorphosis. Science 326(5958):1403-1405.

Rewitz KF, Yamanaka N, O'Connor MB (2010) Steroid hormone inactivation is required during the juvenile-adult transition in Drosophila. Dev Cell 19(6):895-902.

Rewitz KF, Yamanaka N, O'Connor MB (2013) Developmental checkpoints and feedback circuits time insect maturation. Curr Top Dev Biol 103:1-33.

Reynolds SE, Samuels RI (1996) Physiology and Biochemistry of Insect Moulting Fluid. Advances in Insect Physiology 26:157–232.

Richards AG, Richards PA (1977) The peritrophic membranes of insects. Ann Rev Entomol 22:219-240.

Riddiford LM (1980) Insect endocrinology: action of hormones at the cellular level. Annu Rev Physiol 42:511-28.

Riddiford LM, Hiruma K, Zhou X, Nelson CA (2003) Insights into the molecular basis of the hormonal control of molting and metamorphosis from Manduca sexta and Drosophila melanogaster. Insect Biochem Mol Biol 33(12):1327-1338.

Riddiford LM (2007) Juvenile hormone action: A 2007 perspective. J Insect Phys 54:895-901.

Riddiford LM, Truman JW, Mirth CK, Shen YC (2010) A role for juvenile hormone in the prepupal development of Drosophila melanogaster. Development 137(7):1117-1126.

Rieger AM, Nelson KL, Konowalchuk JD, Barreda DR (2011) Modified annexin V/propidium iodide apoptosis assay for accurate assessment of cell death. J Vis Exp (50):2597.

Roa J, García-Galiano D, Castellano JM, Gaytan F, Pinilla L, Tena-Sempere M (2010) Metabolic control of puberty onset: new players, new mechanisms. Mol Cell Endocrinol 324(1-2):87-94.

Roller L, Zitnanová I, Dai L, Simo L, Park Y, Satake H, Tanaka Y, Adams ME, Zitnan D (2010) Ecdysis triggering hormone signaling in arthropods. Peptides 31(3):429-41.

Rubin GM, Lewis EB (2000) A brief history of Drosophila's contributions to genome research. Science 287(5461), 2216-2218.

Sahle FF, Gebre-Mariam T, Dobner B, Wohlrab J, Neubert RH (2015) Skin diseases associated with the depletion of stratum corneum lipids and stratum corneum lipid substitution therapy. Skin Pharmacol Physiol 28(1):42-55.

Saito J, Kimura R, Kaieda Y, Nishida R, Ono H (2016) Characterization of candidate intermediates in the Black Box of the ecdysone biosynthetic pathway in Drosophila melanogaster: Evaluation of molting activities on ecdysteroid-defective larvae. J Insect Physiol 93-94:94-104.

Sánchez-Higueras C, Sotillos S, Castelli-Gair Hombría J (2014) Common origin of insect trachea and endocrine organs from a segmentally repeated precursor. Curr Biol 24(1):76-81.

Sánchez-Higueras C, Hombría JC (2016) Precise long-range migration results from short-range stepwise migration during ring gland organogenesis. Dev Biol 414(1):45-57.

Sandelin A, Wasserman WW, Lenhard B (2004) ConSite: web-based prediction of regulatory elements using cross-species comparison. Nucleic Acids Res 32(Web Server issue):W249-252.

Sarraf-Zadeh L, Christen S, Sauer U, Cognigni P, Miguel-Aliaga I, Stocker H, Köhler K, Hafen E (2013) Local requirement of the Drosophila insulin binding protein imp-L2 in coordinating developmental progression with nutritional conditions. Dev Biol 381(1):97-106.

Sass M, Kiss A, Locke M (1994) The localization of surface integument peptides in tracheae and tracheoles. J Insect Phys 40(7):561–575.

Sawin-McCormack EP, Sokolowski MB, Campos AR (1995) Characterization and genetic analysis of Drosophila melanogaster photobehavior during larval development. J Neurogenet 10(2):119-35.

Schiesari L, Kyriacou CP, Costa R (2011) The hormonal and circadian basis for insect photoperiodic timing. FEBS Lett 585(10):1450-1460.

Schneiderman HA, Gilbert LI (1964) Control of growth and development in insects. Science 143(3604):325-333.

Schubiger M, Wade AA, Carney GE, Truman JW, Bender M (1998) Drosophila EcR-B ecdysone receptor isoforms are required for larval molting and for neuron remodeling during metamorphosis. Development 125(11):2053-2062.

Schubiger M, Truman JW (2000) The RXR ortholog USP suppresses early metamorphic processes in Drosophila in the absence of ecdysteroids. Development 127(6):1151-1159.

Shahbazian D, Roux PP, Mieulet V, Cohen MS, Raught B, Taunton J, Hershey JW, Blenis J, Pende M, Sonenberg N (2006) The mTOR/PI3K and MAPK pathways converge on eIF4B to control its phosphorylation and activity. EMBO J 25(12):2781-2791.

Shaik KS, Wang Y, Aravind L, Moussian B (2014) The Knickkopf DOMON domain is essential for cuticle differentiation in Drosophila melanogaster. Arch Insect Biochem Physiol 86(2):100-106.

Shi JF, Mu LL, Guo WC, Li GQ (2016a) Identification and hormone induction of putative chitin synthase genes and splice variants in Leptinotarsa decemlineata (SAY). Arch Insect Biochem Physiol 92(4):242-58.

Shi JF, Mu LL, Chen X, Guo WC, Li GQ (2016b) RNA interference of chitin synthase genes inhibits chitin biosynthesis and affects larval performance in Leptinotarsa decemlineata (Say). Int J Biol Sci 12(11):1319-1331.

Shimada-Niwa Y, **Niwa R** (2014) Serotonergic neurons respond to nutrients and regulate the timing of steroid hormone biosynthesis in Drosophila. Nat Commun 5:5778.

Shiotsuki T, Hua YJ, Tsugane T, Gee S, Hammock BD (2005) Optimization of an enzyme-linked immunosorbent assay for ecdysteroids. Journal of Insect Biotechnology and Sericology 74(1):1-4.

Shubitz LF, Trinh HT, Perrill RH, Thompson CM, Hanan NJ, Galgiani JN, Nix DE (2014) Modeling nikkomycin Z dosing and pharmacology in murine pulmonary coccidioidomycosis preparatory to phase 2 clinical trials. J Infect Dis 209(12):1949-1954.

Sieber MH, Spradling AC (2015) Steroid Signaling Establishes a Female Metabolic State and Regulates SREBP to Control Oocyte Lipid Accumulation. Curr Biol 25(8):993-1004.

Siegmund T, Korge G (2001) Innervation of the ring gland of Drosophila melanogaster. J Comp Neurol 431(4):481-491.

Smagghe G, Carton B, Decombel L, Tirry L (2001) Significance of absorption, oxidation, and binding to toxicity of four ecdysone agonists in multi-resistant cotton leafworm. Arch Insect Biochem Physiol 46(3):127-139.

Stümpges B, Behr M (2011) Time-specific regulation of airway clearance by the Drosophila J-domain transmembrane protein Wurst. FEBS Lett 585(20):3316-3321.

Sun J, Zhou Y (2015) Design, synthesis and insecticidal activity of novel phenylurea derivatives. Molecules 20(3):5050-5061.

Swale DR, Engers DW, Bollinger SR, Gross A, Inocente EA, Days E, Kanga F, Johnson RM, Yang L, Bloomquist JR, Hopkins CR, Piermarini PM, Denton JS (2016) An insecticide resistance-breaking mosquitocide targeting inward rectifier potassium channels in vectors of Zika virus and malaria. Sci Rep 6:36954.

Sweeton D, Parks S, Costa M, Wieschaus E (1991) Gastrulation in Drosophila: the formation of the ventral furrow and posterior midgut invaginations. Development 112(3):775-789.

Talamillo A, Sánchez J, Cantera R, Pérez C, Martín D, Caminero E, Barrio R (2008) Smt3 is required for Drosophila melanogaster metamorphosis. Development 135(9):1659-1668.

Talbot WS, Swyryd EA, Hogness DS (1993) Drosophila tissues with different metamorphic responses to ecdysone express different ecdysone receptor isoforms. Cell 73(7):1323-1337.

Tang WJ, Fernandez JG, Sohn JJ, Amemiya CT (2015) Chitin is endogenously produced in vertebrates. Curr Biol 25(7):897-900.

Thomsen SF (2014) Atopic dermatitis: natural history, diagnosis, and treatment. ISRN Allergy 2014:354250.

Thummel CS, Burtis KC, Hogness DS (1990) Spatial and temporal patterns of E74 transcription during Drosophila development. Cell 61(1):101-111.

Thummel CS (1996) Flies on steroids--Drosophila metamorphosis and the mechanisms of steroid hormone action. Trends Genet 12(8):306-310.

Thummel CS (2002) Ecdysone-regulated puff genes 2000. Insect Biochem Mol Biol 32(2):113-120.

Tian H, Peng H, Yao Q, Chen H, Xie Q, Tang B, Zhang W (2009) Developmental control of a lepidopteran pest Spodoptera exigua by ingestion of bacteria expressing dsRNA of a non-midgut gene. PLoS One 4(7):e6225.

Tiklová K, Tsarouhas V, Samakovlis C (2013) Control of airway tube diameter and integrity by secreted chitin-binding proteins in Drosophila. PLoS One 8(6):e67415. doi: 10.1371.

Togawa T, Dunn WA, Emmons AC, Nagao J, Willis JH (2008) Developmental expression patterns of cuticular protein genes with the R&R Consensus from Anopheles gambiae. Insect Biochem Mol Biol 38(5):508-519.

Tonning A, Hemphälä J, Tång E, Nannmark U, Samakovlis C, Uv A (2005) A transient luminal chitinous matrix is required to model epithelial tube diameter in the Drosophila trachea. Dev Cell 9(3):423-430.

Tonning A, Helms S, Schwarz H, Uv AE, Moussian B (2006) Hormonal regulation of mummy is needed for apical extracellular matrix formation and epithelial morphogenesis in Drosophila. Development 133(2), 331-341.

Tsai CC, Kao HY, Yao TP, McKeown M, Evans RM (1999) SMRTER, a Drosophila nuclear receptor coregulator, reveals that EcR-mediated repression is critical for development. Mol Cell 4(2):175-186.

Tsigos I, Martinou A, Kafetzopoulos D, Bouriotis V (2000) Chitin deacetylases: new, versatile tools in biotechnology. Trends Biotechnol 18(7):305-312.

Urness LD, **Thummel CS** (1990) Molecular interactions within the ecdysone regulatory hierarchy: DNA binding properties of the Drosophila ecdysone-inducible E74A protein. Cell 63(1):47-61.

Urness LD, **Thummel CS** (1995) Molecular analysis of a steroid-induced regulatory hierarchy: the Drosophila E74A protein directly regulates L71-6 transcription. EMBO J 14(24):6239-6246.

Uryu O, Ameku T, Niwa R (2015) Recent progress in understanding the role of ecdysteroids in adult insects: Germline development and circadian clock in the fruit fly Drosophila melanogaster. Zoological Lett 2;1:32.

Uv A, Moussian B (2010) The apical plasma membrane of Drosophila embryonic epithelia. Eur J Cell Biol 89(2-3):208-211.

Vannini L, Bowen JH, Reed TW, Willis JH (2015) The CPCFC cuticular protein family: Anatomical and cuticular locations in Anopheles gambiae and distribution throughout Pancrustacea. Insect Biochem Mol Biol 65:57-67.

van Smeden J, Bouwstra JA (2016) Stratum Corneum Lipids: Their Role for the Skin Barrier Function in Healthy Subjects and Atopic Dermatitis Patients. Curr Probl Dermatol 49:8-26.

Vincent JF, Wegst UG (2004) Design and mechanical properties of insect cuticle. Arthropod Struct Dev 33(3):187-199.

Vinetz JM, Valenzuela JG, Specht CA, Aravind L, Langer RC, Ribeiro JM, Kaslow DC (2000) Chitinases of the avian malaria parasite Plasmodium gallinaceum, a class of enzymes necessary for parasite invasion of the mosquito midgut. J Biol Chem 275(14):10331-10341.

Walker JA, Gouzi JY, Long JB, Huang S, Maher RC, Xia H, Khalil K, Ray A, Van Vactor D, Bernards R, Bernards A (2013) Genetic and functional studies implicate synaptic overgrowth and ring gland cAMP/PKA signaling defects in the Drosophila melanogaster neurofibromatosis-1 growth deficiency. PLoS Genet 9(11):e1003958.

Walkiewicz MA, Stern M (2009) Increased insulin/insulin growth factor signaling advances the onset of metamorphosis in Drosophila. PLoS One 4(4):e5072.

Walsh AL, Smith WA (2011) Nutritional sensitivity of fifth instar prothoracic glands in the tobacco hornworm, Manduca sexta. J Insect Physiol 57(6):809-818.

Wang S, Jayaram SA, Hemphälä J, Senti KA, Tsarouhas V, Jin H, Samakovlis C (2006) Septate-Junction-Dependent Luminal Deposition of Chitin Deacetylases Restricts Tube Elongation in the Drosophila Trachea. Current Biology 16, 180–185.

Wang S, Meyer H, Ochoa-Espinosa A, Buchwald U, Onel S, Altenhein B, Heinisch JJ, Affolter M, Paululat A (2012a) GBF1 (Gartenzwerg)-dependent secretion is required for Drosophila tubulogenesis. J Cell Sci 125(Pt 2):461-472.

Wang Y, Fan HW, Huang HJ, Xue J, Wu WJ, Bao YY, Xu HJ, Zhu ZR, Cheng JA, Zhang CX (2012b) Chitin synthase 1 gene and its two alternative splicing variants from two sap-sucking insects, Nilaparvata lugens and Laodelphax striatellus (Hemiptera: Delphacidae). Insect Biochem Mol Biol 42(9):637-646.

Warren JT, Wismar J, Subrahmanyam B, Gilbert LI (2001) Woc (without children) gene control of ecdysone biosynthesis in Drosophila melanogaster. Mol Cell Endocrinol 181(1-2):1-14.

Warren JT, Petryk A, Marques G, Jarcho M, Parvy JP, Dauphin-Villemant C, O'Connor MB, Gilbert LI (2002) Molecular and biochemical characterization of two P450 enzymes in the ecdysteroidogenic pathway of Drosophila melanogaster. Proc Natl Acad Sci U S A 99(17): 11043-11048.

Warren JT, Petryk A, Marqués G, Parvy JP, Shinoda T, Itoyama K, Kobayashi J, Jarcho M, Li Y, O'Connor MB, Dauphin-Villemant C, Gilbert LI (2004) Phantom encodes the 25-hydroxylase of Drosophila melanogaster and Bombyx mori: a P450 enzyme critical in ecdysone biosynthesis. Insect Biochem Mol Biol 34(9):991-1010.

Wieschaus E, Nüsslein-Volhard C, Jürgens G (1984) Mutations affecting the pattern of the larval cuticle in Drosophila melanogaster III. Zygotic loci on the X-chromosome and fourth chromosome. Roux's Arch Dev Biol 193:296-307.

Wigglesworth VB (1947) The corpus allatum and the control of metamorphosis in insects. Nature 159(4052):872.

Wigglesworth VB (1948) The Insect Cuticle. Biol Rev Camb Philos Soc 23(4):408-451.

Wigglesworth VB (1960) The epidermal cell and the metamorphosis of insects. Nature 188:358-359.

Wigglesworth VB (1985) Sclerotin and lipid in the waterproofing of the insect cuticle. Tissue Cell 17(2):227-248.

Wismar J, Habtemichael N, Warren JT, Dai JD, Gilbert LI, Gateff E (2000) The mutation without children(rgl) causes ecdysteroid deficiency in third-instar larvae of Drosophila melanogaster. Dev Biol 226(1):1-17.

Wolfgang WJ, Riddiford LM (1986) Larval cuticular morphogenesis in the tobacco hornworm, Manduca sexta, and its hormonal regulation. Dev Biol 113(2):305-316.

Wolfgang WJ, Fristrom D, Fristrom JW (1986) The pupal cuticle of Drosophila: differential ultrastructural immunolocalization of cuticle proteins. J Cell Biol 102(1):306-311.

Wolfgang WJ, Fristrom D, Fristrom JW (1987) An assembly zone antigen of the insect cuticle. Tissue Cell 19(6), 827-838.

Wilkin MB, Becker MN, Mulvey D, Phan I, Chao A, Cooper K, Chung HJ, Campbell ID, Baron M, MacIntyre R (2000) Drosophila dumpy is a gigantic extracellular protein required to maintain tension at epidermal-cuticle attachment sites. Curr Biol 10(10):559-567.

Willis JH (2010) Structural cuticular proteins from arthropods: annotation, nomenclature, and sequence characteristics in the genomics era. Insect Biochem Mol Biol 40(3):189-204.

Wingen C, Stümpges B, Hoch M, Behr M (2009) Expression and localization of clathrin heavy chain in Drosophila melanogaster. Gene Expr Patterns 9(7):549-554.

Wu VM, Beitel GJ (2004) A junctional problem of apical proportions: epithelial tube-size control by septate junctions in the Drosophila tracheal system. Curr Opin Cell Biol 16(5):493-499.

Xi Y, Pan PL, Ye YX, Yu B, Xu HJ, Zhang CX (2015) Chitinase-like gene family in the brown planthopper, Nilaparvata lugens. Insect Mol Biol 24(1):29-40.

Xie XJ, Hsu FN, Gao X, Xu W, Ni JQ, Xing Y, Huang L, Hsiao HC, Zheng H, Wang C, Zheng Y, Xiaoli AM, Yang F, Bondos SE, Ji JY (2015) CDK8-Cyclin C Mediates Nutritional Regulation of Developmental Transitions through the Ecdysone Receptor in Drosophila. PLoS Biol. 2015 Jul 29;13(7):e1002207. doi: 10.1371/journal.pbio.1002207.

Yamada M, Murata T, Hirose S, Lavorgna G, Suzuki E, Ueda H (2000) Temporally restricted expression of transcription factor betaFTZ-F1: significance for embryogenesis, molting and metamorphosis in Drosophila melanogaster. Development 127(23):5083-5092.

Yamanaka N, Rewitz KF, O'Connor MB (2013) Ecdysone control of developmental transitions: lessons from Drosophila research. Annu Rev Entomol 58:497-516.

Yang TL (2011) Chitin-based materials in tissue engineering: applications in soft tissue and epithelial organ. Int J Mol Sci 12:1936-1963.

Yao TP, Segraves WA, Oro AE, McKeown M, Evans RM (1992) Drosophila ultraspiracle modulates ecdysone receptor function via heterodimer formation. Cell 71(1):63-72.

Yao TP, Forman BM, Jiang Z, Cherbas L, Chen JD, McKeown M, Cherbas P, Evans RM (1993) Functional ecdysone receptor is the product of EcR and Ultraspiracle genes. Nature 366(6454):476-479.

Yoshiyama T, Namiki T, Mita K, Kataoka H, Niwa R (2006) Neverland is an evolutionally conserved Rieske-domain protein that is essential for ecdysone synthesis and insect growth. Development 133(13):2565-2574.

Younes I, Rinaudo M (2015) Chitin and chitosan preparation from marine sources. Structure, properties and applications. Mar Drugs 13(3):1133-1174.

Young SC, Yeh WL, Gu SH (2012) Transcriptional regulation of the PTTH receptor in prothoracic glands of the silkworm, Bombyx mori. J Insect Physiol 58(1):102-109.

Zamore PD (2001) RNA interference: listening to the sound of silence. Nat Struct Biol 8(9), 746-750.

Zeidler MP, Tan C, Bellaiche Y, Cherry S, Häder S, Gayko U, Perrimon N (2004) Temperature-sensitive control of protein activity by conditionally splicing inteins. Nat Biotechnol 22(7):871-876.

Zitnan D, Ross LS, Zitnanova I, Hermesman JL, Gill SS, Adams ME (1999) Steroid induction of a peptide hormone gene leads to orchestration of a defined behavioral sequence. Neuron 23(3):523-535.

Zitnan D, Zitnanová I, Spalovská I, Takác P, Park Y, Adams ME (2003) Conservation of ecdysis-triggering hormone signalling in insects. J Exp Biol 206(Pt 8):1275-1289.

Zhang J, Zhang X, Arakane Y, Muthukrishnan S, Kramer KJ, Ma E, Zhu KY (2011a) Comparative Genomic Analysis of Chitinase and Chitinase-Like Genes in the African Malaria Mosquito (Anopheles gambiae). PLoS ONE 6(5): e19899. doi:10.1371/journal.pone.0019899.

Zhang Z, Xu J, Sheng Z, Sui Y, Palli SR (2011b) Steroid receptor co-activator is required for juvenile hormone signal transduction through a bHLH-PAS transcription factor, methoprene tolerant. J Biol Chem 286(10):8437-8447.

Zhang J, Zhang X, Arakane Y, Muthukrishnan S, Kramer KJ, Ma E, Zhu KY (2011c) Identification and characterization of a novel chitinase-like gene cluster (AgCht5) possibly derived from tandem duplications in the African malaria mosquito, Anopheles gambiae. Insect Biochem Mol Biol. 2011 Aug;41(8):521-528.

Zhang X, Lei Y, Ma Z, Kneeshaw D, Peng C (2014) Insect-induced tree mortality of boreal forests in eastern Canada under a changing climate. Ecol Evol 4(12):2384-2394.

Zhou X, Riddiford LM (2002) Broad specifies pupal development and mediates the 'status quo' action of juvenile hormone on the pupal-adult transformation in Drosophila and Manduca. Development 129(9):2259-2269.

Zhu Q, Deng Y, Vanka P, Brown SJ, Muthukrishnan S, Kramer KJ (2004) Computational identification of novel chitinase-like proteins in the Drosophila melanogaster genome. Bioinformatics 20(2):161-169.

Zhu Q, Arakane Y, Beeman RW, Kramer KJ, Muthukrishnan S (2008a) Characterization of recombinant chitinase-like proteins of Drosophila melanogaster and Tribolium castaneum. Insect Biochem Mol Biol 38(4):467-477.

Zhu Q, Arakane Y, Beeman RW, Kramer KJ, Muthukrishnan S (2008b) Functional specialization among insect chitinase family genes revealed by RNA interference. Proc Natl Acad Sci U S A 105(18):6650-6655.

Zhu W, Wang D, Liu T, Yang Q (2016) Production of N-Acetyl-d-glucosamine from Mycelial Waste by a Combination of Bacterial Chitinases and an Insect N-Acetyl-d-glucosaminidase. J Agric Food Chem 64(35):6738-6744.